



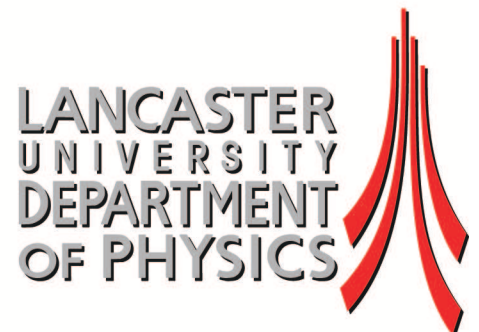
***International Conference on
Quantum Fluids and Solids 2012***

15th-21st August 2012

Lancaster University, UK

Co-chairs: S. N. Fisher and G. R. Pickett

Conference Handbook



International Advisory and Program Committee:

Shaun Fisher (Lancaster, co-chair)	George Pickett (Lancaster, co-chair)
Sébastien Balibar (Paris)	Natalia Berloff (Cambridge)
Moses Chan (Penn State)	Franco Dalfovo (Trento)
Seamus Davis (Cornell)	Volodya Dmitriev (Moscow)
Volodya Eltsov (Helsinki)	Henri Godfrin (Grenoble)
Bill Halperin (Northwestern)	Wolfgang Ketterle (Cambridge, Mass.)
Eunseong Kim (Daejeon)	Kimitoshi Kono (Riken)
Yoonseok Lee (Florida)	Jeevak Parpia (Cornell)
Jukka Pekola (Helsinki)	Emil Polturak (Technion)
Jim Sauls (Northwestern)	John Saunders (Royal Holloway, U of London)
Ladik Skrbek (Prague)	Peter Skyba (Kosice)
Makoto Tsubota (Osaka)	Grigori Volovik (Helsinki)

Local Organising Committee:

Shaun Fisher (co-chair), Lancaster University	George Pickett (co-chair), Lancaster University
Ian Bradley, Lancaster University	Andrei Golov, Manchester University
Tony Guénault, Lancaster University	Richard Haley, Lancaster University
Peter McClintock, Lancaster University	John Saunders, Royal Holloway, U of London
Viktor Tsepelin, Lancaster University	

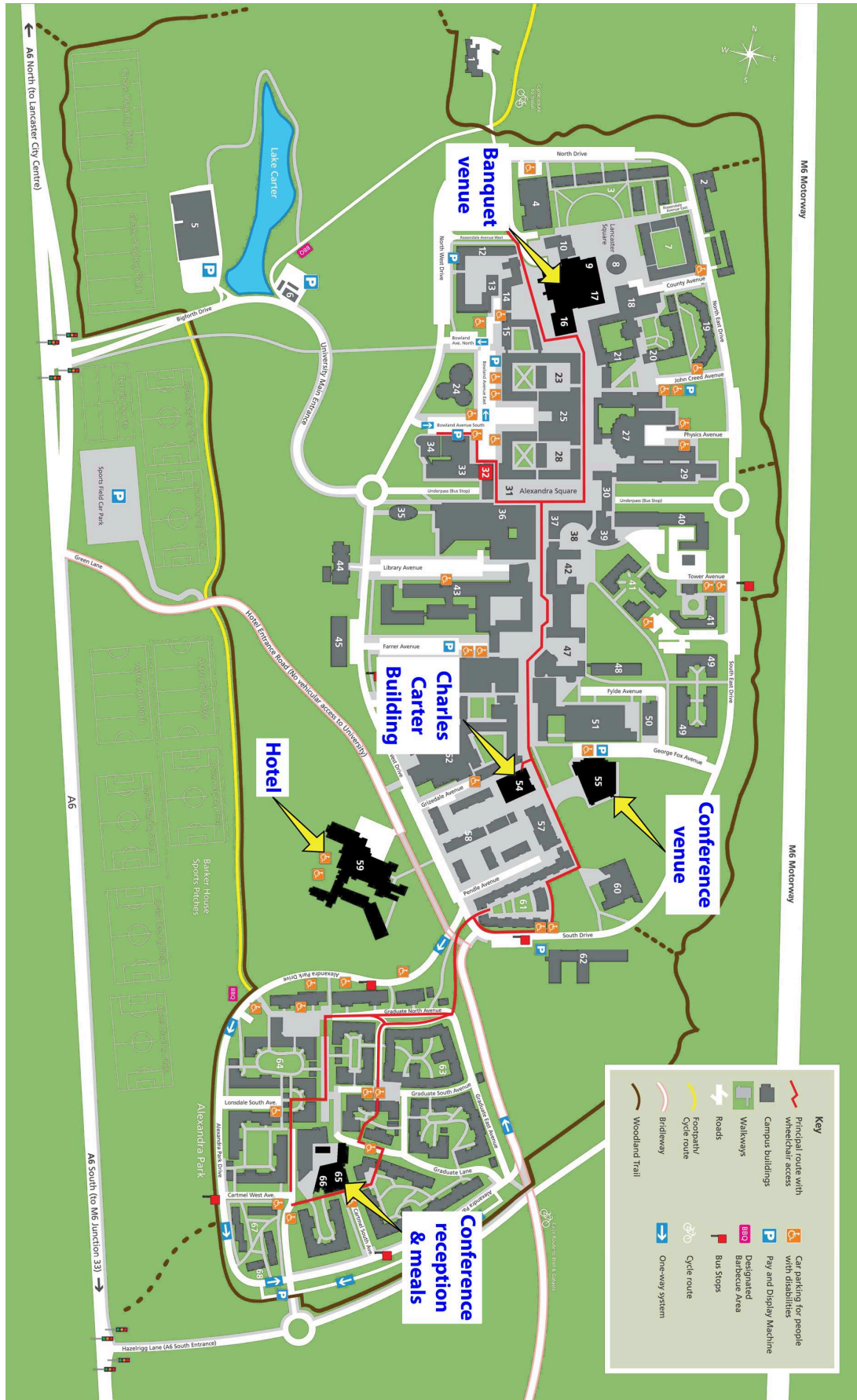
Conference Sponsors



vspace*5mm

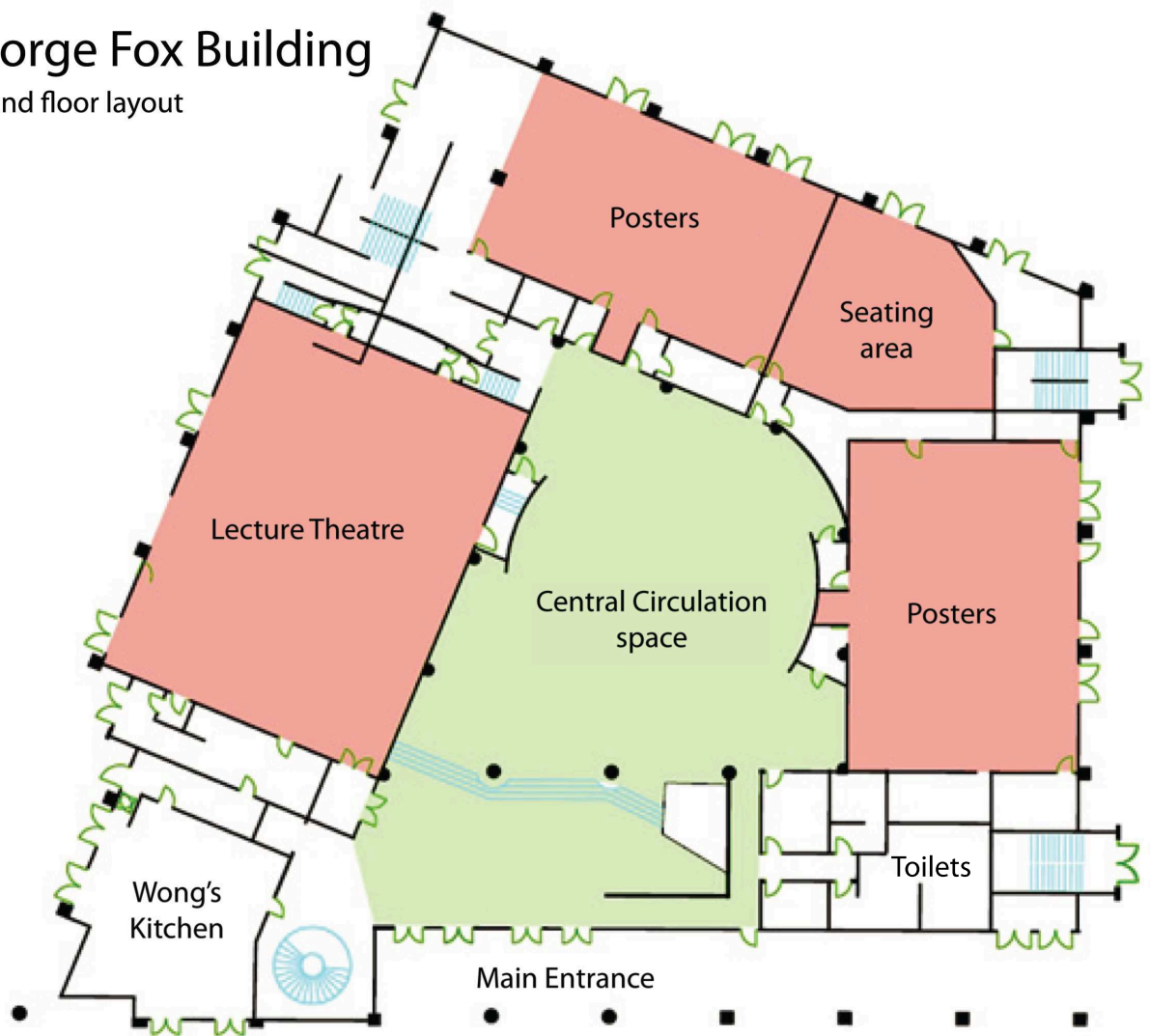


1 Maps and General Arrangements



George Fox Building

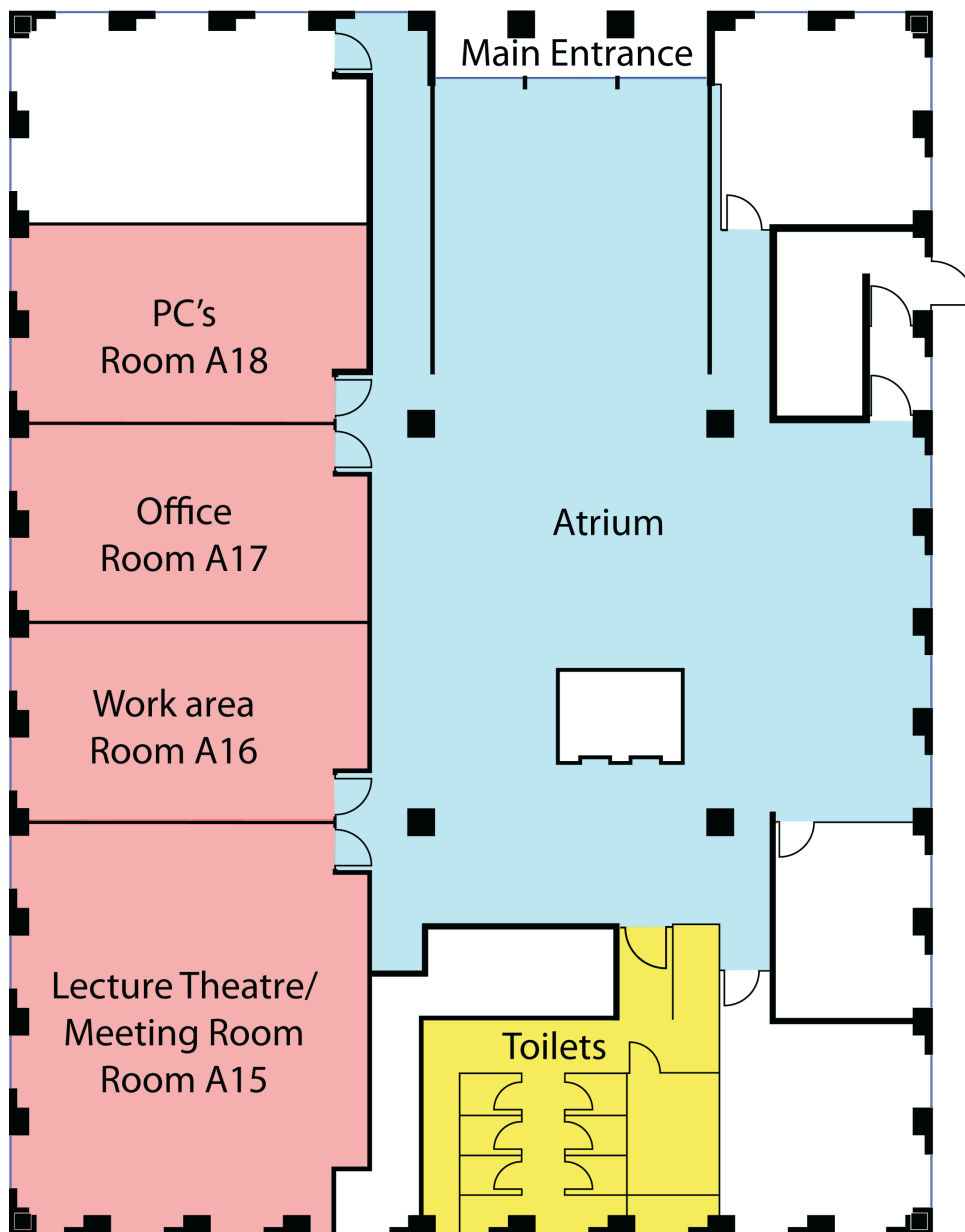
ground floor layout



The main conference venue is the **George Fox Building** at the south end of campus. Registration and reception will be in the **Barker House Farm** complex a few hundred meters away on **Alexandra Park** adjacent to the standard en-suite accommodation. The **Lancaster House Hotel** is nearby.

All oral sessions are held in the main lecture theatre, labelled Lecture Theatre 1, of the George Fox Building. Poster sessions are held in the adjacent rooms. Between the two poster rooms is room with tables and chairs to permit small group discussions.

Charles Carter Building



From Thursday August 16th, the **conference office** will be in room A17 on the ground floor of the **Charles Carter Building**, immediately opposite the entrance to the George Fox Building. The office will be open from 0830 to 1930. There are **computer terminals** for email with a support technician available on the first day of the conference in room A18. There is a work area in A16 with tables and chairs, suitable for small group discussions. There is also a medium sized lecture room (A15) with a projector suitable for larger group discussion/presentation. Contact the office if you wish to use these two rooms.

2 Scientific Programme

2.1 Morning Sessions Overview

	09:00–10:40		11:10–12:30	12:30–13:50
Thursday August 16	Opening ceremony & QFS Related Systems	coffee	Thin Fluid Films	lunch
Friday August 17	Quantum Turbulence I	coffee	Quantum Gases II	lunch
Saturday August 18	Quantum Solids I	coffee	Quantum Turbulence II	lunch
Sunday August 19	excursion			
Monday August 20	Aerogel	coffee	Quantum Solids II	lunch
Tuesday August 21	Low Dimensional Systems	coffee	QFS Analogue Systems & Closing ceremony	

Coffee and snacks will be served in the central circulation space of the George Fox building.

For those who have purchased **lunches** and **evening meals**, these are available at 12:30 and 19:00 respectively in the Barker House Farm restaurant.

The **conference banquet** will be held on Sunday August 19th in the Great Hall at 19:00, after the return from the excursions. All delegates and accompanying persons have been reserved a space at the banquet. The Great Hall is situated at the north end of campus about 15 minutes walk from the Barker House Farm complex.

2.2 Afternoon Sessions Overview

13:50–15:10		15:40–17:00	17:00–19:00	
Quantum Gases I	coffee	Vortices	Poster session 1	Thursday August 16
Mechanical Quantum Behaviour	coffee	Quantum Fluids	Poster session 2	Friday August 17
Unconventional BECs	coffee	New Techniques & Devices	Poster session 3	Saturday August 18
excursion				Sunday August 19
Electrons on Helium	coffee	Quantum Solids & Fluids	Poster session 4	Monday August 20
				Tuesday August 21

In case of emergency, the internal emergency telephone number is 999. Lancaster University security can also be contacted on internal telephones using 94541 and external telephones 01524 594541. Dialing 999 on a telephone that is not part of the campus internal telephone system (e.g. a mobile or a telephone in Lancaster) will connect you to the national emergency services (Police, Fire, Ambulance) at which point you will be asked to specify which service you want.

The QFS organisers can be contacted on

+44(0)7511922503, +44(0)7511322480 or +44(0)7511922505

in an emergency.

2.3 Thursday August 16th

09:00	Opening Ceremony		
Session 1: QFS Related Systems		Chair: Henri Godfrin	
09:40	O1.1	Nils Andersson	Neutron stars - the hottest superfluids in the Universe
10:00	O1.2	Robert Grisenti	In situ spectroscopic investigation of rapid structural transformations in supercooled quantum molecular liquids
10:20	O1.3	Dave Lee	ESR and optical spectroscopy studies of nitrogen atoms stabilized in nitrogen- helium condensates
10:40	coffee break		
Session 2: Thin Fluid Films		Chair: Masaru Suzuki	
11:10	O2.1	Francis Gasparini	Specific heat and superfluid density of ^4He near T_λ of a 33.6 nm film formed between Si wafers
11:30	O2.2	Yuichi Okuda	Strong suppression of the Kosterlitz-Thouless transition in a ^4He film under high pressure
11:50	O2.3	Priya Sharma	Effect of rough walls on transport in mesoscopic ^3He films
12:10	O2.4	Andrew Casey	Superfluid ^3He confined in nanofluidic cells
12:30	lunch		
Session 3: Quantum Gases I		Chair: Eckhard Krotscheck	
13:50	O3.1	Michael Köhl	Two-dimensional Fermi gases of ultracold atoms [keynote talk]
14:30	O3.2	Brian Anderson	Two-dimensional quantum turbulence in dilute-gas Bose-Einstein condensates
14:50	O3.3	Francesco Ancilotto	Shock waves in strongly interacting Fermi gas from time-dependent density functional calculations
15:10	coffee break		
Session 4: Vortices		Chair: Matti Krusius	
15:40	O4.1	Philip Stamp	Dynamics of a superfluid vortex
16:00	O4.2	Mihail Silaev	Dissipation in Fermi superfluids at ultralow temperatures
16:20	O4.3	Daniel Golubchik	Experimental determination of the mass of a vortex in a superconducting film
16:40	O4.4	David Weir	Defect formation in superconducting rings: external fields and finite-size effects
17:00	P1	Poster session 1	

2.4 Friday August 17th

Session 5: Quantum Turbulence I			Chair: Ladik Skrbek
09:00	O5.1	Makoto Tsubota	Hydrodynamic instability and turbulence in quantum fluids [keynote talk]
09:40	O5.2	Simone Babuin	Steady and decaying two-fluid quantum turbulence in a bellows-driven ^4He superflow
10:00	O5.3	Jaakko Hosio	Quantum turbulence in rotating superfluid $^3\text{He-B}$ in the $T = 0$ limit
10:20	O5.4	Carlo Barenghi	Spectra and statistics of velocity fluctuations in quantum turbulence
10:40	coffee break		
Session 6: Quantum Gases II			Chair: Susana Hernández
11:10	O6.1	Martin Zwierlein	Strongly interacting Fermi gases: Thermodynamics, lower dimensions and synthetic gauge fields
11:30	O6.2	Hiromitsu Takeuchi	Tachyon condensation and brane annihilation in Bose-Einstein condensates: spontaneous symmetry breaking in a lower-dimensional subspace
11:50	O6.3	Sergey Vasiliev	Electron spin waves in atomic hydrogen gas
12:10	O6.4	Vanderlei Bagnato	Quantum turbulence in an atomic trapped superfluid: general characteristics and observation of power law in the kinetic energy spectrum
12:30	lunch		
Session 7: Mechanical Quantum Behaviour			Chair: John Owers-Bradley
13:50	O7.1	Andrew Cleland	Mechanical resonators in the quantum regime [keynote talk, EPS invited speaker]
14:30	O7.2	Mika Sillanpää	Circuit QED with a hybrid of micromechanical resonator and transmon qubit
14:50	O7.3	Pertti Hakonen	Towards microwave optomechanics with graphene mechanical resonators
15:10	coffee break		
Session 8: Quantum Fluids			Chair: Minoru Kubota
15:40	O8.1	Osamu Ishikawa	Investigation of intrinsic angular momentum in rotating superfluid $^3\text{He-A}$ phase
16:00	O8.2	Oleg Kirichek	A neutron reflectometry study of the liquid helium surface
16:20	O8.3	Takeshi Mizushima	Symmetry protected topological order and spin susceptibility in superfluid $^3\text{He-B}$
16:40	O8.4	Humphrey Maris	Experimental investigation of exotic negative ions in superfluid helium
17:00	P2	Poster session 2	

2.5 Saturday August 18th

Session 9: Quantum Solids I		Chair: John Beamish	
09:00	O9.1	Sébastien Balibar	The quantum plasticity of helium crystals [keynote talk]
09:40	O9.2	Hans Lauter	Superfluid components within solid helium
10:00	O9.3	Alexander Balatsky	Defects and glassy dynamics in solid ^4He : Perspectives and current status
10:20	O9.4	Bob Hallock	Mass flux measurements in solid ^4He : status and new work
10:40	coffee break		
Session 10: Quantum Turbulence II		Chair: Sergey Nemirovskii	
11:10	O10.1	Edouard Sonin	Symmetry of Kelvin-wave dynamics and the Kelvin-wave cascade in the $T = 0$ superfluid turbulence
11:30	O10.2	Risto Hänninen	Kelvin-wave spectrum of a pinned vortex
11:50	O10.3	Yuri Sergeev	Decay regimes and spectra of quantum turbulence at low temperatures
12:10	O10.4	Hideo Yano	Vortex emission from quantum turbulence generated by a vibrating wire in superfluid ^4He
12:30	lunch		
Session 11: Unconventional BECs		Chair: Reyer Jochemsen	
13:50	O11.1	Natalia Berloff	Universality and pattern forming in polariton condensates [keynote talk]
14:30	O11.2	Yuriy Bunkov	Magnetic BEC and spin superfluidity in antiferromagnetics
14:50	O11.3	Vladimir Eltsov	Self trapping and relaxation of magnon condensates in superfluid $^3\text{He-B}$
15:10	coffee break		
Session 12: New Techniques & Devices		Chair: Harry Kojima	
15:40	O12.1	Gary Ihas	MWN collaboration: multi-faceted approach to quantum turbulence
16:00	O12.2	Eddy Collin	Nonlinear dynamics in nanomechanical resonators
16:20	O12.3	Yoonseok Lee	Investigation of transport properties in thin films of liquid ^3He using MEMS devices
16:40	O12.4	Andrei Golov	Excimer molecules as tracer particles for study of quantum turbulence in superfluid ^4He
17:00	P3	Poster session 3	

2.6 Monday August 20th

Session 13 Aerogel		Chair: Jeevak Parpia	
09:00	O13.1	Bill Halperin	New chiral phases of superfluid ^3He stabilized by anisotropic silica aerogel [keynote talk]
09:40	O13.2	Vladimir Dmitriev	NMR Studies of superfluid ^3He in “nematically ordered” aerogel
10:00	O13.3	Igor Fomin	Effect of structural correlations in aerogel on thermodynamic properties of superfluid ^3He
10:20	O13.4	Yutaka Sasaki	Existence of dense superfluid ^3He - ^4He mixture in aerogel
10:40	coffee break		
Session 14: Quantum Solids II		Chair: Eunseong Kim	
11:10	O14.1	Séamus Davis	Interplay of rotational relaxational and shear dynamics in solid ^4He
11:30	O14.2	Hyoungsoon Choi	Quantized circulation in solid helium-4 under rotation
11:50	O14.3	Daisuke Takahashi	Possible quantum oscillation of non-classical rotational inertia of solid ^4He in vycor by DC rotation
12:10	O14.4	Moses Chan	Is solid helium a superfluid?
12:30	lunch		
Session 15: Electrons on Helium		Chair:	
13:50	O15.1	Paul Leiderer	Electrons on liquid helium in confined geometry - a unique Coulomb system [keynote talk]
14:30	O15.2	Kimitoshi Kono	Transport of electrons on helium channels
14:50	O15.3	Hiroki Ikegami	Probing Chirality in Superfluid ^3He -A
15:10	coffee break		
Session 16: Quantum Solids & Fluids		Chair: Emil Polturak	
15:40	O16.1	Alexander Andreev	Resonant tunneling systems in ^4He crystals: alternative to supersolidity
16:00	O16.2	Peter Moroshkin	Spectroscopy of atomic bubbles in liquid and solid helium
16:20	O16.3	Victor Efimov	Free decay of acoustic turbulent energy cascades in superfluid ^4He
16:40	O16.4	Jim Sauls	Surface states, edge currents, and chiral symmetry of superfluid ^3He -A
17:00	P4	Poster session 4	

2.7 Tuesday August 21st

Session 17: Low Dimensional Systems Chair: John Saunders			
09:00	O17.1	Hiroshi Fukuyama	Physics of two-dimensional helium films: Recent studies of monolayer ^3He and ^4He on graphite [keynote talk]
09:40	O17.2	Junko Taniguchi	Superfluidity and BEC of ^4He confined in a one-dimensional channel
10:00	O17.3	Luciano Reatto	^3He and ^4He on graphene-fluoride and graphane: prediction of novel fluid, superfluid and supersolid phases
10:20	O17.4	David Cobden	Phases, transitions, and novel phenomena in monolayers of ^4He and other gases on individual carbon nanotubes
10:40	coffee break		
Session 18: QFS Analogue Systems Chair:			
11:10	O18.1	Henry Tye	^3He superfluid as a model for the cosmic landscape in string theory [keynote talk]
11:50	Closing Ceremony		

3 Posters

Poster should be mounted at the start of the day of your poster presentation and removed at the end of the poster session. Poster boards are identified by a number. Each poster has an identifier of the form **Px.y** where **x** gives to the number of the poster session and **y** identifies the poster board. For example, P3.17 will be in poster session 3 on Saturday August 18th on poster board 17. Posters 1–36 are in the room on right as you enter the building whilst posters 37–60 are directly ahead.

The lists below gives the presenting author only, see the complete abstracts for further details.

3.1 Thursday August 16th

Defoort, M.	P1.1	Silicon nitride mechanical nano-resonators
Kirichek, O.	P1.2	Ultra-low temperature sample environment for neutron scattering experiments
Shibahara, A.	P1.3	Characterisation of microcoils as local probes for helium NMR
Casey, A.	P1.4	A practical DC SQUID current sensing noise thermometer for low temperature measurements
Kondaurova, Luiza P.	P1.5	Numerical study on decay of the vortex tangle at zero temperature
Rogova, S.	P1.6	Diffusion and Thermal Diffusion Influence on Temperature Relaxation in Superfluid ^3He - ^4He Mixtures
Collett, C.A.	P1.7	Nonlinear field-dependence and f -wave interactions in superfluid ^3He
Papoular, D. J.	P1.8	Cooling by Heating a Superfluid
Bešlić, I.	P1.9	Quantum Monte Carlo simulation of spin-polarized deuterium
Nemirovskii, Sergey K.	P1.10	Energy spectrum of the 3D velocity field, induced by vortex tangle
Miah, S.	P1.11	Superstatistical Approach to Quantum Fluid
Ikegami, H.	P1.12	Probing Chirality in Superfluid ^3He -A
Choi, H. C.	P1.13	Evidence of Knudsen-Hydrodynamic Crossover in Normal Fluid ^3He in 98% Aerogel
Gonzalez, M.	P1.14	Unusual Behavior of a MEMS Resonator in Superfluid ^4He
Lichtenegger, T.	P1.15	Spin-density fluctuations in liquid ^3He
Holler, R.	P1.16	Multi-pair and exchange effects in the dynamic structure of 2D- ^3He
Nakamura, S.	P1.17	Heat Capacity and Vapor Pressure Measurements of 2D ^4He on ZYX Graphite
Wu, Hao	P1.18	Excitation spectrum and Spin Current on the surface of ^3He -B
Wacks, D.H.	P1.19	Shell model of superfluid turbulence
Hawthorne, Dean L.	P1.20	Simulations of non-linear spin dynamics in spin polarized dilute ^3He - ^4He mixtures
Sheshin, G.	P1.21	Transition to turbulence regime in ^3He - ^4He solutions: ^3He condensation on quantized vortices
Gritsenko, I.	P1.22	Frequency characteristics of a quartz tuning fork immersed in He II
Schmoranzner, D.	P1.23	Crosstalk between quartz tuning forks in He II
Woods, A.	P1.24	Hydrodynamic Properties of a Low Frequency Resonator in Normal and Superfluid ^4He
Mateo, D.	P1.25	Electron photo-ejection from bubble states in liquid ^4He
Heikkinen, P.J.	P1.26	Bose-Einstein condensation of magnons in rotation-controlled traps in superfluid ^3He -B

Ikegami, H.	P1.27	Unexpected Density Dependence of Mobility of Electron Bubbles Trapped below the Free Surface of Normal ^3He
Nemirovskii, Sergey K.	P1.28	Fluctuations of the vortex line density in turbulent flows of quantum fluids
Nemchenko, E.K.	P1.29	Heat flow from solid to liquid He II due to inelastic processes of phonons interaction
Abdurakhimov, L.V.	P1.30	Study on the instability of He-II surface induced by second sound
Obara, K.	P1.31	Acoustic Observation of Textural Transition of Superfluid $^3\text{He-A}$ in Slab
Fukui, A.	P1.32	Enhancement of Magnetization in Liquid ^3He at Aerogel Interface
Melnikovskiy, L.A.	P1.33	Roton Parametric Resonance
Tsutsumi, Y.	P1.34	Quasiparticle States for the Superfluid ^3He B-Phase in a Cylinder
Glyde, H.R.	P1.35	Phonon-roton modes and Bose-Einstein condensation in liquid ^4He
Azuah, R.T.	P1.36	Bose-Einstein condensation in liquid ^4He under pressure
Nava, M.	P1.37	Ground state and excitations in a film of ^3He
Panochko, G.	P1.38	The ^3He impurity states in ^4He
Yamaguchi, A.	P1.39	Recent Spin Pump Experiments on Superfluid $^3\text{He-A}_1$
Mateo, D.	P1.40	Real time dynamics of the desorption of atomic impurities from ^4He
Takeuchi, Hiromitsu	P1.41	Spin Susceptibility of Proximity-Induced Odd-Frequency State in Aerogel/Superfluid ^3He System
Surovtsev, E.	P1.42	Contribution of spacial transverse fluctuations of order parameter to superfluid properties of ^3He in aerogel
Ghosh, A.	P1.43	Generation of multi-electron bubbles under pulsed electric fields
Yudin, A.N.	P1.44	Pulse NMR Studies of Superfluid ^3He in squeezed “Nematically Ordered” Aerogel
Kunimatsu, T.	P1.45	Texture of Rotating Superfluid $^3\text{He-A}$ phase in a single narrow cylinder
Zmeev, D.E.	P1.46	Observation of Crossover from Ballistic Regime to Diffusion for Excimer Molecules in Superfluid ^4He
Zhelev, N.	P1.47	Torsion Pendulum energy dissipation due to ^3He in aerogel. Dissipation signature of the A-phase
Minoguchi, T.	P1.48	Density functional theory and Bose statistics for the freezing of superfluid ^4He
Rysti, J.	P1.49	Mechanical oscillators immersed in inviscid compressible fluids
Sato, D.	P1.50	The Temperature Dependence of Heat Capacity in 2D Liquid Puddles of ^3He on Grafoil
Munday, L.L.E.	P1.51	Second Sound Attenuation of Decaying Quantum Grid Turbulence in Liquid Helium-4
Arrayás, M.	P1.52	Phenomenological modelling of the A-B interface
Senin, A.A.	P1.53	NMR Studies of Superfluid ^3He in Squeezed “Nematically Ordered” Aerogel
Schanen, R.	P1.54	The superfluid ^3He AB interface probed by quartz tuning forks
Ikeda, Ryusuke	P1.55	Competition between Anisotropy and Disorder in a Toy Model of Superfluid ^3He in Globally Anisotropic Aerogel
Sultan, A.	P1.56	Experimental determination of the static structure factor of Fermi Liquid ^3He in two-dimensions

3.2 Friday August 17th

Malik, G.P.	P2.1	A study of the experimental features of ^{87}Rb , ^{23}Na and ^7Li via a linearly perturbed harmonic oscillator potential
Hufnagl, D.	P2.2	Stability of a bilayer system of strongly correlated dipolar Bosons
Holler, R.	P2.3	Spin Structure function of a cold Fermi gas
Mullin, W. J.	P2.4	Amplitude control of quantum interference
Tempere, J.	P2.5	Quasicondensation and pseudogap in two-dimensional Fermi gases
Wada, N.	P2.6	A New Superfluid Transition of ^4He Films in Three-Dimensional Topology
Krotscheck, E.	P2.7	Correlated BCS State of Ultracold Fermi Gases
Nitta, M.	P2.8	Vortons and 3D skyrmions from domain wall pair annihilations in BECs
Zillich, R. E.	P2.9	Roton Excitations and Stability of the Anisotropic Two-Dimensional Dipolar Bose Gas
Proukakis, N. P.	P2.10	<i>Ab Initio</i> Stochastic Modelling of Low-Dimensional Bose Gas Experiments
Hernández, E.S.	P2.11	Effects of stationary vortices in the structure of pair currents in a fermion superfluid.
Gordillo, M.C.	P2.12	Bosonic hard-rods in one dimensional optical lattices
Tsubota, M.	P2.13	Spin Turbulence and the $-7/3$ Power Law in a Trapped Spin-1 Spinor Bose-Einstein Condensate
Arahata, E.	P2.14	Dynamical Simulation of Sound Propagation in a Highly Elongated Trapped Bose Gas at Finite temperatures
Aoki, Yusuke	P2.15	Spin turbulence made by the oscillating magnetic field in a spin-1 spinor Bose-Einstein condensate
Ishino, S.	P2.16	Instability of overlapped vortices rotating in opposite directions in binary Bose-Einstein condensates
Hayashi, S.	P2.17	Helical shear-flow instability in the phase-separated two-component Bose-Einstein Condensates
Borgh, M.O.	P2.18	Topological Interface Engineering in a Spinor Bose-Einstein Condensate
Kashimura, T.	P2.19	Magnetic properties and strong-coupling corrections in an ultracold Fermi gas with population imbalance
Watanabe, R.	P2.20	Two-dimensional pseudogap effects of an ultracold Fermi gas in the BCS-BEC crossover region
Hanai, R.	P2.21	Superfluid phase transition and strong-coupling effects in an ultracold Fermi gas with mass imbalance
Hernández, E.S.	P2.22	Pure pairing modes in trapped fermion systems
Takahashi, D.A.	P2.23	Solutions of bosonic and fermionic one-dimensional Bogoliubov-de Gennes equations: a unified treatment and generalizations
Inotani, D.	P2.24	Phase transition from p_x -wave state to $p_x + ip_y$ state and single-particle properties in a one-component superfluid Fermi gas with a p -wave Feshbach resonance
Kusumura, T.	P2.25	Energy spectra of the superfluid velocity made by quantized vortices in two-dimensional quantum turbulence
Proment, D.	P2.26	Vortex knots in a Bose-Einstein condensate
Tinh, B.D.	P2.27	Ac fluctuation resistivity in high- T_c superconductors
Allen, A.J.	P2.28	Finite Temperature Vortex Dynamics in Trapped Bose Gases
Sherwin, L.K.	P2.29	Energy spectrum of counterflow turbulence
Kimura, Y.	P2.30	Anomalous Acoustic Absorption in Liquid Helium

White, A. C.	P2.31	Measures of vortex clustering in Bose–Einstein condensates
Apushkinsky, E.	P2.32	Nonlinear motion of vortices in HTSC after interacting with external Rf field.
Marakov, A.	P2.33	Visualization technique for determining the structure functions of normal-fluid turbulence in superfluid ^4He
Suramlishvili, N.	P2.34	Three-dimensional modelling of Andreev scattering in turbulent $^3\text{He-B}$
Hietala, N.	P2.35	Spin-Down to Rest of the Superfluid Component in Different Geometries
Skrbek, L.	P2.36	Analysis of Solid Particles' Motion in Thermal Counterflow
Baggaley, A.W.	P2.37	Vortex density fluctuations in quantum turbulence
Walmsley, P.M.	P2.38	Observation of vortex ring emission within turbulent vortex tangles in superfluid ^4He at low temperatures
Walmsley, P.M.	P2.39	Rotating quantum turbulence in superfluid ^4He in the $T = 0$ limit
Guise, E.	P2.40	Design and Characterisation of a Detector for Quasiparticle Imaging Studies and Quantum Turbulence in Superfluid ^3He
Mineda, Y.	P2.41	Decay of Counterflow Quantum Turbulence in Superfluid ^4He
Nakatsuji, A.	P2.42	Propagation of quantized vortices driven by an oscillating sphere in superfluid ^4He
Kubo, H.	P2.43	Time-of-flight Measurements of Vortex Rings Emitted from Quantum Turbulence in Superfluid ^4He
Galantucci, L.	P2.44	Normal fluid profiles in a Helium II counterflow channel
Sciacca, M.	P2.45	Waves in a quantized vortex line in superfluid helium
Williams, P.	P2.46	Comparison of the Turbulent Drag Coefficient For Low and High Frequency Vibrating Grids in Superfluid $^3\text{He-B}$
Williams, P.	P2.47	Direct Measurements of the Energy Dissipated by Quantum Turbulence in Superfluid $^3\text{He-B}$
Salman, H.	P2.48	Self-reconnecting Quantized Vortices in Superfluid Turbulence
Cox, T.	P2.49	Inertial effects on the motion of a vortex in a Bose-condensed gas
Lawson, C.R.	P2.50	Anomalous damping of a low frequency vibrating wire in superfluid $^3\text{He-B}$ due to vortex shielding
Tsepelin, V.	P2.51	The onset of vortex production by a vibrating wire in superfluid $^3\text{He-B}$

3.3 Saturday August 18th

Nafidi, A.	P3.1	Isovalent substitution and heat treatments control of T_c , chain oxygen disorder and structural phase transition in high T_c superconductors
Dubyna, D. S.	P3.2	Nonequilibrium superconductivity in double tunnel junction with spatially inhomogeneous superconducting electrode
Chaudhury, R.	P3.3	Kohn anomaly and acoustic properties of superconductors
Durajski, A.P.	P3.4	The high pressure superconductivity in CaLi_2 compound: the thermodynamic properties
Ahlstrom, S.L.	P3.5	Thermal conductivity measurements of $\text{Dy}_2\text{Ti}_2\text{O}_7$ (Spin Ice) and $\text{Y}_2\text{Ti}_2\text{O}_7$ in the temperature range 15 mK to 20 K
Sonin, E.B.	P3.6	Spin superfluidity, coherent spin precession, and magnon BEC
Yamaguchi, A.	P3.7	Crystal size effects on ferromagnetic heavy fermion compound UGe_2
Rybalko, A.S.	P3.8	New features of a glassy phase in solid helium at the supersolid region
Chishko, K. A.	P3.9	Metastable States of ^3He - ^4He Solid Solutions in Pre-separation Region
Kojima, H.	P3.10	Solid ^4He Probed Simultaneously by Torsional Oscillator and Ultrasound
Nomura, R.	P3.11	Self-Organized Criticality in Quantum Crystallization of ^4He in Aerogel
Polturak, E.	P3.12	Identification of a Dislocation Related Dissipation Mechanism in High Temperature Mobile Solid ^4He
Todoshchenko, I.A.	P3.13	Faceting of vicinal surfaces on ^4He crystals
Iwasa, I.	P3.14	Dislocation-Pinning Mechanism for the Hysteresis of Torsional-Oscillator Experiments on Solid Helium
Haziot, A.	P3.15	Quantum plasticity in ^4He crystals
Mi, X.	P3.16	Anomalous Behavior of Solid ^4He in Porous Vycor Glass
Maris, H. J.	P3.17	Frequency Shifts of Torsional Oscillators Due to Elasticity
Minoguchi, T.	P3.18	Possible crystallization wave in thin film of He-4 on a smooth surface
Vitiello, S. A.	P3.19	Effects of a ^3He impurity on the elastic anomalies of ^4He at $T = 0$
Kubota, M.	P3.20	Vortex lines penetration rejection below supersolid transition T_c of hcp He
Nomura, R.	P3.21	Left-over Superfluid ^4He in Aerogel and Its Crystallization by Cooling
Mezhov-Deglin, L.P.	P3.22	Low-Temperature Anomalies in Thermal Conductivity of the Plastically Deformed Crystals due to the Phonon-Kink Scattering
Vekhov, Ye.	P3.23	Dissipative superfluid mass flux through solid ^4He
Mukharski, Y.	P3.24	Neutron and X-ray experiments in solid ^4He
Brazhnikov, M. Yu.	P3.25	Simultaneous measurements of the thermal conductivity and response to torsional oscillations of solid ^4He
Kunimi, Masaya	P3.26	Excitation spectrum and stability analysis of a supersolid
Cowan, B.	P3.27	Two-Mode Torsional Oscillator Study of Solid Helium
Kim, S.S.	P3.28	Lattice Dynamics of ^3He Impurities in Solid ^4He : An NMR Study
Takahashi, T.	P3.29	Ripening of Splashed ^4He Crystals by Acoustic Waves in Zero Gravity
Khmelenko, V.V.	P3.30	Energy release channels during destruction of impurity-helium condensates

Birchenko, A.P.	P3.31	Pressure Relaxation and NMR Measurements in hcp 1% ^3He in ^4He Quenched Crystals
Tsuiki, T.	P3.32	Depletion of NCRI of solid ^4He confined in Vycor glass under DC rotation
Ohgoe, T.	P3.33	Commensurate supersolid in lattice bosons
Kato, Yusuke	P3.34	Josephson effect in two-dimensional supersolids
Krainyukova, N.V.	P3.35	Simple Statistics for Cooperative Motion in Solid ^4He and Supersolidity
Bossy, J.	P3.36	Modes of amorphous solid helium
Mulders, N.	P3.37	More on the shear modulus of solid helium
Shin, J.	P3.38	Simultaneous Measurements of Torsional Oscillator and Shear Modulus of Solid Helium
Mikhin, N.P.	P3.39	Spin-lattice relaxation in rapidly grown helium crystal with 1% impurity of ^3He
Haziot, A.	P3.40	Dissipation and dislocations density in ^4He crystals
Fefferman, A.D.	P3.41	Absence of pressure transmission through a helium solid/liquid/solid double junction
Fefferman, A.D.	P3.42	Predictions of the Granato-Lucke model assuming a distribution of dislocation lengths
Tempere, J.	P3.43	Resonant enhancement of the FFLO superfluid state by a 1D optical potential
Yamashita, K.	P3.44	Gas-Solid Phase Transition in Hardcore-like Systems
Choi, Jaewon	P3.45	Shear Modulus Measurement of Ultrapure Solid Helium-4
Mukharski, Y.	P3.46	Precise measurements of the lattice constant solid ^4He
Choi, H.	P3.47	Quantized Circulation in Solid Helium-4 under Rotation
Merdan, M.	P3.48	Longitudinal excitations in triangular lattice antiferromagnets

3.4 Monday August 20th

Saini, L.K.	P4.1	Effect of Form Factor on Ground-state Properties of Electron Quantum Bilayers
Smorodin, A.V.	P4.2	Surface electrons transport over structured silicon substrate
Antsygina, T.N.	P4.3	Magnetization of Dense ^3He Monolayers Adsorbed on Graphite
Rovenchak, A.	P4.4	Finite systems of 1D and 2D harmonic oscillators obeying fractional statistics with a complex parameter
Momoi, T.	P4.5	Spin nematic order in the multiple-spin exchange model on the triangular lattice
Nafidi, A.	P4.6	Correlation between band structure and magneto- transport properties in HgTe/CdTe two-dimensional far-infrared detector superlattice
Mezhov-Deglin, L.P.	P4.7	Interaction of cold neutrons with impurity gel samples of heavy water and deuterium in superfluid He-II; structural transformations in high dispersed icy samples at low temperatures
Konopko, L.	P4.8	Quantum Interference of Surface States in Bismuth Nanowires in Transverse Magnetic Fields
Nikolaeva, A.	P4.9	Influence Weak and High Magnetic Field in Longitudinal and Transverse Configuration on Magneto- thermoelectric Properties Quantum Bi- wires
Meisel, Mark W.	P4.10	Magnetic Response of $\mathbf{S} = \mathbf{2}$ Linear-Chain Antiferromagnets at Low Temperatures and in High Magnetic Fields
Reatto, L.	P4.11	^3He and ^4He on graphene–fluoride and graphane: prediction of novel fluid, superfluid and supersolid phases
Gordillo, M.C.	P4.12	H_2 physisorbed on graphane
Gordillo, M.C.	P4.13	Phase diagrams of ^4He on flat and curved environments
Narayan, V.	P4.14	Evidence of Novel Quasiparticles in a Strongly Interacting Two-Dimensional Electron System: Giant Thermopower and Metallic Behaviour
Matsushita, Taku	P4.15	One-Dimensional Superfluid ^4He Adsorbed in Nanochannels
Aubry, G.	P4.16	Critical behaviour of the liquid gas transition of ^4He confined in a silica aerogel
Babichenko, V.S.	P4.17	Many-Body Effects in the Spatially Separated Electron and Hole Layers in the Coupled Quantum Wells
Tanaka, T.	P4.18	Superfluidity of ^4He in a well-controlled nanopore array
Mezhov-Deglin, L.	P4.19	On Effective Mass of Charged Clusters in Cryogenic Electrolytes
Karasevskii, A.I.	P4.20	Low-temperature thermodynamic properties of nanocrystals
Krainyukova, N.V.	P4.21	Instability of Small Deuterium Clusters in Superfluid Helium near the λ Point
Taborek, P.	P4.22	Superfluid Onset and 2D phase transitions of Helium-4 on Lithium and Sodium
Badrutdinov, A.	P4.23	Relaxation of hot electrons on helium in ripplon scattering regime
Murakawa, S.	P4.24	Superfluid ^4He in Nanopore Array: Toward the Josephson Effect at Arbitrary Temperatures
Tanatar, B.	P4.25	Collective Modes in Bilayer Dipolar Gases and the Drag Effect
Arnold, F.	P4.26	SQUID-NMR of Helium-3 on a new Exfoliated Graphite Substrate
Shin, Hyeondeok	P4.27	Effects of ^3He Impurities on the Superfluid Response of the ^4He Monolayer on a C_{20} Molecule
Kim, Byeongjoon	P4.28	Structural and Superfluid Properties of the ^4He Monolayer on a C_{28} Molecule
Kent, K.	P4.29	A New Exfoliated Graphite Substrate for Measurements of Adsorbed Gases
Yager, B.	P4.30	NMR Identification of Possible One-Dimensional Behaviour of Helium-3 in Nanopores

Noda, K.	P4.31	Slippage of ^4He Films and Precursor Phenomenon of Superfluidity
Iwata, Y.	P4.32	Ultrasound Attenuation of Confined ^4He near the Quantum Critical Point
Bešlić, I.	P4.33	Liquid and solid ^4He clusters adsorbed on graphene
Markić, L. Vranješ	P4.34	Quantum Monte Carlo simulations of spin-polarized hydrogen in 2D and on the surface of liquid helium
Hieda, M.	P4.35	^3He Effect on 2D Superfluid in ^3He - ^4He Mixture Films on Gold
Taniguchi, Junko	P4.36	Double torsional oscillator measurements for ^4He confined in 1D nanoporous medium FSM16 with 2.8-nm channel
Matsushita, Taku	P4.37	Atomic motion in low-coverage helium film adsorbed in FSM nanochannels
Morishita, Masashi	P4.38	Heat Capacity of Very Dilute ^3He - ^4He Films on Graphite
Spathis, P.	P4.39	Imbibition of liquid helium in silica aerogels
Levitin, L.V.	P4.40	Superfluid ^3He Confined in a Single 100 nm Slab
Watanabe, M.	P4.41	Self Oscillation of Electrons on the Surface of Superfluid ^4He
Zimmerman, A.	P4.42	Growth and Characterization of Anisotropic Silica Aerogel
Fear, M.J.	P4.43	A New Compact Rotating Dilution Refrigerator
Garg, D.	P4.44	Thermometry in normal liquid ^3He using a Quartz Tuning fork viscometer
Shirahama, K.	P4.45	A Compact Rotating Cryostat for Superfluid ^4He Studies
Jang, S.	P4.46	Absolute Positioning Application of Capacitive Sensor
Jochemson, R.	P4.47	SRD1000 and CMN1000 sensors for precision thermometry below 8 K

4 Abstracts

4.1 Invited Oral Presentations: Thursday August 16th

01.1 Neutron stars - the hottest superfluids in the Universe

N. Andersson

School of Mathematics, University of Southampton, Southampton, UK

In this talk I will summarise the astrophysical evidence for superfluidity (and superconductivity) in neutron stars, the extreme density remnants of supernova explosions. Based on general arguments these systems have long been expected to have superfluid cores (due to Cooper pairing of neutrons, etc), but it is only recently that observations have reached the point where they begin to constrain the theory. I will discuss new data concerning radio pulsar glitches, where vortex unpinning plays a key role in explaining the observed phenomenology. I will also show how the "real-time" cooling of the remnant in Cassiopeia A (the youngest known neutron star) allows us to infer the presence of superfluid components at densities beyond nuclear saturation. Finally, I will consider a list of outstanding questions in this area of research and discuss whether laboratory insights may help us make progress in the future.

01.2 In situ spectroscopic investigation of rapid structural transformations in supercooled quantum molecular liquids

R.E. Grisenti^a, M. Kühnel^a, J.M. Fernández^b, G. Tejeda^b, A. Kalinin^a, and S. Montero^b

^aInstitut für Kernphysik, J. W. Goethe-Universität, Max-von-Laue-Str. 1, 60438 Frankfurt am Main, Germany

^bLaboratory of Molecular Fluid Dynamics, Instituto de Estructura de la Materia, CSIC, Serrano 121, 28006, Madrid, Spain

Understanding the exact interplay between the freezing transition and the dynamics in supercooled liquids represents one of the most fundamental and so far unresolved issues in condensed matter physics. Here we employ the liquid microjet technique to experimentally investigate with ns time resolution the crystallization process in supercooled p-H₂ and o-D₂ liquid mixtures. Our results reveal a significant slowing down, with respect to the pure cases, in the crystallization kinetics of the mixtures. We attribute the observed behavior to the quantum nature of the system in terms of zero-point contribution to the interaction potential between the particles. These quantum effects, which are at greatest for o-D₂ impurities surrounded by p-H₂ solvent particles, leads to a local structural relaxation of the surrounding shell of p-H₂ molecules toward the impurity, thereby significantly affecting the local geometry of the system. Thus, our experimental data appear to be particularly appealing in the context of frustration-limited theories of supercooled liquids, providing first experimental evidence for a relationship between the existence of favored local structures in the (supercooled) liquid and the nature of the freezing transition in a quantum binary liquid mixture.

O1.3 ESR and optical spectroscopy studies of nitrogen atoms stabilized in nitrogen-helium condensates

D.M. Lee^a, S. Mao^a, R.E. Boltnev^b, and V.V. Khmelenko^a

^aDepartment of Physics and Astronomy, Texas A&M University, College Station, TX 77843 USA

^bBranch of Institute of Energy Problems of Chemical Physics RAS, Chernogolovka, Moscow region, 142432, Russia

Impurity-helium condensates (IHCs) containing nitrogen and krypton atoms immersed in superfluid ^4He have been studied via continuous wave electron spin resonance (ESR) and optical spectroscopy techniques. The IHCs are gel-like aggregates of nanoclusters composed of impurity species. It was found that the addition of krypton atoms to the nitrogen-helium gas mixture used for preparation of IHCs increases efficiency of stabilization of nitrogen atoms. We have achieved high average ($5 \cdot 10^{19} \text{ cm}^{-3}$) and local ($2 \cdot 10^{21} \text{ cm}^{-3}$) concentrations of nitrogen atoms in krypton-nitrogen-helium condensates. The analysis of ESR lines shows that three different sites exist for stabilization of nitrogen atoms in krypton-nitrogen nanoclusters. Nitrogen atoms are stabilized in the krypton core of nanoclusters, in the nitrogen molecular layer which covers the Kr core and on the surface of the nanoclusters. High concentrations of nitrogen atoms achieved in IHCs provide an important step in the search for magnetic ordering effects at low temperatures. The results of investigations of thermoluminescence dynamics during destruction of nitrogen-helium condensates containing stabilized nitrogen and oxygen atoms will be also discussed.

O2.1 Specific heat and superfluid density of ^4He near T_λ of a 33.6 nm film formed between Si wafers

J.K. Perron and F.M. Gasparini

The University at Buffalo The State University of New York, Buffalo, NY 14260

We report measurements of superfluid density and specific heat of a 33.6 nm film near the superfluid transition. The film is formed between two patterned and directly bonded silicon wafers. These measurements were undertaken with the primary purpose of understanding coupling and proximity effects in a situation when the film was in contact with helium in a larger confinement¹. However, these data are also relevant to issues of correlation-length finite-size scaling. This is the thinnest hard-wall confined film for which such scaling has been tested for the specific heat and superfluid density. One expects that at some small thickness such scaling should fail. We compare our results with previous data of helium in a similar confinement but at larger thickness. We find good agreement with scaling in regions where previous data scaled, and confirm the lack of scaling where previously reported. In our analysis we consider a native oxide growth between the etching and bonding steps of cell fabrication and its effect on our scaling analysis.

1. Perron, J. K. *et al.* (2010). "Coupling and proximity effects in the superfluid transition in ^4He dots". *Nat. Phys.* **6**:499-502.

02.2 Strong Suppression of the Kosterlitz-Thouless Transition in a ^4He Film under High Pressure

Y. Okuda

Department of Physics, Tokyo Institute of Technology, Tokyo 152-8551, Japan

We have found that the surface specularly for ^3He quasiparticle scattering is closely related to the superfluidity and the Kosterlitz-Thouless (KT) transition of ^4He film adsorbed on the surface. The specularly is determined by measurements of the transverse acoustic impedance of bulk liquid ^3He in the normal Fermi liquid region as a function of ^4He thickness. The unique point of our system is that we can control the correlation strength among ^4He atoms in the film by changing the pressure of the bulk ^3He . The observed KT transition temperature (T_{KT}) is significantly suppressed by increasing the pressure, which suggests a strong correlation effect on KT transition. As pressure increased, T_{KT} decreased linearly. Especially at the 3.6 layer of ^4He , it extrapolates to zero at 2.75 MPa. This behavior implies that Quantum Critical Point (QCP) does exist at this pressure in this system. ¹

This work has been performed in cooperation with Satoshi Murakawa, Ryuji Nomura, Masahiro Wasai and Koki Akiyama.

1. S. Murakawa *et al.*, Phys. Rev. Lett. 108, 025302 (2012).

02.3 Effect of Rough Walls on Transport in Mesoscopic ^3He Films

P. Sharma^a, A. Corcoles^b, R.G. Bennett^c, J.M. Parpia^c, B. Cowan^a, A. Casey^a, and J. Saunders^a

^aDepartment of Physics, Royal Holloway University of London, Egham, TW20 0EX, Surrey, UK

^bPresent address, IBM Watson Research Center, Yorktown Heights, NY 10598, USA

^cDepartment of Physics, Cornell University, Ithaca, NY 14853, USA

The interplay of bulk and boundary scattering is explored in a regime where quantum size effects modify mesoscopic transport in a degenerate Fermi liquid film of ^3He on a rough surface. We discuss mass transport and the momentum relaxation time of the film in a torsional oscillator geometry within the framework of a quasiclassical theory that includes the experimentally determined power spectrum of the rough surface. The theory explains the anomalous temperature dependence of the relaxation rate observed experimentally. We model further studies on ^3He confined in nanofluidic sample chambers with lithographically defined surface roughness. The improved understanding of surface roughness scattering can be extended to the analogous system of electrons in metals and suggests routes to improve the conductivity of thin metallic films.

O2.4 Superfluid ^3He confined in nanofluidic cells

A.J Casey^a, L.V. Levitin^a, B. Cowan^a, J. Saunders^a, and J. Parpia^b

^aDepartment of Physics, Royal Holloway, University of London, Egham, Surrey, TW20 0EX, UK

^bDepartment of Physics, Cornell University, Ithaca NY 14853, USA

The superfluid phases, which emerge from the quantum liquid of ^3He atoms close to the absolute zero of temperature, have a rich variety of broken symmetries and non-trivial momentum-space topologies. They exhibit macroscopic quantum phenomena and provide model systems for unconventional superconductivity. Quasiclassical theory provides a framework for detailed predictions of the influence of surfaces on the order parameter and surface/edge excitations.

In this work we have studied such surface effects experimentally by confining superfluid ^3He in a nanofabricated slab-like cavities of thickness comparable to the superfluid pair diameter. We present detailed measurements of the superfluidity of ^3He confined to a 0.7 micron thick slab and preliminary studies of a 100 nm slab. The confinement on a scale comparable to the coherence length of the superfluidity results in a suppression of the order parameter and an alteration of the relative stability of different phases. We observe the confinement to have a profound effect on the phase diagram. NMR is used both to identify the phases and make quantitative measurements of the suppression of the order parameter. The boundary conditions are tuned by preplating the surfaces with ^4He . Measurements with different boundaries show quantitative differences. Our results demonstrate how a spin-triplet p-wave order parameter responds to mesoscopic confinement. Controlled confinement of nanofluidic samples provides a new laboratory in which to search for new classes of order parameter and exotic excitations.

O3.1 Two-dimensional Fermi gases

Michael Köhl

Cavendish Laboratory, University of Cambridge, JJ Thomson Avenue, Cambridge CB3 0HE, United Kingdom

Pairing of fermions is ubiquitous in nature and it is responsible for a large variety of fascinating phenomena like superconductivity, superfluidity of ^3He , the anomalous rotation of neutron stars, and the BEC-BCS crossover in strongly interacting Fermi gases. When confined to two dimensions, interacting many-body systems bear even more subtle effects, many of which lack understanding at a fundamental level. Most striking is the, yet unexplained, effect of high-temperature superconductivity in cuprates, which is intimately related to the two-dimensional geometry of the crystal structure. In particular, the questions how many-body pairing is established at high temperature and whether it precedes superconductivity are crucial to be answered. We report on investigations of trapped two-dimensional atomic Fermi gas in the regimes of strong and weak coupling using momentum-resolved photoemission spectroscopy¹⁻⁴ and collective mode spectroscopy⁵ and find evidence for pseudogap pairing² as well as novel Fermi polaron quasiparticles.³

1. B. Fröhlich et al., Phys. Rev. Lett. 106, 105301 (2011).
2. M. Feld et al., Nature 480, 75 (2011).
3. M. Koschorreck et al., Nature 485, 619 (2012).
4. B. Fröhlich et al., arXiv:1206:5380 (2012).
5. E. Vogt et al., Phys. Rev. Lett. 108, 070404 (2012).

O3.2 Two-dimensional quantum turbulence in dilute-gas Bose-Einstein condensates

Brian P. Anderson

College of Optical Sciences, University of Arizona, Tucson, AZ 85721, USA

Experimental and theoretical studies of dilute-gas Bose-Einstein condensates (BECs) are enabling new developments in the field of two-dimensional quantum turbulence (2DQT). For example, using highly oblate BECs, numerous experimental methods can be used to generate the disordered distributions of quantized vortices associated with 2DQT, and new vortex detection and manipulation techniques are also emerging. In conjunction with this experimental progress, analytical and numerical efforts are uncovering new aspects of the vortices involved in 2DQT, from their dynamics to their relationships with energy spectra. This talk will focus on the physics of quantized vortices in 2DQT, particularly with respect to the common goals of experimental, numerical, and analytical efforts with condensates. We will present an overview of our recent findings on these topics, highlighting experimental capabilities regarding 2DQT and vortex studies in BECs.

O3.3 Shock waves in strongly interacting Fermi gas from time-dependent density functional calculations

F. Ancilotto, L. Salasnich, and F. Toigo

Dipartimento di Fisica e Astronomia "Galileo Galilei" and CNISM
Università di Padova, Via Marzolo 8, 35131 Padova, Italy

Motivated by a recent experiment¹ we simulate the real-time dynamics of two colliding clouds of cold Fermi gas at unitarity conditions by using an extended Thomas-Fermi density functional². At variance with the current interpretation of the experiments, where the role of viscosity is emphasized, we find that a quantitative agreement with the experimental observation of the dynamics of the cloud collisions is obtained within our superfluid effective hydrodynamics approach, where density variations during the collision are controlled by a purely dispersive quantum gradient term. We also suggest different initial conditions where dispersive density ripples can be detected with the available experimental spatial resolution.

1. J. Joseph, J. Thomas, M. Kulkarni and A. Abanov, Phys. Rev. Lett. **106**, 150401 (2011).
2. F. Ancilotto, L. Salasnich and F. Toigo, submitted to Phys. Rev. Lett.

O4.1 Dynamics of a Superfluid Vortex

P.C.E. Stamp^a, L. Thompson^b, and T. Cox^c

^aPacific Institute of Theoretical Physics, University of British Columbia, 6224 Agricultural Rd., Vancouver, BC., Canada V6T 1Z1 ^bDepartment of Physics, Massachusetts Institute of Technology, Cambridge, Massachusetts 02139, USA

^cDepartment of Physics & Astronomy, University of British Columbia, Vancouver, BC V6T 1Z1, Canada

Recently we succeeded in finding the equation of motion for a superfluid Bose vortex at low T, thereby resolving a rather old controversy.¹ The results revealed a new 'quantum regime' in the vortex dynamics, in which retardation effects are important. Here we describe how these results may be tested in low-T experiments on turbulence in He-4, and on single vortex dynamics in 'pancake' atomic BEC systems. The effects of retardation show up in the long-time dynamics. We also show the usefulness of a 'gravitational analogy' to the problem of a cosmic string interacting with spacetime fluctuations.

1. L. Thompson, P. C. E. Stamp. "Quantum Dynamics of a Bose Superfluid Vortex". Phys. Rev. Lett. **108**, 184501 (2012)

O4.2 Dissipative vortex motion in Fermi superfluids at ultra low temperatures

M.A. Silaev

Institute for Physics of Microstructures Russian Academy of Sciences, Nizhny Novgorod, Russia
Department of Theoretical Physics, The Royal Institute of Technology, Stockholm, Sweden
Low Temperature Laboratory, Aalto University, Espoo, Finland

We discuss in detail the recently proposed mechanism of dissipation and damping of the vortex motion in Fermi superfluids at temperatures much smaller than the critical one.¹ In the absence of the heat bath of normal component the kinetic energy of the superflow is transferred to the vortex core fermions due to the accelerated vortex motion. The resulting local heating of the vortex cores creates the heat flux carried by non-equilibrium quasiparticles emitted by moving vortices. Here we study this peculiar kinetics of localized quasiparticles beyond relaxation time approximation, calculate the decrement of Kelvin waves and the total power losses in Kelvin wave cascade realized by the turbulent motion of ³He-B.

1. Silaev, M.A. "Universal mechanism of dissipation in Fermi superfluids at ultralow temperatures" Phys. Rev. Lett. **108**, 045303 (2012).

O4.3 Experimental determination of the mass of a vortex in a superconducting film

D. Golubchik^a, G. Koren^b, and E. Polturak^b

^aLawrence Berkeley National Laboratory, Berkeley, CA, US

^bDepartment of Physics, Technion, Haifa, Israel

We have combined high resolution magneto-optical imaging with an ultra-fast heating/cooling technique to measure the movement of individual vortices in a superconducting film. The motion took place while the film was heated close to T_c , where pinning and viscous forces are relatively small. Under these conditions, vortices move due to the magnetic repulsion between them. We found that a finite vortex mass has to be included in the analysis in order to account for the experimental results. The extent of the motion is consistent with a vortex mass being 3 orders of magnitude smaller than the mass of all the electrons in the core.

O4.4 Defect formation in superconducting rings: external fields and finite-size effects

David J. Weir^a, Roberto Monaco^b, and Ray J. Rivers^c

^aHelsinki Institute of Physics, University of Helsinki, Finland

^bIstituto di Cibernetica del CNR, Comprensorio Olivetti, Italy

^cTheoretical Physics Group, Blackett Laboratory, Imperial College London, UK

Consistent with the predictions of Kibble and Zurek, scaling behaviour has been seen in the production of fluxoids during temperature quenches of superconducting rings. However, both experimental and theoretical understanding of deviations from the canonical behaviour has since improved. Technical developments, including laser heating and the use of long Josephson tunnel junctions, have improved the quality of data that can be obtained.

Approaching the topic from a theoretical point of view, we shall interpret recent results for defect formation in Niobium rings. We make use of large-scale 3D simulations of quenches of small, thin superconducting rings of various geometries, at nonzero external field. Informed by both simulation and experiment, we comment on analytical approximations that can yield the correct physics for both causality-limited and size-limited regimes for arbitrary external magnetic field and trapping probability.

4.2 Poster Presentations: Thursday August 16th

P1.1 Silicon nitride mechanical nano-resonators

M. Defoort, K. Lulla, C. Blanc, O. Bourgeois, Yu.M. Bunkov, H. Godfrin, and E. Collin

Institut Néel - CNRS Grenoble, France

We report on experiments performed in vacuum at low temperatures on nanomechanical silicon nitride doubly-clamped resonators. Different samples have been studied, with different in-built stresses ranging from low-stress (about 100 MPa) to high-stress (about 1 GPa). The mechanical properties (frequency, Q-factor, non-linear behavior) have been characterized as a function of this intrinsic axial load.

P1.2 Ultra-low temperature sample environment for neutron scattering experiments

O. Kirichek, R.B.E. Down, J. Keeping, L.V. Linfitt, and Z.A. Bowden

ISIS, STFC Rutherford Appleton Laboratory, Harwell Science and Innovation Campus, Didcot, UK

Today almost a quarter of all neutron scattering experiments performed at neutron scattering facilities require sample temperatures below 1K [1]. However, a global shortage of helium gas can seriously jeopardies low temperature experimental programmes of neutron scattering laboratories. Luckily the progress in cryo-cooler technology offers a new generation of cryogenic systems with significantly reduced consumption and in some cases nearly complete elimination of cryogens. Here we discuss new cryogen free dilution refrigerators developed by ISIS facility in collaboration with Oxford Instruments such as the powerful cryogen free dilution refrigerator designed for big and heavy sample cells. We also discuss new approach which makes standard dilution refrigerator inserts cryogen-free if they are used with cryogen-free cryostats such as 1.5K top-loader or re-condensing cryostat with a variable temperature insert. First scientific results obtained from the neutron scattering experiments with these refrigerators are also going to be discussed.

1. O. Kirichek, *Modern Phys. Lett. B* **26** 1230006 (2012).

P1.3 Characterisation of microcoils as local probes for helium NMR

A. Shibahara^a, A. Casey^a, C. Lusher^a, D. Drung^b, Th. Schurig^b, and C. Assmann^b

^aDepartment of Physics, Royal Holloway University of London, Egham, UK

^bPhysikalisch Technische Bundesanstalt, Abbestrasse 2-12, Berlin, Germany

Previous NMR studies of superfluid helium in a slab geometry have been carried out with the pickup coil encompassing the entire helium cell. However, as features such as domain boundaries could be present, it would be of interest to develop a local probe with an increased spatial resolution to detect spins from various positions within the nanofluidic cell. The first generation of microcoils with a multiturn square loop size of $400\ \mu\text{m} \times 400\ \mu\text{m}$ have been fabricated by PTB Berlin using UV lithography. The calculated inductance is 105 nH. For readout, these microcoils are coupled to a low noise DC SQUID with input inductance 29 nH in a tuned input configuration. Calculations for the sensitivity of the microcoils are presented. For characterisation purposes, NMR signals from helium-3 gas at 1 bar, 4.2 K, were successfully measured with a resonance frequency of 930 kHz with the expected SNR. In this experiment, the helium gas was in direct contact with the microcoil. However, for the superfluid experiment, although the spin density is much greater, the microcoils must be able to sense spins through a cell wall. Silicon cavities with walls thinned down to $100\ \mu\text{m}$ are being developed for this purpose.

P1.4 A practical DC SQUID current sensing noise thermometer for low temperature measurements

A. Casey, L. Levitin, C. Lusher, and A. Shibahara

Department of Physics, Royal Holloway, University of London, Egham, Surrey, TW20 0EX, UK

Thermometry below 4K over the operating temperature range of a dilution refrigerator, or in particular a nuclear demagnetisation cryostat, normally requires the use of several thermometers operating on different principles. We have developed dc SQUID-based noise thermometers which cover the temperature range from 4 K to below 1 mK. These thermometers measure a current produced by the thermal Johnson noise in a resistive element. Improvements in SQUID performance have lead to the ability to produce a higher bandwidth device that is fast and relatively easy to use. The performance of this thermometer on both a nuclear demagnetisation cryostat and an Oxford Instruments cryogen-free dilution refrigerator are reported.

P1.5 Numerical study on decay of the vortex tangle at zero temperature.

Luiza P. Kondaurova and Sergey K. Nemirovskii

Institute of Thermophysics SB RUS, Novosibirsk, Russia

We submit the results of the numerical study on the decay of the quantum turbulence in the absence of the normal component of superfluid helium. Computations were fulfilled inside of the fixed domain with the use of the vortex filament method. The purpose of this study was to ascertain the role of various factors arising in the numerical procedure such as change in length in the reconnection processes, procedures regulating the amount of points, the eliminations of very small loops below the space resolution, evaporation of the loops from the volume, and the effect of boundary conditions. We would like to stress that the widely accepted mechanism - the cascade-like transferring of the energy by nonlinear Kelvin waves (and radiation of sound) - was not considered. One of the reasons is that space resolution along the lines did not allow to detect generation of high harmonics, moreover, to get harmonics, which really radiate sound. In addition, the use of the method assumes that the fluid is incompressible. Simulations have been performed for the cubic domain with transparent walls embedded in an unbounded space, and for the cube with the solid smooth walls. The calculations showed that in the case of unlimited space of the decay of quantum turbulence caused by the evaporation of vortex loops, which is realized in the diffusion-like manner. The rate of the attenuation of the vortex line density agrees with the one, predicted by the diffusion theory of the nonuniform vortex tangle. In the case of the cube with the solid walls the main decay is also due to the diffusion of vortex loops to the boundaries. The vortex loops, whose ends are sliding on a smooth wall, execute the sophisticated motion with many subsequent reconnections and fragmentations. As a result there appear smaller loops with a size of few spatial resolution. Indirect comparison with the experiments shows that the time of decay agrees with the measured data.

P1.6 Diffusion and Thermal Diffusion Influence on Temperature Relaxation in Superfluid ^3He - ^4He Mixtures

K. Nemchenko and S. Rogova

Energy Physics Department, Karazin Kharkiv National University, Kharkiv, Ukraine

Formation of a stationary state in quantum superfluid ^3He - ^4He mixtures is described in this paper. The problem is considered on a segment with the heat flow switched at the left end and with the constant temperature at the right end. Second sound mode contribution and dissipative mode contribution is studied. The problem is solved at arbitrary temperatures and concentrations of ^3He and this needs the accounting of diffusion and thermal diffusion processes in superfluid ^3He - ^4He mixtures.

P1.7 Nonlinear field-dependence and f -wave interactions in superfluid ^3He

C.A. Collett, J. Pollanen, J.I.A. Li, W.J. Gannon, and W.P. Halperin

Department of Physics and Astronomy, Northwestern University, Evanston, IL 60208, USA.

We present the results of transverse acoustics studies in superfluid ^3He - B at fields up to 0.11 T. Using acoustic cavity interferometry, we observe the acoustic Faraday effect for a transverse sound wave propagating along the magnetic field, and we measure Faraday rotations of the polarization up to 1710° . We use these results to calculate the splitting of the imaginary squashing mode, an order parameter collective mode with total angular momentum $J = 2$, and report nonlinear field splitting at frequencies above the mode frequency. We find that the theory for the field dependence of the acoustic dispersion relation must be extended to order higher than linear, and that theories for the Landé g -factor and the f -wave interaction strength, x_3^{-1} , cannot be simply extended to frequencies above the mode frequency. Nonetheless, with our present data we can make an accurate extrapolation to low magnetic field and compare with previous work, and we show that the pairing interaction in the f -wave channel is attractive at a pressure of $P = 6$ bar.

P1.8 Cooling by Heating a Superfluid

D. J. Papoular, G. Ferrari, L.P. Pitaevskii, and S. Stringari

INO-CNR BEC Center and Dipartimento di Fisica, Universita di Trento, Povo, Italy

We consider a uniform superfluid confined in two compartments connected by a superleak and initially held at equal temperatures. If one of the two compartments is heated, a fraction of the superfluid will flow through the superleak. We show that, under certain thermodynamic conditions, the atoms flow from the hotter to the colder compartment, contrary to what happens in the fountain effect observed in superfluid Helium. This flow causes quantum degeneracy to increase in the colder compartment. In superfluid Helium, this novel thermomechanical effect takes place in the phonon regime of very low temperatures. In dilute quantum gases, it occurs at all temperatures below T_c . The increase in quantum degeneracy reachable through the adiabatic displacement of the wall separating the two compartments will also be discussed.

1. Papoular, D.J., Ferrari, G., Pitaevskii, L.P., and Stringari, S. (2012). "Increasing Quantum Degeneracy by Heating a Superfluid". In preparation.

P1.9 Quantum Monte Carlo simulation of spin-polarized deuterium

I. Bešlić^a, L. Vranješ Markić^b, J. Casulleras^a, and J. Boronat^a

^aDepartament de Física i Enginyeria Nuclear, Campus Nord B4-B5, Universitat Politècnica de Catalunya, E-08034 Barcelona, Spain

^bFaculty of Science, University of Split, HR-21000 Split, Croatia

The ground-state properties of spin-polarized deuterium ($D\downarrow$) at zero temperature are obtained by means of the diffusion Monte Carlo calculations within the fixed-node approximation. Three $D\downarrow$ species have been investigated ($D\downarrow_1$, $D\downarrow_2$, $D\downarrow_3$), corresponding respectively to one, two and three equally occupied nuclear spin state. Influence of the backflow correlations on the ground-state energy of the systems under investigation is also explored. The calculations have been performed using several interatomic potentials and the quantum nature of the three $D\downarrow$ species is discussed. When the phase of the system is liquid, we have obtained the equilibrium density and we have compared it with previous approximate description.

P1.10 Energy spectrum of the 3D velocity field, induced by vortex tangle

Sergey K. Nemirovskii

Institute of Thermophysics, Novosibirsk, Russia

A review of various theoretical and numerical methods on the determination of the energy spectra $E(k)$ of 3D-velocity field, induced by chaotic vortex lines is proposed. This problem is closely related to the sacramental question whether a chaotic set of vortex filaments can mimic real hydrodynamic turbulence. The quantity $\langle \mathbf{v}(\mathbf{k})\mathbf{v}(-\mathbf{k}) \rangle$ can be exactly calculated, provided that we know the probability distribution functional $\mathcal{P}(\{\mathbf{s}(\xi, t)\})$ of vortex loops configurations. The knowledge of $\mathcal{P}(\{\mathbf{s}(\xi, t)\})$ is identical to the full solution of the problem of quantum turbulence and, in general, \mathcal{P} is unknown. In the talk I discuss the following issues: The first group of reviewed methods deals with the exactly solvable models. This case includes standard vortex configurations such as a straight line, vortex array and ring. Independent chaotic loops of various fractal dimension as well as interacting loops in the thermodynamic equilibrium also permit analytical solution. In spite of that these models are far from the real quantum turbulence, they provide valuable information, concerning relation between vortex lines configurations and 3D energy spectrum, which these lines generate. The second group is based on the so-called differential approximation. The basic idea of this method is the derivation of the differential equation describing the evolution of energy in k space. This approach is pure phenomenological, it is necessary to "guess" the proper form of this equation. The method is useful for involved situations e.g., in case of finite temperature. We also describe and comment on the method of an obtaining the 3D velocity $E(k)$ spectrum from the 1D Kelvin waves spectrum $E_{KW}(k)$ equating these two quantities. We are also review works on the determination of the energy spectra from direct numerical simulations. Both the works based on the vortex filament method and on the Gross-Pitaevskii equation are discussed and comparison between them is made.

P1.11 Superstatistical Approach to Quantum Fluid

S. Miah and C. Beck

School of Mathematical Science, Queen Mary, University of London, England

Recent studies on quantum turbulence have shown that the velocity statistics of a tracer particle obey power law statistics ^{1,2} rather than Gaussian statistics as observed in classical turbulence ^{3,4}. A superstatistical model ⁴ is constructed for a Lagrangian tracer particle in a quantum turbulent flow. The result is in excellent agreement with a recent experiment done by Paoletti *et al.*¹ to observe the motion of tracer particles in quantum turbulent flow of superfluid ⁴He.

1. M. Paoletti, M. Fisher, D. Lathrop, K.Sreenivasan, Phys. Rev.Lett. **101** 154501(2008).
2. A.C. White, C.F. barengi, N.P. Proukakis, A.J. Youd, and D.H. Wacks, Phy. Rev. Lett. **104**, 075301(2010)
3. A. Vincent and M. Meneguzzi, J. Fluid Mech. **225** 1 (1991).
4. A. Noullez, G. Wallace, W. Lempert, R.B. Miles and U. Frisch, J. Fluid Mech. **339** 287 (1997).
5. C.Beck, Phys. Rev.Lett. **98**, 064502(2007).

P1.12 Probing Chirality in Superfluid ³He-A

H. Ikegami and K. Kono

Advanced Science Institute, RIKEN, Wako, Saitama 351-0198, Japan

We report the first detection of chirality in superfluid ³He-A by observing a novel effect, intrinsic Magnus effect,^{1,2} experienced by a traveling impurity. An impurity traveling in a plane perpendicular to the l vector experiences the intrinsic Magnus force in the direction perpendicular to both its velocity and the l vector, as a result of the skew scattering of quasiparticles by the impurity. We investigated the intrinsic Magnus effect for charged impurities, electron bubbles, trapped below the free surface of superfluid ³He at a depth about 35 nm by transport of electron bubbles along the surface. In this configuration, the l vector aligns uniformly normal to the surface, and the electrons bubbles traveling along the surface would be subjected to the intrinsic Magnus force. We observed transverse current associated with the intrinsic Magnus effect. The transverse currents show two types of temperature dependences, which are equal in magnitude but opposite in sign, and these two correspond to the l vector pointing parallel ($+l$) and anti-parallel ($-l$) to the surface normal. After repeating many cooling runs from normal state, we find that the ratio between $+l$ and $-l$ emerging just below T_c is asymmetric about the direction of magnetic field.

1. R. H. Salmelin *et al.*, Phys. Rev. Lett. **63**, 868 (1989).
2. R. H. Salmelin and M. M. Salomaa, Phys. Rev. B **41**, 4142 (1990).

P1.13 Evidence of Knudsen-Hydrodynamic Crossover in Normal Fluid ^3He in 98% Aerogel

H. C. Choi^a, B. H. Moon^a, N. Masuhara^a, M. W. Meisel^a, Y. Lee^a, H. Takeuchi^b, S. Higashitani^b, K. Nagai^b, and N. Mulders^c

^aNHMFL and Department of Physics, University of Florida, Gainesville, Florida, USA

^bGraduate School of Integrated Arts and Sciences, Hiroshima University, Kagamiyama, Higashi-Hiroshima, Japan

^cDepartment of Physics and Astronomy, University of Delaware, Newark, Delaware, USA

Extensive ultrasound attenuation measurements were performed to understand the effect of the high porosity aerogel on the mass transport in liquid ^3He . Owing to the strong temperature dependence of the quasiparticle mean free path in the normal fluid and the unique geometrical structure of high porosity aerogel, this system is expected to exhibit complex flow phenomena. Evidence of the Knudsen-hydrodynamic crossover is clearly demonstrated by a drastic change in the temperature dependence of ultrasound attenuation in 98% porosity aerogel. Our theoretical analysis shows that the frictional sound damping caused by the drag force is governed by distinct laws in the two regimes, providing excellent agreement with the experimental observation.¹ This work provides an important contribution toward unified understanding of complex flow phenomena in porous media.

Supported by the Grant-in-Aids from MEXT, Japan through No. 21540365 and No. 22103003, and also by NSF under DMR-0803516 (YL) and DMR-0654118 (NHMFL), and the State of Florida.

1. H. Takeuchi *et al.*, Phys. Rev. Lett. **108**, 225307 (2012).

P1.14 Unusual Behavior of a MEMS Resonator in Superfluid ^4He

M. Gonzalez^a, P. Zheng^a, B. H. Moon^a, E. Garcell^a, Y. Lee^a, and H. B. Chan^b

^aDepartment of Physics, University of Florida, Gainesville, Florida, USA

^bDepartment of Physics, The Hong Kong University of Science and Technology, Clear Water Bay, Hong Kong

Novel mechanical resonators based on the micro-electro-mechanical systems (MEMS) technology were developed for the study of superfluid ^4He . The MEMS device is composed of two parallel plates, one movable plate suspended by four serpentine springs and the substrate, forming a shear mechanical oscillator.¹ A specific device with a $1.25\ \mu\text{m}$ gap was tested in the superfluid phase of ^4He . The device exhibits an extreme sensitivity to the excitation level below 400 mK *i.e.*, extreme nonlinearity and hysteretic behavior. The anomalies are reminiscent of quantum turbulence and vorticity effects observed in other mechanical oscillators such as tuning forks or vibrating grids. Details on the fabrication and operation of the device are also presented.

This work is supported by NSF (YL) under DMR-0803516 and DMR-1205891.

1. M. Gonzalez, P. Bhupathi, B.H. Moon, P. Zheng, G. Ling, E. Garcell, H.B. Chan, and Y. Lee, J. Low Temp. Phys. **162**, 662 (2011).

P1.15 Spin–density fluctuations in liquid ^3He

T. Lichtenegger^a and E. Krotscheck^{a,b}

^aJohannes Kepler University, Linz, Austria

^bUniversity at Buffalo–SUNY, Buffalo, New York, USA

Progress on the microscopic understanding of density fluctuations in liquid ^3He at $T = 0\text{K}$ has been made recently, employing a variational approach in terms of single– and double–pair fluctuations from the correlated ground state to find the dynamic structure function of the system.¹ We extend here the same manifestly microscopic techniques to the description of spin–density waves in 3D liquid ^3He and find good agreement with experiments.² Our calculations show that this excitation branch is a macroscopic manifestation of exchange effects. The inclusion of pair fluctuations, *i.e.* intermediate states that can not be described by the quantum numbers of a single particle, is essential for a quantitative description of the physics. These lead to both an energy dependent renormalization of the exchange interaction, and to self-energy corrections to the single-particle spectrum.

1. Böhm *et al.* (2010). “Dynamic many-body theory: Dynamics of strongly correlated Fermi fluids”. *Phys. Rev. B* 82, 224505

2. Fåk *et al.* (1998). “Temperature dependence of spin–density fluctuations in liquid ^3He ”. *J. Low Temp. Phys.* 110, 417–424

P1.16 Multi-pair and exchange effects in the dynamic structure of 2D- ^3He

R. Holler^a, E. Krotscheck^{a,b}, R. Hobbiger^a, and M. Panholzer^a

^aInstitute for Theoretical Physics, JKU Linz, Austria

^bDepartment of Physics, University at Buffalo, SUNY Buffalo NY 14260

We examine the effect of fermionic exchange interactions on the dynamic structure function of two-dimensional ^3He within a manifestly microscopic theory of excitations. Exchanges have various consequences at different wave lengths and densities, ranging from change of Landau-damping at low densities over significant change of the effective mass at large wave numbers to being of little relevance for intermediate wave numbers.

Another very important aspect included in our calculations are pair fluctuations – excitations that can not be described by the quantum numbers of a single particle. While not changing the features of long wave length excitations, they induce a finite width to the collective mode outside the particle-hole continuum. In the intermediate momentum regime, where one would expect a “roton minimum” in a Bose fluid with the same interaction and density, pair fluctuations cause a visible shift of the strength of the dynamic structure function towards lower energies and cause a very sharp collective mode. This effect is slightly enhanced by inclusion of exchange corrections and was reported by Godfrin *et al.*¹

1. H. Godfrin, M. Meschke, H.-J. Lauter, A. Sultan, H. M. Böhm, E. Krotscheck & M. Panholzer: *Observation of a roton collective mode in a two-dimensional Fermi liquid*, *Nature* **483**, 576 (2012).

P1.17 Heat Capacity and Vapor Pressure Measurements of 2D ^4He on ZYX Graphite

S. Nakamura, K. Matsui, T. Matsui, and Hiroshi Fukuyama

Department of Physics, Graduate School of Science, The University of Tokyo, Japan

The heat capacity and the vapor pressure of the first and second layers of ^4He on ZYX graphite were measured with high precisions. Crystallinity of ZYX is much better than Grafoil, the most commonly-used exfoliated graphite substrate. This allows us to distinguish different phases in 2D ^4He much more clearly and may provide us qualitatively different insights into this 2D Bosonic system. First, we measured the heat capacity at densities around the $\sqrt{3} \times \sqrt{3}$ phase ($\rho_{c1} = 6.37 \text{ nm}^{-2}$) in the 1st layer. We found a significant asymmetric density dependence of the peak amplitude of heat capacity, *i.e.*, a precipitous decrease by half within 0.05 nm^{-2} above ρ_{c1} and only 5% reduction at densities in 0.12 nm^{-2} below ρ_{c1} . By contrast, in previous experiments with Grafoil, the asymmetry was much weaker and stretched for 0.5 nm^{-2} . Second, we measured the vapor pressure at densities around that for the 2nd layer promotion ($\rho_{1 \rightarrow 2}$). We could determine $\rho_{1 \rightarrow 2} = 11.5 \pm 0.2 \text{ nm}^{-2}$ from a stepwise decrease in the density dependence of the calculated isosteric heat. The value is consistent with our own heat capacity isotherms in the second layer, but not with previous determination (12.0 nm^{-2}) with Grafoil. Third, we studied the heat capacity of the second layer in a density region where the gas-liquid transition is insisted to occur. We found a highly pronounced peak at $T = 0.75 \text{ K}$ at densities below 16.5 nm^{-2} , confirming the gas-liquid transition, as well as a much broader anomaly around $T = 0.9 \text{ K}$ at densities from 16.5 to 18.7 nm^{-2} . Those two anomalies are clearly distinguished each other, while they were not with Grafoil substrate. The latter anomaly seems to be accompanied with the Kosterlitz-Thouless (KT) transition into the superfluid phase in 2D ^4He , the measured density evolution does not follow the simple KT theory.

P1.18 Excitation spectrum and Spin Current on the surface of $^3\text{He-B}$

Hao Wu and J. A. Sauls

Department of Physics, Northwestern University, Evanston, Illinois, 60208, USA

The surface excitation spectrum and spin current of $^3\text{He-B}$ with specular reflection is discussed. We report calculations of surface the Andreev bound state and continuum spectrum, and present the results for spin current density on the surface of $^3\text{He-B}$. Surface states with momentum \vec{p}_{\parallel} are spin polarized transverse to \vec{p}_{\parallel} . A non-vanishing ground-state spin current is confined on the surface within a few coherence lengths. The temperature dependence of the spin current originates from the Majorana branches of excitations, and exhibits power law behavior for $T \ll T_c$ in the fully gapped B-phase.

P1.19 Shell model of superfluid turbulence

D.H. Wacks and C.F. Barenghi

Joint Quantum Centre Durham-Newcastle, School of Mathematics and Statistics, Newcastle University, Newcastle upon Tyne NE1 7RU, United Kingdom

Superfluid helium consists of two inter-penetrating fluids, a viscous normal fluid and an inviscid superfluid, coupled by a mutual friction. We develop a two-fluid shell model to study superfluid turbulence. We investigate the energy spectra and the balance of fluxes between the two fluids as a function of temperature in continuously forced turbulence, and, in the absence of forcing, the decay of turbulence. We furthermore investigate deviations from the $k^{-5/3}$ spectrum caused by the mutual friction force. We compare our results with experiments and existing calculations. We find that, at sufficiently low temperatures a build-up of energy develops at high wavenumbers suggesting the need for a further dissipative effect, such as the Kelvin wave cascade and phonon emission [1].

1. Wacks, D.H., and Barenghi, C.F. (2011) “Shell model of superfluid turbulence”, Phys. Rev. B 84, 184505.

P1.20 Simulations of non-linear spin dynamics in spin polarized dilute ^3He - ^4He mixtures

Dean L. Hawthorne^a, Scott Wilde^b, and D.M. Lee^{b,c}

^aLaboratory of Ornithology, Cornell University, Ithaca, NY 14850, USA

^bDepartment of Physics & Astronomy, Texas A&M University, 4242 TAMU, College Station, TX 77843, USA

^cLaboratory of Atomic & Solid State Physics, Clark Hall, Cornell University, Ithaca NY 14853, USA

Studies of spin dynamics of highly polarized dilute mixtures of ^3He in superfluid ^4He have been performed by various researchers over the past three decades. One series of experiments performed at Cornell University in the early 1990's revealed a novel long timescale excitation.¹ We present the numerical solution of the non-linear Leggett spin dynamics equation in one spatial dimension subject to boundary conditions consistent with the Cornell experiments. Experimentally observed phenomena are composed of a train of bursts in the transverse magnetization lasting several seconds. The simulations capture the time evolution of the individual bursts localized in time. Preliminary results of two dimensional simulations are also presented.

1. Nunes, G. Jr., Jin, C., Hawthorne, D. L., Putnam, A. M., Lee, D. M. (1992). “Spin-polarized ^3He - ^4He solutions: Longitudinal spin diffusion and nonlinear spin dynamics”. Phys. Rev. B. **46**, 9082

P1.21 **Transition to turbulence regime in ^3He - ^4He solutions: ^3He condensation on quantized vortices**

G. Sheshin, I. Gritsenko, V. Chagovets, A. Zadorozhko, and E. Rudavskii

B.Verkin Institute for Low Temperature Physics and Engineering, Kharkov, Ukraine

By the method of oscillating tuning fork we carried out researches of passing to the turbulent mode of flow in He II and superfluid solution of ^3He in ^4He at the temperatures range from 100 mK to 2.2 K. By the kink on the volt - ampere characteristics, the critical velocity of the turbulence appearance was determined. It is established that the critical velocity temperature dependence is differs strongly from that in pure ^4He and is non-monotonous. Unlike ^4He , the step-by-step anomalies on resonance curves we observed which is, presumably, is stimulated by instability of the vortex system under the conditions where the core of the vortex is filled by the atoms of ^3He . It was shown that such anomalies appear at the temperature lower ~ 0.8 K, at the same time at more low temperature (lower than 0.5 K) they appear only at the velocity grate then critical velocity of appearing turbulence in pure ^4He ¹.

1. G.A. Sheshin, A.A. Zadorozhko, E.Y. Rudavskii, V.K. Chagovets, L. Skrbek and M. Blazhkova, Low Temp. Phys 34, 875 (2008);

P1.22 **Frequency characteristics of a quartz tuning fork immersed in He II**

I. Gritsenko, A. Zadorozhko, and G. Sheshin

B.Verkin Institute for Low Temperature Physics and Engineering, Kharkov, Ukraine

The effect of dissipation on frequency characteristics of tuning forks was measured, the dissipation being induced by acoustic radiation of different wavelengths, excited by tuning forks. The tuning forks immersed in superfluid helium had 32, 77 and 90 kHz resonance frequencies. The fork resonance frequencies f was measured at $T=370\text{mK}$ in the pressure range between SVP and 24.9 atm. Most of the tuning forks studied was in a commercial can. It is found that $\lambda > 0.6$ cm the frequency dependence is determined by the relationship between density and pressure. It is established that a decrease in wavelength gives rise to the effect of acoustic radiation on fork oscillation frequency. In the case where the sound wavelength is equal to the can internal diameter there occurs an acoustic resonance at witch the turbulence of acoustic dissipation on oscillation frequency is maximum. On further reduction of λ , the frequency varies in a jump and reaches values higher than the fork frequency in vacuum.

P1.23 Crosstalk between quartz tuning forks in He II

D. Schmoranzer, M. La Mantia, and L. Skrbek

Faculty of Mathematics and Physics, Charles University in Prague, Czech Republic

We present a set of our experimental results on crosstalk of non-electrical origin between two or more quartz tuning forks immersed in the same volume of helium gas, liquid or superfluid. Our aim is to compare these results with various observations of other groups and to propose an explanation of this puzzling phenomenon. To the best of our knowledge, notable crosstalk has so far only been observed in superfluid helium (both in the two-fluid regime and at very low temperatures), which our results confirm. Although crosstalk between tuning forks has rarely been seen to behave in a strictly systematic manner, we demonstrate some of its most significant properties – amplitude dependence within a short time span, long-term temporal instability, effects of the geometry of the setup and of obstacles placed between the tuning forks. As the most likely explanation, we ascribe the observations to acoustic emission [1,2] and to the coupling of both interacting tuning forks to standing acoustic modes inside the experimental volume [3], emphasizing the necessity of dispersive and non-linear phenomena in sound propagation, and especially the importance of second sound for understanding the observations at temperatures within the two-fluid regime ($1\text{ K} < T < 2.17\text{ K}$). Finally, we suggest simple precautions leading to suppression of excessive acoustic crosstalk between oscillating objects in He II.

[1] D. Schmoranzer et al., *J. Low Temp. Phys.* **163**, 317 (2011)

[2] D.I. Bradley et al., *Phys. Rev. B* **85**, 014501 (2012)

[3] D. Garg et al., *Phys. Rev. B* **85**, 144518 (2012)

P1.24 Hydrodynamic Properties of a Low Frequency Resonator in Normal and Superfluid ^4He

A. Woods, S.L. Ahlstrom, D.I. Bradley, M. Človečko, S.N. Fisher, D. Garg, A.M. Guénault, E. Guise, R.P. Haley, G.R. Pickett, M. Poole, R. Schanen, and V. Tsepelin

Department of Physics, Lancaster University, UK

Mechanical resonators such as vibrating wires and tuning forks are widely used for the study of quantum fluids. In this study we focus on the properties of a low frequency (approximately 50 Hz) goal-post shaped vibrating wire. The wire was mounted in a cell containing two pressure sensors and an array of quartz tuning forks with a range of resonant frequencies between 6 kHz and 160 kHz.

We present measurements of the force-velocity response for the wire and tuning forks over a wide range of velocities spanning the transition from laminar to turbulent flow. We compare the behaviour of classical turbulence, measured in normal fluid above 2.2 K, and quantum turbulence over a wide range of temperatures down to below 3 mK.

We have also investigated the frequency dependence of the turbulent drag by measuring the wire response over a range of frequencies using a technique based on measuring the wire position with nearby pick-up coils.

P1.25 Electron photo-ejection from bubble states in liquid ^4He

J. Barragán^a, D. Mateo^a, M. Pi^a, F. Salvat^a, M. Barranco^a, and H.J. Maris^b

^a Departament ECM, Facultat de Física, and IN²UB, Universitat de Barcelona. Diagonal 645, 08028 Barcelona, Spain

^bDepartment of Physics, Brown University, Providence, Rhode Island 02912, USA

Within finite-range density-functional theory, we have addressed the photo-ejection of electrons hosted in ^4He bubbles as a function of pressure at zero temperature. It is shown that, contrarily to the $1s \rightarrow 1p$ and $1s \rightarrow 2p$ transitions that show up in the whole pressure range up to solidification, there is a transition to a loosely bound $3p$ state that disappears at $p \sim 1.7$ bar. Realistic predictions for the photo-ejection cross section are made using a model¹ that has been proved to accurately reproduce the experimental infrared absorption transitions as a function of pressure.^{2,3}

1. Grau V., Barranco M., Mayol R., and Pi M., Phys. Rev. B **73**, 064502 (2006).
2. Grimes C. C. and Adams G. A., Phys. Rev. B **41**, 6366 (1990).
3. Grimes C. C. and Adams G. A., Phys. Rev. B **45**, 2305 (1992).

P1.26 Bose-Einstein condensation of magnons in rotation-controlled traps in superfluid $^3\text{He-B}$

P.J. Heikkinen^a, S. Autti^a, Yu.M. Bunkov^b, V.B. Eltsov^a, J.J. Hosio^a, M. Krusius^a, G.E. Volovik^{a,c}, and V. Zavjalov^a

^aO. V. Lounasmaa Laboratory, Aalto University, P.O. Box 15100, 00076 AALTO, Finland

^bInstitute Néel, CNRS, Grenoble, France

^cLandau Institute for Theoretical Physics, Kosygina 2, 119334 Moscow, Russia

In superfluid ^3He non-thermal (pumped) magnons spontaneously form a Bose-Einstein condensate as the magnetization starts to precess with common frequency and coherent phase in a large sample volume in an external field. In our experiments at pressure 0.5 bar and at temperatures down to $0.14 T_c$ a 3-dimensional potential trap for magnons is formed in the axially symmetric order-parameter texture of $^3\text{He-B}$ with additional minimum in the polarizing magnetic field. Trap shape can be controlled by adjusting the strength of the minimizing field or by rotating the sample both in vortex-free and vortex states. Using continuous wave NMR techniques we can simultaneously populate the selected excited level and the ground state of the trap with magnons leading to coexistence of two condensates [1]. They both exhibit a long lifetime after switching off the pumping. Relaxation process is not generally exponential but depends on the trap profile, which changes with increasing number of magnons in the trap from approximately harmonic to a box-like. The relaxation rate is proportional to the density of thermal quasiparticles, which is expected for the relaxation via spin diffusion. A close proximity of the free surface of $^3\text{He-B}$ to the condensate causes additional relaxation through coupling to mechanical oscillations of the surface.

1. S. Autti *et. al.*, Phys. Rev. Lett. **108**, 145303 (2012).

P1.27 **Unexpected Density Dependence of Mobility of Electron Bubbles Trapped below the Free Surface of Normal ^3He**

H. Ikegami, T. Matsumoto, and K. Kono

Advanced Science Institute, RIKEN, Wako, Saitama 351-0198, Japan

We have performed mobility measurements of electron bubbles trapped below the free surface of normal ^3He at temperatures between 5 and 100 mK. We find that the mobility increases with increasing temperature, and that the increase at high temperatures is more significant for higher densities of electron bubbles. The observed mobility has no dependence on depth of the electron bubbles, indicating that the surface excitations have no contributions to the mobility. The observed increase of mobility as a function of density suggests that the Coulomb interaction between electron bubbles plays an important role for the momentum transfer from the electron bubble to ^3He quasiparticles.

P1.28 **Fluctuations of the vortex line density in turbulent flows of quantum fluids**

Sergey K. Nemirovskii

Institute of Thermophysics, Novosibirsk, Russia

We present the study of fluctuations of the Vortex Line Density (VLD) $\langle \delta\mathcal{L}(\omega) \delta\mathcal{L}(-\omega) \rangle$ in turbulent flows of quantum fluids. Two cases have been considered. The first one is the counterflowing (Vinen) turbulence, where vortex lines are disordered, and quantity $\mathcal{L}(t)$ is governed by the Vinen equation. The second case is the quasi-classic turbulence, where vortex lines are believed to form so called vortex bundles, and the dynamics of VLD obeys the HVBK equations. The latter case, is of a special interest, since the series of recent experiments demonstrates the $\omega^{-5/3}$ dependence for spectrum VLD, instead of $\omega^{1/3}$ law, typical for spectrum of vorticity. The main position of our work is that relations $\mathcal{L} = \gamma^2 v_{ns}^2$ for Vinen case and $\mathcal{L} = |\nabla \times \mathbf{v}_s| / \kappa$ for quasi-classic turbulence are valid only for steady situation (rotation). For any nonstationary situation, in particular in fluctuating turbulent flow there is retardation between instantaneous value of the local relative velocity and quantity $\kappa\mathcal{L}$. This retardation tends to diminish, in accordance with some inner dynamics, which has the relaxation character. In both cases the relaxation dynamics of VLD is related to fluctuations of the relative velocity, however if for the Vinen disordered turbulence rate of temporal change for $\mathcal{L}(t)$ is directly depends on $\delta\mathbf{v}_{ns}$, for the HVBK dynamics it depends on $\nabla \times \delta\mathbf{v}_{ns}$. As a result for the disordered case the spectrum $\langle \delta\mathcal{L}(\omega) \delta\mathcal{L}(-\omega) \rangle$ coincides with the spectrum $\omega^{-5/3}$ of the normal fluid turbulence. In case of the bundle arrangement, the spectrum of the VLD coincides with the $\omega^{1/3}$ spectrum of vorticity field. Both spectrum are valid up to frequencies of the order of inverse time of relaxation, after which they acquire additional factor ω^{-2} . From comparison with recent experiments by Roche et al. we can conclude that the structure of the vortex line configuration in turbulent flow is closer to the disordered state.

P1.29 **Heat flow from solid to liquid He II due to inelastic processes of phonons interaction**

I.N. Adamenko and E.K. Nemchenko

V.N.Karazin Kharkiv National University, Svobody Sq. 4 Kharkiv, 61022, Ukraine

The quantum theory for description of creation of phonons in superfluid helium by a solid heater is developed in this work. This problem first came up after experimental discover of temperature gap on He II - solid interface (Kapitza gap). The first theoretical description of this problem was given by I.M.Khalatnikov [1]. Since then this problem has been intensively investigated by experimentators and theoreticians. Despite this there is no complete agreement between theory and experiment until now.

A new approach to solve this problem is proposed. The main idea is account of not only elastic mechanism of creation and annihilation phonons [1], but also a number of inelastic processes on He II - solid interface.

The proposed model allows to calculate the explicit expressions for heat flux from heater to superfluid helium were calculated. The expression for the heat flux via the elastic channel calculated in the framework of present hydrodynamic theory exactly coincides with the well-known formula obtained in the acoustic-mismatch theory [1]. It was shown that heat flux due to inelastic processes under certain conditions can be in order of magnitude to the flux due to elastic processes.

1. I.M. Khalatnikov (1965) "Introduction to the Theory of Superfluidity". New York, Benjamin

P1.30 **Study on the instability of He-II surface induced by second sound**

L.V. Abdurakhimov^a, I.A. Remizov^a, I.M. Khalatnikov^b, and A.A. Levchenko^a

^aInstitute of Solid State Physics RAS, Chernogolovka, Russia

^bLandau Institute for Theoretical Physics, Chernogolovka, Russia

We present preliminary results of experimental study of surface waves induced by second sound propagating in the bulk of the superfluid helium-4. Previously it was observed that He-II surface lost its stability above critical value of the input power¹. Surface waves whose frequency was much less than that of the pumping second sound developed. Several theoretical models were suggested to explain the instability^{1,2,3}. Our experimental data confirm that the formation of low-frequency wave can be related to the instability of He-II surface in the presence of constant heat flow proposed by S.E. Korshunov³.

1. P.W. Egolf, J.L. Olsen, B. Roehricht, D.A. Weiss, Physica B **169**, 217 (1991)
2. I.M. Khalatnikov, M. Kroyter, JETP **88**, 626 (1999)
3. S.E. Korshunov, Europhys. Lett. **16**, 673 (1991)

P1.31 Acoustic Observation of Textural Transition of Superfluid $^3\text{He-A}$ in Slab

C. Kato, K. Obara, Y. Kimura, H. Yano, O. Ishikawa, and T. Hata

Graduate School of Science, Osaka City University, Osaka 558-8585, Japan

Superfluid ^3He is one of the material that gives us an ideal system to study the basic property of the spin triplet p-wave condensates. We have studied the sound propagation mechanism in anisotropic superfluid in a narrow space. The fourth sound is a peculiar sound propagating in such a confined space that normal-fluid component is clamped to the wall by its viscosity, and it is able to obtain the superfluid density from its velocity. We adopted the stack of parallel plates as a confined space, whose thickness is 12, 25, and 50 μm . There are two intentions to use such thicknesses; first, these are comparable to the viscous penetration depth. It means that normal-fluid component is not completely clamped and is possible to be driven by the acoustic resonance technique. Since in A-phase, the motion of normal-fluid component may associate with the spatial orientation of the energy gap, it is possible to understand how the flow of normal-fluid component affects the ℓ -texture. Second, these length are comparable to the dipole coherence length, so that our geometry also has an advantage of controlling ℓ -texture. Since, in A-phase, superfluid density is a tensor quantity depending on the direction of the fluid oscillation relative to ℓ -vector¹, it is possible to verify whether ℓ -texture is deformed by the orientational effect or not.

We performed the sound experiments at 29 bar both in zero magnetic field and in the weak magnetic field normal to the slabs. We found that, in zero magnetic field, a uniform ℓ -texture is realized in all of slabs, however, in the weak magnetic field, we observed the signature of the textural transition due to the competition between the dipole-dipole interaction and the orientational effect of ℓ -vector.

1. J. E. Berthold, R. W. Gianetta, E. N. Smith and J. D. Reppy, Phys. Rev. Lett., **37**, 1138 (1976).

P1.32 Enhancement of Magnetization in Liquid ^3He at Aerogel Interface

A. Fukui, K. Kondo, C. Kato, K. Obara, H. Yano, O. Ishikawa, and T. Hata

Graduate School of Science, Osaka City University, Osaka, Japan

A novel feature of condensate state in liquid ^3He is predicted theoretically, which consists of spin triplet s-wave Cooper pairs¹. Such a spin triplet s-wave state will appear inside aerogel near the surface boundary contacting with superfluid $^3\text{He-B}$, and the enhancement of magnetization due to s-wave state is theoretically expected². In order to detect this proximity effect, we made the interface in columnar glass tube which is coated with 2.5 layer ^4He , and set a saddle shape NMR coil surrounding the interface. At 11 bar and 24 bar, we found that superfluidity in ^3He in aerogel near the interface never occurred, even at considerably low temperatures. At 24 bar below $T/T_c = 0.392$, we observed the enhancement of magnetization which increases with decreasing temperatures. In this poster, we will discuss whether the enhancement is caused by s-wave Cooper pairs.

1. S. Higashitani et al., JLTP, 155, 83-97 (2009).

2. Yasushi NAGATO, Seiji HIGASHITANI, and Katsuhiko NAGAI, J. Phys. Soc. Jpn. 78 (2009) 123603.

P1.33 Roton Parametric Resonance

L.A. Melnikovsky

Russian Academy of Sciences, P.L.Kapitza Institute for Physical Problems, Moscow, Russia

An ultra-narrow damping resonance was discovered in the recent experiments¹ with electromagnetic whispering gallery resonators submerged in superfluid ⁴He. We show that observed line-width is consistent with parametric excitation of a macroscopic coherent roton state. The parametric instability band is selected by the roton slowness.

1. A.S. Rybalko, S.P. Rubets, E.Ya. Rudavskii, V.A. Tikhii, S.I. Tarapov, R.V. Golovashchenko, and V.N. Derkach, "Microwave experiments in He II. New features of undamped superfluid flows" *Low Temp. Phys.* **34**, 497 (2008).

P1.34 Quasiparticle States for the Superfluid ³He B-Phase in a Cylinder

Y. Tsutsumi^a, T. Kawakami^b, and K. Machida^b

^aCondensed Matter Theory Laboratory, RIKEN, 2-1 Hirosawa, Wako, Saitama 351-0198, Japan

^bDepartment of Physics, Okayama University, Okayama 700-8530, Japan

At an edge of the superfluid ³He among topological superfluids, the surface Andreev bound state emerges by the pairing symmetry owing to the bulk-surface correspondence. Due to the quasiparticles in the surface Andreev bound state, namely Majorana fermions, the spin density operator is Ising-like polarized perpendicular to the surface in the B-phase.¹ It follows that spin susceptibility will become anisotropic.² We expect the anisotropy of the spin susceptibility to be observed by NMR experiments. In ISSP, University of Tokyo, high-speed rotating cryostat for the superfluid ³He in a narrow cylinder has been used to investigate the intrinsic angular momentum and textures with vortices in the A-phase by NMR measurement. Signals from the Majorana fermions may be included in NMR spectra which were observed also in the B-phase. Moreover, when vortices are created in a cylinder by rotation, the coupling between Majorana fermions in vortices and those at a edge may be observed. Motivated by the experiment, we obtain quasiparticle states and spin susceptibility for the superfluid ³He B-phase in a cylinder on the basis of the quasiclassical theory. Then, we discuss signals from the Majorana fermions how to emerge into NMR spectrum.

1. S. B. Chung and S.-C. Zhang, *Phys. Rev. Lett.* **103**, 235301 (2009).
2. Y. Nagato, S. Higashitani, and K. Nagai, *J. Phys. Soc. Jpn.*, **78**, 123603 (2009).

P1.35 Phonon-roton modes and Bose-Einstein condensation in liquid ^4He

J. Bossy^a, J. Ollivier^b, H. Schober^c, and H.R. Glyde^d

^aInstitut Néel, CNRS-UJF, BP 166, 38042 Grenoble Cedex 9, France.

^bInstitut Laue-Langevin, BP 156, 38042 Grenoble, France.

^cInstitut Laue-Langevin, BP 156, 38042 Grenoble, France and Université Joseph Fourier, UFR de Physique, F38041 Grenoble Cedex 9, France.

^dDepartment of Physics and Astronomy, University of Delaware, Newark, Delaware 19716-2593, USA.

We present neutron scattering measurements of the phonon-roton (P-R) and layer modes of liquid ^4He confined in 47 Å pore diameter MCM-41 under pressure up to 38 bar. The data shows unambiguously that the P-R mode exists at low temperature only. As temperature is increased there is a gradual transfer of intensity from the P-R mode to the normal liquid response, which lies at a lower energy at higher pressure. The transfer takes place with no observable mode broadening. At $T = 1.6\text{ K}$ there is no longer P-R mode in liquid ^4He at $p = 34\text{ bar}$. The loss of P-R modes is identified with the loss of Bose-Einstein condensation (BEC). Layer modes in 25 Å gelsil and MCM-41 are also observed. The mode giving rise to the specific heat, c_V , of liquid ^4He in porous media (e.g. gelsil under pressure) at higher temperature is the layer mode since the energy of the mode extracted from c_V and the layer mode that we observe have the same energy. The layer mode survives up to a higher temperature than the P-R mode.

1. J. Bossy, J. Ollivier, H. Schober and H. R. Glyde (2012) “Phonon-Roton Modes in Liquid ^4He coincide with Bose-Einstein Condensation.” *Euro. Phys. Lett.* **98**, 50068 (2012)

P1.36 Bose-Einstein condensation in liquid ^4He under pressure

S.O. Diallo^a, D.L. Abernathy^a, R.T. Azuah^b, O. Kirichek^c, J.W. Taylor^c, and H.R. Glyde^d

^aSpallation Neutron Source, Oak Ridge National Laboratory, Oak Ridge, TN 37831, USA

^bNIST Center for Neutron Research, Gaithersburg, Maryland 20899-8562, USA and Department of Materials Science and Engineering, University of Maryland, College Park, Maryland 20742-2115, USA

^cISIS Spallation Neutron Source, STFC, Rutherford Appleton Laboratory, Didcot, OX11 0QX, United Kingdom

^dDepartment of Physics and Astronomy, University of Delaware, Newark, Delaware 19716-2593, USA.

We present neutron scattering measurements of Bose-Einstein condensation, the atomic momentum distribution and Final State effects in liquid ^4He under pressure¹. The condensate fraction at low temperature is found to decrease from $n_0 = 7.25 \pm 0.75\%$ at SVP ($p \simeq 0$) to $n_0 = 3.2 \pm 0.75\%$ at pressure $p = 24\text{ bar}$. This indicates an $n_0 = 3.0\%$ in the liquid at the liquid/solid co-existence line ($p = 25.3\text{ bar}$). The pressure dependence of n_0 is reproduced by Monte Carlo calculations within observed error. The atomic momentum distribution $n(\mathbf{k})$ has high occupation of low k states and differs significantly from a Gaussian (e.g. a classical $n(\mathbf{k})$). Both $n(\mathbf{k})$ and the Final state function broaden with increasing pressure, reflecting the increased localization of the ^4He in space under increased pressure. In separate measurements and calculations², the temperature dependence of $n_0(T)$ at 24 bars near the solidification line has also been measured and calculated. Future measurements are discussed.

1. H. R. Glyde, S. O. Diallo, R. T. Azuah, O. Kirichek, and J. W. Taylor (2011), *Phys. Rev. B* **83**, 100507(R); *Phys. Rev. B* **84**, 184506. 2. S. O. Diallo, R. T. Azuah, D. L. Abernathy, R. Rota, J. Boronat, and H. R. Glyde (2012), *Phys. Rev. B* **85**, 140505.

P1.37 Ground state and excitations in a film of ^3He

M. Nava^a, A. Motta^a, D.E. Galli^a, S. Moroni^b, and E. Vitali^a

^aDipartimento di Fisica, Università degli Studi di Milano, via Celoria 16, 20133 Milano, Italy

^bIOM-CNR DEMOCRITOS National Simulation Center and SISSA, via Bonomea 265, 34136 Trieste, Italy

We have performed a Quantum Monte Carlo study of a two-dimensional bulk sample of interacting $1/2$ -spin structureless fermions, a model of ^3He adsorbed on a variety of preplated graphite substrates. We computed the equation of state, the polarization energy and we challenged the microscopic characterization of zero-sound mode and particle-hole excitations. We show that it is indeed possible to have access to ground state and excited state properties in Fermi systems starting from imaginary time correlation functions, of a fictitious collection of Bose particles, evaluated via “exact” Quantum Monte Carlo simulations. This is particularly appealing since recent neutron scattering experiments on ^3He films have shown for the first time evidence of a zero-sound mode. Relying on an ab-initio theoretical approach, which extends the method already used by ourselves [*Phys. Rev. B* 85, 184401 (2012)], we have been able to capture the different excitations in the system. Our theory uses as only input the form of the pair interaction potential among ^3He atoms. The approach is in principle exact and relies on the ability to obtain robust inversion of the Laplace transform in ill-posed conditions [*Phys. Rev. B* 82, 174510 (2010)]. We have been able to “separate” the collective mode from the particle-hole structure, focusing in particular to the roton region, where the re-emergence of the zero-sound mode is considered to be a very important point for many-body physics. Finally, we have introduced a variational approximation of the dynamical structure factor $S(q, \omega)$ of the Fermi liquid, finding an impressive agreement with experiments.

P1.38 The ^3He impurity states in ^4He

G. Panochko and I.O. Vakarchuk

Department for Theoretical Physics, Ivan Franko National University of Lviv, Ukraine

In this paper we study the impurity states in quantum fluids based on construction of the density matrix for all temperatures. We consider a set of spinless Bose-particles of mass m each with coordinates $\mathbf{r}_1, \dots, \mathbf{r}_N$, which are moving in a volume of V , together with an impurity atom of mass M and coordinate \mathbf{r} . Our task is to find the density matrix of the system described by the Hamiltonian written in the representation of collective variables. This quantity includes all the information about the system. In particular, the diagonal element of the density matrix integrated over all the variables is the partition function of the system “Bose-liquid + impurity”. Averaging the expression for the density matrix over the states of the liquid, the one-particle reduced density matrix of the system is found. Its Fourier image allows to find the distribution of momenta of the system “liquid helium + impurity”. The estimation of the effective mass of the ^3He impurity in ^4He is made.

P1.39 Recent Spin Pump Experiments on Superfluid $^3\text{He-A}_1$

A. Yamaguchi^a, N. Kamada^a, G. Motoyama^a, A. Sumiyama^a, Y. Aoki^b, Y. Okuda^b, M. Kubota^c, and H. Kojima^d

^aGraduate School of Material Science, University of Hyogo, Kamigori, Hyogo 678-1297, Japan

^bTokyo Institute of Technology, Meguro-ku, Tokyo 152-8550, Japan

^cInstitute for Solid State Physics(ISSP), University of Tokyo, Kashiwanoha, Chiba 277-8581, Japan

^dSerin Physics Laboratory, Rutgers University, Piscataway, New Jersey 08854, USA

The superfluid $^3\text{He A}_1$ phase, containing a spin-polarized condensate allows us to explore the dynamics of superfluid spin current. In the mechano-spin effect (MSE), a mechanically applied pressure gradient and a superleak-spin filter enable to directly boost spin polarization of ^3He in a small chamber. Recently, we are developing new apparatus for achieving greater enhancement of spin density. A development of a new-type ^3He -hydraulic actuator has been reported elsewhere.¹ We present here a construction of new-type of superleak-spin-filter made of packed powder aluminum oxide. The packed powder superleak is popular in study of superfluid ^4He , but not established for that of the superfluid ^3He . The details of the new type superleak will be presented. The nuclear demagnetization cryostat of ISSP, Univ. Tokyo which has been used for this experimental activity, was heavily damaged by the 2011 East Japan (Higashi Nihon) earthquake. The repair work and earthquake damage protection strengthening will be also mentioned .

1. A. Yamaguchi, et al. in LT26 conference proceedings, to be published.

P1.40 Real time dynamics of the desorption of atomic impurities from ^4He

D. Mateo^a, A. Hernando^b, M. Pi^a, M. Barranco^a, E. Loginov^c, M. Langlet^c, and M. Drabbles^c

^a Departament ECM, Facultat de Física, and IN²UB, Universitat de Barcelona. Diagonal 645, 08028 Barcelona, Spain

^b Laboratoire Collisions, Agrégats, Réactivité, IRSAMC, Université Paul Sabatier 118 route de Narbonne 31062 - Toulouse CEDEX 09, France

^c Laboratoire de Chimie Physique Moléculaire, Swiss Federal Institute of Technology Lausanne (EPFL), CH-1015 Lausanne, Switzerland

The desorption of Ag atoms in helium nanodroplets following the $5p \leftarrow 5s$ transition has been investigated within a three-dimensional, time-dependent density functional approach. We have compared the theoretical results for the velocity at which the Ag atom is expelled from the drop with the experimental data. Similar studies have been done with Na and Li atoms,¹ but Ag presents two additional interesting features: first, Ag resides in the bulk of the drop and its velocity is largely dampened by the surrounding helium, being thus a natural probe for superfluidity in finite clusters; second, the possibility to excite to a particular J state in the $5p$ manifold means that it is a good impurity to study exciplex formation.

1. A. Hernando et al, Phys. Chem. Chem. Phys. **14**, 3996 (2012)

P1.41 **Spin Susceptibility of Proximity-Induced Odd-Frequency State in Aerogel/Superfluid ^3He System**

Seiji Higashitani^a, Hirimitsu Takeuchi^a, Shigemasa Matsuo^a, Yasushi Nagato^b, and Katsuhiko Nagai^a

^aGraduate School of Integrated Arts and Sciences, Hiroshima University, Kagamiyama 1-7-1, Higashi-Hiroshima 739-8521, Japan

^bInformation Media Center, Hiroshima University, Kagamiyama 1-4-2, Higashi-Hiroshima 739-8511, Japan

The proximity effect at the interface of superfluid ^3He partly filled with aerogel under external magnetic field is discussed. This system can be regarded as a dirty Fermi liquid/spin-triplet superfluid junction. Our attention is mainly paid to the case when the aerogel layer is in the normal state owing to the impurity pair-breaking effect by the aerogel. In our previous work¹, we have shown that the odd-frequency s -wave Cooper pair dominates the proximity-induced superfluidity in the aerogel layer. In this work, we study the response of the odd-frequency state to magnetic field. Using the quasiclassical Green's function, we have calculated the spatial dependence of the spin magnetization in the aerogel/superfluid ^3He -B system with magnetic field perpendicular to the interface. We show that the spin magnetization is strongly enhanced due to the formation of the odd-frequency s -wave Cooper pairs. The observation of this spin-magnetization enhancement gives an evidence of the proximity-induced odd-frequency s -wave Cooper pairs.

1. Higashitani, S., Nagato Y. and Nagai, K. (2009) J. Low Temp. Phys. **155**, 83-97.

P1.42 **Contribution of spacial transverse fluctuations of order parameter to superfluid properties of ^3He in aerogel**

E. Surovtsev

Kapitza Institute for Physical Problems, Moscow, Russia

It was experimentally shown that in uniaxially compressed silica aerogel the order parameter of the A-like phase is more suppressed than the B-like phase order parameter, i.e. the ratio of Leggett frequencies $\frac{\Omega_A}{\Omega_B}$ is less than in the case of pure ^3He .¹ Such behavior can be explained by consideration of the orientational fluctuations of the A-like phase order parameter induced by aerogel. In the absence of global uniaxial anisotropy of aerogel this type of fluctuations leads to Larkin-Imry-Ma state for the A-phase order parameter. In order to calculate the contribution of spacial fluctuations the method developed by Larkin and Ovchinnikov is used. We found fluctuation corrections to the temperature of superfluid transition, squared order parameter and the superfluid density of the A-like and B-like phases of ^3He that arise from correlations between aerogel particles. The main difference of the orientational fluctuations from the longitudinal ones is that the orientational fluctuations give temperature independent contribution to the squared order parameter. Therefore the effect of this type of fluctuations is not confined by the temperature region near T_c .

1. V.V. Dmitriev, et.al., Pis'ma v ZhETF, V91, 669 (2010).

P1.43 Generation of multi-electron bubbles under pulsed electric fields

V. Vadakkumbatt^a, E.M. Joseph^b, A. Pal^a, and A. Ghosh^b

^aDepartment of Physics, Indian Institute of Science, Bangalore, India

^bCentre for Nano Science and Engineering, Indian Institute of Science, Bangalore, India

We studied the generation of multielectron bubbles (MEBs) in superfluid helium upon the application of a pulsed electric field. We found the statistical distribution of the charge of individual MEBs to be strongly dependent on the duration of the electric field pulse. The rate and probability of MEB generation in relation to the temporal characteristics of the applied field was also investigated.

P1.44 Pulse NMR Studies of Superfluid ³He in squeezed “Nematically Ordered” Aerogel

V.V. Dmitriev, D.A. Krasnikhin, A.A. Senin, and A.N. Yudin

Kapitza Institute, Moscow, Russia

Results of pulse NMR experiments in superfluid ³He confined by “nematically ordered” aerogel¹ are presented. Similarly to the previous paper², where anisotropic aerogel with stretching deformation was used, two types of spin states were obtained in “nematically ordered” aerogel – ordered spin nematic (SN) and disordered spin glass (SG) state. Dependencies of frequency shift on tipping angle were obtained. These data, in principle, can be used to determine coefficients of ABM order parameter with polar distortion.

1. R. Sh. Askhadullin et. al., JETP Letters **95**, 355 (2012).
2. V. V. Dmitriev et. al., JETP Letters **91**, 599 (2010).

P1.45 Texture of Rotating Superfluid $^3\text{He-A}$ phase in a single narrow cylinder

T. Kunimatsu^b, H. Nema^c, R. Ishiguro^d, M. Kubota^a, T. Takagi^e, Y. Sasaki^f, and O. Ishikawa^b

^aISSP, The University of Tokyo, Kashiwa, 277-8581, Japan

^bGraduate School of Science, Osaka City University, Osaka, 558-8585, Japan

^cFaculty of Science and Engineering, Chuo University, Tokyo, 112-8551, Japan

^dDepartment of Physics, Faculty of Science, Tokyo University of Science, Tokyo, 162-8681, Japan

^eDepartment of Applied Physics, Fukui University, Fukui, 910-8507, Japan

^fResearch Center for Low Temperature and Materials Sciences, Kyoto University, Kyoto, 606-8502, Japan

We have studied textures of the rotating superfluid $^3\text{He-A}$ in a single narrow cylinder by NMR measurement. In a narrow cylinder, the characteristic textures such as Mermin-Ho texture¹ can be formed in order to minimize the free energy of the system determined by the effect of the wall, the magnetic field, the dipole interaction, the flow of the superfluid and so on. We observed three types of NMR absorption spectra according to the processes to form A-phase in a narrow cylinder. A texture shows a characteristic spectrum and we can determine the texture of the observed spectrum by comparing the resonance frequency of NMR spectrum with the calculated one of the spin wave mode. We present the stabilization and the phase diagram of texture of the rotating superfluid $^3\text{He-A}$ in a single narrow cylinder.

1. N. D. Mermin and Tin-Lun Ho, Phys. Rev. Lett. **36**, 594 (1976)

P1.46 Observation of Crossover from Ballistic Regime to Diffusion for Excimer Molecules in Superfluid ^4He

D.E. Zmeev^a, F. Papkour^b, P.M. Walmsley^b, A.I. Golov^b, P.V.E. McClintock^a, S.N. Fisher^a, W. Guo^c, D.N. McKinsey^c, G.G. Ihas^d, and W.F. Vinen^e

^aPhysics Department, Lancaster University, Lancaster, UK

^bSchool of Physics and Astronomy, The University of Manchester, Manchester, UK

^cDepartment of Physics, Yale University, New Haven, Connecticut, USA

^dDepartment of Physics, University of Florida, Gainesville, Florida, USA

^eSchool of Physics and Astronomy, University of Birmingham, Birmingham, UK

Einstein's model for Brownian motion suggests that the particle moves ballistically between collisions with the molecules of the surrounding medium. As the medium gets more rarified, the free path of the particle increases until the particle becomes ballistic on a macroscopic scale. Superfluid helium at low temperatures poses as a convenient reservoir for the gas of phonons with its density changing with temperature as T^4 . If one uses a Brownian particle, whose size is much smaller than the wavelength of phonons k , the particle will experience Rayleigh scattering with the cross-section $\sigma \propto k^{-4} \propto T^4$. Overall, the free path of such Brownian particle ℓ would scale as T^8 , and its behaviour can be scanned through many orders of magnitude of ℓ in a narrow temperature range. This would allow the regime intermediate between ballistic motion and diffusion to be studied. One such probing particle is the helium excimer molecule, which in liquid helium forms a bubble of 1.3 nm in diameter. We report the measurement of the temperature dependence of the time of flight of helium excimer molecules $\text{He}_2^*(a^3\Sigma_u^+)$ in superfluid ^4He and find that the molecules behave ballistically below ~ 100 mK and exhibit Brownian motion above ~ 200 mK. In the intermediate temperature range the transport cannot be described by either model.

P1.47 **Torsion Pendulum energy dissipation due to ^3He in aerogel. Dissipation signature of the A-phase**

N. Zhelev^a, R.G. Bennett^a, J. Pollanen^b, E.N. Smith^a, W.P. Halperin^b, and J.M Parpia^a

^aCornell University, Ithaca, NY, USA

^bNorthwestern University, Evanston, IL, USA

A torsion pendulum excited at acoustic frequencies was used to measure the dissipation (Q^{-1}) and period shift of ^3He confined in a 98% open aerogel, compressed by 10% along the axial direction. Data was taken in the range between 100 mK and T_c , as well as below T_c for a series of pressures. After accounting for bulk and empty cell contributions, Q^{-1} is seen to be pressure and temperature independent in the normal state. The dissipation is larger than expected, which can be accounted for either by invoking a very long frictional relaxation time as modeled by Higashitani et. al.¹, or by taking into account the internal friction in the aerogel that is affected by mass loading of ^3He . In contrast, the dissipation in the superfluid state depends strongly on temperature and pressure. The A phase (observed on cooling) shows a higher dissipation than the B phase (observed on warming); the excess dissipation is greater at high pressures.

1. S. Higashitani, M. Miura, M. Yamamoto, and K. Nagai, Phys. Rev. B **71**, 134508 (2005).

P1.48 **Density functional theory and Bose statistics for the freezing of superfluid ^4He**

T. Minoguchi^a, M. Nava^b, F. Tramonto^b, and D.E. Galli^b

^aInstitute of Physics, University of Tokyo, Meguro, Tokyo, Japan

^bDipartimento di Fisica, Universita' degli Studi di Milano, Milano, Italy

Density functional theory (DFT) so far has experienced pathological results in the description of the freezing of superfluid ^4He , even with the use of the best accurate inputs, namely the density response function (DRF) and the equation of state (EOS) of the superfluid. In fact, while the second order approximation of Ramakrishnana-Yussouf type gives a too much stable solid phase, a non-perturbative treatment called modified weighted density approximation (MWDA) gives, on the other hand, a too stable superfluid phase. We have found that a MWDA calculation indeed provides better results if we take DRF and EOS input of a system of liquid ^4He in which Bose statistics has been suppressed. The input data has been obtained via Path Integral Monte Carlo (PIMC) simulations of a system of distinguishable ^4He atoms. The DRF has been obtained from the dynamic structure factors extracted, via the Genetic Inversion via Falsification of Theories (GIFT) method, from imaginary time density–density correlation functions. Our results indicate that DRF and EOS of superfluid ^4He should not be used as input for MWDA calculations; a better choice is to use DRF and EOS of the “normal” fluid ^4He which reproduces the loss of Bose–Einstein condensation at freezing.

P1.49 Mechanical oscillators immersed in inviscid compressible fluids

J. Rysti and J. Tuoriniemi

Low Temperature Laboratory, Aalto University, PO BOX 15100, 00076 AALTO, Finland

Mechanical resonators of different kinds are widely used to probe, for example, the properties of superfluid helium. When immersed in fluid medium, the oscillator response changes due to added inertia and dissipation compared to that of vacuum. The surrounding fluid is often assumed incompressible to simplify the analysis. This approximation is justified by noting that the wavelength of sound is much larger than the relevant length scale of the resonator. We study mechanical oscillators with various geometries by means of numerical simulations. The results demonstrate that compressibility of the medium has a significant effect even when the conditions for the incompressibility approximation are assumed to hold. Therefore in precise measurements compressibility should be taken into account. In particular, we examine the effect of the fluid compressibility on a quartz tuning fork resonator immersed in superfluid helium.

P1.50 The Temperature Dependence of Heat Capacity in 2D Liquid Puddles of ^3He on Grafoil

D. Sato, K. Naruse, T. Matsui, and Hiroshi Fukuyama

Department of Physics, The University of Tokyo, Japan

The two-dimensional (2D) ^3He system has long been thought as the only material which stays gaseous at the ground state.¹ On the other hand, our recent heat-capacity (C) measurements of the third layer of ^3He on graphite² suggested the existence of a self-bound liquid phase. However, there are several arguments on this experiment that the liquid might be stabilized by the quasi two-dimensionality, indirect interactions mediated by surface excitations of the underlayer, etc, and might not be representative of the ground state of ^3He in strictly 2D. In this presentation, we report a result of new heat-capacity measurements of three different ^3He monolayers, i.e., the first, second, and third layer of ^3He at $T \leq 80$ mK. Surprisingly, all the three monolayers show the gas-liquid transitions with approximately the same liquid density ρ_{c0} ($= 0.6 - 0.9 \text{ nm}^{-2}$). This strongly indicates that the ground state of 2D ^3He is a liquid phase. We also discuss density variations of the T -dependence of C in the puddle region. The measured $C(T)$ follows the known expression, $C_F = \gamma T - \alpha T^2$, for 2D liquid ^3He with spin fluctuations. In the second layer, the ratio α/γ is not fixed within the puddle region unlike the simple expectation from the two phase coexistence idea. Instead, it increases rapidly with increasing total density, i.e., areal ratio of the liquid phase. This may be indicative of the size effect of the liquid puddle, which inhibits long wave-length spin fluctuations, due to the micro-platelet structure of the exfoliated graphite substrate (Grafoil).

1. M. D. Miller and L. H. Nosanow, J. Low Temp. Phys. **32**, 145 (1978).

2. D. Sato *et al.*, J. Low Temp. Phys. **158**, 201 (2010).

P1.51 **Second Sound Attenuation of Decaying Quantum Grid Turbulence in Liquid Helium-4**

L.L.E. Munday^b, K.J. Thompson^a, W. Guo^d, W.F. Vinen^c, P.V.E. McClintock^b, S.N. Fisher^b, J.H. Yang^a, and G.G. Ihas^a

^aDepartment of Physics, University of Florida, Florida, USA

^bPhysics Department, Lancaster University, Lancashire, UK

^cPhysics Department, University of Birmingham, Birmingham, UK

^dPhysics Department, Yale University, Connecticut, USA

Second sound attenuation is being used to investigate the decay of quantum turbulence in superfluid ⁴He at 1-2K. The investigation has been undertaken to better understand the effect of grid design, and channel size, on the energy spectrum of QT. Of particular interest is the low wave number part of the energy decay spectrum^{1,4}. The isotropic and homogeneous quantum grid turbulence is produced using a new linear motor which magnetically pulls a 1cm² grid velocities within the range of 1 to 150mm/s. The capabilities of the new linear motor² are demonstrated, as well as expectations of the vortex line density as a function of time measured by the second sound transducers⁵.

1. Skrbek, L., Donnelly, R.J., Niemela, J.J. (2000) "Four regimes of Decaying Grid Turbulence in a Finite Channel". *Physical Review Letters*, 85, 14
2. Thompson, K.J. (2012). "Energy Decay in Superfluid Helium-4". PHD Thesis, University of Florida.
4. Stalp, S.R., Skrbek, L., Donnelly, R.J. (1999). "Decay of grid Turbulence in a Finite Channel". *Physical Review Letters*, 82
5. Stalp, S.R. (1999), "Decay of Grid Turbulence in Superfluid Helium". PhD Thesis, University of Oregon.

P1.52 **Phenomenological modelling of the A-B interface**

M. Arrayás

Área de Electromagnetismo, Univ. Rey Juan Carlos, Spain

We present the investigations of a phenomenological model describing the A-B interface¹. In some ongoing experiments at Lancaster by the ULT group a shaped magnetic field is used to stabilise and manipulate the phase boundary between A and B, with the B phase being stable up to a critical field of 340 mT.

We have calculated the equilibrium profile for realistic magnetic fields and boundary conditions, being our final goal to simulate the interface behaviour when subjected to perturbations, and to see how its properties may be modified by defects that can exist within it. We will discuss some work on progress in order to determine the influence on the dynamics when an inertia mass per unit area of the interface is considered.

1. S. Yip and A. J. Leggett, *Phys. Rev. Lett.* **57**, 345

P1.53 NMR Studies of Superfluid ^3He in Squeezed “Nematically Ordered” Aerogel

V.V. Dmitriev, E.E. Efimenko, D.A. Krasnikhin, A.A. Senin, and A.N. Yudin

Kapitza Institute, Moscow, Russia

Results of continuous wave nuclear magnetic resonance (CW NMR) measurements in superfluid ^3He confined to “nematically ordered” aerogel are reported. This aerogel consists of Al_2O_3 strands which are nearly parallel to each other at macroscopic distances. Aerogel samples with different squeeze rate (10% and 40%) in direction transverse to the strands were used. Temperature dependencies of CW NMR shift for different orientations of magnetic field are presented. We have found that for magnetic field oriented along the direction of the squeezing the CW NMR shift is zero in some range of temperatures $T_p < T < T_{ca}$. On further cooling the positive NMR shift appears. It is possible that for $T_p < T < T_{ca}$ the theoretically predicted polar phase exists.

P1.54 The superfluid ^3He AB interface probed by quartz tuning forks

D.I. Bradley, M. Fear, S.N. Fisher, A.M. Guénault, R.P. Haley, C.R. Lawson, G.R. Pickett, R. Schanen, and V. Tsepelin

Department of Physics, Lancaster University, Lancaster, LA1 4YB, United Kingdom

We are studying the AB phase boundary in superfluid ^3He at low temperatures in the pure condensate ballistic limit. The phase change between A and B is an exemplar first order transition, and the interface between the two is arguably the most highly ordered to which there is experimental access. The A phase order parameter transforms coherently through the interface to that of the B phase over a distance of the order of a few coherence lengths. However, no direct measurements of the boundary region have yet been undertaken. Our experimental cell consists of a vertical cylinder of superfluid, 5.7 cm long and 1.2 cm in diameter. We create and stabilize the AB interface across the cylinder using a controllable magnetic field gradient. At zero pressure the transition from B to A occurs at a field on the order of 0.3 T. Ramping the field gradient moves the AB interface up and down the cylinder, converting B phase to A phase and vice versa. The motion and properties of the interface are inferred from the behaviour of quartz tuning fork resonators that project into the superfluid from the sidewalls of the cylinder. These resonators are sensitive to the density of broken Cooper pair quasiparticle excitations, and are thus used to detect any changes as the interface is moved through the cell. Such changes are due to several effects, for example simple heating, the presence of defects, or the underlying order parameter texture of the surrounding superfluid phase. Here we present measurements of the interaction of quartz tuning forks with the AB interface itself, and their response when immersed in B phase whose energy gap structure has been severely distorted by the large magnetic field.

P1.55 **Competition between Anisotropy and Disorder in a Toy Model of Superfluid ^3He in Globally Anisotropic Aerogel**

Ryusuke Ikeda

Department of Physics, Kyoto University, Kyoto 606-8502, Japan

Recently, two intriguing experiments have been reported of superfluid ^3He in radially compressed (or, uniaxially stretched) aerogels [1,2]. As a first step for addressing this issue, we consider here the competition between the stretched anisotropy and quenched disorder in superfluid ^3He -A phase. We find based on the self-consistent harmonic approximation that, for instance, upon cooling, the anisotropy becomes more relevant than disorder. This tendency is opposite to that seen in the experiment [1] and suggests that it is insufficient to focus only on the hydrodynamic degrees of freedom like the \mathbf{l} -vector. Together with possible appearance of the polar phase [2,3], it seems to be necessary to take account of the amplitude change of the superfluid order parameter.

1. Pollanen J., et al., "New chiral phases of superfluid ^3He stabilized by anisotropic silica aerogel", *Nature Physics* 8, 317 (2012).
2. Askhadullin R. Sh. et al., "Phase diagram of superfluid ^3He in "nematically ordered" aerogel", *Pis'ma v ZhETF* v.95, 355 (2012).
3. Aoyama K. and Ikeda R., "Pairing states of superfluid ^3He in uniaxially anisotropic aerogel", *Phys. Rev. B* 73, 060504(R) (2006).

P1.56 **Experimental determination of the static structure factor of Fermi Liquid ^3He in two-dimensions**

A. Sultan^a, M. Meschke^b, H. Lauter^c, and H. Godfrin^a

^aInstitut Néel, CNRS et Université Joseph Fourier, BP 166, 38042 Grenoble cedex 9, France

^bLow Temperature Laboratory, Aalto University, PO Box 15100, 0076 Aalto, Finland

^cInstitut Laue-Langevin, Grenoble, France and Oak Ridge National Laboratory, Oak Ridge, USA

We have recently shown that a submonolayer liquid liquid ^3He film sustains zero-sound at large wave-vectors (*Nature* **483**, 576, 2012). The static structure factor, the Fourier transform of the atomic radial distribution function, is obtained here from the neutron inelastic data by integrating over the accessible energy range the experimental values of $S(Q,\omega)$. The experimental results agree well with Quantum Monte Carlo and Dynamical Many-Body Theory calculations.

4.3 Invited Oral Presentations: Friday August 17th

O5.1 Hydrodynamic Instability and Turbulence in Quantum Fluids

Makoto Tsubota

Department of Physics, OCARINA, Osaka City University, JAPAN

Superfluid turbulence consisting of quantized vortices is called quantum turbulence (QT). Quantum turbulence and quantized vortices were discovered in superfluid ^4He about 50 years ago, and have been thoroughly studied experimentally, theoretically and numerically. Since the early efforts were mostly limited to thermal counterflow, however, QT has absorbed little interest of scientists in other fields. Two kinds of innovation has occurred from the mid of 90's.¹ One is in the field of superfluid helium; the comparison between QT and conventional classical turbulence has been studied. Statistical quantities such as energy spectra and probability distribution function of the velocity field are now investigated theoretically and experimentally. Visualization technique has developed rapidly in these years, which succeeded in the direct visualization of quantized vortices. The other innovation is the realization of atomic Bose-Einstein condensation in 1995. The modern optical technique has enabled us to control and visualize directly the condensate and quantized vortices. The early studies of quantized vortices in atomic Bose-Einstein condensates (BECs) were chiefly limited to vortex lattices under rotation, while the recent studies start to reveal hydrodynamic instability and even QT in atomic BECs.² In this talk, starting with some research history of the topics, I will discuss the important motivation of studying quantum hydrodynamics. The latter half part is devoted to the discussions of some modern interesting topics.

1. Halperin, W. P. and Tsubota, M. (2009). Progress in Low Temperature Physics Vol. XVI. Elsevier, Amsterdam.
2. Tsubota, M. and Kasamatsu, K. arXiv: 1202.1863.

O5.2 Steady State and Decay of Quantum Turbulence of a Bellows-Driven Superfluid ^4He Channel Flow

S. Babuin^a, M. Stammeier^{b,c}, E. Varga^b, M. Rotter^b, and L. Skrbek^b

^aInstitute of Physics ASCR, Na Slovance 2, 182 21 Prague, Czech Republic

^bFaculty of Mathematics and Physics, Charles University, Ke Karlovu 3, 121 16 Prague, Czech Republic

^cPresent address: Department of Physics, ETH Zurich, Schafmattstr. 16, CH-8093 Zürich, Switzerland

Novel results will be presented on the quantum turbulence of a net flow of ^4He superfluid component in flow channels, where the through-flow of viscous normal component is prevented by plugging the channel ends with superleak filters. The flows are generated by a low temperature bellows assembly, as opposed to the more commonly used helium fountain pump. The temperature range is $1.35 \text{ K} \leq T \leq 1.95 \text{ K}$ at the saturated vapour pressure, and the flow channels are 115 mm long, with square cross-sections of 7 mm or 10 mm in side. Turbulence is quantified by measuring the length of vortex lines per unit volume, L , by the attenuation of second sound propagating perpendicular to the flow. The turbulent steady state is characterized by $L^{1/2} = \gamma(T)(v - v_c)$, where v is the mean superflow velocity and v_c the critical velocity for the onset of turbulence. This formally agrees with the Vinen phenomenological model for thermal counterflow turbulence, and the coefficient $\gamma(T)$ agree with previous thermal pure superflow and counterflow experiments. The critical velocity $v_c \approx 0.2 \text{ cm/s}$ is roughly temperature and channel-width independent. When the bellows drive is suddenly stopped, the character of decay of L depends on the length of vortex lines present in the steady state, and less so on temperature. Generally, for low steady state L the decay obeys the t^{-1} behaviour predicted by the Vinen model, but if L grows sufficiently then at late times the decay is consistent with the $t^{-3/2}$ character observed also in classical fluids.

O5.3 Quantum Turbulence in Rotating Superfluid ${}^3\text{He-B}$ in the $T \rightarrow 0$ limit

V.B. Eltsov^a, P.J. Heikkinen^a, J.J. Hosio^a, R. Hänninen^a, M. Krusius^a, V.S. L'vov^b, and G.E. Volovik^{a,c}

^aO.V. Lounasmaa Laboratory, Aalto University, P.O. Box 15100, 00076 AALTO, Finland

^bDepartment of Chemical Physics, The Weizmann Institute of Science, Rehovot 76100, Israel

^cLandau Institute for Theoretical Physics, Kosygina 2, 119334 Moscow, Russia

Quantum turbulence (motion of tangled and reconnecting quantized vortices) can be triggered in a rotating superfluid by a step change in rotation velocity. In ${}^3\text{He-B}$ at high temperatures mutual friction between the normal and superfluid components provides both the angular momentum transfer to the superfluid component and the energy dissipation during spin-up or spin-down. How do these processes occur in the $T \rightarrow 0$ limit, where the density of the normal component is exponentially depleted, and what is the role of turbulence? We study these questions both experimentally and with numerical simulations of vortex dynamics on the example of spin-up of the initially vortex-free superfluid through the propagation of the turbulent vortex front along the axis of a cylindrical container. Using NMR measurements of the vortex propagation and direct calorimetric measurements of the energy dissipation [1] we determine the propagation velocity of the front and the angular velocity of the superfluid behind it down to temperatures of $0.14T_c$. The results are fit to a phenomenological model of the front as a function of the mutual friction parameter $\alpha(T)$, which can be measured *in situ*. We show that the turbulence substantially enhances the effect of the mutual friction in the dissipation, owing to the cascade of energy to smaller length scales, but the angular momentum transfer is not significantly improved by the turbulence. This mismatch results in the decoupling of the superfluid from the rotating frame in the $T \rightarrow 0$ limit. A finite residual coupling is, however, observed in the experiments [2] and we discuss its possible sources.

1. J.J. Hosio *et al.*, Phys. Rev. Lett. **107**, 135302 (2011). 2. J.J. Hosio *et al.*, arXiv:1204.6172.

O5.4 Energy spectra and coherent structures in quantum turbulence

C.F. Barenghi^a, A.W. Baggaley^a, A. Shukurov^a, and Y.A. Sergeev^b

^aJoint Quantum Centre Durham-Newcastle, School of Mathematics and Statistics, Newcastle University, Newcastle upon Tyne NE1 7RU, United Kingdom

^bJoint Quantum Centre Durham-Newcastle, School of Mechanical and System Engineering, Newcastle University, Newcastle upon Tyne NE1 7RU, United Kingdom

Recent numerical calculations have shown that interacting vortex lines can organise themselves so that the kinetic energy distribution over the length scales has the same $k^{-5/3}$ Kolmogorov scaling that is observed in ordinary turbulence, where k is the wavenumber. It is also found [1] that the spectrum of the fluctuations of the vortex line density has the $f^{-5/3}$ scaling typical of a passive quantity, where f is the frequency. Both effects are independent of temperature, and have been observed in helium II. Alongside the spectra, we observe another important feature: the vorticity is not uniform in space, but tends to concentrate in metastable bundles of vortex lines [2], similar to the coherent vortex structures which are observed in ordinary turbulence.

1. Baggaley, A.W., and Barenghi, C.F. (2011), “Vortex-density fluctuations in quantum turbulence”, Phys. Rev. B **84**, 020504(R).

2. Baggaley, A.W., Barenghi, C.F., Shukurov, A., and Sergeev, Y.A. (2012), “Coherent structures in quantum turbulence”, Europhys. Lett. **98**, 26002.

O6.1 Strongly Interacting Fermi Gases: Thermodynamics, Lower Dimensions and Topological Phases

M.W. Zwierlein

Center of Ultracold Atoms, Department of Physics, and Research Laboratory of Electronics, Massachusetts Institute of Technology, Cambridge, MA, USA

Strongly interacting gases of ultracold fermions have become an amazingly rich test-bed for many-body theories of fermionic matter. I will present high-precision measurements on the thermodynamics of a strongly interacting Fermi gas across the superfluid transition¹. The onset of superfluidity is directly observed in the compressibility, the chemical potential, the entropy, and the heat capacity. Our measurements provide benchmarks for current many-body theories on strongly interacting fermions. Novel topological phases of matter are predicted for fermionic superfluids in the presence of spin-orbit coupling. We created and detected spin-orbit coupling in an atomic Fermi gas². For energies within the spin-orbit gap, the system acts as a spin diode. To fully inhibit transport, we create a spin-orbit coupled lattice with spinful band structure. In the presence of s-wave interactions, such systems should display induced p-wave pairing, topological superfluidity, and Majorana edge states.

1. Mark Ku, Ariel Sommer, Lawrence Cheuk, and Martin W. Zwierlein “Revealing the Superfluid Lambda Transition in the Universal Thermodynamics of a Unitary Fermi Gas.” *Science* 335, 563 (2012)

2. Lawrence W. Cheuk, Ariel T. Sommer, Zoran Hadzibabic, Tarik Yefsah, Waseem S. Bakr, and Martin W. Zwierlein “Spin-Injection Spectroscopy of a Spin-Orbit Coupled Fermi Gas” preprint arXiv: 1205.3483 (2012)

O6.2 Tachyon Condensation and Brane Annihilation in Bose-Einstein Condensates: Spontaneous Symmetry Breaking in a Lower-dimensional Subspace

H. Takeuchi^a, K. Kasamatsu^b, M. Tsubota^c, and M. Nitta^d

^aGraduate School of Integrated Arts and Sciences, Hiroshima University, Japan

^bDepartment of Physics, Kinki University, Japan

^cDepartment of Physics and The Osaka City University Advanced Research Institute for Natural Science and Technology (OCARINA), Osaka City University, Japan

^dDepartment of Physics and Research and Education Center for Natural Sciences, Keio University, Japan

In brane cosmology, the Big Bang is hypothesized to occur by the annihilation of the brane–anti-brane pair in a collision, where the branes are three-dimensional objects in a higher-dimensional Universe. Spontaneous symmetry breaking accompanied by the formation of lower-dimensional topological defects, *e.g.* cosmic strings, is triggered by the so-called ‘tachyon condensation’, where the existence of tachyons is attributable to the instability of the brane–anti-brane system. Here, we propose a groundbreaking system to simulate the tachyon condensation due to brane-pair-annihilation in two-component atomic Bose–Einstein condensates.¹ In this system, three-dimensional formation of vortices from a domain-wall annihilation is considered a kink formation due to spontaneous symmetry breaking in a two-dimensional subspace. Our numerical experiments show that the following relaxation dynamics obey the scaling law in phase ordering kinetics. We hope that this study motivates experimental researches for this novel phenomenon of spontaneous symmetry breaking in condensed matter systems.^{1,2}

1. H. Takeuchi, K. Kasamatsu, M. Tsubota, M. Nitta, arXiv:1205.2330.

2. M. Nitta, K. Kasamatsu, M. Tsubota, H. Takeuchi, *Phys. Rev. A* **85**, 053639 (2012).

O6.3 Electron spin waves in atomic hydrogen gas

S. Vasiliev^a, O. Vainio^a, J. Ahokas^a, S. Sheludiyakov^a, D. Zvezdov^b, and K.-A. Suominen^a

^aDepartment of Physics and Astronomy, University of Turku, 20014 Turku, Finland

^bKazan Federal University, 420008, 18 Kremlyovskaya St, Kazan, Russia

We present a high magnetic field study of electron spin waves in atomic hydrogen gas compressed to high densities of $\sim 10^{18} \text{ cm}^{-3}$ at temperatures 0.26 - 0.6 K [1]. We observed a variety of spin wave modes caused by the identical spin rotation effect with strong dependence on the spatial profile of the polarizing magnetic field. We demonstrate confinement of these modes in regions of strong magnetic field and manipulate their spatial distribution by changing the position of the field maximum. At high enough densities of hydrogen atoms we observed a sharp and strong peak in the ESR spectrum originating from the spin wave modes trapped in magnetic field maximum. We observed emergence of spontaneous coherence of the transversal magnetization, similar to that of the homogeneously precessing domain in liquid ^3He , which can be interpreted as Bose-Einstein condensation of magnons [2].

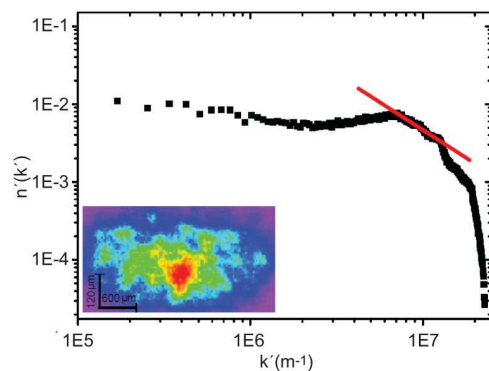
1. O. Vainio *et.al.*, Phys. Rev. Lett **108**, pp. 185304 (2012)
2. Yu. M. Bunkov, and G. E. Volovik, J. Phys. Condens. Matter **22**, pp. 164210 (2010).

O6.4 Quantum turbulence in an atomic trapped superfluid: general characteristics and observation of power law in the kinetic energy spectrum

V.S. Bagnato, G.D. Telles, R. Shiozaki, G. Bagnato, and P.E.S. Tavares

Instituto de Fisica de São Carlos, Universidade de São Paulo, São Paulo, Brazil

We discuss general aspects related to the experimental production of Quantum Turbulence in a sample of *Rb* atoms composing a Bose-Einstein condensate kept in a harmonic trap. From the vortex tangle formation up to evolution to a granulate state is analyzed. In special, the macroscopic manifestation of



the tangle configuration is discussed and the spectrum of kinetic energy of a turbulent sample is measured. Turbulence is produced by an oscillatory field as described in previous work. The analysis is performed to identify the inertial range of momentum and associated with the appearance of the power law dependence. We found that all the turbulent cloud of our experiment showed a regime where $n(k) \sim k^{-\delta}$. Comparison with the Kolmogorov $-5/3$ power law is performed. Details of the experiment are presented in the figure.

Figure: The momentum distribution and the power-law behavior in $n(k)$.

Support from FAPESP, CNPq and CAPES.

07.1 Mechanical resonators in the quantum regime

A. N. Cleland

Department of Physics, University of California, Santa Barbara CA 93106 USA

The UCSB superconducting quantum circuits group has been developing superconducting and mechanical systems for fundamental experiments in quantum mechanics. The Josephson junction provides an extremely nonlinear electrical circuit element that can be used as an “electronic atom”, and is the central active element in our circuitry. This unique device can detect and manipulate single quanta of energy, and has been used to demonstrate simple quantum algorithms. We have used this device to demonstrate full quantum control over microwave-frequency photons in electromagnetic resonators, and more recently that we could measure the ground state of a mechanical resonator, as well as create and manipulate individual phonons. I will describe how we create and measure individual mechanical quanta; I will briefly outline an ongoing project to couple a superconducting circuit to a telecommunications optical signal via a mechanical element.

1. M. Hofheinz et al., “Generation of Fock states in a superconducting quantum circuit”, *Nature* 454, 310-314 (2008).
2. M. Hofheinz et al., “Synthesizing arbitrary quantum states in a superconducting resonator”, *Nature* 459, 546-549 (2009).
3. A.D. O’Connell et al., “Quantum ground state and single-phonon control of a mechanical resonator”, *Nature* 464, 697-703 (2010).
4. M. Mariani et al., “Implementing the quantum von Neumann architecture with superconducting circuits”, *Science* 334, 61 (2011).

07.2 Hybrid circuit cavity quantum electrodynamics with a micromechanical resonator

J.-M. Pirkkalainen, S.U. Cho, Jian Li, G.S. Paraoanu, P.J. Hakonen, and M.A. Sillanpää

Low Temperature Laboratory, Aalto University, P.O. Box 15100, FI-00076 Aalto, Finland

Hybrid quantum systems with inherently distinct degrees of freedom play a key role in many physical phenomena. A strong coupling can make the constituents lose their individual character and form entangled states. The properties of these collective excitations, such as polaritons of light and phonons in semiconductors, can combine the benefits of each subsystem. In the emerging field of quantum information control, a promising direction is provided by the combination between long-lived atomic states and the accessible electrical degrees of freedom in superconducting cavities and qubits. Here we demonstrate the possibility to integrate circuit cavity quantum electrodynamics with phonons. Besides coupling to a microwave cavity, our superconducting transmon qubit interacts with a resonant phonon mode in a micromechanical resonator, allowing the combination of long lifetime, strong tunable coupling, and ease of access. We measure the phonon Stark shift, as well as the splitting of the transmon qubit spectral line into motional sidebands representing transitions between electromechanical polaritons formed by phonons and the qubit. In the time domain, we observe coherent sideband Rabi oscillations between the qubit states and phonons. This advance may allow for storage of quantum information in long-lived phonon states, and for investigations of strongly coupled quantum systems near the classical limit.

07.3 Towards microwave optomechanics with graphene mechanical resonators

X. Song^a, M. Oksanen^a, M. Sillanpää^a, H.G. Craighead^b, J.M. Parpia^b, and P. Hakonen^a

^aLow Temperature Laboratory, Aalto University, P.O. Box 15100, FI-00076 Aalto, Finland

^bCenter for Materials Research, Cornell University, Ithaca, New York 14853, USA

We have developed a micromanipulation technique that can be used to transfer and assemble suspended graphene into nanoscale mechanical resonators.¹ This new technique enables us to take advantage of a localized gate in close proximity to the sample, which improves the sensitivity of RF-cavity readout schemes by reducing the parasitic contributions. In our experiments on a series of graphene samples at temperatures 30 mK - 4.2 K, we obtained resonance frequencies up to 178 MHz, a sensitivity of about 50 fm/ $\sqrt{\text{Hz}}$, and an effective resonator mass down to 10^{-18} kg. The achieved combination of high frequency, high sensitivity, and low mass show that our fabrication technique and RF reflection measurement scheme hold promise for investigations of NEMS structures in the regime where the mechanical motion is quantized. In our latest experiments, we have employed a symmetrized electrical cavity,² which has allowed us to detect thermally induced motion in the sub-Kelvin regime; the sensitivity of this setup will be sufficient to reach the quantum limit once the coupling coefficient of the electrical cavity to the mechanical resonator and the microwave measurement setup is optimized. Furthermore, we are investigating the interplay of electrical and mechanical degrees of freedom by detecting shot noise in suspended graphene.

1. X. Song, M. Oksanen, M. Sillanpää, H. Craighead, J. Parpia, P. Hakonen, *Stamp transferred suspended graphene mechanical resonators for radio-frequency electrical readout*, Nano Lett. **12**, 198 (2012).

2. F. Massel, T. T. Heikkilä, J.-M. Pirkkalainen, S. U. Cho, H. Saloniemi, P. Hakonen, and M. A. Sillanpää, *Microwave amplification with nanomechanical resonators*, Nature **480**, 351 (2011).

08.1 Investigation of Intrinsic Angular Momentum in Rotating Superfluid ³He-A phase

O. Ishikawa^b, T. Kunimatsu^b, H. Nema^c, R. Ishiguro^d, M. Kubota^a, T. Takagi^e, and Y. Sasaki^f

^aISSP, The University of Tokyo, Kashiwa, 277-8581, Japan^bGraduate School of Science, Osaka City University, Osaka, 558-8585, Japan^cFaculty of Science and Engineering, Chuo University, Tokyo, 112-8551, Japan^dDepartment of Physics, Faculty of Science, Tokyo University of Science, Tokyo, 162-8681, Japan^eDepartment of Applied Physics, Fukui University, Fukui, 910-8507, Japan

^fResearch Center for Low Temperature and Materials Sciences, Kyoto University, Kyoto, 606-8502, Japan

We have studied textures of the rotating superfluid ³He-A in a single narrow cylinder by NMR measurement. In a narrow cylinder, the characteristic textures such as Mermin-Ho texture¹ can be observed and we identified a few types of textures by the resonance frequencies of NMR spectra. When the texture has the angular momentum, the system makes a change of texture to have lower energy under rotation by itself. Such a textural change gives rise to the change of the satellite peak frequency in NMR signal. By measuring the peak frequency as a function of the rotation velocity, we can estimate the quantity of the intrinsic angular momentum in the chiral p-wave superfluid ³He-A phase. We present that the intrinsic angular momentum was detected by the rotational dependence of the peak frequency in Mermin-Ho texture as proposed by Takagi².

1. N. D. Mermin and Tin-Lun Ho, Phys. Rev. Lett. **36**, 594 (1976)

2. T. Takagi, Physica. **B194-196**, 833 (1994).

08.2 A neutron reflectometry study of the liquid helium surface

O. Kirichek^a, N.D. Vasilev^b, C.J. Kinane^a, T.R. Charlton^a, S. Langridge^a, and P.V.E. McClintock^b

^aISIS, STFC Rutherford Appleton Laboratory, Harwell Science and Innovation Campus, Didcot, UK

^bDepartment of Physics, Lancaster University, Lancaster LA1 4YB, UK

We report the first neutron reflectometry measurements from the free surface of isotopically pure liquid ⁴He. The results are compared with reflectometry from helium of the natural ³He/⁴He isotopic ratio $x_3 \simeq 2 \times 10^{-7}$, and from stronger mixtures of $x_3 = 0.001$ and 0.005 . In each case, the reflectivity of the liquid surface was measured as a function of the momentum transfer vector Q_z . The measurements were repeated at $T = 2.3, 1.5$ and 0.4 K. At the relatively high temperatures 2.3 K and 1.5 K there was almost no difference in reflectivity between pure ⁴He and the mixtures. However, at the lower temperature of 0.4 K a significant difference was observed between reflectivity from the pure ⁴He surface and from the isotopic mixtures. The shape of the reflectivity curve at low temperature suggests the presence of a substantial number of ³He atoms close to the surface. The most likely explanation of the observations is that they arise as the result of ³He atoms becoming trapped in Andreev levels – quantum states of ³He atoms near to the free surface of liquid ⁴He – a phenomenon that was predicted theoretically by Andreev almost fifty years ago [1]. We comment that it will be of immediate interest to undertake reflectometry on polarised neutrons (and in a magnetic field), which will give us information about the spin dynamics of 2D ³He complementary to that from NMR measurements. In the (very) long term, studies in the μ K range could seek evidence for 2D ³He superfluidity [2].

1. A. F. Andreev, *Sov. Phys. JETP* **23** 939 (1966).

2. P.A. Sheldon and R.B. Hallock, *Phys. Rev. Lett.* **77**, 2973 (1996).

08.3 Symmetry Protected Topological Order and Spin Susceptibility in Superfluid ³He-B

Takeshi Mizushima^a, Masatoshi Sato^b, and Kazushige Machida^a

^aDepartment of Physics, Okayama University, Okayama 700-8530, Japan

^bThe Institute for Solid State Physics, The University of Tokyo, Chiba, 277-8581, Japan

The superfluid ³He-B has been recognized as a textbook example of topological superfluids. The topological order is protected by the time-reversal symmetry as well as the particle-hole symmetry, giving rise to the Majorana Ising spin as a consequence of the bulk-edge correspondence. Here, we clarify the interplay of a Zeeman magnetic field and dipole interaction on surface helical Majorana fermions of superfluid ³He-B. We first reveal that even without the time-reversal symmetry, the B-phase under a magnetic field in a particular direction stays topological due to a discrete symmetry, that is, in a symmetry protected topological phase.¹ It is shown that the Ising spin character of the helical Majorana fermion is a direct consequence of the symmetry protected topological order. Based on the quasiclassical theory, we quantitatively demonstrate that the competition between the dipole interaction and the magnetic field involves the topological phase transition and simultaneously the spontaneous breaking of the discrete symmetry. This quantum phase transition is accompanied by novel behaviors of spin susceptibilities on the surface.

1. T. Mizushima, M. Sato, and K. Machida, arXiv:1204.4780.

08.4 Experimental Investigation of Exotic Negative Ions in Superfluid Helium

W. Wei, Z. Xie, G.M. Seidel, and H.J. Maris

Department of Physics, Brown University, Providence, Rhode island 02912, USA

We have constructed a new apparatus designed to study the exotic negative ions in superfluid helium-4 previously observed by Doake and Gribbon, Ihas and Sanders, and Eden and McClintock. The ions are generated in an electrical discharge in the vapor above the surface of the liquid and the mobility is measured by the time-of-flight method. The cryostat includes a high cooling power continuously-operating 1 K pot which make it possible to perform experiments under stable conditions for extended periods of time. We have detected eleven exotic ions with distinct mobilities, have measured their mobility as a function of temperature, and studied how the strength of the different ions varies with the conditions of the electrical discharge.

In addition to the peaks in the time-of-flight signal due to the different exotic ions, there is a smoothly varying and continuous background signal. This background varies with drift field in a way that indicates that it arises from negative ions with a continuous distribution of mobilities. This is a striking result because it implies that these ions have a continuous size distribution. We will discuss the constraints this result imposes on the possible origin of these ions.

Work supported by the US National Science Foundation under grant No DMR 0965728.

4.4 Poster Presentations: Friday August 17th

P2.1 A study of the experimental features of ^{87}Rb , ^{23}Na and ^7Li via a linearly perturbed harmonic oscillator potential

G.P. Malik^a and V.S. Varma^b

^aTheory Group, School of Environmental Sciences, Jawaharlal Nehru University, New Delhi 110067, India; Present address: B 208 Sushant Lok I, Gurgaon 122002, India

^bAmbedkar University - Delhi, Lothian Road, Kashmere Gate, Delhi 110006, India

We show that the observed features of the Bose-Einstein condensates of ^{87}Rb , ^{23}Na and ^7Li can be understood by modelling the experimental set up used for each of these by a linearly perturbed harmonic oscillator potential

$$V(r) = \frac{1}{2}m\omega^2 \left[r^2 + 2 \left(\frac{kT}{m\omega^2} \right)^{1/2} br \right]$$

where b is a dimensionless parameter and the other variables have their usual significance. We fix b by substituting the density of states corresponding to $V(r)$ into the equation for the number of excited states at any temperature and appealing to the experimental data at $T = T_c$. The values of b thus found for the three condensates are: $-0.17709(^{87}\text{Rb})$, $1.69225(^{23}\text{Na})$, $1.28844(^7\text{Li})$ — which are discussed. We are thus enabled to: a) calculate the number of atoms in the excited states at any T and b) study how T_c would vary with b for each of the condensates. We also draw attention to earlier work in diverse fields where such T -dependent Hamiltonians have found a useful application.

This work cites 12 references.

P2.2 Stability of a bilayer system of strongly correlated dipolar Bosons

D. Hufnagl^a, V. Apaja^b, and R.E. Zillich^a

^aInstitut für Theoretische Physik, Johannes Kepler Universität, Linz, Austria

^bNanoscience Center, Department of Physics, University of Jyväskylä, Finland

Due to the anisotropy and the long range of the dipole–dipole interaction, ultracold dipolar gases are a very promising field of research, and the experimental advances in generating Feshbach-associated molecular quantum gases have led to a growing interest in this field.

We study polarized dipolar Bose systems in a pancake shaped trap, where we also introduce a tunnel barrier to go from the limit of a single quasi-2D layer, to the limit of two quasi-2D layers. We discuss instabilities due to dimerization in one layer and the associated signature of a roton in the spectrum. For the case of two layers we investigate the dependence of the stability on the distance of these layers. In this case destabilization is a result of ordering due to the inter-layer attraction of the dipoles. Additionally, depending on the distance of the layers and the height of the tunnel barrier, we observe the transition from two coupled systems to two uncoupled, identical systems. This transition is clearly visible in the splitting of the first and the second excitation mode.

For the ground state calculations we use the hypernetted–chain Euler Lagrange method and for the calculation of the excitations we use the correlated basis function method. Both methods include two-body correlations, which means they can be used to describe strongly interacting systems.

P2.3 Spin Structure function of a cold Fermi gas

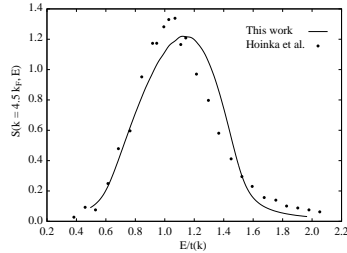
R. Holler^a, E. Krotschek^b, T. Lichtenegger^a, G. Astrakharchik^c, and J. Boronat^c

^aInstitute for Theoretical Physics, JKU Linz, Austria

^bDepartment of Physics, University at Buffalo, SUNY Buffalo NY 14260

^cDepartament de Física i Enginyeria Nuclear, Universitat Politècnica de Catalunya, Barcelona, Spain

We present theoretical calculations for the dynamic structure function of a cold Fermi gas near the unitary limit. The time-dependent Hartree-Fock theory is adequate for the purpose; local effective interactions can be generated¹ by demanding that the m_0 sum rule reproduces the density- and spin- structure functions provided by Monte Carlo calculations. Our results agree, in the spin-channel, quite well with recent measurements².



The figure shows the comparison between the experimental spin dynamic structure function $S(k, E)$ and our theoretical results (xRPA).

1. N. Iwamoto, E. Krotschek, and D. Pines: Phys. Rev. **B29**, 3936 (1984).
2. S. Hoinka, M. Lingham, M. Delehay, and C. J. Vale: *Dynamic spin response of a strongly interacting Fermi gas*, arXiv:1203.4657v1

P2.4 Amplitude control of quantum interference

W. J. Mullin^a and F. Laloë^b

^aDepartment of Physics, University of Massachusetts, Amherst, Massachusetts 01003 USA

^bLaboratoire Kastler Brossel, ENS, UPMC, CNRS; 24 rue Lhomond, 75005 Paris, France

Usually, the oscillations of interference effects are controlled by relative phases. We show that varying the amplitudes of quantum waves, for instance by changing the reflectivity of beam splitters, can also lead to quantum oscillations and even to Bell violations of local realism. We first study theoretically a generalization of the Hong-Ou-Mandel experiment to arbitrary source numbers and beam splitter transmittivity. We then consider a Bell type experiment with two independent sources, and find strong violations of local realism for arbitrarily large source number N ; for small N , one operator measures essentially the relative phase of the sources and the other their intensities. Since, experimentally, one can measure the parity of the number of atoms in an optical lattice more easily than the number itself, we assume that the detectors measure parity.

P2.5 Quasicondensation and pseudogap in two-dimensional Fermi gases

J. Tempere, S. N. Klimin, and J. T. Devreese

TQC, Universiteit Antwerpen, Belgium

The phase diagrams for an imbalanced Fermi gas with s-wave pairing, confined to two dimensions in an optical lattice, are obtained accounting for both phase and amplitude fluctuations. For this purpose, we use the Gaussian pair fluctuation formalism of Hu, Liu and Drummond, reformulated in the context of functional integrals. Special attention is paid to the pseudogap paired state above the Berezinskii-Kosterlitz-Thouless transition temperature. The amplitude of the order parameter is other than zero in the pseudogap state, while the phase coherence is absent. The Gaussian pair fluctuation approach yields a convergent fermion density for the paired state in 2D, in contrast to the usual Nozières and Schmitt-Rink approach. Owing to fluctuations, the pairing temperature for the pseudogap state can be substantially lowered with respect to the mean-field critical temperature. This difference is especially drastic in the strong-coupling regime. The obtained pairing temperatures are in agreement with recent experimental data on pseudogap pairing of ultracold fermionic atoms in two dimensions. The obtained results can shed light on the pseudogap state for high-temperature superconductors.

This work was supported financially by the Research Foundation - Flanders (FWO).

P2.6 A New Superfluid Transition of ^4He Films in Three-Dimensional Topology

N. Wada^a, T. Matsushita^a, M. Hieda^a, and R. Toda^b

^aDepartment of Physics, Nagoya University, Nagoya 464-8602, Japan

^bLow Temperature Center, University of Tokyo, Yayoi, Tokyo 113-0032, Japan

We have studied a superfluid transition of ^4He films formed in three-dimensional (3D) nanopores of HMM-2 of which pores 2.7 nm in diameter are connected in 3D with the period (3D topological length) 5.5 nm[1]. At very dilute fluid densities, the ^4He thin films show a typical 3D superfluid transition of a 3D atomic gas; density dependence of the transition temperature T_C is described by that of the Bose-Einstein condensation (BEC) temperature of a 3D atomic gas, the observed superfluid density shows $T^{2/3}$ -dependence, and so on. It is due to the thermal de Broglie wavelength $\lambda_T = h/\sqrt{2\pi m k_B T}$ being as long as the 3D topological length at T_C . At higher densities where λ_T at T_C is much shorter than the 3D length, the 2D topology of the films causes a crossover from the normal fluid to a 2D condensate state, followed by the 3D superfluid transition at the lower temperature. The transition at T_C shows a tiny but sharp peak of the heat capacity just at the superfluid onset temperature. The transition from the 2D condensate state to the 3D long-range-ordered superfluid state is completely different from the 2D Kosterlitz-Thouless transition of the ^4He films formed on a flat substrate.

1. R. Toda, et. al, Phys. Rev. Lett. **99**, 255301 (2007).

P2.7 Correlated BCS State of Ultracold Fermi Gases

E. Krotscheck^{a,b}, D. Mateo^c, and R. E. Zillich^b

^aDepartment of Physics, University at Buffalo SUNY Buffalo NY 14260

^bInstitut für Theoretische Physik, Johannes Kepler Universität, Linz, Austria

^cDept. E.C.M., Facultat de Física, Universitat de Barcelona, Spain

Fermi gases with attractive effective interactions are superfluid due to pairing. For weak interactions, this pairing is well described by the BCS wave function, which neglects pair correlations. Here we present calculations for homogeneous Fermi gases, based on the Fermi-hypernetted chain (FHNC-EL) method, which takes into account correlations. We show that the pair distribution function $g_{\uparrow\downarrow}(r)$ for two fermions with opposite spin greatly deviates from the usual BCS assumption of unity. Instead $g_{\uparrow\downarrow}(r)$ exhibits a large peak that increases as the s -wave scattering length a becomes more and more negative. Based on the FHNC-EL ground state, we use a *correlated* BCS wave function and derive the pairing gap equation that includes interactions renormalized by the correlations. For a square well and a Lennard-Jones interaction model, we compare the results for the pair distribution functions $g_{\uparrow\downarrow}(r)$ and $g_{\uparrow\uparrow}(r)$ and for the pairing gap Δ for a wide range of densities and potential strengths. We discuss the low density regime, where the results are universal and depend only on $k_F a$, with k_F the Fermi wave number. However, we are mostly interested in the deviations from the universal low density limit, and show results for the non-universal regime at higher densities where many-body effects become important.

P2.8 Vortons and 3D skyrmions from domain wall pair annihilations in BECs

M. Nitta^a, K. Kasamatsu^b, M. Tsubota^c, and H. Takeuchi^d

^aDepartment of Physics and Research and Education Center for Natural Sciences, Keio University, Japan

^bDepartment of Physics, Kinki University, Japan

^cDepartment of Physics and The Osaka City University Advanced Research Institute for Natural Science and Technology (OCARINA), Osaka City University, Japan

^dGraduate School of Integrated Arts and Sciences, Hiroshima University, Japan

We study a mechanism to create a vorton or three-dimensional skyrmion in phase-separated two-component BECs with the order parameters Ψ_1 and Ψ_2 of the two condensates. We consider a pair of a domain wall (brane) and an anti-domain wall (anti-brane) stretched by vortices (strings), where the Ψ_2 component with a vortex winding is sandwiched by two domains of the Ψ_1 component. The vortons appear when the domain wall pair annihilates. Experimentally, this can be realized by preparing the phase separation in the order Ψ_1 , Ψ_2 and Ψ_1 components, where the nodal plane of a dark soliton in Ψ_1 component is filled with the Ψ_2 component with vorticity. By selectively removing the filling Ψ_2 component gradually with a resonant laser beam, the collision of the brane and anti-brane can be made, creating vortons.

1. M. Nitta, K. Kasamatsu, M. Tsubota, H. Takeuchi, Phys. Rev. A **85**, 053639 (2012).
2. H. Takeuchi, K. Kasamatsu, M. Tsubota, M. Nitta, arXiv:1205.2330.

P2.9 Roton Excitations and Stability of the Anisotropic Two-Dimensional Dipolar Bose Gas

R. E. Zillich^a, A. Macia^b, D. Hufnagl^a, F. Mazzanti^b, and J. Boronat^b

^aInstitut für Theoretische Physik, Johannes Kepler Universität, Linz, Austria

^bDepartament de Física i Enginyeria Nuclear, Universitat Politècnica de Catalunya, Barcelona, Spain

Ultracold quantum gases of molecules with electric dipole moments can be strongly interacting even at low density. We investigate a polarized dipolar Bose gas in two dimensions when the polarization axis is tilted with respect to the system normal and thus the dipolar interaction becomes anisotropic. The gas is strongly interacting in one direction and – depending on the polarization angle – weakly interacting in the other direction. After previous studies of the low-density behavior of this system [1], we focus here on the high density regime and study the effect of anisotropy on the roton excitations (calculated by dynamic many-body theory [2]), and on the nature of phase transitions towards a solid-like state similar to the smectic phase of a liquid crystal. Depending on the density and polarization direction, we find a tendency of the system towards long-range order along the strongly interacting direction. This tendency manifests itself as an instability of the gas phase against plane wave fluctuations of the pair distribution function in that direction. At even higher density, our path integral ground state simulations show the formation of stripe patterns, corresponding to a quantum phase transition to a smectic-like phase. Close to the phase transition, the roton energy in the strongly interacting direction tends towards zero, and one can find two roton excitations in a given direction.

[1] A. Macia, F. Mazzanti, J. Boronat, and R. E. Zillich, *Phys. Rev. A* **84**, 033625 (2011).

[2] C. E. Campbell and E. Krotscheck, *Phys. Rev. B* **80**, 174501 (2009).

P2.10 *Ab Initio* Stochastic Modelling of Low-Dimensional Bose Gas Experiments

N. P. Proukakis, S. P. Cockburn, and D. Gallucci

Joint Quantum Centre (JQC) Durham–Newcastle, School of Maths & Stats, Newcastle University, UK

Low-dimensional Bose gases are known to exhibit enhanced fluctuations, making them harder to model. In this talk, we present an *ab initio* self-consistent stochastic method capable of fully accounting for both phase and density fluctuations. This method is known as the stochastic Gross-Pitaevskii equation (SGPE), and the present work explicitly demonstrates excellent *ab initio* agreement with six weakly-interacting cold atom experiments^{1,2,3}.

In the context of one-dimensional systems we show in the regime $\mu < \hbar\omega_{\perp}$ that this model accurately reproduces¹ densities and density fluctuations in atom chip experiments of Bouchoule *et al.* (PRL **97**, 250403 (2006); PRL **105**, 230402 (2010)) and van Druten *et al.* (PRL **100**, 090402 (2008)); in the regime $\mu < \text{few } \hbar\omega_{\perp}$ we also demonstrate² excellent reconstruction of earlier quasi-one-dimensional phase fluctuation experiments in the group of Alain Aspect (PRL **91**, 010405 (2003); EPJD **35**, 155 (2005)).

The SGPE is also shown to give an excellent *ab initio* description of weakly-interacting, finite temperature two-dimensional Bose gases, reproducing³ the recent universality and scale invariance experiment of Chin *et al.* (Nature **470**, 236 (2011)). We acknowledge funding from EPSRC (EP/F055935/1).

1. S. P. Cockburn, D. Gallucci and N. P. Proukakis, “Quantitative study of quasi-one-dimensional Bose gas experiments via the stochastic Gross-Pitaevskii equation”, *Phys. Rev. A* **84**, 023613 (2011).

2. D. Gallucci, S. P. Cockburn and N. P. Proukakis, “Phase coherence in quasicondensate experiments: an *ab initio* analysis via the stochastic Gross-Pitaevskii equation”, cond-mat/1205.6075

3. S. P. Cockburn and N. P. Proukakis, “*Ab Initio* Modelling of Two-Dimensional Bose Gases”, Preprint

P2.11 **Effects of stationary vortices in the structure of pair currents in a fermion superfluid.**

E.S. Hernández^a, P. Capuzzi^a, and L. Szybisz^b

^aDepartment of Physics, FCEN, University of Buenos Aires and CONICET, Argentina

^bTandar Laboratory, Atomic Energy Commission, and CONICET, Argentina

We examine the structure of stationary vortices in a two species superfluid of ${}^6\text{Li}$ atoms in the frame of the recently developed fluid-dynamical scheme¹, that includes the pair density and its associated pair current and pair kinetic energy in addition to the fields appearing in the hydrodynamical description of normal fluids. We are able to show that the presence of any nonvanishing particle velocity field gives rise to the appearance of a pair current. As a reference, we consider a stationary vortex with cylindrical geometry in an unpolarized fluid, and examine the effects of the rotational velocity field on the spatial structure of the gap in various approximations, that progressively include higher truncation levels within the fluid-dynamical frame. We show that it is necessary to reach the full version of fermion fluid-dynamics, including the kinetic energy densities of both spin species and of the Cooper pairs, in order to analyse the spatial profiles of the pair current and to establish the role of the particle current in their formation.

1. Capuzzi, P., Hernández, E.S., and Szybisz, L. (2012). “Cold Fermions with Pairing Interactions: New Results based on a Fluid-dynamical Description”, *J. Low Temp. Phys* **166**, 242.

P2.12 **Bosonic hard-rods in one dimensional optical lattices**

F. de Soto and M.C. Gordillo

Universidad Pablo de Olavide, Sevilla, Spain

Diffusion Monte Carlo simulations on the subject of bosonic hard rods trapped in one dimensional optical lattices are presented. The existence of incompressible Mott Insulator phases for integer fillings is deduced from the behavior of the energy per particle as a function of the density. The analysis of the pair distribution functions and structure factors suggest the existence of fluid-like phases for shallow optical lattices that evolve to solid-like arrangements when the confinement is deep enough.

P2.13 Spin Turbulence and the $-7/3$ Power Law in a Trapped Spin-1 Spinor Bose-Einstein Condensate

M. Tsubota and K. Fujimoto

Department of Physics, Osaka City University, JAPAN

We numerically study the spin turbulence in a two-dimensional trapped spin-1 spinor Bose-Einstein condensate, focusing on the energy spectrum. The spin turbulence in the trapped system is generated through the instability of the initial helical structure of the spin density vector. The spectrum of the spin-dependent interaction energy in the ferromagnetic case becomes to exhibit the $-7/3$ power law as the spin turbulence develops, which was confirmed in a uniform system by the counterflow instability.¹ Hence the spin turbulence with the $-7/3$ energy spectrum is robust independently of how to make the turbulence.

1. K. Fujimoto and M. Tsubota, Phys. Rev. A **85**, 033642 (2012).

P2.14 Dynamical Simulation of Sound Propagation in a Highly Elongated Trapped Bose Gas at Finite temperatures

E. Arahata^a and T. Nikuni^b

^aDepartment of Basic Science, The University of Tokyo, Japan

^bDepartment physics, Tokyo University of Science, Japan

Recently, there has been renewed interest in second sound mode in superfluid Bose and Fermi gases. Sound propagation in Bose-condensed gases has been observed when the thermal cloud is in the hydrodynamic regime and the system is therefore described by the two-fluid model by using highly elongated (cigar-shaped) traps.¹ This experimental work has reported some success, with evidence for a second sound mode in superfluid Bose gases, while there was no clear signature of first sound mode. In order to clearly demonstrate the two fluid dynamics of second sound, it will be important to observe both first and second sound. We study this problem by using Zaremba-Nikuni-Griffin(ZNG) formalism² that consists of a generalized GP equation for a condensate and a semiclassical kinetic equation for the thermal component. In order to deal with a highly-anisotropic trap potential we extend the ZNG formalism by expanding the field operator in terms of radial wavefunctions. We dynamically simulate sound propagation by numerically evolving the coupled ZNG equations. We then discuss the possibility of experimental observation of the second sound mode.

1. R. Meppelink, S. B. Koller, and P. van der Straten, Phys. Rev. A **80**, 043605 (2009).

2. E. Zaremba, T. Nikuni, and A. Griffin, J. Low Temp. Phys. **116**, 277 (2009).

P2.15 **Spin turbulence made by the oscillating magnetic field in a spin-1 spinor Bose-Einstein condensate**

Yusuke Aoki^a and Makoto Tsubota^{a,b}

^aDepartment of Physics, Osaka City University, Japan

^bThe OCU Advanced Research Institute for Natural Science and Technology (OCARINA), Osaka City University, Japan

We numerically study spin turbulence made by the oscillating magnetic field in a two-dimensional homogeneous spin-1 spinor Bose-Einstein condensate. We confine ourselves to the case of the ferromagnetic interaction, where the ground state is ferromagnetic. By the oscillating magnetic field along some direction makes the system unstable. At first, the spin density vector revolves in the plane perpendicular to the magnetic field, exciting long-wavelength modes. Secondly, appear some vector components along the magnetic field. Finally, the system becomes spin turbulence. In terms of the energy spectrum of the spin-dependent interaction energy, the peak appears first at low wave number region. Gradually, the peak shifts from low to high wave number region. Eventually, the spectrum exhibits the $-7/3$ power law. The $-7/3$ power law is confirmed by the scaling analysis using the hydrodynamic equation of the spinor Bose-Einstein condensate.

P2.16 **Instability of overlapped vortices rotating in opposite directions in binary Bose-Einstein condensates**

S. Ishino^a, M. Tsubota^{a,b}, and H. Takeuchi^c

^aDepartment of Physics, Osaka City University, Osaka, Japan

^bThe OCU Advanced Research Institute for Natural Science and Technology, Osaka City University, Osaka, Japan

^cGraduate School of Integrated Arts and Science, Hiroshima University, Hiroshima, Japan

We theoretically study the instability of vortices in pancake-shaped trapped binary miscible Bose-Einstein condensates (BECs). We consider that a quantized vortex is at the center of each condensate and the two BECs rotate in the opposite directions. The overlapped vortices relatively rotate but do not totally rotate. Therefore the circulation in total is zero, so we call it "zero-quantum vortex". When we focus on a local point, we can regard this system as countersuperflow, two counterpropagating miscible superflows. The countersuperflow instability happens in the counterpropagating binary miscible BECs above a critical relative velocity and nucleates quantized vortices in the bulk^{1,2}. We apply the countersuperflow instability to our present system to investigate the instability of the zero-quantum vortices. Then we find out that the vortices are unstable and some modes with angular momentum are amplified. We also show the dynamics of the vortices when the system becomes unstable by numerically solving the Gross-Pitaevskii equations. The numerical results are consistent with the linear analysis of the countersuperflow and shows non-trivial phenomenon that the vortices spontaneously multiplies.

1. H. Takeuchi, S. Ishino, and M. Tsubota, Phys. Rev. Lett. **105**, 205301 (2010).
2. S. Ishino, M. Tsubota, and H. Takeuchi, Phys. Rev. A. **83**, 063602 (2011).

P2.17 Helical shear-flow instability in the phase-separated two-component Bose-Einstein Condensates

S. Hayashi^a, S. Ishino^a, M. Tsubota^{a,b}, and H. Takeuchi^c

^aDepartment of Physics, Osaka City University, Japan

^bThe OCU Advanced Research Institute for Natural Science and Technology (OCARINA), Osaka City University, Japan

^cGraduate School of Integrated Arts and Sciences, Hiroshima University, Japan

The shear-flow instability in phase-separated two fluids is called Kelvin-Helmholtz instability (KHI)¹. When the relative velocity between the two fluids exceeds a critical velocity, the vortex sheet along the interface becomes dynamically unstable to amplify interface modes. Also in phase-separated two-component Bose-Einstein condensates, KHI is realized and the interface modes are amplified^{2,3}. In this work, we theoretically study the helical shear-flow instability by considering the case where one component forms a quantized vortex and the other component is localized in the vortex core with an uniform velocity along the core. When the core size is sufficiently large, the analysis of quantum KHI for a flat interface is applicable. On the other hand, when the core size reduces to be comparable to the interface thickness, the instability is much affected by the outer vortex. We investigate the helical shear-flow instability using two analysis models. One is the interface wave model treating only the interface motion and the other is the Bogoliubov-de Gennes model.

1. S. Chandrasekhar, Hydrodynamic and Hydromagnetic Stability
2. H. Takeuchi, N. Suzuki, K. Kasamatsu, H. Saito, and M. Tsubota, Phys. Rev. B **81**, 094517 (2010)
3. N. Suzuki, H. Takeuchi, K. Kasamatsu, M. Tsubota and H. Saito, Phys. Rev. A **82**, 063604 (2010)

P2.18 Topological Interface Engineering in a Spinor Bose-Einstein Condensate

M.O. Borgh and J. Ruostekoski

School of Mathematics, University of Southampton, United Kingdom

Interfaces between topologically distinct regions are important, for example in exotic superconductivity, early-universe cosmology and superfluid liquid ³He. Here we propose an experimentally feasible scheme for creating topologically non-trivial coherent interfaces between regions with different broken symmetries in a spinor Bose-Einstein condensate (BEC).¹ Defects, such as vortices, must either terminate at such a boundary, or connect non-trivially across it to another object. As an application of topological interface engineering we consider a coherent boundary between ferromagnetic and polar regions in a spin-1 BEC. We identify basic interface-crossing defect solutions and minimise their energy to find examples of intriguing defect structures, resulting from the energetics of a hierarchy of characteristic length scales.^{2,3} Here this leads, for example, to an “Alice arch” defect on the interface with the topological charge of a monopole. Our example illustrates how interface engineering in ultracold gases can be employed to study properties of field-theoretical solitons in an experimentally accessible system. The scheme can be extended to quantum gases with even richer phenomenology, such as spin-2 and 3 BECs and optical-lattice systems.

1. Borgh, M. O. and Ruostekoski, J. (2012). “Topological interface engineering and defect crossing in ultracold atomic gases”. Phys. Rev. Lett. in press. arXiv:1202.5679
2. Lovegrove, J., Borgh, M. O. and Ruostekoski, J. (2012). “Energetically stable singular vortex cores in an atomic spin-1 Bose-Einstein condensate”. Phys. Rev. A in press. arXiv:1204.6347
3. Ruostekoski, J. and Anglin, J. R. (2003). “Monopole Core Instability and Alice Rings in Spinor Bose-Einstein Condensates”. Phys. Rev. Lett. **91**, 190402.

P2.19 Magnetic properties and strong-coupling corrections in an ultracold Fermi gas with population imbalance

T. Kashimura, R. Watanabe, and Y. Ohashi

Department of Physics, Keio University, Japan

We investigate magnetic properties of an ultracold Fermi gas with population imbalance. In the presence of population imbalance, it is well known^{1,2} that the strong-coupling theory developed by Nozières and Schmitt-Rink (which is frequently referred to as the NSR theory, or Gaussian fluctuation theory)³ leads to thermodynamically unphysical results in the BCS-BEC crossover region. We clarify that this problem originates from inconsistent treatments with respect to pseudogap effects associated with pairing fluctuations and magnetic fluctuations in the NSR theory. We show that these failures can be eliminated by properly including higher order fluctuation effects in the Cooper channel, beyond the ordinary T -matrix approximation. Calculated spin susceptibility based on our extended T -matrix theory is found to well agree with the recent experiment on ${}^6\text{Li}$ ⁴.

1. X.-J. Liu and H. Hu, *Europhys. Lett.* **75**, 364 (2006).
2. M. M. Parish, *et al.*, *Nat. Phys.* **3**, 124 (2007).
3. P. Nozières and S. Schmitt-Rink, *J. Low Temp. Phys.* **59**, 195 (1985).
4. C. Sanner, *et al.*, *Phys. Rev. Lett.* **106**, 010402 (2011).

P2.20 Two-dimensional pseudogap effects of an ultracold Fermi gas in the BCS-BEC crossover region

R. Watanabe^a, S. Tsuchiya^b, and Y. Ohashi^a

^aDepartment of Physics, Faculty of Science and Technology, Keio University, Yokohama, Japan

^bDepartment of Physics, Faculty of Science, Tokyo University of Science, Tokyo, Japan

We investigate single-particle properties and pseudogap effects in the BCS-BEC crossover regime of a two-dimensional trapped Fermi gas. Within the framework of a combined strong-coupling T -matrix theory with the local density approximation, we self-consistently determine the superfluid transition temperature T_c and Fermi chemical potential. We then examine single-particle properties, such as the local density of states and the local spectral weight, in the BCS-BEC crossover region above T_c . We clarify how the low-dimensionality and spatial inhomogeneity affect the pseudogap appearing in these quantities. We also compare our results with the recent photoemission experiment on a two-dimensional ${}^{40}\text{K}$ Fermi gas¹. Our results would be useful for clarifying pseudogap phenomena in the BCS-BEC crossover regime of a two-dimensional Fermi gas.

1. Feld, M., Fröhlich B., Vogt E., Koschorreck M., and Köhl M., *Nature* **480**, 75 (2011).

P2.21 Superfluid phase transition and strong-coupling effects in an ultracold Fermi gas with mass imbalance

R. Hanai, T. Kashimura, R. Watanabe, D. Inotani, and Y. Ohashi

Faculty of Science and Technology, Keio University, Japan

We investigate the superfluid phase transition and effects of mass imbalance in the BCS-BEC crossover regime of an interacting Fermi gas. We point out that the ordinary Gaussian fluctuation theory and the strong-coupling T -matrix theory, that are now widely used to study the BCS-BEC crossover physics in the mass-balanced case, give unphysical results in the presence of mass imbalance. To overcome this serious problem, we extend the T -matrix theory to include higher-order self-energy corrections. Using this, we determine the phase diagram of a Fermi gas in terms of temperature, interaction strength, and the ratio of mass imbalance. Since various Fermi superfluids with mass imbalance, such as a ^{40}K - ^6Li Fermi atom gas, exciton condensate (where the electron mass is different from the hole mass), and color superconductivity, have recently attracted much attention, our results would be useful for further development of Fermi superfluid theory.

P2.22 Pure pairing modes in trapped fermion systems

E.S. Hernández^a, P. Capuzzi^a, and L. Szybisz^b

^aDepartment of Physics, FCEN, University of Buenos Aires and CONICET, Argentina

^bTandar Laboratory, Atomic Energy Commission, and CONICET, Argentina

We present numerical predictions for the shape of the pairing fluctuations in harmonically trapped atomic ^6Li with two spin projections, based on the fluid-dynamical description of cold fermions with pairing interactions. In previous works it has been shown that when the equilibrium of a symmetric mixture is perturbed, the linearised fluid-dynamic equations decouple into two sets, one containing the sound mode of fermion superfluids and the other the pairing mode. The latter corresponds to oscillations of the modulus of the complex gap and is driven by the kinetic energy densities of the particles and of the pairs. Assuming proportionality between the heat flux and the energy gradient, the particle kinetic energy undergoes a diffusive behavior and the thermal conductivity is the key parameter for the relaxation time scale. We examine a possible range of values for this parameter and find that the shape of the pairing oscillation is rather insensitive to the precise value of the transport coefficient. Moreover, the pairing fluctuation is largely confined to the center of the trap, and the energy of the pairing mode is consistent with the magnitude of the equilibrium gap.

P2.23 Solutions of bosonic and fermionic one-dimensional Bogoliubov-de Gennes equations: a unified treatment and generalizations

D.A. Takahashi^a, S. Tsuchiya^b, R. Yoshii^c, and M. Nitta^d

^aDepartment of Basic Science, The University of Tokyo, Tokyo, 153-8902, Japan

^bDepartment of Physics, Faculty of Science, Tokyo University of Science, Tokyo 162-8601, Japan

^cYukawa Institute of Theoretical Physics, Kyoto University, Kyoto 606-8502, Japan

^dDepartment of Physics, Keio University, Hiyoshi 4-1-1, Yokohama, Kanagawa 223-8521, Japan

Bogoliubov-de Gennes (BdG) equations are widely used to describe the physics of quasiparticles in both bosonic and fermionic quantum condensed systems. The equivalent equation also appears in the polyacetylene¹ and the chiral Gross-Neveu model.² In our poster, we show that the BdG equations for bosonic and fermionic systems can be solved^{3,4} when the problem can be mapped to the Ablowitz-Kaup-Newell-Segur system.^{5,6} As an example, we treat the bosonic BdG equation for integrable spin-1 BECs⁷ and the linearized fermionic BdG equation when the condensate has a multi-kink profile.⁸

1. H. Takayama, Y. R. Lin-Liu, and K. Maki, PRB **21** (1980) 2388.
2. D. J. Gross and A. Neveu, PRD **10** (1974) 3235.
3. D. A. Takahashi, JPSJ **80**, 015002 (2011).
4. D. A. Takahashi, S. Tsuchiya, R. Yoshii, and M. Nitta, arXiv:1205.3299.
5. M. J. Ablowitz, D. J. Kaup, A. C. Newell, H. Segur, Stud. Appl. Math. **53** (1974) 249.
6. F. Correa, G. V. Dunne, M. S. Plyushchay, Ann. Phys. **324** (2009) 2522.
7. M. Uchiyama, J. Ieda, and M. Wadati, JPSJ **75** (2006) 064002.
8. S. Okuno and Y. Onodera, JPSJ **52** (1983) 3495; J. Feinberg, Ann. Phys. **309** (2004) 166.

P2.24 Phase transition from p_x -wave state to $p_x + ip_y$ state and single-particle properties in a one-component superfluid Fermi gas with a p -wave Feshbach resonance

D. Inotani^a, M. Sigrist^a, and Y. Ohashi^a

^aDepartment of Physics, Keio University, 3-14-1 Hiyoshi, Kohoku-ku, Yokohama 223-8522, Japan

^bInstitut für Theoretische Physik, ETH Zürich, CH-8093 Zürich, Switzerland

We investigate superfluid properties of a single-component Fermi gas with a tunable anisotropic p -wave pairing interaction. In this system, because of the splitting of a p -wave Feshbach resonance into two p_x component and p_y and p_z components by a magnetic dipole-dipole interaction^{1,2}, a phase transition from the p_x -wave pairing state to the $p_x + ip_y$ -wave state is expected in the superfluid phase below T_c ³. In this poster presentation, within the framework of the strong-coupling Gaussian fluctuation theory, we determine the phase transition temperature T_0 ($< T_c$) from the p_x -wave state to the $p_x + ip_y$ -wave state, as functions of the interaction strength and the magnitude of the splitting of resonances. Near T_0 , although the system is in the superfluid phase with a large magnitude of the p_x -wave superfluid order parameter, pairing fluctuations in the $p_x + ip_y$ -wave channel are found to become strong, affecting single-particle excitations. To see this in a clear manner, we also calculate single-particle density of states, as well as spectral weight, near $T_0 < T_c$.

1. C. A. Regal, C. Ticknor, J. L. Bohn, and D. S. Jin, Phys. Rev. Lett. **90**, 053201 (2003).
2. J. Zhang et al., Phys. Rev. A **70**, 030702(R) (2004).
3. V. Gurarie, L. Radzihovsky, and A. V. Andreev, Phys. Rev. Lett. **94**, 230403 (2005).

P2.25 Energy spectra of the superfluid velocity made by quantized vortices in two-dimensional quantum turbulence

T. Kusumura^a, M. Tsubota^{a,b}, and H. Takeuchi^c

^aDepartment of Physics, Osaka City University, Sumiyoshi-ku, Osaka 558-8585, Japan

^bThe OCU Advanced Research Institute for Natural Science and Technology (OCSARINA), Osaka City University

^cGraduate school of Integrated Arts and Sciences, Hiroshima University, Higashi-Hiroshima Japan

We discuss the configuration of vortices in two-dimensional (2D) quantum turbulence (QT), studying the energy spectra (ES) of superfluid velocity and the probability distribution function (PDF) of the distance between two quantized vortices. In order to consider the correlation of vortices, we decompose the ES into the self-energy spectra $E_{self}(k)$ and the interactive energy spectra $E_{int}(k)$. In our work, we define QT with $E_{int}(k) = 0$ as the *uncorrelated turbulence* and QT with $E_{int}(k) \neq 0$ as the *correlated turbulence*. To closely investigate $E_{int}(k)$, we decompose the PDF into two terms, namely the (auto-) correlation function of the distribution with like sign vortices and the (cross-) correlation function of the distribution with opposite sign vortices, which allows us to discuss the configuration of vortices. In this paper, we propose a method of directly connecting the ES to the configuration of vortices.

We apply the above method to 2D QT described by Gross-Pitaevskii equation. We make 2D QT from many dark solitons which decay to a lot of vortices and eventually lead to 2D QT. Our simulation shows that the QT is the *correlated turbulence* from the ES and consists of many pairs of opposite sign vortices. By considering both the ES and the PDF, we are able to well understanding what configuration of vortices the QT has.

P2.26 Vortex knots in a Bose-Einstein condensate

D. Proment^a, M. Onorato^a, and C.F. Barenghi^b

^aDipartimento di Fisica, Università degli Studi di Torino, Torino, Italy. And: INFN, Sezione di Torino, Torino, Italy

^bSchool of Mathematics and Statistics, Newcastle University, Newcastle upon Tyne, United Kingdom

I will present a method for numerically building a quantum vortex knot state in the single scalar field wave function of a Bose-Einstein condensate. I will show how the two topologically simplest vortex knots wrapped over a torus evolve and may preserve their shapes by reporting results of the integration in time of the governing Gross-Pitaevskii equation.¹

In particular, I will focus on how the velocity of a vortex knot depends on the ratio of poloidal and toroidal radius: in a first approximation it is linear and, for smaller ratio, the knot travels faster. Finally, I will display mechanisms of vortex breaking by reconnections which produce simpler vortex rings whose number depends on initial knot topology.

1. Proment, D., Onorato, M., and Barenghi, C. F. (2012). "Vortex knots in a Bose-Einstein condensate". *Physical Review E* 85, 036306.

P2.27 **Ac fluctuation resistivity in high- T_c superconductors**

B.D. Tinh

Department of Physics, Hanoi National University of Education, Vietnam

We use the time-dependent Ginzburg-Landau to calculate ac fluctuation conductivity and resistivity in type-II superconductor in 3D model under magnetic field. Thermal fluctuations are assumed to be strong enough to melt the Abrikosov vortex lattice created by the magnetic field into a vibrating vortex liquid and marginalize the effects of the vortex pinning by inhomogeneities. The nonlinear interaction term in dynamics is treated within self-consistent Gaussian approximation. We obtain expressions the complex conductivity and resistivity summing all Landau levels which are applicable essentially to whole liquid phase and are compared to experimental data on high- T_c superconductor $\text{YBa}_2\text{Cu}_3\text{O}_{7-\delta}$.

P2.28 **Finite Temperature Vortex Dynamics in Trapped Bose Gases**

A.J. Allen^a, C.F. Barenghi^a, E. Zaremba^b, and N.P. Proukakis^a

^aJoint Quantum Centre (JQC) Durham-Newcastle, School of Mathematics and Statistics, Newcastle University, Newcastle upon Tyne, NE1 7RU, UK.

^bDepartment of Physics, Queens University, Kingston, Ontario, K7L 3N6, Canada.

We study the precession of an off-centered vortex in a finite temperature, harmonically-trapped atomic condensate. In the absence of a thermal cloud, it is well understood the vortex rotates at a constant radius, as recently confirmed experimentally [1]. However, the thermal cloud induces a frictional force on the vortex, thereby leading it to a gradual decay. By an extension of earlier work [2], we perform a detailed quantitative study of the role of the dynamics of the thermal cloud on the experimentally-relevant quantities of vortex decay rate, precession frequency, and vortex core brightness, highlighting the importance of the various collisional processes involved. We model the system by a dissipative Gross-Pitaevskii equation for the condensate, self-consistently coupled to a quantum Boltzmann equation for the thermal modes, which additionally includes collisional processes which transfer atoms between these two subsystems (Zaremba-Nikuni-Griffin formalism, ‘ZNG’) [3].

1. D.V. Freilich, D.M. Bianchi, A.M. Kaufman, T.K. Langin, D.S. Hall, *Science* **329**, 1182 (2010).
2. B. Jackson, N.P. Proukakis, C.F. Barenghi, and E. Zaremba, *PRA* **79**, 053615 (2009).
3. E. Zaremba, T. Nikuni, and A. Griffin, *JLTP* **116**, 277 (1999).

P2.29 Energy spectrum of counterflow turbulence

L.K. Sherwin^a, A.W. Baggaley^a, C.F. Barenghi^a, and Y.A. Sergeev^b

^aJoint Quantum Centre Durham-Newcastle, School of Mathematics and Statistics, Newcastle University, Newcastle upon Tyne NE1 7RU, United Kingdom

^bJoint Quantum Centre Durham-Newcastle, School of Mechanical and System Engineering, Newcastle University, Newcastle upon Tyne NE1 7RU, United Kingdom

We perform numerical simulations of counterflow turbulence in superfluid ^4He driven by a constant heat flux. We determine the energy spectrum and other properties of counterflow turbulence, such as the spatial homogeneity of the vorticity and the curvature of the vortex lines. We find that the distribution of the kinetic energy of the vortices over the length scales is concentrated at intermediate wavenumbers. We conclude that counterflow turbulence lacks the concentration of energy at the largest scales which has been measured when liquid helium is stirred by a rotating propeller [1]. In addition we present an experimentally feasible technique, which could be used to infer the existence of vortex bundles in mechanically driven, quasi-classical, quantum turbulence.

1. Maurer, J., and Tabeling, P. (1998) “Local investigation of superfluid turbulence”, *Europhys. Lett.* **43**, 29-34.

P2.30 Anomalous Acoustic Absorption in Liquid Helium

Y. Kimura, K. Obara, H. Yano, O. Ishikawa, and T. Hata

Graduate School of Science, Osaka City University, Japan

We have studied the nonlinear acoustic response in a quantum fluid and found the new class of turbulence. The experimental setup was very simple as follows; the PZT driver and the receiver transducers were attached at the both ends of the cylindrical cavity that is filled with liquid ^4He , and standing waves were excited and detected by them continuously. The frequency was kept at the resonance frequency of the liquid column by PLL technique. In the lower driving-amplitude regime, we found that the I/O relations were linear. However, in the higher driving-amplitude regime, we found strong and unsteady absorption with a turbulent waveform. In this presentation, we will focus on the stochastic properties of the inception of the turbulence, and show the amplitude dependence of the probability that the turbulent response takes place in a fixed time-span. We found that the probability obeyed “asymmetric S curve” function with the threshold pressure P_T^1 . We also measured the ambient pressure dependence of P_T , and revealed that this absorption is caused by the formation of the vapor bubble. The class of the cavitation is not homogeneous but heterogeneous, because the bubble arises from the surface of the transducer where the acoustic pressure takes its maximum value, and, whose surface has a lot of crevices that can hold vapor nuclei. The acoustic absorption is caused by the bubble motion². The special feature of ^4He being the quantum liquid has appeared in the ultra-fast latent-heat transfer during the bubble nucleation and annihilation process, which corresponds to the evaporation and the liquefaction, respectively.

1. S. Balibar, *J. Low Temp. Phys.* **129**, 363, (2002).
2. Y. Hao, A. Prosperetti, *Phys. Fluids* **11**, 2008, (1999).

P2.31 Measures of vortex clustering in Bose–Einstein condensates

A. C. White, C. F. Barenghi, and N. P. Proukakis

Joint Quantum Centre (JQC) Durham-Newcastle, School of Mathematics and Statistics, Newcastle University, Newcastle upon Tyne, NE1 7RU, UK.

We extend available methods for creating vortices in 2D atomic Bose-Einstein condensates by demonstrating that a moving obstacle, in the form of an elongated paddle, can be used to stir a condensate in two quite different ways, to create clusters of like-signed vortices, or induce vortices that are dispersed. The size of atomic condensates and number of vortices present are small in comparison to larger classical and quantum turbulent fluid systems where a huge number of length scales is excited. We introduce new statistical measures of clustering based on Ripley's K-function and nearest neighbor techniques which are suitable to the small size and number of vortices in atomic condensates. These measures are applied to analyze the evolution and decay of clustering. The theoretical techniques we present are accessible to experimentalists and extend the current methods of inducing 2D quantum turbulence in Bose-Einstein condensates.

P2.32 Nonlinear motion of vortices in HTSC after interacting with external Rf field.

D. Apushkinskaya^a, E. Apushkinsky^b, and M. Astrov^c

^aDepartment of Mathematics, Saarland University, Germany

^bExperimental Physics Department, St. Petersburg State Polytechnical University, St. Petersburg, Russia

^cD.V. Efremov Scientific Research Institute of Electrophysical Apparatus, St. Petersburg, Russia

We consider a type II superconductor (SC) placed in a dc magnetic field with the value above the lower critical one. This magnetic field penetrates inside SC in the form of individual vortices, which may be "pinned" to the SC crystal lattice in sites of its defect. Also an ac radio-frequency field (orthogonal to a dc field) is applied on the boundary of our SC. The ac field simulates vortex oscillations on the boundary surface of SC, they are transformed into lattice oscillations through the pinning centers and induce a propagating sound wave. Spreading into SC such a wave causes the vortex oscillations in the whole volume.

Assume that in the vortex core superconductivity does not exist. So, along the vortex there is the interface separating the SC state from the normal one. If an external influence is sufficiently strong, we can neglect the vortex mass in the equation of the vortex motion and reduce this equation to the parabolic one. As a result, we get a free boundary problem, where a-priori unknown free boundary describes the set of points at which transition from SC state to the normal state or vice versa is realized.

From the general theory of free boundary problems we get some information about regularity and singularity of the interface between SC and normal state, as well as about qualitative properties of the vortex tension and damping of the vortex oscillations.

P2.33 Visualization technique for determining the structure functions of normal-fluid turbulence in superfluid ^4He

Wei Guo^a, [A. Marakov](#)^b, G.G. Ihas^b, D. McKinsey^a, and W.F. Vinen^c

^aDepartment of Physics, Yale University, Connecticut, United States

^bDepartment of Physics, University of Florida, Florida, United States

^cSchool of Physics and Astronomy, University of Birmingham, UK

Metastable helium molecules have been shown to be ideal tracers for the study of normal-fluid flow in superfluid ^4He above 1K. These molecules can be visualized using a laser-induced-fluorescence technique. Although so far the fluorescence does not allow single-molecule imaging, practical technique can still be developed to extract quantitative information of the flow field. In an on-going experiment, we use a focused femtosecond laser pulse to create a thin line of He_2 molecules in helium. Such a line of molecules can be easily imaged. Studying the drift and distortion of the molecular line in a turbulent flow shall allow us to measure the flow velocity fluctuations and hence determine the structure functions of the normal-fluid turbulence. We discuss in detail the range of turbulence length scale that can be examined in this experiment.

P2.34 Three-dimensional modelling of Andreev scattering in turbulent $^3\text{He-B}$

N. Suramlishvili^a, C. F. Barenghi^a, A. W. Baggaley^a, and Y. A. Sergeev^b

^aJoint Quantum Centre Durham-Newcastle, School of Mathematics and Statistics, Newcastle University, Newcastle upon Tyne, NE1 7RU, United Kingdom

^bJoint Quantum Centre Durham-Newcastle, School of Mechanical and Systems Engineering, Newcastle University, Newcastle upon Tyne, NE1 7RU, United Kingdom

We are concerned with numerical modelling of Andreev scattering technique^{1,2} which is used for detection of quantized vortices in $^3\text{He-B}$. We report the results of numerical analysis of Andreev reflection by three-dimensional turbulent structures. In particular, we are interested whether Kelvin waves propagating along vortex filaments might significantly change the cross-sections of Andreev scattering by individual vortex lines. We also analyze the Andreev scattering by a dense vortex tangle and a gas of vortex rings, thus aiming at calculating, and comparing with experiment³, the spectral characteristics of the retroreflected beam of thermal excitations.

1. S. N. Fisher, A. J. Hale, A. M. Guénault, and G. R. Pickett, *Phys. Rev. Lett.* **86**, 244 (2001).

2. D. I. Bradley *et al.*, *Phys. Rev. Lett.* **95**, 035301 (2005).

3. D. I. Bradley *et al.*, *Phys. Rev. Lett.* **101**, 065302 (2008).

P2.35 Spin-Down to Rest of the Superfluid Component in Different Geometries

N. Hietala and R. Hänninen

O.V. Lounasmaa Laboratory, Aalto University, Finland

At constant rotation velocity vortices form a regular array where the superfluid component is in solid body motion with the container. After a sudden stop of rotation the new equilibrium state is one with no vortices where the superfluid component is at rest. We study, by using the vortex filament model and numerical simulations, the spin-down of superfluid component of $^3\text{He-B}$ in different geometries. We analyze the homogeneity and isotropy of the vortex tangle during the decay. In geometries cylindrically symmetric with respect to the initial rotation axis the motion of vortices is laminar. The polarization of the tangle remains high, most of the reconnections take place in a thin turbulent boundary layer and the vortex length decay as $L \propto t^{-1}$. These results are in good agreement with the Helsinki measurements¹. When the cylindrical symmetry is broken, i.e. by tilting the cylinder with respect to the rotation axis or in a cubic geometry, the decay of vortices becomes turbulent at low temperatures. The polarization doesn't remain as high as in the laminar case, number of reconnections increases and the decay is faster, $L \propto t^{-3/2}$. We determine the turbulent decay time as a function of temperature. We study also the transition from laminar to turbulent by varying the tilt angle of the cylinder. The critical tilt angle, above which the decay becomes turbulent, is independent of temperature, at least for temperatures $T \geq 0.20T_c$.

1. V.B. Eltsov *et al.*, Phys. Rev. Lett. **105**, 125301 (2010).

P2.36 Analysis of Solid Particles' Motion in Thermal Counterflow

M. La Mantia, D. Duda, M. Rotter, and L. Skrbek

Faculty of Mathematics and Physics, Charles University, Ke Karlovu 3, 121 16 Prague, Czech Republic

An experimental setup¹ has recently been devised to investigate by visualization cryogenic flows of liquid ^4He and address unresolved problems of quantum turbulence. The main feature of the newly implemented apparatus lays in the possibility of obtaining chosen amounts of micron-sized solid tracers made of hydrogen, deuterium or a mixture of the two, the latter option being attractive as it could lead to the generation of neutrally buoyant particles. Thermal counterflow experiments have been performed and the motion of solid hydrogen and deuterium tracers studied by using the particle tracking velocimetry technique. It is shown that the obtained results are consistent with the two-fluid model describing the behaviour of He II. The different aggregation process of hydrogen and deuterium tracers, role of rotating particles in thermal counterflow and evidence of non-Gaussian distribution of tracers velocities are also discussed. The setup appears to be well-suited to the task of analyzing cryogenic flows and the outcome gives us confidence in our current and future investigations. The former are mainly focused on the study of flows around bluff bodies in thermal counterflow, which do not seem to be yet sufficiently understood, while the latter will initially address cryogenic flows around oscillating objects, not yet analyzed by visualization.

We thank S. Babuin, G. Bewley, T.V. Chagovets, L. Dolezal, E. Fonda, V. Pilcova, D. Schmoranzer, F. Soukup and B. Vejr for fruitful discussions and valuable help and acknowledge the support of GACR P203/11/0442.

1. La Mantia, M. *et al.*, (2012) Rev. Sci. Instrum. 83, 055109.

P2.37 Vortex density fluctuations in quantum turbulence

A.W. Baggaley^a, J. Laurie^b, and C.F. Barenghi^a

^aJoint Quantum Centre Durham-Newcastle, School of Mathematics and Statistics, University of Newcastle, Newcastle upon Tyne, NE1 7RU, UK

^bLaboratoire de Physique, École Normale Supérieure de Lyon, 46 allée d'Italie, 69007, Lyon, France

Turbulence in the low temperature phase of liquid helium is a complex state in which a viscous normal fluid interacts with an inviscid superfluid. In the former vorticity consists of eddies of all sizes and strengths; in the latter vorticity is constrained to quantized vortex lines. We compute the frequency spectrum of superfluid vortex density fluctuations and obtain the same, experimentally observed^{1,2}, $f^{-5/3}$ scaling. We show that the scaling can be interpreted in terms of the spectrum of reconnecting material lines. We also develop a novel technique to identify intense vortical regions and analyse their contribution to the energy spectrum of the superfluid component.

1. Roche, P. E., Diribarne, P., Didelot, T., Français, O., Rousseau, L., and Willaime, H. (2007) "Vortex density spectrum of quantum turbulence", *Europhys. Lett.* 77, 66002.

2. Bradley, D. I., Fisher, S. N., Guénault, A. M., Haley, R. P., O'Sullivan, S., Pickett, G. R., and Tsepelin, V. (2008) "Fluctuations and correlations of pure quantum turbulence in superfluid ³He-B", *Phys. Rev. Lett.* 101, 065302.

P2.38 Observation of vortex ring emission within turbulent vortex tangles in superfluid ⁴He at low temperatures

P.M. Walmsley, M.J. Fear, and A.I. Golov

School of Physics and Astronomy, University of Manchester, Manchester, M13 9PL, UK

We have developed a new technique to probe the internal dynamics of turbulent vortex tangles at length scales less than the typical intervortex spacing where classical-like behaviour is no longer possible due to the quantization of vorticity. We injected electron bubbles into a cubic container with sides of length 4.5 cm filled with superfluid ⁴He at temperatures below 1 K. When there is no turbulent tangle present, ballistic charged vortex rings travel across the container with a time of flight $\simeq 1$ s. However, when the container is filled with a dense vortex tangle and seeded with charge in the vicinity of the injector, we find that for $T < 0.5$ K, a fraction of the charge travels across the container quickly (< 0.2 s). Such fast transport of charge does not occur at the slightly higher temperature of 0.7 K. These observations can be explained if, at $T < 0.5$ K, vortex reconnections within the tangle lead to the emission of very small charged rings. These rings are initially emitted isotropically, but when an electric field is applied they are rapidly redirected towards the collector electrode. We will show how the observed ring emission depends on the structure, polarization and density of the vortex tangle. One potential explanation for why this does not happen at $T > 0.7$ K is that the damping provided by mutual friction prevents the fractalization of vortex lines at the small length scales where self-reconnections can lead to the emission of small rings. Instead, the trapped charge drifts slowly with the vortex tangle.

P2.39 Rotating quantum turbulence in superfluid ^4He in the $T = 0$ limit

P.M. Walmsley and A.I. Golov

School of Physics and Astronomy, University of Manchester, Manchester, M13 9PL, UK

Observations of quantum turbulence in pure superfluid ^4He in a container rotating at angular velocity Ω_0 and $T < 0.2$ K are reported. New techniques of large-scale forcing (rotational oscillations of the cubic container at frequency ω and amplitude $\Delta\Omega$) and detecting (monitoring ion transport along the axis of rotation) turbulence were implemented. With increasing the amplitude of forcing, three states of vortex lines near the rotational axis were observed. In the first one, from 0 to $\Delta\Omega_{c1}$, the rectilinear vortex lines are perturbed but not reconnecting yet. In the second one, between $\Delta\Omega_{c1}$ and $\Delta\Omega_{c2}$, a boundary layer of vortex tangle near the axial walls coexists with perturbed rectilinear vortex lines. Above $\Delta\Omega_{c2}$ a bulk vortex tangle fills the cell. Above $\Delta\Omega_{c2}$, the vortex line length, measured using charged vortex rings, increases rapidly. Resonances of inertial waves are observed in both laminar and turbulent states. We show how the critical amplitudes vary when driven both on and off the inertial wave resonances.

P2.40 Design and Characterisation of a Detector for Quasiparticle Imaging Studies and Quantum Turbulence in Superfluid ^3He

D.I. Bradley, M. Človečko, S.N. Fisher, A.M. Guénault, E. Guise, R.P. Haley, G.R. Pickett, and V. Tsepelin

Department of Physics, Lancaster University, UK

Our aim in this work is the visualisation of vortex dynamics in superfluid $^3\text{He-B}$ in the pure quantum regime. To achieve this, we will create a “video” camera consisting of a two-dimensional array of detectors to be illuminated by the quasiparticle gas in the superfluid. At low temperatures quasiparticles in $^3\text{He-B}$ are highly ballistic, but are Andreev scattered by vortices. Hence, a tangle of vortices (quantum turbulence) will cast a shadow when illuminated by a beam of quasiparticles. We will image the shadow with the detector array. Each pixel in the array is formed by a cylindrical channel in a copper block, and placed at the centre of each channel is a miniature quartz tuning fork. In $^3\text{He-B}$, the damping of the forks provides a measure of the local density of quasiparticles proportional to the quasiparticle flux incident on each pixel. To simplify the design we use custom-made 1-D arrays of miniature tuning forks, each carrying five forks with thicknesses of either $50\ \mu\text{m}$ or $75\ \mu\text{m}$. All the forks have a tine width $90\ \mu\text{m}$ but with graduated lengths varying from $1400\ \mu\text{m}$ to $1900\ \mu\text{m}$, to give each a unique and well-separated resonant frequency ranging from 20kHz to 40kHz. We have mounted five such arrays in a copper holder to create a detector of twenty-five pixels. This should allow us to make crude images of quantum turbulence, and other structures, with both time and spatial resolution. Here we present the results of the characterisation of the arrays in vacuum at 4.2K and in normal and superfluid ^4He . The arrays work well in this configuration and the next stage is to transfer the concept to superfluid $^3\text{He-B}$.

P2.41 Decay of Counterflow Quantum Turbulence in Superfluid ^4He

Y. Mineda^a, M. Tsubota^{a,b}, and W.F. Vinen^c

^aDepartment of Physics, Osaka City University, Sumiyoshi-Ku, Osaka 558-8585, Japan

^bThe OCU Advanced Research Institute for Natural Science and Technology (OCARINA), Osaka City University, Sumiyoshi-Ku, Osaka 558-8585, Japan

^cSchool of Physics and Astronomy, University of Birmingham B15 2TT, United Kingdom

We simulated the decay of counterflow quantum turbulence from a statistically steady state at $T=1.9[\text{K}]$. There are parameters which characterize the decay and the steady state turbulence. We calculated by using the vortex filament model with the full Biot-Savart law. In the statistically steady state, we can estimate the parameter c_2 which represents the relationship between the curvature of the vortex lines and the mean distance between vortices, obtaining $c_2 = 1.99 \pm 0.38$ at $T=1.9[\text{K}]$. The decay of quantum turbulence is described by the solution of the Vinen equation¹ which includes the temperature-dependent parameter χ_2 , $\chi_2 = 5.48 \pm 0.88$. The simulation of decay turbulence shows that the vortex line density decays as t^{-1} power law, which is consistent with the solution of the Vinen equation with $\chi_2 = 5.48$.

1. W.F. Vinen, *Proc. R. Soc. London, Ser. A* **240**, 114, (1957); **240**, 128, (1957); **242**, 493, (1957); **243**, 400, (1958).

2. W.F. Vinen and J.J. Niemela, *J. Low Temp. Phys.* **52**, 189 (1983).

P2.42 Propagation of quantized vortices driven by an oscillating sphere in superfluid ^4He

A. Nakatsuji^a, M. Tsubota^{a,b}, and H. Yano^a

^aDepartment of Physics, Osaka City University, Japan

^bThe OCU Advanced Research Institute for Natural Science and Technology (OCARINA), Osaka City University, Japan

We performed numerical simulation of quantum turbulence at 0K generated from remnant vortices by an oscillating sphere. The remnant vortices are extended by the sphere and form a tangle with emitting vortex loops. As time passes, the length of vortices in a computational volume becomes statistical steady. We investigate in the statistical steady state the distribution of the length of vortex loops and anisotropy of their propagation caused by the sphere. The propagation of the emitted vortex loops is anisotropic along the oscillation direction of the sphere. The obtained results are comparable with the experiments using vibrating wires in superfluid ^4He .

P2.43 Time-of-flight Measurements of Vortex Rings Emitted from Quantum Turbulence in Superfluid ^4He

H. Kubo, A. Nishijima, Y. Nago, K. Obara, H. Yano, O. Ishikawa, and T. Hata

Graduate School of Science, Osaka City University, Japan

In the present work, we report the time-of-flights of vortex rings emitted from a turbulent region in superfluid ^4He at low temperatures. We used a vortex-free vibrating wire as a vortex detector. The vortex-free wire can detect only the first colliding vortex during vibration, though it will be refreshed after the vibration stop and be able to detect a vortex again¹.

We measured a flight period from the start of turbulence generation to the vortex detection in the distance between a generator and a detector repeatedly, finding the Poisson distribution of observed periods with a non-detection period t_0 and a mean detection period t_1 . Period t_0 corresponds to a generation time plus a time-of-flight of a vortex ring. By studying two characteristic periods t_0 and t_1 for two flight distances, we find that both periods t_0 and t_1 increase with increasing flight distance. A ring velocity estimated from period t_0 suggests that sizes of vortex rings emitted from the generated turbulence distribute to a range smaller than a generator thickness or a generator vibration amplitude. Vortex rings are emitted radially from a turbulence region, at least in the direction of generator vibration.

1. R. Goto, S. Fujiyama, H. Yano, M. Tsubota, *et al.*, *Phys. Rev. Lett.* **100**, 045301 (2008).

P2.44 Normal fluid profiles in a Helium II counterflow channel

L. Galantucci^a and M. Sciacca^b

^aDipartimento di Ingegneria Strutturale, Politecnico di Milano, Italy

^bDipartimento SAgA, Università di Palermo, Italy

The turbulent and laminar nature of the normal fluid flow is numerically investigated in a two-dimensional Helium II channel counterflow. In particular, the stationary profile of the normal fluid is analysed for varying vortex-line densities, in order to compare the numerical results with the experimental studies of Guo *et al.* who observe a flat profile, orthogonal to the heat flux applied, and assert the turbulent nature of the normal fluid for the heat flux range studied.

1. W. Guo, S.B. Cahn, J.A. Nikkel, D.N. McKinsey, “Visualization study of counterflow in superfluid helium-4 using metastable helium molecules”, *Phys. Rev. Lett.* **105**, 045301, 2010.

P2.45 Waves in a quantized vortex line in superfluid helium

M. Sciacca^a, T. Brugarino^b, M.S. Mongiovì^b, and D. Jou^c

^aDipartimento SAgA, Università di Palermo, Italy

^bDipartimento DIEETCAM, Università di Palermo, Italy

^cDepartament de Física, Universitat Autònoma de Barcelona, Spain

We perform a series of studies devoted to the dynamics of Kelvin waves in a vortex line in superfluid helium and in an eulerian fluid. First we find out that the Hall-Vinen equation for the motion of a vortex line is not properly correct and we theoretically suggest corrections for its improvement. Then, in order to study the dynamics of Kelvin waves along a slender vortex, the Hall-Vinen equation is approximated by the Local Induction Approximation and the Fukumoto's approximation. We propose some exact solutions of the obtained equations, which can be applied both in superfluid helium and in eulerian fluid. All the results are finally addressed to the recent discussion on the Kelvin wave cascade at very low temperature in a superfluid helium.

P2.46 Comparison of the Turbulent Drag Coefficient For Low and High Frequency Vibrating Grids in Superfluid ³He-B

D.I. Bradley, S.N. Fisher, A.M. Guénault, R.P. Haley, G.R. Pickett, V. Tsepelin, and P. Williams

Physics Department, Lancaster University, Lancaster, LA1 4YB. United Kingdom

We present measurements of the dissipative turbulent drag of a low frequency vibrating grid in superfluid ³He-B at temperatures below 180 μ K and at pressures up to 3.8 Bar. We have compared our low frequency grid with a higher frequency grid made from the same copper mesh [1]. We find a substantially lower turbulent drag coefficient at lower frequencies. We also compare our measurements to those of a similar low frequency grid device (again with the same mesh) measured in superfluid ⁴He at temperatures below 20 mK. In this case we find that the turbulent drag coefficient is very similar for the two superfluids [2].

1. Bradley, D.I. et al. "The Damping of a Quartz Tuning Fork in Superfluid ³He-B at Low Temperatures." *Journal of Low Temperature Physics* **157** (5-6) 2009.
2. Bradley, D.I. et al. "The turbulent drag on a low frequency vibrating grid in superfluid ⁴He at very low temperatures." *Physical Review B* **85** (22) 2012.

P2.47 **Direct Measurements of the Energy Dissipated by Quantum Turbulence in Superfluid $^3\text{He-B}$**

D.I. Bradley, S.N. Fisher, A.M. Guénault, R.P. Haley, G.R. Pickett, V. Tsepelin, and P. Williams

Physics Department, Lancaster University, Lancaster, LA1 4YB. United Kingdom

We present new measurements of the energy dissipation by quantum turbulence in superfluid $^3\text{He-B}$. We use a black body radiator bolometer with an order of magnitude less heat leak than our previous measurements [1], allowing us to detect power levels an order of magnitude smaller than before. This allows better measurements of the late time limiting behaviour. Our measurements are consistent with the quantum turbulence having a classical-like Kolmogorov spectrum. We determine the Kolmogorov constant to have the value of around 2.

1. Bradley, D. I. et al. “Direct Measurement of the Energy Dissipated by Quantum Turbulence.” *Nature Physics* **7** (4) 2011.

P2.48 **Self-reconnecting Quantized Vortices in Superfluid Turbulence**

H. Salman^a and A. Baggaley^b

^aSchool of Mathematics, University of East Anglia, Norwich, UK

^bSchool of Mathematics & Statistics, Newcastle University, Newcastle upon Tyne, NE1 7RU

Current theories on superfluid turbulence in the ultra low temperature regime indicate that the turbulence can simultaneously support a quasiclassical Kolmogorov cascade at low wavenumbers and a Kelvin wave driven cascade at higher wavenumbers. This Kelvin wave cascade persists up to scales where the curvature of the vortex line becomes of the order of the healing length upon which energy is radiated in the form of phonons. An immediate question that naturally arises that is of fundamental importance to our understanding of this superfluid turbulent state is “How is the energy transferred from the large scales to the small scales where it can be radiated as phonons?”. It has been argued by some authors [1] that at intermediate scales, a bottleneck forms since the transfer of energy by a Kolmogorov cascade is greater than in the Kelvin wave cascade. Other authors [2] have ruled out the bottleneck scenario by identifying the process of self-recrossings of individual quantized vortices as a mechanism for transferring energy. In this work, we simulate the scenario of self-recrossings of quantised vortices using a microscopically accurate model in the form of the Gross-Pitaevskii equation. Different vortex configurations are studied and results are compared with a hierarchy of vortex filament models of varying degrees of complexity.

1. L’vov, V.S., Nazarenko, S.V., Rudenko, O. (2007). “Bottleneck crossover between classical and quantum superfluid turbulence.” *Phys. Rev. B* **76**, 024520.

2. Kozik, E.V., Svistunov, B.V. (2009). “Theory of Decay of Superfluid Turbulence in the Low-Temperature Limit.” *J. Low Temp. Phys.* **156**, 215.

P2.49 Inertial effects on the motion of a vortex in a Bose-condensed gas

T. Cox^a and P.C.E. Stamp^b

^aDepartment of Physics, University of British Columbia, Vancouver, BC, Canada V6T 1Z1

^bDepartment of Physics and Pacific Institute of Theoretical Physics, University of British Columbia, Vancouver, BC, Canada V6T 1Z1

We study the motion of a vortex under the influence of a harmonic force in an approximately two dimensional trapped Bose-condensed gas. The Hall-Vinen-Iordanskii equations, modified to include a fluctuational force and an inertial mass term, are solved for the vortex motion. The mass of the vortex has a strong influence on the time it takes the vortex to escape the trap. Since the vortex mass also depends on the trap size we have an additional dependence on the trap size in the escape time which we compare to the massless case.

P2.50 Anomalous damping of a low frequency vibrating wire in superfluid ³He-B due to vortex shielding

D.I. Bradley, M. Fear, S.N. Fisher, A.M. Guénault, R.P. Haley, C.R. Lawson, G.R. Pickett, R. Schanen, and V. Tsepelin

Department of Physics, Lancaster University, Lancaster, LA1 4YB, United Kingdom

We have investigated the behaviour of a low frequency vibrating wire [1] in the B phase of superfluid helium-3 at zero pressure and temperatures around $0.15 T_C$. The vibrating wire has a goalpost shape with a 25 mm leg length and 8 mm crossbar. It has a low resonant frequency around 60 Hz. Placed in a vertical magnetic field of ~ 100 mT, it is forced into oscillatory motion by passing an ac current through the wire. Its velocity can be inferred from the ac Faraday voltage generated as the crossbar sweeps through the magnetic field. At low velocities the motion of the wire is impeded by its intrinsic (vacuum) damping and by the scattering of thermal quasiparticles. At higher velocities we would normally expect the motion to be further damped by the creation of quantized vortices and broken Cooper pair excitations. However, for a range of temperatures, as we increase the driving force we observe a sudden *decrease* in the damping of the wire. This indicates that the wire is shielded from thermal quasiparticles by quantized vortex lines created by the wire itself.

1. Bradley, D. I. et al. (2011). "A New Device for Studying Low or Zero Frequency Mechanical Motion at Very Low Temperatures" *Journal of Low Temperature Physics* **165**, 3-4, (114-131).

P2.51 **The onset of vortex production by a vibrating wire in superfluid $^3\text{He-B}$**

D.I. Bradley^a, S.N. Fisher^a, A. Ganshin^b, A.M. Guénault^a, R.P. Haley^a, M.J. Jackson^a, G.R. Pickett^a, and V. Tsepelin^a

^aDepartment of Physics, Lancaster University, Lancaster, LA1 4HP, UK

^bPresent address: Laboratory for Elementary-Particle Physics, Cornell University, USA.

We present measurements of the force-velocity response of a vibrating wire resonator in superfluid $^3\text{He-B}$ at very low temperatures. At low velocities the response is dominated by intrinsic (vacuum) damping whilst at high velocities it is dominated by pair-breaking. At intermediate velocities there is a series of small plateaus where the velocity often shows small oscillations. We believe that the behavior results from the stretching of vortices pinned to the wire. The vortices grow and self-reconnect, emitting a vortex ring. The behavior is very sensitive to the presence of surrounding vortices generated by a neighboring vibrating wire.

4.5 Invited Oral Presentations: Saturday August 18th

09.1 The quantum plasticity of helium crystals

S. Balibar, A. Haziot, X. Rojas, A. Fefferman, and J. Beamish*

Laboratoire de Physique Statistique de l'ENS,
associé au CNRS et aux Universités Paris Diderot et P.M. Curie,
24 rue Lhomond, 75231 Paris Cedex 05 (France)

The plasticity of crystals is usually attributed to the motion of their dislocations. Solid helium offers unique opportunities to study the basic mechanisms of this plasticity. This is because it can be prepared and studied at low temperature without any impurity and with very low dislocation densities. Taking advantage of these exceptional properties, we have discovered that, in the absence of impurities and at low enough temperature, helium crystals do not resist to shear in one particular direction because dislocations may glide by quantum tunneling along the basal planes of the hexagonal structure. This "quantum plasticity" is reversible and disappears as soon as traces of ^3He impurities bind to dislocations or if their mobility is damped by collisions with thermal phonons.

I will explain why this plasticity is an alternative explanation in many - but not all - "torsional oscillator experiments" where supersolidity was invoked to explain rotation anomalies in the same crystals.

This work is supported by grants from ERC (AdG 247258-SUPERSOLID) and from NSERC Canada.

*permanent address: Department of Physics, University of Alberta, Edmonton, Canada

09.2 Liquid Helium in Solid Helium

H. Lauter^a, E. Krotscheck^b, E. Katz^c, M. Koza^c, V.V. Lauter^d, I. Kalinin^e, and A.V. Puchkov^e

^aOak Ridge National Laboratory, Oak Ridge, USA

^bDepartment of Physics, University at Buffalo SUNY, Buffalo New York, USA

^cInstitut Laue-Langevin, Grenoble, France

^dOak Ridge National Laboratory, Oak Ridge, USA

^eInstitute for Physics and Power Engineering, Obninsk, Russia

We demonstrate that a localized superfluid component exists at high pressures within solid helium in aerogel. Its existence is deduced from the observation, by neutron scattering, of two sharp phonon-roton spectra, which are clearly distinguishable from modes in bulk superfluid helium. These roton excitations show gap parameters different from those observed in the bulk fluid at freezing temperature. One of the modes vanishes by increasing the temperature to 1.3K. Comparison with many body calculations suggests that the model that reproduces the observed data best is that of superfluid double layers within the solid and at the helium-substrate interface.

09.3 Defects and glassy dynamics in solid ^4He : Perspectives and current status

A.V. Balatsky^a, M.J. Graf^a, N. Nussinov^b, and J.J. Su^c

^aLos Alamos National Laboratory, Los Alamos, New Mexico 87545, USA

^bDepartment of Physics, Washington University, St. Louis, Missouri 63160, USA

^cGinzton Laboratory, Stanford University, Stanford, California 94305, USA

We review the anomalous behavior of solid ^4He at low temperatures with particular attention to the role of structural defects present in solid. The discussion centers around the possible role of two level systems and structural glassy components for inducing the observed anomalies. We propose that the origin of glassy behavior is due to the dynamics of defects like dislocations formed in ^4He . Within the developed framework of glassy components in a solid, we give a summary of the results and predictions for the effects that cover the mechanical, thermodynamic, viscoelastic, and electro-elastic contributions of the glassy response of solid ^4He . Our proposed glass model for solid ^4He has several implications:

- 1) The anomalous properties can be accounted for by allowing defects to freeze out at lowest temperatures. The dynamics is governed by glasslike (glassy) relaxation processes and the distribution of relaxation times varies significantly between different torsional oscillator, shear modulus, and dielectric function experiments.
- 2) Any defect freeze-out will be accompanied by thermodynamic signatures consistent with entropy contributions from defects. It follows that such entropy contribution is much smaller than the required superfluid fraction, yet it is sufficient to account for excess entropy at lowest temperatures.
- 3) We predict a Cole-Cole type relation between the real and imaginary part of the response functions for rotational and planar shear that is occurring due to the dynamics of defects. Similar results apply for other response functions.
- 4) We predict low-frequency electro-elastic features in defect rich ^4He crystals. These predictions allow one to directly test the ideas and very presence of glassy contributions in ^4He .

09.4 Mass flux measurements in solid ^4He : status and new work

R.B. Hallock

Laboratory for Low Temperature Physics, Dept. of Physics., Univ. of Mass., Amherst, MA, USA

A brief review of some of the mass flux measurements in the presence of solid ^4He conducted at the University of Massachusetts in collaboration with Michael Ray will be presented, with an emphasis on the temperature dependence of the flux at fixed pressure. These experiments, off but near the melting curve, showed a rising flux with falling temperature below 650 mK, and a sharp minimum in the flux in the vicinity of 75 mK¹. The flux was seen to be unstable in the vicinity of the flux minimum. More recent work done in collaboration with Yegor Vekhov is generally consistent with previous work, but has studied in much more detail the behavior of the flux for $T > 100$ mK. In this work, the thermo-mechanical effect in superfluid helium was again used: an applied temperature difference was used to create a changing chemical potential difference, $\Delta\mu$, across a solid helium-4 sample. The flux, F , was studied in detail as a function of $\Delta\mu$ and temperature near 25.7 bar². We find that at fixed temperature the flux depends on $\Delta\mu$ in a nonlinear way, $F \sim (\Delta\mu)^b$, with b independent of temperature; $b \approx 0.32$. We also find that at fixed $\Delta\mu$ the flux can be represented by $F \sim -\ln(T/\tau)$, with $\tau \approx 630\text{mK}$. These experiments, with a concentration on our recent work, will be described and possible interpretations, including the evidence for Bosonic Luttinger liquid behavior, will be discussed.

1. M.W. Ray and R.B. Hallock, Phys. Rev. Letters 100, 235301 (2008); 105, 145301 (2010) and Phys. Rev. B 79, 224302 (2009); 84, 144512 (2011).
2. Ye. Vekhov and R.B. Hallock, arXiv cond-mat 1205.5751.

O10.1 Symmetry of Kelvin-wave dynamics and the Kelvin-wave cascade in the $T = 0$ superfluid turbulence

E.B. Sonin

Racah Institute of Physics, Hebrew University of Jerusalem, Givat Ram, Jerusalem 91904, Israel

The talk will discuss the implications of tilt symmetry (symmetry with respect to tilting of the coordinate axis with respect to which vortex motion is studied) in the nonlinear dynamics of Kelvin waves. The conclusion is that although the spectrum of a Kelvin wave is not tilt-invariant, this does not compromise the tilt invariance of the Kelvin-wave cascade that is currently being vividly debated in the theory of superfluid turbulence. This conclusion supports the assumption of locality in the analysis of the Kelvin-wave cascade.

The effect of strong kelvon interaction on the power-law exponent for the Kelvin-wave cascade is also considered. It is argued that there is no universal power law in the Kelvin-wave cascade, which may depend on power input into the cascade. The power laws between $k^{-3.4}$ and k^{-3} for the kelvon distribution function are possible.

Finally a simple picture of the crossover from the classical Kolmogorov cascade to the quantum Kelvin-wave cascade is suggested, which does not encounter a mismatch problem of the energy distributions at the crossover and does not require a broad intermediate interval for realization of the crossover.

O10.2 Kelvin-wave spectrum of a pinned vortex

R. Hänninen and N. Hietala

O.V. Lounasmaa Laboratory, Aalto University, Finland

At low temperatures the Kelvin-wave cascade is expected to play an important role in energy dissipation. We illustrate with numerical simulations that the theoretical spectra are not robust. Stable results require fine-tuning of the drive and dissipation. When a drive is applied in a configuration, which resembles one applied in experiments, different Kelvin spectra are found. For example, a vortex driven with pinned end points results in a spectrum $|w_k| \propto k^{-\eta}$ with $\eta \approx 1.88$.¹

The effect of mutual friction damping on the Kelvin wave cascade is of central interest. As expected, dissipation increases rapidly when more small-scale structure is present. We estimate the temperature where novel dissipation mechanism beyond mutual friction may become relevant in experiments with superfluid ⁴He and ³He-B.

We also demonstrate that the interaction of Kelvin waves of finite amplitude gives rise to new effects compared to theory, which is derived in the small amplitude limit. For example, even the local induction approximation (LIA) results in a nonzero cascade. This cascade, due to finite amplitude, dominates in numerical simulations (whether LIA or Biot-Savart) where the periodic boundary conditions discretize the spectrum and the “normal” Kelvin wave cascade with $3 \leftrightarrow 3$ scattering is suppressed because energy and momentum conservation cannot be simultaneously satisfied.

1. R. Hänninen: Steady-state spectrum of Kelvin waves on a quantized vortex at finite temperatures, arXiv:1104.4926.

O10.3 Decay regimes and spectra of quantum turbulence at low temperatures

Y A. Sergeev^a, C.F. Barenghi^b, and A.W. Baggaley^b

^aJoint Quantum Centre Durham-Newcastle, School of Mechanical and Systems Engineering, Newcastle University, Newcastle upon Tyne, NE1 7RU, United Kingdom

^bJoint Quantum Centre Durham-Newcastle, School of Mathematics and Statistics, Newcastle University, Newcastle upon Tyne, NE1 7RU, United Kingdom

We address a long-standing question of hydrodynamic natures of the ultraquantum ($L \sim t^{-1}$, where L is the vortex line density) and the quasiclassical ($L \sim t^{-3/2}$) decay regimes of quantum turbulence in the zero-temperature limit. We present a numerical model which reproduces both the quasiclassical and the ultraquantum regimes in the case where turbulence is generated, as in the experiments^{1,2}, by forcing at some intermediate length scale. By examining the time-dependent energy spectra, probability distribution function of the vortex line curvature, and the energy transfer to the regions of large and small wavenumbers, we determine the conditions leading to either quasiclassical or ultraquantum decay. We also identify the mechanism of generation of large-scale flow structures resulting in the formation of the Kolmogorov spectrum and, after the forcing has been stopped, in the quasiclassical decay of quantum turbulence.

1. P. M. Walmsley and A. I. Golov, Phys. Rev. Lett. **100**, 245301 (2008).
2. D. I. Bradley *et al.*, Phys. Rev. Lett. **96**, 035301 (2006).

O10.4 Vortex Emission from Quantum Turbulence Generated by a Vibrating Wire in Superfluid ⁴He

H. Yano, H. Kubo, Y. Nago, A. Nishijima, K. Obara, O. Ishikawa, and T. Hata

Graduate School of Science, Osaka City University, Japan

An oscillating obstacle generates a quantum turbulence in superfluids, when vortices remained attached to obstacle surfaces or vortex rings collided with it during oscillation.^{1,2} A turbulence provides a source of vortex rings; however, the characteristics of these vortex rings are not clear. In the present work, we report the flight of vortex rings generated from quantum turbulence in superfluid ⁴He, using two vibrating wires as a source of vortex rings and a detector of a vortex ring. A vortex-free vibrating wire can detect only the first colliding vortex ring, though it will be refreshed after low vibration and be able to detect a vortex ring again.¹

By measuring time-of-flights of vortex rings repeatedly, we find the velocity and direction distributions of vortex rings emitted from quantum turbulence. At finite temperatures, the time-of-flight of a detectable vortex ring increases linearly with the mutual friction between a vortex and a normal fluid component, suggesting that small, therefore rapid, vortex rings dissipate between the wires and only large vortex rings may reach the detector. We estimate the ring size of a detectable vortex from the flight distance and the mutual friction, finding that emitted vortex rings are distributed to a size comparable with a turbulence region.

1. R. Goto, S. Fujiyama, H. Yano, M. Tsubota, *et al.*, Phys. Rev. Lett., **100**, 045301 (2008).
2. Y. Nago, M. Inui, H. Yano, *et al.*, Phys. Rev. B, **82**, 224511 (2010).

O11.1 Universality and pattern forming in polariton condensates

N.G. Berloff

Department of Applied Mathematics and Theoretical Physics, University of Cambridge, Wilberforce Road, Cambridge, CB3 0WA, United Kingdom

At the root of any universal behavior of pattern-forming systems lies common theoretical description, which is independent of the system considered. Such common theoretical framework is achieved when the detailed microscopic description is reduced to an order parameter equation. Starting with a generic laser model based on the Maxwell-Bloch equations the models of nonequilibrium condensates can be derived and analyzed based on the assumption of a smooth crossover between lasers and nonequilibrium condensates [1]. Exciton-polaritons, hybrids of excitons and photons in semiconductor microcavities, and magnons, which are elementary excitations – quantized spin waves – of a magnetic system, are two of several examples of quasi-particles inside solids which present opportunities to explore condensation and pattern formation.

In my talk I will draw the analogy between lasers, exciton-polariton and magnon condensates emphasising the similarities and differences in modelling and pattern forming behavior of these system. Using microcavities on a semiconductor chip supporting two-dimensional polariton condensates we directly visualize the formation of a spontaneously oscillating quantum fluid. This system is created on the fly by injecting polaritons at two or more spatially separated pump spots.

1.N.G. Berloff and J. Keeling “Universality in modelling non-equilibrium polariton condensates,” book chapter in ”Quantum Fluids: hot-topics and new trends”, eds. A. Bramati and M. Modugno, Springer Verlag (2012).

O11.2 Magnetic BEC and spin superfluidity in antiferromagnetics

Yu. M. Bunkov^a, E. N. Alakshin^b, R. R. Gazizulin^b, A. V. Klochkov^b, V. V. Kuz'min^b, and M. S. Tagirov^b

^aInstitute Neel, CNRS, Grenoble, France

^bKazan (Volga Region) Federal University, Kazan, Russia

The Spin Superfluidity and Bose-Einstein condensation (BEC) of magnons have been observed previously in superfluid ³He. Indeed, the ³He superfluidity itself forms the corresponding profile of magnetic energy and does not involved directly to the Spin Superfluidity. It was a challenge to observe the similar phenomena in a solid body magnetic materials. We have found experimentally the effect of magnon BEC on a nuclear spin waves mode in antiferromagnetic CsMnF₃ and MnCO₃. It has the same properties as a magnon BEC states in ³He-A in aerogel. The last experiments shows the existence of “persistent” signal in these systems.

1. Yu. M. Bunkov, E. M. Alakshin, R. R. Gazizulin, A.V. Klochkov, V.V. Kuzmin, V.S. L'vov, and M.S. Tagirov. (2012). “High T c spin superfluidity in antiferromagnets”. Phys. Rev. Lett. 108, 177002.

O11.3 Self trapping and relaxation of magnon condensates in superfluid $^3\text{He-B}$

V.B. Eltsov^a, S. Autti^a, Yu.M. Bunkov^b, P.J. Heikkinen^a, J.J. Hosio^a, M. Krusius^a, G.E. Volovik^{a,c}, and V. Zavjalov^a

^aO.V. Lounasmaa Laboratory, Aalto University, P.O. Box 15100, 00076 AALTO, Finland

^bInstitute Néel, CNRS, Grenoble, France

^cLandau Institute for Theoretical Physics, Kosygina 2, 119334 Moscow, Russia

In superfluid $^3\text{He-B}$ traps for bosonic magnon excitations can be formed by the order-parameter texture and the applied profile of the static magnetic field. At temperatures around $0.2T_c$ and below we pump magnons to the trap using NMR techniques and create macroscopic occupation of the ground or of a selected excited level. Such magnons form Bose-Einstein condensates as demonstrated by the long-lived coherent spin precession after switching the pumping off. This is the first realization of the BEC at an excited level of the trap [1]. The orbital texture is flexible and as the magnon occupation number increases the profile of the trap gradually changes from harmonic to a square well with walls almost impenetrable to magnons. This is the first experimental example of Bose-Einstein condensation in a box and an analog of the MIT bag model of hadrons in QCD [2].

With decreasing temperature the life time of the magnon condensates rapidly increases and reaches minutes. Our measurements of the relaxation rate in a rotating sample filled with vortex lines clearly demonstrate two contributions to the relaxation: One contribution is proportional to the density of the bulk thermal quasiparticles and the other is approximately temperature-independent but increases linearly with the vortex density. We discuss whether the latter contribution can be attributed to Majorana fermions bound to the vortex cores.

1. S. Autti *et al.*, Phys. Rev. Lett. **108**, 145303 (2012). 2. S. Autti *et al.*, Pis'ma ZhETF **95**, 610 (2012).

O12.1 MWN Collaboration: Multi-Faceted Approach to Quantum Turbulence

G.G. Ihas

Department of Physics, University of Florida, Gainesville, Florida 32607, USA

Five universities (Birmingham, Florida, Lancaster, Manchester, and Yale) began collaborating 2 years ago to study some of the basic problems faced in quantum turbulence. To date, ^4He has been the fluid, with its quantized vorticity and 2-fluid behaviour. Vorticity has been created by rotating a bucket, and turbulence by sudden cessation of rotation, in a wide range of temperatures down to 20 mK. Thermal counterflow has been used just below the λ point. Grids pushed by superconducting actuators or floppy grids vibrating on superconducting wires have been used at millikelvin and higher temperatures. Excited helium molecules (excimers) have been used as small, neutral probes of turbulence, and as tracer particles with laser fluorescence. Second sound and MEMS pressure probes are also used. Three posters and one other talk at this conference expand on the works presented here^{1,2,3,4}. These projects supported in part by US NSF DMR-1007974 and DMR-1007937 and UK EPSRC EP/H04762X/1 and EP/I003738/1.

1. D.E. Zmeev, F. Papkour, P.M. Walmsley, A.I. Golov, P.V.E. McClintock, S.N. Fisher, W. Guo, D.N. McKinsey, G.G. Ihas, and W.F. Vinen, Observation of Crossover from Ballistic to Diffusion Regime for Excimer Molecules in Superfluid ^4He ; 2. W. Guo, D.N. McKinsey, A. Marakov, K.J. Thompson, G.G. Ihas, W.F. Vinen, Visualization Technique for Determining the Structure Functions of Normal-fluid Turbulence in Superfluid ^4He ; 3. L.E. Munday, K.J. Thompson, G.G. Ihas, R. Chapurin, P.V.E. McClintock, W.F. Vinen, S.N. Fisher, and J.H. Yang, Second Sound Attenuation of Decaying Quantum Grid Turbulence in Liquid ^4He ; 4. A. Golov, Excimer molecules as tracer particles for study of quantum turbulence in superfluid ^4He , QFS Session 12.

O12.2 Nonlinear dynamics in nanomechanical resonators

E. Collin^a, M. Defoort^a, K. Lulla^a, C. Blanc^a, J-S. Heron^a, T. Moutonet^a, F. Pistolesi^b, O. Bourgeois^a, Yu.M. Bunkov^a, and H. Godfrin^a

^aInstitut Néel - CNRS Grenoble, France

^bLOMA - CNRS Bordeaux, France

Nanomechanical devices have attracted recently the interest of physicists for both applications and their fundamental understanding. Indeed, these artificial mechanical devices can be studied and controlled in such an accurate way that they become model systems in which fundamental issues of (here classical) mechanics can be addressed.

We present results on a special type of goalpost-shaped nanomechanical devices studied at low temperatures. Particular care is taken in calibrating the setup and understanding the resonance properties of the system [1]. Using a linear excitation technique (magnetomotive) combined with a strongly nonlinear one (capacitive), we can efficiently tune nonlinear effects in the nanoresonator. Parametric amplification with an exceptional gain has been realized and applied to the study of thin films anelasticity [2]. Audio-mechanical mixing has been demonstrated [3]. Finally, the physical issue of dynamic bifurcation, of ubiquitous interest in physics (linked to thermal activation of Josephson junctions, the kinetics of chemical reactions, the dynamics of magnetic macro-molecules...), is presented [4].

[1] E. Collin *et al.*, Rev. Sci. Instrum. In press (04/2012).

[2] E. Collin *et al.*, Phys. Rev. B **84**, 054108 (2011).

[3] M. Defoort *et al.*, Appl. Phys. Lett. **99**, 233107 (2011).

[4] M. Defoort *et al.*, article under preparation.

O12.3 Investigation of Transport Properties in Thin Films of Liquid ³He Using MEMS Devices

Y. Lee^a, M. Gonzalez^a, P. Zheng^a, E. Garcell^a, and H.B. Chan^b

^aDepartment of Physics, University of Florida, Gainesville, Florida, USA

^bDepartment of Physics, The Hong Kong University of Science and Technology, Clear Water Bay, Hong Kong

Using a commercial micro-machining process, novel MEMS oscillators were designed, manufactured, and characterized for the study of thin films of quantum fluids.¹ The MEMS device, composed of a pair of parallel plates separated by a well-defined gap, gives access to physics in the high Knudsen regime and allows investigation of surface scattering effects in thin films of quantum fluids. Detailed measurements on the mechanical properties of an oscillator submerged in liquid ³He were performed in a wide range of temperature between 20 and 800 mK and at pressures of 3, 21 and 29 bar. In the Fermi liquid regime, when the bulk contribution to the damping is subtracted, these measurements show a distinct peak in the coefficient of damping and a reduction in the fluid mass coupled to the oscillator below 100 mK. This work demonstrates the potential of MEMS devices as a novel probe in a wide range of low temperature experiments, in particular, in quantum fluids such as superfluid ³He films.

This work is supported by NSF (YL) under DMR-0803516 and DMR-1205891.

1. M. Gonzalez, P. Bhupathi, B.H. Moon, P. Zheng, G. Ling, E. Garcell, H.B. Chan, and Y. Lee, J. Low Temp. Phys. **162**, 662 (2011).

O12.4 Excimer Molecules as Tracer Particles for Study of Quantum Turbulence in Superfluid ^4He

D.E. Zmeev^b, F. Papkour^a, P.M. Walmsley^a, A.I. Golov^a, P.V.E. McClintock^b, S.N. Fisher^b, W. Guo^c, D.N. McKinsey^c, G.G. Ihas^d, and W.F. Vinen^e

^aSchool of Physics and Astronomy, The University of Manchester, Manchester, UK

^bPhysics Department, Lancaster University, Lancaster, UK

^cDepartment of Physics, Yale University, New Haven, Connecticut, USA

^dDepartment of Physics, University of Florida, Gainesville, Florida, USA

^eSchool of Physics and Astronomy, University of Birmingham, Birmingham, UK

Excimer molecules He_2^* are good candidates for tracer particles in the studies of the microscopic dynamics of tangles of quantized lines in superfluid ^4He in the zero-temperature limit: they are small, passive, long-lived; they can be injected in situ, are expected to be trapped on vortex cores and can be visualised using laser-induced fluorescence.

In this work we studied dynamics of the molecules in the stationary superfluid as well as in the presence of vortices generated by either rotation or ion injection. The molecules, created by electrons field-emitted from a tungsten tip, travelled several centimetres to gridded detector electrodes; the detection field being $10^4 - 10^5$ V/cm. We were able to measure the time of flight of the molecules at temperatures below 300 mK and interpret the results in terms of interaction with phonons.

In the presence of vortex lines, fewer molecules reach the detector; the corresponding trapping diameter of the molecules on vortices was found to be 100 nm at zero pressure.

We have also demonstrated that a turbulent tangle, produced using an auxiliary tungsten tip, can be decorated with the molecules.

4.6 Poster Presentations: Saturday August 18th

P3.1 Isovalent substitution and heat treatments control of T_c , chain oxygen disorder and structural phase transition in high T_c superconductors

A. Aboukassima^a, A. Nafidi^a, H. Chaib^a, B. Marí Soucase^b, K. Chander Singh^c, and B. Hartiti^d

^aLPMC Nano RE, University Ibn Zohr, Agadir, Morocco^bLaboratory of Optoelectronics, Universitat Politècnica de València, Spain.^cDepartment of chemistry, M.D.University, Rohtak, India.

^dLPMAER, University Hassan II Mohammédia, Morocco.

We report here on the preparation, X-ray diffraction with Rietveld refinement, AC magnetic susceptibility measurements and effect of heat treatments in $(Y_{1-x}Nd_x)SrBaCu_3O_{6+z}$. Each sample was subject to two types of heat treatment: oxygen annealing [O] and argon annealing followed by oxygen annealing [AO]. For each x, the [AO] heat treatment increases the orthorhombicity $\varepsilon = (b - a)/(b + a)$ (for $0 < x < 1$), T_c (for $x > 0.2$ and by 9.8 K for $x = 1$) and the distance $d[Cu(1)-(Sr/Ba)]$ (decrease T_c) for $x < 0.25$ and decrease it (increase T_c) for $x > 0.25$. When x increase from 0 to 1, ε decreases to 0 with transition from orthorhombic to tetragonal structure. $\varepsilon[O]$ decreases with $T_c[O]$. However, $T_c[AO]$ decreases with $\varepsilon[AO]$ until $x = 0.2$, increases for $x = 0.4$ and after it decreases by 9.8 K to 77.2 K for $x = 1$ [AO]. A remarkable correlations were observed between $T_c(x)$ and the volume of the unit cell $V(x)$; and between $T_c(x) = T_c[AO] - T_c[O]$ and $\delta\varepsilon(x)$. A combination of several factors such as decrease in $d[Cu(1)-(Sr/Ba)]$; increase in cationic and chain oxygen ordering; the number $p_{sh}(x)$ of holes by Cu(2)-O2 superconducting plans and in-phase purity for the [AO] samples may account for the observed data.

P3.2 Nonequilibrium superconductivity in double tunnel junction with spatially inhomogeneous superconducting electrode

E. M. Rudenko, I. V. Korotash, A. A. Krakovny, and D. S. Dubyna

G.V.Kurdyumov Institute for Metal Physics, N.A.S. of Ukraine

The study of nonequilibrium superconductivity (NS) from the viewpoint of both fundamental physics and practical application is of considerable interest. Nonequilibrium processes occurring in superconducting electrodes with a spatially inhomogeneous order parameter (SIOP) can not be described within the frameworks of the existing theory¹ which has been proposed for electrodes with a spatially homogeneous distribution parameter. Therefore, for further advancement of nonequilibrium theory for electrodes with SIOP extensive experimental evidence is to be accumulated. For this purpose, single and double tunnel junctions with SIOP electrodes have been produced and their current-voltage characteristics (CVCs) at the temperature of 4.2 K measured. These CVCs allow us to draw conclusions concerning various mechanisms leading to NS in the electrodes with SIOP. Influence of the injection current on the energy gap and the proximity effect parameter of the inhomogeneous electrode have been studied. The effective quasiparticle recombination time has been estimated.

1. V.F. Elesin, V.E. Kondratov, A. S. Suhih, Sol. State Phys., **21**, 3226 (1979).

P3.3 Kohn anomaly and acoustic properties of superconductors

R. Chaudhury

S.N. Bose National Centre For Basic Sciences, Calcutta, India

Interacting electron fluid at low temperature provides a fascinating ground for condensed matter physicists, both theoreticians and experimentalists to test various ideas involving the many-body aspects of microscopic physics. In the presence of attractive interaction mediated by phonons, the electron fluid existing in the form of an ordinary 3-dimensional Fermi Liquid can undergo superconducting instability. One manifestation of this phase transition appears as a distinct difference in the behaviour of the acoustic dispersion and attenuation in the normal and superconducting phases, arising from Kohn anomaly related effects. The occurrences of anomalies and singularities in the dispersion and lifetime of acoustic phonons are shown to be characterized functionally differently in the two phases. The origin of this difference is traced to the distinct nature of the energy spectrum of the quasi-particles in the two phases. The results are discussed in the background of recent experiments performed in superconducting *Pb* and *Nb*¹. Some conjectures are made regarding the possible scenarios for various types of non-conventional superconductors.

1. Chaudhury, R. and Das, M.P. (2010). “Kohn Anomaly Energy in Conventional Superconductors Equals Twice the Energy of the Superconducting Gap : How and Why?”. *International Journal of Modern Physics B* 24, 5172; Aynajian P. et al (2008). “Energy Gaps and Kohn Anomalies in Elemental Superconductors”. *Science* 319, 1509.

P3.4 The high pressure superconductivity in CaLi₂ compound: the thermodynamic properties

R. Szcześniak, A.P. Durajski, and P.W. Pach

Institute of Physics, Częstochowa University of Technology, Poland

The thermodynamic properties of the superconducting state in CaLi₂ at 60 GPa have been described. The numerical analysis has been conducted in the framework of the Eliashberg formalism. It has been shown that: (i) the critical value of the Coulomb pseudopotential is equal to 0.20, what corresponds to the value of 1794.85 meV for the Coulomb potential; (ii) the critical temperature (T_C) cannot be calculated correctly by using the McMillan and Allen-Dynes (AD) formula, so the AD formula has been re-parameterized; (iii) the dimensionless ratios: $T_C C^N(T_C) / H_C^2(0)$, $(C^S(T_C) - C^N(T_C)) / C^N(T_C)$ and $2\Delta(0) / k_B T_C$ take the non-BCS values: 0.157, 1.78 and 3.85, respectively. The symbol C^N represents the specific heat in the normal state, C^S denotes the specific heat in the superconducting state, $H_C(0)$ is the thermodynamic critical field near the temperature of zero Kelvin, and $\Delta(0)$ is the order parameter; (iv) the ratio of the electron effective mass to the electron band mass assumes the high value in the whole range where the superconducting state exist, and its maximum is equal to 2.15 for $T = T_C$.

P3.5 Thermal conductivity measurements of $\text{Dy}_2\text{Ti}_2\text{O}_7$ (Spin Ice) and $\text{Y}_2\text{Ti}_2\text{O}_7$ in the temperature range 15 mK to 20 K

S.L. Ahlstrom, D.I. Bradley, M. Človečko, S. N. Fisher, D. Garg, A.M. Guénault, E. Guise, G.R. Pickett, R.P. Haley, M. Poole, R. Schanen, V. Tsepelin, and A. Woods

Physics Department, Lancaster University, Lancaster, UK

Spin Ice is an interesting material which is able to support magnetic monopoles at low temperatures. We have studied the thermal conductivity of two single crystal compounds; one of $\text{Y}_2\text{Ti}_2\text{O}_7$ and one of $\text{Dy}_2\text{Ti}_2\text{O}_7$. The two samples have very similar structures but the Yttrium compound is non-magnetic and therefore cannot support monopoles. We can therefore investigate the influence of magnetic monopoles on the thermal conductivity. For the thermal conductivity measurements we use three Ruthenium Oxide (RuO_2) resistors. One of these resistors is used as a heater to create a temperature gradient across the sample. The other two resistors are used as thermometers to measure the temperature either side of the sample. These samples are mounted on the mixing chamber of a homemade dilution refrigerator. The temperature was varied from 15 mK to 20 K in magnetic fields of 0 and 3.3 T.

Our measurements show a T^2 dependence for the thermal conductivity of $\text{Dy}_2\text{Ti}_2\text{O}_7$ at low temperatures (< 0.7 K). The thermal conductivity of the $\text{Y}_2\text{Ti}_2\text{O}_7$ sample shows the similar behaviour to the $\text{Dy}_2\text{Ti}_2\text{O}_7$ at higher temperatures. Measurements of the $\text{Y}_2\text{Ti}_2\text{O}_7$ at lower temperatures are still in progress. Also, we present measurements of heating spikes during magnetic field sweeps. These are thought to be associated with step changes in magnetisation resulting in thermal runaway in Spin Ice samples.

P3.6 Spin superfluidity, coherent spin precession, and magnon BEC

E.B. Sonin

Racah Institute of Physics, Hebrew University of Jerusalem, Givat Ram, Jerusalem 91904, Israel

Spin superfluidity, coherent spin precession, and magnon BEC are intensively investigated theoretically and experimentally nowadays. Meanwhile, clear definition and differentiation between these tightly related phenomena is needed. In particular, it is argued that spin stiffness, which leads to existence of coherent spin precession and non-dissipative spin supercurrents, is a necessary but not sufficient condition for spin superfluidity. The latter is defined as a possibility of spin transport on macroscopical distances with sufficiently large spin supercurrents. This possibility is realized at special topology of the magnetic-order-parameter space, such as, e.g., that in easy-plane antiferromagnets. Sufficiently large spin supercurrents mean that they essentially exceed supercurrents existing in domain walls or generated by inhomogeneity of samples, where coherent precession is excited.

P3.7 Crystal size effects on ferromagnetic heavy fermion compound UGe₂

A. Yamaguchi^a, H. Nakano^a, N. Sugimoto^a, G. Motoyama^a, A. Sumiyama^a, H. Kashiwaya^b, and S. Kashiwaya^b

^aGraduate School of Material Science, University of Hyogo, Hyogo, 678-1297, Japan

^bNanoelectronics Research Institute of Advanced Industrial Science and Technology (AIST), Tsukuba, 305-8568, Japan

The heavy-fermion compound UGe₂ is attracting much interests because it shows superconductivity in the ferromagnetic state at low temperature and high pressure. We report here crystal size effects on a magnetization curve for single crystals of UGe₂ at 4.2K. The magnetization curve shows characteristic hysteresis loop with several magnetization jumps. The crystal size dependence of the coercive fields and magnetization jumps might be explained in terms of the nucleation and motion of the magnetic domains. Our plan for magnetization measurements of tiny crystals in low temperature and high pressure, using micro-SQUID magnetometer is also presented.

P3.8 New features of a glassy phase in solid helium at the supersolid region

A.S. Rybalko, A.A. Lisunov, V.A. Maidanov, V.Yu. Rubanskyi, S.P. Rubets, E.Ya. Rudavskii, and E.S. Syrkin

B. Verkin Institute for Low Temperature Physics and Engineering of the National Academy of Sciences of Ukraine, Kharkov, Ukraine

A series of experiments have been performed to find out the conditions for formation of disordered (glassy) state in ³He crystals. The high-precision pressure measurements at constant volume demonstrated that a glassy phase was easily generated in quenched cooled crystals grown under uniform temperature conditions in the presence of big number of nuclei and could be removed only after careful annealing. This result was found in both ³He and ⁴He. It does not depend on the type of quantum statistics and is defined mainly by the conditions of the crystal growth. Analysis of similar measurements also was made for some other cell, where the temperature gradient was created in the process of crystal growth. In that case an additional number of defects, created due to deformation of the crystal, were required for formation of a glassy phase. The degree of crystal deformation achieved in the experiment was sufficient for the formation of glassy phase in solid ⁴He, but not in ³He, where the atoms had higher amplitude of zero-point oscillations.

P3.9 Metastable States of ^3He - ^4He Solid Solutions in Pre-separation Region

K. A. Chishko, T.N. Antsygina, A.A. Lisunov, V.A. Maidanov, V.Y. Rubanskyi, S.P. Rubets, and E.Ya. Rudavskii

B.Verkin Institute for Low Temperature Physics and Engineering, Kharkov, Ukraine

A rigorous thermodynamic theory is applied to interpret the experimentally observed behavior of ^3He - ^4He mixed crystals at arbitrary concentrations $x_3 = 1 - x_4$ of the components. The experiments were performed using the precision barometry method on the solutions with $0.01 \leq x_3 \leq 0.9$. Temperature dependences of the pressure $P(T)$ in homogeneous solid mixtures have been studied both above and below the equilibrium phase separation temperature T_s . With decreasing temperature, as T_s is approached, the pressure increases instead of expected reduction due to decrease in the phonon contribution ($P_{ph} \sim T^4$). Such an increase in pressure continues in the metastable region below T_s until the spinodal temperature where the mixture separates inevitably. Theoretical interpretation of the observed effects shows that the found pressure behavior can be described only with the consistent account for fluctuations in the impurity subsystem which near T_s dominates over phonon contribution into the pressure. The obtained theoretical results are in good quantitative agreement with the experimental data. Density fluctuations give rise to a spontaneous formation of impuriton nano-clusters containing several hundreds of atoms. This estimated size of the fluctuation nano-clusters agrees with the corresponding value obtained from the Lifshis-Slesov phenomenological theory of homogeneous nucleation.

1. T.N. Antsygina, A.A. Lisunov, V.A. Maidanov, V.Y. Rubanskyi, S.P. Rubets, E.Ya. Rudavskii, and K.A. Chishko, *Physica B: Condensed Matter*, **406**, 3870 (2011).

P3.10 Solid ^4He Probed Simultaneously by Torsional Oscillator and Ultrasound

H. Kojima^a, B. Hein^b, J. Goodkind^c, and I. Iwasa^a

^aSerin Physics Laboratory, Rutgers University, New Jersey USA

^bDepartment of Physics, Wuerzburg University, Wuerzburg Germany

^cDepartment of Physics, UCSD, California USA

The interpretation of observed anomalous increases in the frequencies of torsional oscillators (TO) containing solid ^4He as evidence for emergence of a supersolid phase remains controversial. Observed TO measurements are influenced by sample preparation and annealing procedures which presumably affect the sample characteristics and disorder such as dislocation density. The nature of correlation between sample characteristics and TO data has not been clearly established. To search for such correlation, we are carrying out simultaneous measurements of 10 MHz longitudinal ultrasound and TOs (250 ~ 1100 Hz) on the identical solid ^4He samples. Temperature dependence of velocity and attenuation of ultrasound and that of amplitude and frequency of TO are measured in a number of samples. The samples are studied under different preparation procedures of repeating block-capillary growth processes, annealing and applying sudden heating by pulses of high intensity ultrasound. The ultrasound data can be well-described by the Granato-Lücke theory and analyzed to extract variations from one sample to another in the average length and density of the dislocation line and the dissipation due to the line motion. The manner of concomitant variations in the (supersolid) frequency increase in the TO depends on the sample preparation procedure. The frequency increases in freshly grown samples do not show so far clear correlation with the extracted dislocation parameters. Annealing decreases the supersolid frequency shift and increases the dislocation length. Interesting effects of sudden acoustic heating will be discussed.

P3.11 Self-Organized Criticality in Quantum Crystallization of ^4He in Aerogel

R. Nomura, H. Matsuda, A. Ochi, R. Isozaki, R. Masumoto, K. Ueno, and Y. Okuda

Department of Physics, Tokyo Institute of Technology, Japan

Due to a competition between thermal fluctuation and disorder, crystallization of ^4He in aerogel shows a dynamical transition in the growth mode: a creep growth at high temperatures and an avalanche growth at low temperatures¹. Both crystallization rate and nucleation probability measurements indicated that the former is via the thermal activation and the latter is via the macroscopic quantum tunneling. In the quantum tunneling regime, the number of smaller size avalanches was larger and a power law behavior was observed in the avalanche size distribution². This is the first demonstration of the self-organized criticality at low temperatures where the quantum nature dominates the dynamical properties of the system. The exponent of the power law has weak temperature dependence while the cutoff size becomes larger with cooling due to the dissipation.

1. R. Nomura, A. Osawa, T. Mimori, K. Ueno, H. Kato and Y. Okuda. "Competition between thermal fluctuations and disorder in the crystallization of ^4He in aerogel". Phys. Rev. Lett. 101, 175703 (2008).
2. R. Nomura, H. Matsuda, R. Masumoto, K. Ueno and Y. Okuda. "Macroscopic Quantum Tunneling and Avalanche Size Distribution of ^4He Crystallization in Aerogel". J. Phys. Soc. Jpn. 80, 123601 (2011).

P3.12 Identification of a Dislocation Related Dissipation Mechanism in High Temperature Mobile Solid ^4He

E. Polturak, A. Eyal, and E. Livne

Department of Physics, Technion - Israel Institute of Technology, Haifa 32000, Israel

Disordered single crystals of solid ^4He contained inside a torsional oscillator behave as if part of the solid is decoupled from the oscillator. Overall, this behavior of disordered single crystals closely resembles the low temperature effects currently under debate regarding their interpretation in terms of supersolidity. However, disordered single crystals exhibit such effects up to temperatures as high as 1.9K. Here, we report a systematic study of the temperature and stress dependence of the internal friction associated with the motion of the disordered solid inside the torsional oscillator. We found that there exists a characteristic energy scale of about 3K for this process. The temperature dependence of the dissipation is consistent with the internal friction being dominated by climb of individual dislocations.

P3.13 Faceting of vicinal surfaces on ^4He crystals

I.A. Todoshchenko^a, M.S. Manninen^a, and A.Ya. Parshin^b

^aO.V. Lounasmaa Laboratory, Aalto University, P. O. Box 15100, 00076 AALTO, Finland

^bP.L. Kapitza Institute, Kosygina 2, Moscow, 119334, Russia

We observe and analyze the kinetics of high order facets with Miller index up to $N = 23$ on the surface of ^4He crystals in a wide temperature range. For the first time, we have been able to measure the dynamics of growing and melting facet in the one set of data. It was found that the data are described well in the terms of spiral growth model. We have measured the step energies for vicinal facets and found them to scale rather slowly with the step height, in contrast to the earlier predictions. We explain the slow scaling by the weak coupling model and found the qualitative agreement between the theoretical and the experimental values of step energies. At higher temperatures we have observed a drop in the step energy value in the vicinity of roughening transition. We are discussing the unexpectedly high roughening transition temperatures of vicinal facets.

P3.14 Dislocation-Pinning Mechanism for the Hysteresis of Torsional-Oscillator Experiments on Solid Helium

I. Iwasa

Kanagawa University, Japan

One of the explanations for the "supersolid" phenomena, i. e. the anomaly of the torsional-oscillator (TO) period containing solid ^4He , is the dislocation-vibration model,¹ which assumes pinning of dislocation segments by ^3He impurities. The model predicts the TO-period change to be proportional to ΛL^2 , where Λ is the dislocation density and L the average pinning length. The dependences of the TO-period on the temperature, T , and the ^3He concentration, x_3 , are described by the T - and x_3 - dependences of the average pinning length.

In order to analyze the hysteresis of the TO period with respect to the rim velocity² and the temperature³ based on the dislocation-vibration model, the stress-induced breakaway and thermal unpinning of dislocations from ^3He impurities are considered. Pinning of dislocations by and unpinning of dislocations from ^3He impurity atoms depending on the history of temperature and rim velocity play an important role. It turns out that longer dislocation segments are not pinned at larger rim velocity even when the sample is cooled to the lowest temperature. By introducing a distribution for the network pinning lengths, the amplitude dependence and the hysteresis of the TO period are explained quantitatively.

1. Iwasa, I. (2010). Phys. Rev. B 81, 104527.
2. Aoki, Y. et al. (2007). Phys. Rev. Lett. 99, 015301.
3. Clark, A.C. et al. (2008). Phys. Rev. B 77, 184513.

P3.15 Quantum plasticity in ^4He crystals

A. Haziot^a, A. Fefferman^a, X. Rojas^a, J. Beamish^b, and S. Balibar^a

^aLaboratoire de Physique Statistique, ENS, Paris, France

^bUniversity of Alberta, Edmonton, Canada

We have applied very small shear stresses (of order 1 microbar) to oriented single ^4He crystals, and directly measured their response as a function of temperature (from 15 mK to 1 K), orientation, crystal quality, ^3He concentration, frequency and shear stress magnitude. For particular orientations, we have found a spectacular evidence for a giant plasticity associated with the elastic coefficient c_{44} which nearly vanishes around 200 mK. Other elastic coefficients show no measurable anomaly. The strong reduction of c_{44} (85% in high quality crystals) is in very good agreement with the current model where dislocations soften the crystal if they are able to glide by quantum tunnelling in the basal plane of the hexagonal structure. The tunnelling is clearly possible in a region between pinning by ^3He impurities (at low T) and damping by thermal fluctuations (at higher T). Our analysis of the damping of the dislocation motion leads to the dislocation density and their pinning length. Some connexion with the issue of supersolidity will be also presented.

P3.16 Anomalous Behavior of Solid ^4He in Porous Vycor Glass

X. Mi and J. D. Reppy

Laboratory of Atomic and Solid State Physics and the Cornell Center for Materials Research, Cornell University, Ithaca, New York 14853-2501

The low temperature properties of solid ^4He contained in porous Vycor glass have been investigated utilizing a two-mode compound torsional oscillator¹. At low temperatures, we find period shift signals for the solid similar to those reported by Kim and Chan², which were taken at the time as evidence for a supersolid helium phase. The supersolid is expected to have properties analogous to those of a conventional superfluid, where the superfluid behavior is independent of frequency and the ratio of the superfluid signals observed at two different mode periods will depend only on the ratio of the sensitivities of the mode periods to mass-loading. In the case of helium studies in Vycor, one can compare the period shift signals seen for a conventional superfluid film with signals obtained for a supersolid within the same Vycor sample. We find, contrary to our own expectations, that the signals observed for the solid display a marked period dependence not seen in the case of the superfluid film. This surprising result suggests that the low temperature response of solid ^4He in a Vycor is more complex than previously assumed and cannot be thought of as a simple superfluid.

1. X. Mi, and J. D. Reppy, Phys. Rev. Lett. **108**, 225305 (2012).
2. E. Kim, and M.H.W. Chan, Nature **427**, 225 (2004).

P3.17 Frequency Shifts of Torsional Oscillators Due to Elasticity

H. J. Maris

Department of Physics, Brown University, Providence, Rhode Island 02912, USA

Torsional oscillators have been used in many experiments to investigate the possible supersolid behavior of solid helium. In these experiments it is usually assumed that the change in the oscillator frequency arises from the change in the effective moment of inertia of the solid helium; this change arises from a superfluid component which does not rotate with the oscillator. However, as has been pointed out by several authors, changes in the elasticity of the helium can also produce frequency shifts. These shifts have approximately the same temperature dependence as is observed; the question is whether they are large enough to explain the results that have been obtained.

We discuss one particular way in which the helium elasticity enters. The torsion rod is attached to the bottom plate of the torsion cell. When the oscillator vibrates, the part of this plate near to the torsion rod undergoes torsion. This, in turn, results in torsion of the helium sample adjacent to the plate. The stiffness of this helium makes a contribution to the effective torsion constant of the oscillator structure, and so when the helium stiffness changes a frequency shift results. We present a calculation of the magnitude of this effect for a typical oscillator.

Work supported by the US National Science Foundation under grant No DMR 0965728.

P3.18 Possible crystallization wave in thin film of He-4 on a smooth surface

T. Minoguchi

Institute of Physics, University of Tokyo, Komaba 3-8-1, Tokyo 153-8902, JAPAN

We address a possibility of a novel crystallization wave for He-4 layers adsorbed on atomically smooth surface such as graphite. For appropriate amount of deposition, He-4 adsorption forms a solid bilayer underneath a superfluid layer at low temperatures. The crystallization wave in such a system is shown to be new in the sense that the deformation of solid is longitudinal, while the ordinary crystallization wave is transverse. We adopt here the mobile dislocation assumption proposed by Hosomi et. al.¹ That is, line dislocations or domain walls embedded in the solid bilayer are highly mobile enough to be responsible for experimentally observed mass decoupling (or solid bilayer sliding) when overlayer is empty or normal liquid layer. As for the case of superfluid overlayer, on the other hand, the mass decoupling dramatically stops which may be the sign of a cross talk between solid bilayer and superfluid overlayer. We in fact find that the coupling between the superfluid and the solid is possible through mass flow condensing into or leaving from the dislocations, and oscillating as a novel crystallization wave. The energy spectrum of the crystallization wave is found for the simplest and the most interesting case where the dislocations are parallelly embedded: $\omega(k) = \eta \frac{k}{\sqrt{k^2 + \kappa^2}}$, where κ is the inverse dislocation width and η the wave velocity being the geometric mean of superfluid density ρ_s and dislocation -dislocation interaction. We note that the crystallization wave becomes soft when $\rho_s \rightarrow 0$. We emphasize that this crystallization wave is nothing but a two dimensional 'superclimb' phenomenon.

1. Hosomi, N., Taniguchi, J., Suzuki, M. and Minoguchi, T. (2009). "Dynamical sticking of a solid He-4 film with superfluid overlayer". Physical Review B.

P3.19 Effects of a ^3He impurity on the elastic anomalies of ^4He at $T = 0$

S. A. Vitiello^a and Renato Pessoa^b

^aInstituto de Física Gleb Wataghin, Universidade Estadual de Campinas - Unicamp, Campinas - SP, Brazil

^bInstituto de Física, Universidade Federal de Goiás, Goiânia - GO, Brazil

Effects of ^3He impurities on the elastic constants of ^4He are investigated in a range of densities varying from 0.029 to 0.035 \AA^{-3} . The linear compressibility assumes the isotropic character one expects for an *hcp* crystal with a constant value of the structure axis ratio c/a . This normal behavior is not observed in a computer simulation with our model but without impurities [1]. In this last situation we see deviations from the expected value of the elastic relation in a way that follows the behavior of the experimental supersolid fraction. Our present results for ^4He are in agreement with the observations made of shear anomalies and on torsional oscillators experiments with a concentration of about 0.1% of ^3He .

1. Renato Pessoa, M. de Koning and S. A. Vitiello, "Elastic constants and supersolidity in solid *hcp* ^4He "

P3.20 Vortex lines penetration & rejection below supersolid transition T_c of *hcp* He

M. Kubota^a, K. Rogacki^b, M. Yagi^a, N. Shimizu^a, Y. Yasuta^a, A. Kitamura^c, and S. Harada^c

^aInstitute for Solid State Physics, the University of Tokyo, Kashiwa, Chiba, Japan

^bInst. of Low Temp. and Structure Research, Polish Academy of Sciences, Wroclaw, Poland.

^cGrad. School of Sci. & Tech., Niigata University, Ikarashi 2-8050, Nishi-ku, Niigata, Japan

Penzev *et al.*, reported the onset of the vortex fluid state in *hcp* He about 500 mK¹ using sensitive torsional oscillator (TO) technique, and Yagi *et al.*², reported possible vortex lines penetration by observing linearly increasing dissipation signal as the DC rotation speed Ω , while no change of the non-linear rotational susceptibility *NLRS* up to 0.6 rad/sec speed for the "equilibrium state"^{3,4}, a branch of the hysteric loop found below $T_c \sim 57-75$ mK^{3,4}. We show the rejection of the vortices in the "excited state" in the loop³ as well. In the present paper we discuss that the origin of the hysteresis in terms of quantized vortices physics, just in the same manner as for type II superconductors with smooth surface in comparison to the "penetration length"⁵ which is expected to be infinite for the supersolid or superfluids.

1. A. Penzev, Y. Yasuta, and M. Kubota, Phys Rev Lett Vol.101, (2008). 2. M. Yagi, A. Kitamura, N. Shimizu, Y. Yasuta, M. Kubota, J. Low Temp. Phys. (2011) 162, 492-499; *ibid*, 162, 754-761. 3. M. Kubota, *et. al.*, J. Low Temp. Phys. (2011) 162, 483-491. 4. M. Kubota, submitted to J Low Temp. Phys. special issue on solid ^4He ; arXiv:1203.6824. 5. de Gennes, "Superconductivity in Metals and Alloys", Benjamin, Lecture notes from a course given in 1962-1963, p.76-80. (1965).; C.P. Bean and J.D. Livingston, Phys. Rev. Lett. Vol.12, 14-16, (1964).

P3.21 Left-over Superfluid ^4He in Aerogel and Its Crystallization by Cooling

H. Matsuda, A. Ochi, R. Isozaki, R. Nomura, and Y. Okuda

Department of Physics, Tokyo Institute of Technology, Japan

Using a variable volume cell, we were able to crystallize ^4He in aerogels at a constant temperature. The whole crystallization process was monitored visually thanks to the transparency of the aerogel. Two different crystallization processes of ^4He in aerogels are observed: creep at high temperatures and avalanche at low temperatures^{1,2}. In a 96% porosity aerogel, we noticed that ^4He in some part of the aerogel was left over as a liquid incidentally, whereas other parts of the aerogel were completely crystallized. Once such a situation was formed, the liquid could not be crystallized any more by applying further pressure. This is presumably because a supply path of ^4He atoms from the bulk crystal was blocked by the crystals in the aerogel. This left over liquid, however, was found to start to crystallize via avalanches by cooling below a particular temperature. Since the crystallization pressure in aerogel should be naively temperature independent at low temperature as the bulk crystallization pressure, the crystallization by cooling is rather unusual. Possible explanation will be a decrease of the crystallization pressure in aerogel in a low temperature region, or supersolidity of crystals in aerogel playing some role in crystallization.

1. R. Nomura, H. Matsuda, R. Masumoto, K. Ueno and Y. Okuda. "Macroscopic Quantum Tunneling and Avalanche Size Distribution of ^4He Crystallization in Aerogel". J. Phys. Soc. Jpn. 80, 123601 (2011).
2. R. Nomura, A. Osawa, T. Mimori, K. Ueno, H. Kato and Y. Okuda. "Competition between thermal fluctuations and disorder in the crystallization of ^4He in aerogel". Phys. Rev. Lett. 101, 175703 (2008).

P3.22 Low-Temperature Anomalies in Thermal Conductivity of the Plastically Deformed Crystals due to the Phonon-Kink Scattering

S.I. Mukhin^a, J. Ostaay^b, A.A. Levchenko^c, and L.P. Mezhov-Deglin^c

^aMoscow Institute for Steel and Alloys, Russia

^bLorentz Institute for Theoretical Physics, Holland

^cInstitute of Solid State Physics, Chernogolovka, Russia

In samples where the phonon (lattice) thermal conductivity plays the main role in heat flux transfer processes (quantum crystals¹, metal crystals in superconducting state², semimetals³) a strong scattering of thermal phonons on the mobile kinks on dislocation lines induced under weak deformation of initially perfect samples seems to be the natural explanation of the experimentally observed anomalies in temperature dependences of their thermal conductivity. The model for inelastic scattering of quasiparticles on mobile kinks was proposed earlier by one of us⁴ for explanation of the peculiarities in electronic component of thermal conductivity of the bent copper crystals.

1. L.P. Mezhov-Deglin and A.A. Levchenko, Sov. Phys. JETP 55, 166 (1982); Sov. Phys. JETP 59, 1234 (1984); Sov. J. Low Temp. Phys. 10, 581 (1984); and Sov. J. Low Temp. Phys. 11, 617 (1985); also "Physics of Phonons". Lecture Notes in Physics, 1987, Volume 285, 438-443 (1987).
2. L.P. Mezhov-Deglin, Sov. Phys. JETP 50(2), 734 (1979).
3. V.N. Kopylov, L.P. Mezhov-Deglin, Sov. Phys. Solid State, 15, 8 (1973).
4. S.I. Mukhin, Sov. Phys. JETP 64, 81 (1986); L.P. Mezhov-Deglin, S.I. Mukhin, Low Temp. Phys. 37 (10), 806 (2011).

P3.23 Dissipative superfluid mass flux through solid ^4He

Ye. Vekhov and R. B. Hallock

Laboratory for Low Temperature Physics, Department of Physics, University of Massachusetts, Amherst, MA 01003

The thermo-mechanical effect in superfluid helium is used to create a chemical potential difference, $\Delta\mu$, across a solid ^4He sample[1]. This $\Delta\mu$ causes a flow of helium atoms from one reservoir filled with superfluid helium to another through solid helium. The solid helium sample is separated from the reservoirs by Vycor rods that allow only the superfluid component to flow[2]. With an improved technique, measurements of the flow, F , at several fixed solid helium temperatures, T , have been made as function of $\Delta\mu$. And, measurements of F (in the range $100 < T < 650$ mK) have been made as a function of temperature for several fixed values of $\Delta\mu$ [3]. The temperature dependence of the flow above 100 mK is confirmed to show attenuation of the flux with increasing temperature. The dependence of F on $\Delta\mu$ indicates that the flow has a dissipative character. The implications of this and the relevance to existing theoretical ideas concerning solid helium will be presented.

[1] M.W. Ray and R.B. Hallock, Phys. Rev. Letters 105, 145301 (2010) and Phys. Rev. B 84, 144512 (2011).

[2] M.W. Ray and R.B. Hallock, Phys. Rev. Letters 100, 235301 (2008) and Phys. Rev. B 79, 224302 (2009).

[3] Ye. Vekhov and R.B. Hallock, arXiv cond-mat 1205.5751

P3.24 Neutron and X-ray experiments in solid ^4He .

Y. Mukharski^a, A. Braslau^a, and J. Bossy^b

^aCEA-Saclay/DSM/IRAMIS/SPEC; 91191 Gif sur Yvette, Cedex; France.

^bInstitut Néel, CNRS et Université Joseph Fourier, BP 166, 38042 Grenoble Cedex 9, France

We will present results on neutron and X-ray scattering in solid ^4He in the range of parameters where supersolidity is observed. The measurements address, among other questions, the viability of two possible mechanisms of supersolidity: via a metastable amorphous phase and via metastable vacancies. We have attempted to observe a glassy phase by neutron scattering and found that it is impossible to do this through total scattering, as it would be common in a classical solid, due to the extremely large inelastic diffuse signal related to the anomalously strong zero-point motion of helium atoms. Results from energy-resolved elastic scattering are heavily influenced by multiple scattering of neutrons, yet allow us to put the limit on the concentration of an amorphous phase to $\sim 5\%$ in a polycrystal with millimetre-size crystallites and to 0.5% in a single crystal. The values of NCRIf expected from these limits should be much lower, although exact values depend strongly on a particular model of glass-related supersolidity.

To check for existence of metastable vacancies, we measured simultaneously the lattice constants of a single crystal sample and its dielectric constant, from which the density can be deduced. The results indicate the absence of metastable vacancies or interstitials within a precision of $\sim 2 \cdot 10^{-4}$.

P3.25 Simultaneous measurements of the thermal conductivity and response to torsional oscillations of solid ^4He

M. Yu. Brazhnikov^a, D. E. Zmeev^b, and A. I. Golov^a

^aThe University of Manchester, Manchester M13 9PL, UK

^bLancaster University, Lancaster LA1 4YB, UK

In our experiments the anomalous response to torsional oscillations of solid ^4He is examined along with its thermal conductivity. Polycrystalline samples of ^4He grown in an annular cell by the blocked capillary method have been studied before and after annealing. In previous experiments with either isotopically pure ^4He or ^4He with about 0.3 ppm ^3He , no correlation has been found between the low-temperature shift of the resonant frequency of oscillator and phonon mean free path [1]. Investigations of samples with a higher concentration of ^3He impurities are ongoing. With increasing ^3He concentration the crossover temperature T^* of the frequency shift increases, at the same time the dissipation peak as a function of normalized temperature T/T^* broadens. The phonon mean free path of a sample with 2.5 ppm ^3He is ten times larger than in pure ^4He . Annealing always resulted in an increase of the phonon mean path and decrease of the width of the dissipation peak. Monitoring free relaxation allowed us to obtain the dependences of the resonant frequency and dissipation on the angular amplitude A . These dependences are similar to the corresponding temperature dependences if one replaces T with A^γ . However, the scaling exponent $\gamma = 0.75$ differs from 0.43 observed in [2].

1. D. E. Zmeev and A. I. Golov, Phys. Rev. Lett. **107**, 065302 (2011).

2. E. J. Pratt, B. Hunt, V. Gadagkar, M. Yamashita, M. J. Graf, A. V. Balatsky, J. C. Davis. Science **332**, 821 (2011).

P3.26 Excitation spectrum and stability analysis of a supersolid

Masaya Kunimi and Yusuke Kato

Department of Basic Science, The University of Tokyo, Japan

Supersolid is a state that has superfluidity and solidity. This state is expected to realize in solid ^4He ¹⁻² and ultra cold atomic gases with a long range interaction³⁻⁴.

In order to investigate superfluidity of supersolids, the nature of excited states of the supersolid phase is essential. We obtained the excitation spectrum in two-dimensional supersolid phase in the frame work of the Gross-Pitaevskii equation with a soft-core interaction⁵⁻⁶ and the Bogoliubov equation⁷. There are three gapless branches in the supersolid phase: Bogoliubov mode, transverse phonon mode, and longitudinal phonon mode.

Calculating the excitation spectra of current-carrying states (, which corresponds to the persistent current states), we obtain the stability phase diagram. We found that superfluid phase, supersolid phase, and stripe phase are stable or metastable against the superflow.

1. E. Kim and M. H. W. Chan, Nature (London) **427**, 225 (2004), Science **305**, 1941 (2004).

2. N. Prokof'ev, Adv. Phys. **56**, 381 (2007).

3. S. Balibar, Nature **464**, 176 (2010).

4. M. Boninsegni and N. V. Prokof'ev, Rev. Mod. Phys. **84**, 759 (2012).

5. Y. Pomeau and S. Rica, Phys. Rev. Lett. **72**, 2426 (1994).

6. H. Watanabe and T. Brauner, Phys. Rev. D, **85**, 085010 (2012).

7. M. Kunimi and Y. Kato, arXiv:1205.2126.

P3.27 Two-Mode Torsional Oscillator Study of Solid Helium

B. Cowan and G. Nichols

Royal Holloway, University of London, UK

We present experimental results exploring the ‘supersolid’ anomaly in ^4He below 100mK.¹ A rigid two-mode compound torsional oscillator is used with resonant modes at 400Hz and 2kHz. By studying two widely spaced frequencies we are able to distinguish between resonant period shifts arising from ‘NCRI’ effects and variation in shear modulus.^{2,3} An in situ pressure gauge allows careful characterisation of annealed crystals to study the effect of disorder on these phenomena.

1. E. Kim and M. H. W. Chan, Nature 427, 225 (2004).
2. J. Day and J. Beamish, Nature 450, 853 (2007)
3. J D Reppy, arXiv:1112.2218 (2011)

P3.28 Lattice Dynamics of ^3He Impurities in Solid ^4He : An NMR Study

S.S. Kim^a, C. Huan^a, D. Candela^b, N.S. Sullivan^a, L. Yin^a, and J.S. Xia^a

^aDepartment of Physics, University of Florida, Gainesville, USA.

^bDepartment of Physics, University of Massachusetts, Amherst, USA.

The results of recent NMR studies of the nuclear spin lattice relaxation of dilute solutions of ^3He impurities in solid ^4He at low temperatures¹ are reviewed in terms of the quantum tunneling of the impurities in the ^4He lattice. The tunneling has a strong dependence on the lattice properties associated with the lattice deformation surrounding the mobile impurities, and the relaxation of the lattice in the wake of the tunneling is expected to determine the NMR relaxation. The observed nuclear spin-lattice relaxation is therefore closely related to the temperature dependence of the shear modulus observed by Beamish and colleagues².

1. Kim, S. S. *et al.* (2011). “NMR Studies of the dynamics of ^3He impurities in the proposed supersolid state of solid ^4He ”, Phys. Rev. Lett. 106,185303.
2. Syshchenko, O. *et al.* (2010) “Frequency dependence and dissipation in the dynamics of solid helium”, Phys. Rev. Lett. 104,19530.

P3.29 Ripening of Splashed ^4He Crystals by Acoustic Waves in Zero Gravity

T. Takahashi, H. Ohuchi, R. Nomura, and Y. Okuda

Department of Physics, Tokyo Institute of Technology, Japan

By developing a refrigerator compatible with a parabolic flight in a small jet plane, ^4He crystals in superfluid was obtained in a zero gravity condition at 0.6 K¹. Sudden reduction of the gravity induces the transformation of crystal shape: at 1 G the largest crystal surface is horizontally flat to minimize the gravitational energy, while at 0 G the crystal relaxes to an equilibrium shape with several facets to minimize the surface energy². Here, we report a ripening of ^4He crystals in superfluid after splashed by acoustic waves. Ripening is a process that smaller crystals melt and larger ones grow to minimize the overall surface energy. At 1 G, the ripening was not observed apparently because it stops growing at a scale of the capillary length of about 1 mm; crystals at lower position grew to minimize the gravitational energy. At 0 G, however, the ripening was observed to a larger scale than 1 mm due to the infinitely long capillary length, exhibiting a novel evolution of crystal shape driven by only the surface energy.

1. T. Takahashi, M. Suzuki, R. Nomura and Y. Okuda “Development of a ^3He refrigerator for possible experiments of solid ^4He on a small jet plane”. *J. Low Temp. Phys.* 162, 733 (2011).
2. T. Takahashi, R. Nomura, and Y. Okuda “ ^4He Crystals in Superfluid under Zero Gravity”. *Phys. Rev. E* 85, 030601(R) (2012).

P3.30 Energy release channels during destruction of impurity-helium condensates

V.V. Khmelenko^a, A.A. Pelmenev^b, I.N. Krushinskaya^b, I.B. Bykhalo^b, R.E. Boltnev^b, and D.M. Lee^a

^aDepartment of Physics and Astronomy, Texas A&M University, College Station, TX 77843 USA

^bBranch of Institute of Energy Problems of Chemical Physics RAS, Chernogolovka, Moscow region, 142432, Russia

Injection of an impurity-helium gas jet passed through a radiofrequency discharge area into a volume of superfluid helium, leads to the growth of nanoclusters of impurity species which form impurity-helium condensates (IHCs). IHCs are porous materials with very low impurity density ($\sim 10^{20} \text{ cm}^{-3}$). High average concentrations of stabilized free radicals can be achieved on the large total surface ($\sim 100 \text{ m}^2/\text{cm}^3$) of the impurity nanoclusters. Warming the IHCs leads to the destruction of the samples and formation of excited atoms and molecules as a consequence of recombination of the stabilized free radicals. We studied the influence of nitrogen content in neon-helium and krypton-helium gas mixtures on the thermoluminescence spectra accompanying the destruction of the IHC samples, which were formed by using these gas mixtures. The energy release channels in the IHC samples were revealed from analysis of the thermoluminescence spectra.

P3.31 Pressure Relaxation and NMR Measurements in hcp 1% ^3He in ^4He Quenched Crystals

A.P. Birchenko, N.P. Mikhin, E.Ya. Rudavskii, and Ye.O. Vekhov

B.Verkin Institute for Low Temperature Physics and Engineering, National Academy of Sciences of Ukraine, Kharkov, Ukraine

The pressure measurements under the constant volume conditions is used for detection the local pressure gradients, which may appear in non-ideal helium samples.¹ The measurements are performed in the temperature range from 1.3 – 2.0 K. Simultaneously, phase structure of $1.0 \pm 0.05\%$ ^3He in ^4He crystals is studied by pulse NMR measurement of D self-diffusion coefficient and T_2 spin-spin relaxation time. It was found, that quenched samples are two-phase systems consisting of the hcp matrix and some inclusions which are characterized by D and T_2 values close to those in liquid phase. At the same time, it has been established that in the quenched samples there is continuous pressure relaxation described by the sum of two exponents with time constants $\tau_1 = 1.2 - 30$ min and $\tau_2 = 30 - 250$ min. The time constants are decreasing when temperature increased, that points on the thermoactivation character of the process. Such pressure behavior may reveal the presence of the disordered phase (liquid droplets) in the quenched hcp crystals, as agreed with NMR measurements. After annealing near melting curve the liquid droplets and pressure relaxation processes has been not observed in quenched hcp samples, and also in the samples which have been grown under make smooth cooling using special thermal stabilization system. The influence of the cell's geometry on the observed effects is discussed.

1. A. Suhel and J. R. Beamish, Phys. Rev. B 84, 094512 (2011).

P3.32 Depletion of NCRI of solid ^4He confined in Vycor glass under DC rotation

T. Tsuiki^a, D. Takahashi^{b,c}, K. Kono^b, and K. Shirahama^a

^aDepartment of Physics, Keio University, Yokohama 223-8522, Japan

^bLow Temperature Phys. Lab., RIKEN, Wako-shi 351-0198, Japan

^cDepartment of General Education, Ashikaga Institute of Technology, Ashikaga 326-8558, Japan

Despite a lot of efforts for understanding putative supersolidity discovered by Kim and Chan,¹ the controversy as to whether the non-classical rotational inertia (NCRI) is due to genuine supersolidity does not come to a conclusion yet. Study of rotation effects may uncover the origin of NCRI.² We report on torsional oscillator (TO) experiment for solid ^4He confined in porous Vycor under DC rotation. In porous media, dislocations are strongly pinned to the porous matrix during rotation. A TO (frequency: 1016 Hz) containing an annular Vycor (inner and outer diameters: 14 and 17 mm) is mounted on the rotating dilution refrigerator at RIKEN. In three solid samples with pressures 5.5 ~ 8.0 MPa, the NCRI clearly decreases as DC angular velocity Ω increases. The magnitude of depletion decreases with increasing torsional oscillation velocity. These features seems similar to the results of bulk solid.² However, some new features appear: The depletion of NCRI is smaller in higher pressure sample. Moreover, the NCRI shows an oscillating structure, which is a combination of a large scale oscillation periodic with inverse of Ω and apparently random but fingerprint-like fluctuations.

1 E. Kim and M. H. W. Chan, Nature **427**, 225 (2004), 2 H. Choi, D. Takahashi, K. Kono, and E. Kim, Science **330**, 1512 (2010); H. Choi, D. Takahashi, W. Choi, K. Kono, and E. Kim, Phys. Rev. Lett. **108**, 105302(2012).

P3.33 Commensurate supersolid in lattice bosons

T. Ohgoe^a, T. Suzuki^b, and N. Kawashima^a

^aInstitute for Solid State Physics, University of Tokyo, Kashiwa, Chiba, Japan

^bResearch Center for Nano-Micro Structure Science and Engineering, Graduate School of Engineering, University of Hyogo, Himeji, Hyogo, Japan

Using an unbiased quantum Monte Carlo method, we have investigated the ground-state phase diagrams of the soft-core Bose-Hubbard model with the nearest-neighbor repulsion on a square lattice and a cubic lattice. The phase diagram includes supersolid phases where superfluidity and solidity coexist. In general, the supersolid states are realized when particles (holes) are added to (removed from) the perfect commensurate solid and delocalize on the solid order, thus, Bose-condensating at low temperatures. Therefore, in general, the supersolid phase appears at incommensurate filling factors. However, we have directly confirmed the presence of a supersolid phase even at a commensurate filling factor, by performing simulations in the canonical ensemble.^{1,2} The commensurate supersolid is realized by unbound interstitial-vacancy pairs in the commensurate solid due to large quantum fluctuations.

1. Ohgoe T, Suzuki T, Kawashima N. (2012). “Commensurate Supersolid of Three-Dimensional Lattice Bosons”. *Phys. Rev. Lett.* **108**, 185302.
2. Ohgoe T, Suzuki T, Kawashima N. (2012). “Ground-State Phase Diagram of the Two-Dimensional Extended Bose-Hubbard Model”. arXiv:1206.3670.

P3.34 Josephson effect in two-dimensional supersolids

Go Anagama^a, Masaya Kunimi^b, and Yusuke Kato^b

^aDepartment of The University of Tokyo, Tokyo 113-0033, Japan

^bDepartment of Basic Science, The University of Tokyo, Tokyo 153-8902, Japan

We show that two-dimensional supersolids can exhibit DC Josephson effect in the presence of a potential barrier in a modified Gross-Pitaevskii equation such that the two-body interaction is finite-ranged^{1,2}. The current-phase relations (the Josephson relation) are obtained for potential barriers with various heights. The present result is consistent with an earlier result³. We compare our result with that of Ref. 1, where superflow around a disk-shaped obstacle has been concluded to be impossible .

1. Pomeau, Y. and Rica, S (1994) “Dynamics of a model of supersolid”. *Physical Review Letters* **72** pp. 2426.
2. Josserand, C., Pomeau, Y. and Rica, S (2007) “Coexistence of ordinary elasticity and superfluidity in a model of a defect-free supersolid”. *Physical Review Letters* **98** pp. 195301.
3. Kunimi, M., Nagai, Y. and Kato, Y. (2011). “Josephson effect in one-dimensional supersolids”. *Physical Review B* **84** pp. 094521.

P3.35 Simple Statistics for Cooperative Motion in Solid ^4He and Supersolidity

N.V. Krainyukova

Institute for Low Temperature Physics and Engineering NASU, Kharkiv, Ukraine

This contribution is an extension of our previous study¹ where within the modified Hartree approach a new term in the interaction, which is presumably responsible for the rotating-like atomic motion in He, was introduced. These findings were shown to be strongly correlated with the neutron scattering experiments. In the suggested here presentation we improve the previous method and introduce correlations in the atomic dynamics via a simple statistic account of cooperative effects in the rotating-like motion. Comparison of calculations with the experiment of Chan et al.² on the heat capacity shows that a correlation length may strongly grow up closely and below the temperature associated with the transition into a 'supersolid state'. A new experiment, which may distinguish the mass decoupling and the modulus stiffening, is suggested.

1. N.V. Krainyukova, J. Low Temp. Phys. **162**, 441 (2011)
2. X. Lin, A. C. Clark, Z. G. Cheng, and M. H.W. Chan, Phys. Rev. Lett. **102**, 125302 (2009)

P3.36 Modes of amorphous solid helium

J. Bossy^a, J. Ollivier^b, H. Schober^c, and H.R. Glyde^d

^aInstitut Néel, CNRS-UJF, BP 166, 38042 Grenoble Cedex 9, France.

^bInstitut Laue-Langevin, BP 156, 38042 Grenoble, France.

^cInstitut Laue-Langevin, BP 156, 38042 Grenoble, France and Université Joseph Fourier, UFR de Physique, F38041 Grenoble Cedex 9, France.

^dDepartment of Physics and Astronomy, University of Delaware, Newark, Delaware 19716-2593, USA.

We present neutron scattering measurements of the dynamic structure factor, $S(Q, \omega)$, of amorphous solid helium confined in 47 Å pore diameter MCM-41 at pressure 48.6 bar. At low temperature, $T = 0.2$ K, we observe $S(Q, \omega)$ of the confined quantum amorphous solid plus the bulk polycrystalline solid lying between the MCM-41 powder grains. We observe an $S(Q, \omega)$ that is a smooth function of ω at low ω characteristic of scattering from phonon modes in a polycrystal. No liquid-like phonon-roton modes or other sharply defined modes at low energy ($\omega < 1.0$ meV) are observed. At higher temperature ($T > 1$ K), the amorphous solid in the MCM-41 pores melts to a liquid which has a broad $S(Q, \omega)$ peaked near $\omega \simeq 0$ characteristic of normal liquid ^4He . At higher ω ($\omega > 1$ meV) the $S(Q, \omega)$ of the liquid and the amorphous solid are similar. Expressions for the $S(Q, \omega)$ of amorphous and polycrystalline solid helium are presented and compared. In previous measurements of liquid ^4He confined in MCM-41 at lower pressure and low temperature, the intensity in the liquid roton mode decreases with increasing pressure and the intensity vanishes at the solidification pressure (38 bars), consistent with no roton in the solid observed here.

P3.37 More on the shear modulus of solid helium

N. Mulders

Department of Physics and Astronomy, University of Delaware, USA

We have made a series of experiments on solid helium-4, using two stacks of piezoelectric transducers that can simultaneously excite, and are able to detect, shear waves in orthogonal shear directions. We find that at temperatures below 100 mK shearing the solid with large amplitude at one frequency affects the shear modulus at different frequencies, and similarly, that shearing in one direction affects the modulus as measured in the orthogonal direction.

P3.38 Simultaneous Measurements of Torsional Oscillator and Shear Modulus of Solid Helium

J. Shin^a, W. Choi^a, J. Choi^a, S. Jang^a, K. Shirahama^b, and E. Kim^a

^aCenter for Supersolid & Quantum Matter Research and Department of Physics, KAIST, Daejeon 305-701, Republic of Korea

^bDepartment of Physics, Keio University, Yokohama 223-8522, Japan

Since the observation of the resonance period drop in a torsional oscillator containing solid helium-4 below 200 mK [1], it has been considered as a possible evidence of the supersolid state. Among various attempts to investigate the characteristics of solid helium, one of the most interesting findings is the shear modulus anomaly which shows remarkable similarities in temperature, frequency, ³He concentration, and drive dependence [2]. Here, we report simultaneous measurements of the TO response and shear modulus anomaly of solid helium at low temperatures by inserting a pair of concentric piezo transducers into the annulus where we measure the TO response. To understand the correlation of NCRI and shear modulus, we measured the interference between two different AC measurements; TO response and shear modulus anomaly. If both are originated from the same microscopic mechanism, then the interference measurements are crucial to understand their correlation.

[1] E. Kim and M. H. W. Chan Nature 427, 225-227 (2004)

[2] J. Day and J. Beamish Nature 450, 853-856 (2007)

P3.39 **Spin-lattice relaxation in rapidly grown helium crystal with 1% impurity of ^3He**

N.P. Mikhin, A.P. Birchenko, E.Ya. Rudavskii, and Ye.O. Vekhov

B.Verkin Institute for Low Temperature Physics and Engineering, National Academy of Sciences of Ukraine, Kharkov, Ukraine

Previously, measurements of the spin-spin relaxation time, T_2 and diffusion coefficient, D in the quenched hcp matrix of dilute ^3He - ^4He mixtures confirmed the presence of liquid inclusions in the matrix. Eventually, T_2 in these inclusions reduced rapidly by an order of magnitude, while the D reduced by some orders of magnitude. This behavior has at least two alternative explanations: either in frame of restricted highly dispersed liquid model or by the vitrification of inclusions. The behavior of the spin-lattice relaxation time T_1 may indicate an adequate model. T_1 in metastable inclusions, as well as in hcp matrix is measured by pulse NMR method in the temperature range 1.25 - 2 K. The comparison with the results of T_2 measurements is allowed to separate out the contributions of coexisting phases to the NMR signal as well as the spin-lattice relaxation rate in these. It is shown that T_1 in both liquid and "vitriform" inclusions is much longer than in the matrix. Mechanisms of spin-lattice relaxation in the inclusions are discussed.

P3.40 **Dissipation and dislocations density in ^4He crystals**

A. Haziot^a, A. Fefferman^a, X. Rojas^a, J. Beamish^b, and S. Balibar^a

^aLaboratoire de Physique Statistique, ENS, Paris, France

^bUniversity of Alberta, Edmonton, Canada

By studying the response of ^4He crystals to an ac-strain (200 to 16,000 Hz), we have measured the dissipation associated to dislocations motion. It is proportional to the frequency and to T^3 at low temperature, in excellent agreement with the "fluttering mechanism", which means that the damping of the dislocations motion is due to collisions with thermal phonons. Our analysis of the real and imaginary parts of the response leads to an accurate determination of the density and of the pinning length of the dislocations.

This work was supported by grants from ERC (AdG 247258-SUPERSOLID) and from NSERC Canada.

P3.41 **Absence of pressure transmission through a helium solid/liquid/solid double junction**

A.D. Fefferman^a, S. Bukhari^b, J.R. Beamish^b, A. Haziot^a, X. Rojas^a, and S. Balibar^a

^aLaboratoire de Physique Statistique de l'ENS, Paris, France

^bDepartment of Physics, University of Alberta, Edmonton, Canada

Porous vycor rods are used to inject mass in solid helium samples or to extract mass from them.¹ In such experiments, one assumes that mass flow is a consequence of a chemical potential difference across the solid-liquid interface at the entrance of the vycor pores. We have studied a solid-liquid-solid double junction at homogeneous temperature. Our two solid phases S1 and S2 were grown at constant volume so that their final pressure was in the range from 25.5 to 33 bar. We applied a stress to S1 with a flexible membrane and we measured a possible pressure change in S2, which was connected to S1 through a liquid region L inside a Vycor rod. We used stresses of order 1 bar in the temperature region from 90 mK to 1.4K. Surprisingly, we could detect a mass current only at high temperature, not in the low temperature region where it was observed by Ray et al.¹ and where supersolidity might exist. The lack of pressure transmission from S1 to S2 implies that either large chemical potential gradients exist in the solid regions or that the chemical potential differences across the S1-L or L-S2 interfaces are not sufficient to allow mass flow. Channels for mass transmission may exist in the solid but were not connected to the liquid phase in our experiment. This work was supported by grants from ERC (AdG 247258-SUPERSOLID) and from NSERC Canada

1. Ray, M. and Hallock, R., "Mass flow through solid ⁴He induced by the fountain effect", PRB (2011).

P3.42 **Predictions of the Granato-Lucke model assuming a distribution of dislocation lengths**

A.D. Fefferman^a, J.R. Beamish^b, A. Haziot^a, and S. Balibar^a

^aLaboratoire de Physique Statistique de l'ENS, Paris, France

^bDepartment of Physics, University of Alberta, Edmonton, Canada

The Granato-Lucke vibrating string model¹ has been used to interpret the damping of dislocation motion in ⁴He crystals.² We discuss here some additions to this theory³ that may lead to a determination of a distribution of the pinning lengths of dislocations, not only its average value and the dislocation density. This work was supported by grants from ERC (AdG 247258-SUPERSOLID) and from NSERC Canada

1. Granato, A. and Lucke, K., "Theory of mechanical damping due to dislocaitons", J. Appl. Phys. (1956).
2. Haziot et al., to be published
3. Ninomiya, T., "Frictional force acting on a dislocation-fluttering mechanism"

P3.43 Resonant enhancement of the FFLO superfluid state by a 1D optical potential

J.P.A. Devreese, J. Tempere, S.N. Klimin, and M. Wouters

TQC, Universiteit Antwerpen, Belgium

In a two component Fermi gas, spin-imbalance leads to a competition between Cooper-pairing with zero momentum and with nonzero momentum. The latter gives rise to the Fulde-Ferrell-Larkin-Ovchinnikov (FFLO) state. Hitherto this state has not been observed in a 3D Fermi gas. We propose a new way to enhance the presence of the FFLO state, by adding a 1D periodic potential. To investigate the effect of this potential, we study the ground state properties of the system, starting from the partition sum of an imbalanced Fermi gas in path-integral representation. To describe the FFLO state, a saddle point is chosen in which the pairs can have nonzero momentum. Minimizing the resulting free energy leads to the phase diagram of the system. The stability region of the FFLO state is found to be greatly enlarged due to the presence of the periodic potential, compared to the ordinary 3D case. We find that the FFLO state can exist at higher spin imbalance if the wavelength of the optical potential becomes smaller. We propose that this concept can be used experimentally to enhance the FFLO state.

[1] Jeroen P.A. Devreese, S.N. Klimin, and J. Tempere, Phys. Rev. A 83, 013606 (2011).

[2] Jeroen P.A. Devreese, M. Wouters, and J. Tempere, J. Phys. B 44, 115302 (2011); Phys. Rev. A 84, 043623 (2011).

This work was supported financially by the Research Foundation - Flanders (FWO).

P3.44 Gas-Solid Phase Transition in Hardcore-like Systems

K. Yamashita^a, Y. Koike^a, Y. Kwon^b, and D. Hirashima^a

^aDepartment of Physics, Nagoya University, Japan

^bDivision of Quantum Phases and Devices, School of Physics, Konkuk University, Korea

It is known that classical hard spheres undergo a phase transition, the Alder transition, from a gas state to a solid state as the system is compressed. A ground state phase diagram of quantum hardcore bosons was also studied and it was also found that the quantum hardcore bosons localize at much more lower density than the classical counterpart.¹ Their result implies that the quantum hardcore systems are much unstable toward solidification and the quantum effect can help the solidification of bose gases. But the quantum effect, the effect of the zero point motion, on the solidification has not been studied carefully except for the variational study by Nosanow *et al.*², where they found no evidence of the solid state stabilized by the zero point motion. The purpose of our work is to examine the effect of the zero point motion on the solidification of quantum systems by studying the gas-solid phase transition where particles interact with hardcore-like potentials. We calculate the ground state energies of each phase using the diffusion Monte Carlo method, and then, we find that the liquid phase is more stabilized as the effect of the zero point motion increases, that is, the quantum effect never help the solidification at zero temperature. We also discuss the quantum effect on the gas-solid phase transition at finite temperature. A competition between thermal fluctuation and zero point motion would cause a crossover from the classical phase transition to the quantum one. In this crossover region, the solid phase would be stabilized by the quantum effect.

1. M. H. Kalos, D. Levesque and L. Verlet, Phys. Rev. A **9**, 2178 (1974).

2. L. H. Nosanow, L. J. Parish and F. J. Pinski, Phys. Rev. **11**, 191 (1975)

P3.45 Shear Modulus Measurement of Ultrapure Solid Helium-4

Jaeho Shin^a, Jaewon Choi^a, Seong Jang^a, Duk-Young Kim^a, Eunseong Kim^a, and Keiya Shirahama^b

^a Center for Supersolid and Quantum Matter Research and Department of Physics, KAIST, Daejeon 305-701, Republic of Korea

^b Department of Physics, Keio University, Yokohama 223-8522, Japan

Since the early observations of the period drop in the torsional oscillator (TO), regarded as the first discovery for supersolidity^{1,2}, the dynamical role of helium-3 impurities in solid helium-4 has been emphasized. Both the magnitude of reduction and temperature dependence of TO period were significantly influenced by the helium-3 impurity concentration³. It has been also proposed that the change in shear modulus found in solid helium-4 at low temperatures, a possible alternative explanation for early TO experiments, can be understood by the dislocation pinning with helium-3 impurities⁴. In order to elucidate the dynamical role of helium-3 impurities to them, the changes in shear modulus has been investigated at extremely low helium-3 concentration of 0.6ppb. We used a pair of concentric piezo-electric transducers to study shear modulus anomaly of isotropically pure solid helium. We investigated temperature, strain, and frequency dependence of shear modulus. The drive and temperature dependent hysteresis will be also discussed with this ultra-pure solid helium

1. E. Kim and M. H. W. Chan, *Nature* 427, 225 (2004)
2. E. Kim and M. H. W. Chan, *Science* 305, 1941 (2004)
3. E. Kim et al, *Phys. Rev. Lett.* 100, 065301 (2008)
4. J. Day and J. Beamish, *Nature* 450, 853 (2007)

P3.46 Precise measurements of the lattice constant solid ⁴He

Y. Mukharski^a, A. Braslau^a, J. Bossy^b, and S. Rabi^c

^aCEA-Saclay/DSM/IRAMIS/SPEC; 91191 Gif sur Yvette, Cedex; France.

^bInstitut Néel, CNRS et Université Joseph Fourier, BP 166, 38042 Grenoble Cedex 9, France

^cSynchrotron SOLEIL, F-91192 Gif Sur Yvette, France

Classical explanation of supersolidity in solid helium is based on existence of vacancies, which persist down to the lowest temperatures. Measurements of the activation energy of the vacancies, indicate that they should be frozen out below 1 K and helium atoms should form commensurate crystal. The same is predicted by numerical QMC calculations. However, some theories¹ predict that number of vacancies decreases polynomially, not exponentially, with temperature. Finally, there is possibility that a number of metastable vacancies persists at zero temperature.

We made high-precision simultaneous measurements of the dielectric constant (easily translated into the density) and the lattice constants of helium crystal to check commensurability of the solid. We conclude that at zero T the concentration of vacancies is below $2 \cdot 10^{-4}$. We have also measured the temperature dependence of the lattice constants by observing several different reflections and found that it is consistent with exponential, and not with polynomial, change. The activation energy is in approximate agreement with earlier measurements. The experimental accuracy does not allow differentiating between Schottky (well-defined end energy) and zone modes of the activation of vacancies.

1. Anderson, P. W., Brinkman, W. F. and Huse, D. A.; *Science* **310**, 1164 (2005).

P3.47 Quantized Circulation in Solid Helium-4 under Rotation

H. Choi^a, D. Takahashi^b, W. Choi^a, K. Kono^b, and E. Kim^a

^aDepartment of Physics, KAIST, Daejeon, South Korea

^bLow Temperature Physics Laboratory, RIKEN, Wako-shi, Japan

Despite people's excitement after the potential discovery of supersolid by Kim and Chan in 2004¹, it is not clear that what they have observed is, in fact, superfluidity within solid. The excitement brought a large number of researchers to pursue the exact nature of solid helium. There is mounting evidence both for and against supersolid, and we present one for the existence of supersolid by performing a torsional oscillator experiment on rotating solid helium. A signal that can be interpreted as suppression of non-classical rotational inertia fraction was seen in solid helium under rotation.² Further investigation of the effect has shown that the suppression of the signal is not continuous under rotation velocity sweep. In fact, the suppression follows a discrete staircase-like change that is periodic in velocity.³ One possible source of such behavior is quantization of superfluid circulation within supersolid.

1. E. Kim and M. H. W. Chan, *Nature* **427**, 225 (2004).
2. H. Choi, D. Takahashi, K. Kono, and E. Kim, *Science* **330**, 1512 (2010).
3. H. Choi, D. Takahashi, W. Choi, K. Kono, and E. Kim, *Physical Review Letters* **108**, 105302 (2012).

P3.48 Longitudinal excitations in triangular lattice antiferromagnets

M. Merdan and Y. Xian

The University of Manchester, Manchester M13 9PL, UK

We study the longitudinal excitations of quantum antiferromagnets on a triangular lattice by a recently proposed microscopic many-body approach based on magnon-density waves. We calculate the full longitudinal excitation spectra of the antiferromagnetic Heisenberg model for a general spin quantum number in the isotropic limit. Similar to the square lattice model, we find that, at the center of the first hexagonal Brillouin zone $\Gamma(\mathbf{q} = 0)$ and at the magnetic ordering wavevectors $\pm[\mathbf{Q} = (4\pi/3, 0)]$, the excitation spectra become gapless in the thermodynamic limit, due to the slow, logarithmic divergence of the structure factor. However, these longitudinal modes on two-dimensional models may be considered as quasi-gapped, as any finite-size effect or small anisotropy will induce a large energy gap, when compared with the counterpart of the transverse spin-wave excitations. We also find that the triangular lattice longitudinal mode is in general softer, with smaller energy gap values, than that of the square lattice model due to the frustrations in the triangle lattice system.

4.7 Invited Oral Presentations: Monday August 20th

O13.1 Stabilization of New Phases of Superfluid ^3He in Anisotropic Silica Aerogel

W.P. Halperin, J. Pollanen, J.I.A. Li, C.A. Collett, W.J. Gannon, A. Zimmerman, and J.A. Sauls

Department of Physics and Astronomy, Northwestern University, Evanston, USA

Superfluid ^3He within highly porous silica aerogel is the realization of homogeneous superfluidity in the presence of quenched disorder. Since the earliest observations in 1995, extensive experimental and theoretical work[1] has shown evidence for various stable superfluid states and order parameter textures. In our recent work at Northwestern University using high quality aerogel samples, we have found extremely sharp phase transitions, $\Delta T_c/T_c$ and $\Delta T_{ab}/T_{ab} \sim 0.1\%$. The NMR experiments[2] with homogeneous isotropic aerogel samples permit identification of the order parameter texture and the superfluid state. They are impurity phases of the axial and isotropic p -wave states, more familiarly known as the A and B-phases of pure ^3He . Uniaxial stretching of this isotropic silica framework produces anisotropic quasi-particle scattering that stabilizes the A-phase over the available range of pressure and temperature down to 0.6 mK in a stretched aerogel.[3] This is in contrast to isotropic aerogel where the phase observed on warming is the B-phase in the zero magnetic field limit. We have also discovered that uniaxial compression leads to stabilization of one, or possible two, equal-spin-pairing states, and that the boundaries between the dominant B-phase and these two states in the $H - T$ phase diagram are quite unexpected. Support from the National Science Foundation, DMR-1103625 is gratefully acknowledged.

1. Yoonseok Lee and Richard P. Haley, Ch. 5 in *Novel Superfluids*, Vol. 1 ed. by Bennemann and Ketterson
2. J. Pollanen *et al.* Phys. Rev. Lett. **107**, 195301 (2011).
3. J. Pollanen *et al.* Nature Physics, **8**, 317 (2012).

O13.2 NMR Studies of Superfluid ^3He in “Nematically Ordered” Aerogel

V. V. Dmitriev, D. A. Krasnikhin, A. A. Senin, and A. N. Yudin

Kapitza Institute, Moscow, Russia

We report results of experiments with superfluid ^3He in “nematically ordered” aerogel. This aerogel consists of Al_2O_3 strands which are nearly parallel to each other. Two kinds of superfluid phases were observed: the low temperature phase and the high temperature phase. NMR properties of the low temperature phase correspond to Balian-Werthamer phase while the high temperature phase presumably has Anderson-Brinkman-Morel order parameter with polar distortion, which value depends on pressure and temperature. We think that, in some range of temperatures just below the temperature of the superfluid transition, the high temperature phase may correspond to pure polar phase. This suggestion agrees with results of our recent experiments which have been done with squeezed aerogel samples.

O13.3 Effect of structural correlations in aerogel on thermodynamic properties of superfluid ^3He

I.A. Fomin and E.V. Surovtsev

P.L. Kapitza Institute for Physical Problems of Russian Academy of Sciences, Moscow

Important difference of aerogel as an impurity in the superfluid ^3He from the ideal impurities of the Abrikosov and Gorkov theory of superconducting alloys is the presence of structural correlations. We show that these correlations substantially enhance the temperature region below the T_c where fluctuations of local density of impurities alter temperature dependence of the absolute square of the average order parameter and of thermodynamic properties of the superfluid, such as specific heat, NMR frequency shift, superfluid density. If correlation radius of impurities is comparable with the coherence length of the superfluid ^3He the effect of fluctuations can extend well into the superfluid region. Lowering of the transition temperature of ^3He and deviation of the thermodynamic properties of its superfluid phase from the standard behavior are expressed in terms of the structure factor of aerogel. Anomaly in temperature dependence is accompanied by significant fluctuations of the magnitude of the order parameter. Comparison with the data for the NMR frequency shift in both superfluid phases of ^3He is made.

O13.4 Existence of Dense Superfluid ^3He - ^4He Mixture in Aerogel

R. Ito^a, Y. Tanaka^a, J. Hitomi^a, R. Toda^a, M. Kanemoto^a, and Y. Sasaki^{a,b}

^aDepartment of Physics, Graduate School of Science, Kyoto University, Kyoto, JAPAN

^bResearch Center for Low Temperature and Materials Sciences, Kyoto University, Kyoto, JAPAN

There has been a controversial issue on whether dense mixture of liquid ^3He and ^4He exists in aerogel at $T = 0$. Penn. State group suggested the existence of dense mixture¹. Cornell group showed the existence of phase-separated droplet of ^4He in the regime of 11% or more of ^4He density². However it is still unclear if ^4He is homogeneously mixed into liquid ^3He in the regime of a few percent of ^4He . We find the existence of the non-phase-separated dense mixture in aerogel near $T = 0$. While studying superfluid ^3He of 2.4 MPa in 97.5%-porosity aerogel with NMR/MRI techniques, we find that the T_C is reduced when more than adequate amount of ^4He for covering the surface of silica strands is introduced. For a sample of which T_C is as low as 0.9 mK, we find that the spin diffusion coefficient in the normal phase is increased by a factor of 1.5 both in high temperature region, where ^3He - ^3He scattering dominates, and in low temperature region, where ^3He -aerogel scattering dominates. This enhancement is attributed to a modification of Landau parameter F_0^a from -0.76 to -0.64, which is a change towards less ferromagnetic direction. This modification of microscopic quantity can be achieved only by diluting liquid ^3He with ^4He in the aerogel and not by a macroscopic coexistence like as phase-separated droplet. This is the first confirmation of the existence of dense superfluid ^3He - ^4He mixture in aerogel.

1. S. B. Kim *et al.*, *PRL***71**, 2268(1993); N. Mulders and M. H. W. Chan, *PRL***75**, 3705(1995).

2. A. Golov *et al.*, *PRL***80**, 4486(1998); G. Lawes *et al.*, *PRL***90**, 195301(2003).

O14.1 Interplay of rotational relaxational and shear dynamics in solid ^4He

J.C. Séamus Davis

Cornell University; Brookhaven National Lab.; University of St. Andrews.

Using a SQUID-based high sensitivity torsional oscillator (TO) technique, we map comprehensively the rotational and relaxational dynamics of solid ^4He throughout the parameter range of the proposed supersolidity. We find evidence that the same microscopic excitations controlling the torsional oscillator motions are generated independently by thermal and mechanical stimulation. Moreover a measure for the relaxation times of these excitations diverges smoothly without any indication for a critical temperature or critical velocity within the parameter ranges proposed for the supersolid transition. Finally, we demonstrate that the combined temperature-velocity dependence of the TO response is indistinguishable from the combined temperature-strain dependence of the solid's shear modulus. This implies that the rotational responses of solid ^4He attributed to supersolidity are associated with generation of the same microscopic excitations as those produced by direct shear strain.

O14.2 Quantized Circulation in Solid Helium-4 under Rotation

H. Choi^a, D. Takahashi^b, W. Choi^a, K. Kono^b, and E. Kim^a

^aDepartment of Physics, KAIST, Daejeon, South Korea

^bLow Temperature Physics Laboratory, RIKEN, Wako-shi, Japan

Despite people's excitement after the potential discovery of supersolid by Kim and Chan in 2004¹, it is not clear that what they have observed is, in fact, superfluidity within solid. The excitement brought a large number of researchers to pursue the exact nature of solid helium. There is mounting evidence both for and against supersolid, and we present one for the existence of supersolid by performing a torsional oscillator experiment on rotating solid helium. A signal that can be interpreted as suppression of non-classical rotational inertia fraction was seen in solid helium under rotation.² Further investigation of the effect has shown that the suppression of the signal is not continuous under rotation velocity sweep. In fact, the suppression follows a discrete staircase-like change that is periodic in velocity.³ One possible source of such behavior is quantization of superfluid circulation within supersolid.

1. E. Kim and M. H. W. Chan, *Nature* **427**, 225 (2004).

2. H. Choi, D. Takahashi, K. Kono, and E. Kim, *Science* **330**, 1512 (2010).

3. H. Choi, D. Takahashi, W. Choi, K. Kono, and E. Kim, *Physical Review Letters* **108**, 105302 (2012).

O14.3 Possible Quantum Oscillation of Non-Classical Rotational Inertia of Solid ^4He in Vycor by DC Rotation

D. Takahashi^{a,c}, T. Tsuiki^b, K. Kono^a, and K. Shirahama^b

^aLow Temperature Phys. Lab., RIKEN, Wako-shi 351-0198, Japan

^bDepartment of Physics, Keio University, Yokohama 223-8522, Japan

^cDepartment of General Education, Ashikaga Institute of Technology, Ashikaga 326-8558, Japan

Recent finding of the reduction of “Non-classical Rotational Inertia (NCRI)” of solid ^4He by DC rotation suggests genuine supersolidity in bulk solid ^4He [1]. It is known that solid ^4He formed in porous Vycor glass also shows a NCRI phenomenon[2]. Search for the DC rotation effect in solid ^4He in Vycor will provide essential information for the nature of NCRI, because in porous media the structure of solid ^4He can be quite different from bulk solid, in particular, no large scale dislocation network exists. We study the effect of rotation on NCRI of solid ^4He confined in a Vycor glass (pore size: 6 nm). A torsional oscillator (resonant frequency: 1016 Hz) containing an annular Vycor (17 and 14 mm in outer and inner diameters) is mounted in the rotating dilution refrigerator at RIKEN. Three solid samples with pressures 5.5 – 8 MPa, having rather large NCRI that is about 10 percent of the total solid ^4He inertia, show the depletion of NCRI by rotating the samples up to angular velocity $\Omega = 4$ rad/sec. The Ω dependence of NCRI has a very interesting oscillating structure, in which the oscillation becomes periodic when NCRI is plotted as a function of Ω^{-1} , suggesting the “de Haas-like quantum oscillation” observed in electrons in metals and semiconductors under magnetic field.

[1] H. Choi *et al.*, Science **330**, 1512(2010); H. Choi *et al.*, Phys Rev. Lett. **108**, 105302(2012), [2] E. Kim and M. Chan, Nature **427**, 225(2004)

O14.4 Is solid helium a superfluid?

M.H.W. Chan

Penn State University, Department of Physics, University Park, PA 16802 USA

O15.1 Electrons on liquid helium in confined geometry - a unique Coulomb system

Paul Leiderer

Department of Physics, University of Konstanz, D 78457 Konstanz, Germany

Electrons the surface of liquid helium or at the interface between phase-separated ^3He - ^4He mixtures are examples of particularly clean and well-defined Coulomb systems, which have been studied for more than four decades and are still providing new insights into the properties of 2-dimensional matter. They are the model counterpart of electrons in MOSFET inversion layers, and a number of phenomena have been observed in these model systems for the first time, the most prominent probably being the transition from an electron fluid to a Wigner crystal state. The electron density can be varied deliberately over many orders of magnitude, so that studies in various regimes of the phase diagram are possible. In this talk first an overview over the properties of the quasi-infinite electron systems at helium interfaces will be presented, followed by results for such systems in confined geometry, like multi-electron bubbles or electron transport in mesoscopic structures such as narrow channels or constrictions, as classical analogues of quantum wires and point contacts.

O15.2 Transport of single electrons on helium channels

K. Kono, D. Rees, and H. Ikegami

Low Temperature Physics Laboratory, RIKEN, Wako-shi, 351-0198 Japan

A capillary condensed helium channel provides versatile means to control single electrons on a liquid He surface [1-3]. Recent developments of this technique will be reviewed. Incorporating micro-fabricated electrode assembly, we have made a point-contact device to observe a single file electron transport. [4] At low temperatures Coulomb interaction between electrons plays an important role to develop a positional ordering in surface state electrons (SSE) on liquid He. Near the point-contact, commensurability between the configuration of electrons and constricting potential profile is important, which gives rise to anomalous transport characteristics. [5]

It was shown that by employing He channels, one can observe decoupling of the electron lattice from a dimple sub-lattice which results from the local pressure due to the electron lattice. [6] The effect had been observed only under perpendicular magnetic fields in bulk SSE on liquid He. Using such He channels, an interesting size effect on the electron lattice melting is observed. The degree of confinement in width results in the modulation of melting behavior of the electron system.

1. P. Glasson, *et al.*, Phys. Rev. Lett. 87, 176802 (2001).
2. G. Papageorgiou, *et al.*, Appl. Phys. Lett. 86, 153106 (2005).
3. F. R. Bradbury, *et al.*, Phys. Rev. Lett. 107, 266803 (2011).
4. D. G. Rees, *et al.*, Phys. Rev. Lett. 106, 026803 (2011).
5. D. G. Rees, H. Totsuji, and K. Kono, Phys. Rev. Lett. 108, 176801 (2012).
6. H. Ikegami, H. Akimoto, and K. Kono, Phys. Rev. Lett. 102, 046807 (2009).

O15.3 Probing Chirality in Superfluid $^3\text{He-A}$

H. Ikegami and K. Kono

Advanced Science Institute, RIKEN, Wako, Saitama 351-0198, Japan

We report the first detection of chirality in superfluid $^3\text{He-A}$ by observing a novel effect, intrinsic Magnus effect,^{1,2} experienced by a traveling impurity. An impurity traveling in a plane perpendicular to the l vector experiences the intrinsic Magnus force in the direction perpendicular to both its velocity and the l vector, as a result of the skew scattering of quasiparticles by the impurity. We investigated the intrinsic Magnus effect for charged impurities, electron bubbles, trapped below the free surface of superfluid ^3He at a depth about 35 nm by transport of electron bubbles along the surface. In this configuration, the l vector aligns uniformly normal to the surface, and the electrons bubbles traveling along the surface would be subjected to the intrinsic Magnus force. We observed transverse current associated with the intrinsic Magnus effect. The transverse currents show two types of temperature dependences, which are equal in magnitude but opposite in sign, and these two correspond to the l vector pointing parallel ($+l$) and anti-parallel ($-l$) to the surface normal. After repeating many cooling runs from normal state, we find that the ratio between $+l$ and $-l$ emerging just below T_c is asymmetric about the direction of magnetic field.

1. R. H. Salmelin *et al.*, Phys. Rev. Lett. **63**, 868 (1989).
2. R. H. Salmelin and M. M. Salomaa, Phys. Rev. B **41**, 4142 (1990).

O16.1 Resonant Tunnelling Systems in ^4He Crystals: Alternative to Supersolidity

A.F. Andreev

Kapitza Institute, Russian Academy of Sciences, Moscow, Russia

A simple model based on the concept of resonant tunnelling clusters of lattice defects is used to explain the low temperature anomalies of ^4He crystals (mass decoupling from a torsional oscillator, shear modulus anomaly, dissipation peaks, heat capacity peak). Mass decoupling is a result of an internal Josephson effect: mass supercurrent inside phase coherent tunneling clusters. Quantitative results are in reasonable agreement with experiments. The characteristic size and the concentration of the clusters are on the order of 10 nm and 10^7 cm^{-3} , respectively. According to the model, mass decoupling is absent in ^3He crystals but shear modulus anomaly is present both in ^3He and ^4He crystals.

1. Andreev, A. F. (2011). “Low-temperature anomalies of ^4He crystals”. JETP Lett. **94**, 129.
2. Andreev, A. F. (2012). “Tunnelling defect nanoclusters in hcp ^4He crystals: alternative to supersolidity”. J. Low Temp. Phys. DOI 10.1007/s10909-011-0455-9.

O16.2 Spectroscopy of atomic bubbles in liquid and solid helium

P. Moroshkin^{a,b}, V. Lebedev^a, and A. Weis^a

^aDepartment of Physics, University of Fribourg, Switzerland

^bInstitute for Applied Physics, University of Bonn, Germany

We investigate properties of open-shell atomic and molecular dopants in liquid and solid ^4He . Despite their small size (typically 1 nm), the defect structures formed by these dopants can be treated as cavities or bubbles embedded into a continuous medium and a hydrodynamic model gives a very accurate description of their observed properties. The spectroscopy of the atomic bubbles is well established since the 1990s (for a recent review see [1]). On the other hand, studies of the atomic bubble dynamics are still scarce. Characteristic vibration frequencies of the nanoscopic bubbles overlap with the spectrum of the elementary matrix excitations. At the same time, the typical bubble size closely matches the wavelength of the resonant phonons. One thus expects a strong coupling between the atomic bubble vibrations and elementary matrix excitations. The details of this resonant interaction at present are not fully understood.

The present contribution gives a brief overview of the atomic bubble theory and of the most recent experiments in the field. In particular, we present a spectroscopic study of transition-metal atoms in liquid and solid helium. Special attention is paid to the effects of the bubble-phonon interaction. We also discuss the perspectives of using the atomic bubbles as nanoscopic probes for the investigation of the properties and dynamics of quantum fluids and solids.

1. P. Moroshkin, A. Hofer, A. Weis, *Physics Reports* **469**, 1 (2008).

O16.3 Free Decay of Acoustic Turbulent Energy Cascades in Superfluid ^4He

V. Efimov^{b,a}, P.V.E. McClintock^b, and A. Ganshin^{b,c}

^aInstitute of Solid State Physics RAS, Chernogolovka, Russia

^bDepartment of Physics, Lancaster University, Lancaster, UK

^cLaboratory for Elementary-Particle Physics, Cornell University, Ithaca, USA.

We report measurements of the free decay of second sound acoustic turbulence [1] in superfluid ^4He in a high- Q resonator. Starting from a resonant stationary state, we discontinuously switch off the external excitation. We then investigate the ensuing spectral evolution as the standing wave decays, thereby gleaning information about the nonlinear inter-mode interactions. We find [2] that the decay of the discrete distribution begins from the high-frequency edge of the spectrum, and then moves towards the pumping range of frequencies. A special feature of this high- Q resonator is that it allows us to separate the linear and nonlinear decay time constants of the main harmonic. The nonlinear decay constant, corresponding to the energy flux through the frequency cascade, was found to be an order of magnitude shorter than the linear decay constant corresponding to the Q -factor of the resonator. The decay time of one harmonic is anomalously long, and possible reasons for this phenomenon will be discussed.

[1] A N Ganshin, V B Efimov, G V Kolmakov, L P Mezhev-Deglin and P V E McClintock, "Observation of an inverse energy cascade in developed acoustic turbulence in superfluid helium", *Phys. Rev. Lett.* **101**, 065303 (2008).

[2] A N Ganshin, V B Efimov and P V E McClintock, "Experiments on second sound acoustic turbulence in superfluid helium: decay of the direct and inverse energy cascades", submitted to *Phys. Rev. E*.

O16.4 Surface states, edge currents, and chiral symmetry of superfluid $^3\text{He-A}$

J.A. Sauls

Department of Physics and Astronomy, Northwestern University, Evanston, Illinois 60201 USA

The spectra of fermionic excitations, pairing correlations and edge currents confined near the boundary of a chiral p-wave superfluid are calculated to leading order in $\hbar/p_f\xi$.¹ Results for the energy- and momentum-resolved spectral functions near a confining boundary reveal the subtle role of the chiral edge states (Weyl fermion branch) in relation to the edge current and the angular momentum of a chiral p-wave superfluid, including the rapid suppression of $L_z(T)$ for $0 \lesssim T \ll T_c$ in the fully gapped 2D chiral superfluid. The edge current and ground-state angular momentum are shown to be sensitive to boundary conditions, and as a consequence the topology and geometry of the confining boundaries. For perfect specular boundaries the edge current accounts for the ground-state angular momentum, $L_z = (N/2)\hbar$, of a cylindrical disk of chiral superfluid with $N/2$ fermion pairs. Non-specular scattering can substantially suppress the edge current. In the limit of perfect retro-reflection the edge states form a flat band of zero modes that are non-chiral and generate no edge current. For a chiral superfluid film confined in a cylindrical toroidal geometry the ground-state angular momentum is, in general, non-extensive, and can have a value ranging from $L_z > (N/2)\hbar$ to $L_z < -(N/2)\hbar$ depending on the ratio of the inner and outer radii and the degree of back scattering on the inner and outer surfaces. Non-extensive scaling of L_z , and the reversal of the ground-state angular momentum for a toroidal geometry, would provide a signature of broken time-reversal symmetry of the ground state of superfluid $^3\text{He-A}$, as well as direct observation of chiral edge currents.

1. J. A. Sauls, Phys. Rev. B 84, 214509 (2011).

4.8 Poster Presentations: Monday August 20th

P4.1 Effect of Form Factor on Ground-state Properties of Electron Quantum Bilayers

L.K. Saini and Mukesh G. Nayak

Department of Applied Physics, S. V. National Institute of Technology, Surat 395 007 Gujarat (India)

The effect of form factor on density modulated ground-state of coupled electron quantum layers (CEQL) is studied by quantum version of Singwi, Tosi, Land, and Sjölander (so called qSTLS) approach at zero temperature. We find that as the electron density in CEQL system is lowered, the system favors the Wigner crystal (WC) phase, the regular periodic arrangement of electrons. The prediction of WC phase gets more support from the study of static structure factor, pair-correlation function and local-field correction factor. Expectedly at the point of instabilities, the intralayer static structure factor shows sharp peak and strong pronounced oscillatory behaviour is observed in pair-correlation function as well as in local-field correction factor at critical electron density. We notice that the inclusion of finite thickness lowered the critical electron density for the onset of WC phase with respect to the ideal CEQL system. We also calculate the ground-state energy and compared our results with the recent ideal CEQL system¹.

1. Moudgil R.K., Senatore G., Saini L.K. (2002). "Dynamic Correlations in Symmetric Electron-Electron and Electron-Hole Bilayers" Phys. Rev. B 66, 205316.

P4.2 Surface electrons transport over structured silicon substrate

A.V. Smorodin, V.A. Nikolaenko, and S.S. Sokolov

B.Verkin Institute for Low Temperature Physics and Engineering of the National Academy of Sciences of Ukraine

A novel zero-dimensional system at helium temperatures is realized. The system is formed by electrons over superfluid helium placed in cylindrical macropores of a structured silicon substrate. It is shown that the pressing electric field, normal to the electron layer can change essentially the potential well for electrons, depending on curvature of the liquid surface. Conductivity of the surface electrons with densities 10^6 to 10^8 cm⁻² is measured at temperatures T=0.5-1.6 K and pressing fields up to 10^3 V/cm. The electron transport along the substrate depends strongly on curvature of the liquid surface in macropores. If the curvature is big and, thereafter the helium film is thin, the electron conductivity has activation nature, typical for the hopping processes. With decreasing the curvature radius the temperature dependence of conductivity becomes smooth. The pressing potential dependence of conductivity has a "dip". The "dip" is not observed for the smallest radii of curvature attained in the experiment. To explain the results obtained we assume formation of the electron clusters around the macropores.

P4.3 Magnetization of Dense ^3He Monolayers Adsorbed on Graphite

T.N. Antsygina, I.I. Poltavsky, M.I. Poltavskaya, and K.A. Chishko

B.Verkin Institute for Low Temperature Physics and Engineering, Kharkov, Ukraine

The second solid ^3He monolayer on graphite provides an excellent example of a nearly perfect $1/2$ - spin nuclear magnet on a triangular lattice. Magnetization of a dense ^3He monolayer is investigated theoretically within a ferromagnetic Heisenberg model (HFM) in an external magnetic field. We employ an analytical approach based on a second-order two-time Green function formalism with a new decoupling scheme that describes properly the HFM thermodynamics for both infinite and finite-sized spin systems in the whole temperature range at arbitrary fields h . In particular, the proposed method improves significantly the description of the 2D HFM at $h < T < J$ (J is an exchange constant) and ultralow magnetic fields $h/J \ll 1$, where the measurements for solid ^3He monolayers are usually made.

The obtained results are used to give a consistent interpretation to a great number of known from literature experimental data on magnetization of the second solid ^3He monolayer in the ferromagnetic regime. It is proved that at dense coverages $\rho \geq 0.22\text{\AA}^{-2}$ the pure Heisenberg behavior of 2D solid ^3He occurs, and the theory is in excellent agreement with the experimental data at all temperatures. The coverage dependences of the exchange constant, saturation magnetization M_{sat} , and average cluster size N are analyzed in detail. The exchange constant is found to display nonmonotonic behavior with increase in coverage, whereas M_{sat} as well as N continuously grow tending to their limiting values.

P4.4 Finite systems of 1D and 2D harmonic oscillators obeying fractional statistics with a complex parameter

A. Rovenchak

Department for Theoretical Physics, Ivan Franko National University of Lviv, Ukraine

Using the previously suggested generalization [1] of the Polychronakos fractional statistics [2], finite systems of 1D and 2D harmonic oscillators are studied. The dependences of critical temperature T_c on the number of particles N are obtained. The critical temperature is defined by the following conditions:

$$\Re \sum_n \frac{g_n}{z_\nu^{-1} e^{\varepsilon_n/T_c} - e^{i\pi\nu}} = N, \quad \Im \sum_n \frac{g_n}{z_\nu^{-1} e^{\varepsilon_n/T_c} - e^{i\pi\nu}} = 0,$$

with g_n being the degeneration of the n th level ($g_n = 1$ for a 1D system and $g_n = n + 1$ for an isotropic 2D system). The parameter $\alpha = e^{i\pi\nu}$ smoothly interpolates between the Bose ($\nu = 0$) and Fermi ($\nu = 1$) distributions; $z_\nu = e^{\mu_\nu/T_c}$ where μ_ν is the bulk value of the chemical potential at the critical temperature, and $\varepsilon_n = \hbar\omega n$ is the energy of the respective level. The analysis of the T_c behaviour allows for better understanding of the nature of the phase transition in the respective systems, which otherwise partly resembles the Bose-condensation as confirmed by the calculated specific heat dependences on the temperature.

1. Rovenchak, A. (2012). "Polychronakos fractional statistics with a complex-valued parameter", J. Phys.: Conf. Ser. (LT26 Proceedings, to appear).

2. Polychronakos, A. P. (1996). "Probabilities and path-integral realization of exclusion statistics", Phys. Lett. B **365**, 202–206.

P4.5 Spin nematic order in the multiple-spin exchange model on the triangular lattice

T. Momoi^a, P. Sindzingre^b, and K. Kubo^c

^aCondensed Matter Theory Laboratory, RIKEN, Japan

^bLaboratoire de Physique Théorique de la Matière Condensée, Université P. et M. Curie, France

^cDepartment of Physics and Mathematics, Aoyama Gakuin University, Japan

Among various triangular-lattice magnetic materials that show spin-liquid-like behaviors, solid helium 3 films on graphite offer an interesting system as it has nearest-neighbor ferromagnetic exchange and competing multiple-spin exchange interactions. For a range of densities bordering on ferromagnetism, spins in solid ³He films exhibit anomalous double-peak structure in specific heat¹ with gapless excitations². It has been an unsolved issue how magnetism of solid ³He films can be described with the multiple-spin exchange (MSE) interactions on the triangular lattice. Recently we figured out that the ground state of the MSE model applicable to thin films of solid ³He possesses an octahedral spin nematic order³. In the presence of magnetic field, it is deformed into an antiferro-quadrupolar order in the perpendicular spin plane, in which lattice Z_3 rotational symmetry is also broken. Furthermore, this model shows a narrow magnetization plateau³ at $m/m_{\text{sat}} = 1/2$, which resembles recent magnetization measurement in solid ³He films⁴.

1. K. Ishida, M. Morishita, K. Yawata, and H. Fukuyama, Phys. Rev. Lett. **79** (1997) 3451.

2. R. Masutomi, Y. Karaki, and H. Ishimoto, Phys. Rev. Lett. **92** (2004) 025301.

3. T. Momoi, P. Sindzingre, and K. Kubo, Phys. Rev. Lett. **108** (2012) 057206.

4. H. Nema, A. Yamaguchi, T. Hayakawa, and H. Ishimoto, Phys. Rev. Lett. **102** (2009) 075301.

P4.6 Correlation between band structure and magneto-transport properties in HgTe/CdTe two-dimensional far-infrared detector superlattice.

A. Idbaha^a, A. Nafidi^a, B. Marí Soucase^b, K. Chander Singh^c, and B. Hartiti^d

^aLPMC Nano RE, University Ibn Zohr, Agadir, Morocco

^bLaboratory of Optoelectronics, Universitat Politècnica de València, Spain.

^cDepartment of chemistry, M.D.University, Rohtak, India.

^dLPMAER, University Hassan II Mohammédia, Morocco.

Theoretical calculations of the electronic properties performed in the envelope function formalism of n-type HgTe ($d_1=8.6$ nm) /CdTe ($d_2=3.2$ nm) superlattices (SLs) have provided an agreement with the experimental data on the magneto-transport behavior. The energy $E(d_2, \Gamma, 4.2$ K), shown that when d_2 increase the gap E_g decrease to zero at the transition semiconductor to semimetal conductivity behavior and become negative accusing a semimetallic conduction. At 4.2 K, the sample exhibits n type conductivity, confirmed by Hall and Seebeck effects, with a Hall mobility of $2.5 \cdot 10^5$ cm²/Vs. This allowed us to observe the Shubnikov-de Haas effect with $n = 3.20 \cdot 10^{12}$ cm⁻². Using the calculated effective mass ($m_{E1}^*(\Gamma) = 0.04 m_0$) of the degenerated electrons gas, the Fermi energy (2D) was $E_F=88$ meV in agreement with 91 meV of thermoelectric power α . In intrinsic regime, $\alpha \sim T^{-3/2}$ and $R_H T^{3/2}$ indicates a gap $E_g = E_1 - HH_1 = 101$ meV in agreement with calculated $E_g(\Gamma, 300$ K) =105 meV The formalism used here predicts that the system is semiconductor for $d_1/d_2 = 2.69$ and $d_2 < 88$ nm. Here, $d_2=3.2$ nm and $E_g(\Gamma, 4.2$ K) = 48 meV so this sample is a two-dimensional far-infrared detector semiconductor ($12\mu\text{m} < \lambda_c < 28\mu\text{m}$).

P4.7 Interaction of cold neutrons with impurity gel samples of heavy water and deuterium in superfluid He-II; structural transformations in high dispersed icy samples at low temperatures

L.P. Mezhov-Deglin^a, V.B. Efimov^a, V.V. Nesvizhevsky^b, and G.V. Kolmakov^c

^aInstitute of Solid State Physics RAS, Chernogolovka, Moscow distr., Russia

^bInstitute Lue Langevin , 6 rue Jules Horowitz, 38042 Grenoble, France

^cNew York City College of Technology, 300 Jay Street, Brooklyn, N.Y.11201, USA

We studied interaction of cold and very cold neutrons with impurity gel samples of heavy water and deuterium in superfluid He-II. The measurements showed that the backbone (dispersion system) of the gels in He-II consists of impurity nanoclusters with characteristic dimensions of a few nm, and liquid helium, which soaks the gel pores (helium in restricted geometry), plays a role of the dispersion medium. Heating the freshly prepared gel samples from 1.66 to 2 K resulted in significant increase of small size (about 1 nm) clusters in the bulk of the sample. From our recent X-ray measurements it followed that the decay of water gel samples on heating them above 4 K resulted in formation of an icy powder composed of a mixture of amorphous and cubic ice grains with the mean sizes of crystals of a few nm. We also discuss the feasibility of utilizing the gel samples and the icy grains for production of ultracold neutrons in He-II and for building nanostructured reflectors for slow neutrons.

P4.8 Quantum Interference of Surface States in Bismuth Nanowires in Transverse Magnetic Fields

L. Konopko^a, T.E. Huber^b, and A. Nikolaeva^a

^aGhitu Institute of Electronic Engineering and Nanotechnologies, ASM, Chisinau, Moldova and International Laboratory of High Magnetic Fields and Low Temperatures, Wroclaw, Poland

^bHoward University Department of Chemistry, 500 College St. N.W., Washington, DC 20059

We report here the observation of quantum oscillations of the transverse magnetoresistance (MR) in single-crystal Bi nanowires with a diameter $d < 80$ nm. The nanowire samples with glass coating were prepared by an improved Ulitovsky technique; they were cylindrical single crystals with the (1011) orientation along the wire axis where the C_3 axis was inclined at an angle of 70° to the wire axis. Earlier [1, 2], we have observed the oscillations of longitudinal MR of Bi nanowires with two periods proportional to h/e and $h/2e$. Nonmonotonic changes of transverse MR that are equidistant in the direct magnetic field were observed at low temperatures in a wide range of magnetic fields up to 14 T. It was recently suggested that bismuth bilayers may manifest quantum spin Hall effect [3]. The Bi crystal can be viewed as a stacking of bilayers with honeycomblike lattice structure along the [111] direction. According to theoretical calculation Z_2 topological number I is odd and Bi bilayer system is inversion symmetric. Probably, transverse MR oscillations arise due to the topological nature of Bi nanowire surface states. Different assumptions about the origin of the observed effect will be discussed.

1. T.E. Huber, A.A. Nikolaeva, L.A. Konopko, M.J. Graf, *Phys. Rev. B* **79**, 201304(R) (2009).

2. L.A. Konopko, T.E. Huber, A.A. Nikolaeva, *J. Low Temp. Phys.* **158**, 523 (2010).

3. S. Murakami, *Phys. Rev. Lett.* **97**, 236805 (2006).

P4.9 Influence Weak and High Magnetic Field in Longitudinal and Transverse Configuration on Magneto-thermoelectric Properties Quantum Bi-wires

A. Nikolaeva^a, L. Konopko^a, T. Huber^b, and Gh. Para^c

^aGhitu Institute of Electronic Engineering and and Nanotechnologies, ASM, Chisinau, Moldova and International Laboratory of High Magnetic Fields and Low Temperatures, Wroclaw, Poland

^bDepartment of Chemistry, Howard University, 500 College St. N.W., DC 20059 Washington, U.S.A

^cGhitu Institute of Electronic Engineering and and Nanotechnologies, ASM, Chisinau, Moldova

This paper report a series of magneto-thermoelectric measurement made on single-crystal Bi nanowires with diameters up to 50 nm in longitudinal and transverse magnetic field 0-14T at temperature range 4.2-300K. Cylindrical Bi single crystals with glass coating were prepared by the high frequency liquid phase casting. We demonstrate that the size maximum on the longitudinal magneto-resistance and magneto-thermopower represents the temperature and dimensional behaviors of the carrier mobility. Anomalies observed on magneto-resistance and magneto-thermopower on 50-70nm Bi-wires is associated with manifestation effect size quantization on 50-70nm Bi-wires. From experimental data it is calculated Power factor and its dependence from diameter, temperature, magnetic field quantum Bi wires. The enhancement the thermoelectric figure of merit for Bi-nanowire is discussed.

P4.10 Magnetic Response of $S = 2$ Linear-Chain Antiferromagnets at Low Temperatures and in High Magnetic Fields

Ju-Hyun Park^a, Olivia N. Risset^b, Muhandis Shiddiq^c, Elisabeth S. Knowles^d, Christopher C. Beedle^a, Matthieu F. Dumont^{b,d}, Stephen Hill^c, Daniel R. Talham^b, and Mark W. Meisel^d

^aNHMFL, Florida State University, Tallahassee, FL 32310-3706, USA

^bDepartment of Chemistry, University of Florida, Gainesville, FL 32611-7200, USA

^cDepartment of Physics and NHMFL, Florida State University, Tallahassee, FL 32310-3706, USA

^dDepartment of Physics and NHMFL, University of Florida, Gainesville, FL 32611-8440, USA

Linear-chain, integer-spin antiferromagnets, commonly known as Haldane systems, have a storied history in the field of quantum spins, with $S = 1$ materials receiving the most attention. The $S = 2$ systems have received less consideration for several reasons, including a smaller Haldane gap, since $\Delta_{S=1} = 0.41 J$ and $\Delta_{S=2} = 0.09 J$, where J is the nearest-neighbor exchange energy. Due to the recent report suggesting Mn(III)F(salen) is a $S = 2$ Haldane system with $J/k_B = 50$ K and no evidence of long-range order down to 2 K [1], we have studied the magnetic response of single-crystals down to 20 mK and in magnetic fields up to 18 T. In addition, we have explored the EPR response of this material and Mn(III)Cl₃(bipy), a Haldane $S = 2$ material with $J/k_B = 35$ K and no evidence of long-range order down to 35 mK [2]. These results will be discussed in the context of the presence of end-chain spins and finite single-ion anisotropy, D . This work was supported, in part, by the NSF through DMR-1005581 (DRT), DMR-0804408 (SH), DMR-1202033 (MWM), and DMR-0654118 (NHMFL).

1. T. Birk *et al.*, Inorg. Chem. **50** (2011) 5312.

2. G.E. Granroth *et al.*, Phys. Rev. Lett. **77** (1996) 1616.

P4.11 ^3He and ^4He on graphene–fluoride and graphane: prediction of novel fluid, superfluid and supersolid phases

M. Nava^a, D.E. Galli^a, M.W. Cole^b, and L. Reatto^a

^aDipartimento di Fisica, Università degli Studi di Milano, via Celoria 16, 20133 Milano, Italy

^bDepartment of Physics, Penn State University, University Park, PA 16802 USA

We present a study of submonolayer He adsorbed on two derivatives of graphene: graphene-fluoride (GF) and graphane (GH). A semiempirical interaction with the substrate is used in state of the art quantum simulations. We predict that both isotopes ^3He and ^4He form anisotropic fluid states at low coverage. The commensurate state analogous to the standard $\sqrt{3} \times \sqrt{3}$ R30° phase that preempts fluid states on graphite turns out to be unstable relative to a fluid state. The commensurate insulating ground state on GF and GH is disfavored by the much smaller inter-site distance (below 1.5 Å) compared to graphite (2.46 Å), implying a large energy penalty for localizing He atoms. The ^4He ground state on both substrates is a self-bound anisotropic superfluid with anisotropic roton excitations and with a superfluid density ρ_s reduced from 100% due to the corrugation of the adsorption potential. In the case of GF such corrugation is so large that $\rho_s = 57\%$ at $T = 0$ K and the superfluid is essentially restricted to move in a multiconnected space, along the bonds of a honeycomb lattice. We predict a superfluid transition temperature $T \simeq 0.25$ (1.1) K for ^4He on GF (GH). At higher coverages we find two kinds of solids, an incommensurate triangular one as well as a novel commensurate state at filling factor 2/7 with 4 atoms in the unit cell. We have evidence that this 2/7 state is supersolid. We conclude that these new platforms for adsorption studies offer the possibility of studying novel phases of quantum condensed matter like an anisotropic Fermi fluid, possibly superfluid, an anisotropic Bose superfluid and a commensurate supersolid.

P4.12 H_2 physisorbed on graphane

C. Carbonell-Coronado^a, F. de Soto^a, C. Cazorla^b, J. Boronat^c, and M.C. Gordillo^a

^aUniversidad Pablo de Olavide, Sevilla, Spain

^bInstitut de Ciència de Materials de Barcelona, Bellaterra, Spain

^cUniversitat Politècnica de Catalunya, Barcelona, Spain

In this work we study the zero-temperature phase diagrams of H_2 adsorbed on the three structures predicted for graphane (chair, boat and washboard graphane), using a diffusion Monte Carlo technique. Graphane is the hydrogenated version of graphene, in which each carbon atom changes its hybridization to sp^3 and forms a covalent bond with a hydrogen atom. Our results show that the ground state of H_2 adsorbed on all three types of graphane is a $\sqrt{3} \times \sqrt{3}$ solid, similar to the structures found both for H_2 and D_2 on graphene. When the H_2 density increases, the system undergoes a first order phase transition to a triangular incommensurate solid. This change is direct in the case of washboard graphane, but indirect via different commensurate structures in the other cases. The total hydrogen weight percentage on the three graphane types in their ground states is in the range 10% to 12%, depending on if one or both graphane surfaces are covered with H_2 .

P4.13 Phase diagrams of ^4He on flat and curved environments

M.C. Gordillo^a and J. Boronat^b

^aUniversidad Pablo de Olavide, Sevilla, Spain

^bUniversitat Politècnica de Catalunya, Barcelona, Spain

By means of diffusion Monte Carlo calculations, we obtained the phase diagrams of a second layer of ^4He on graphene and on the outside of different isolated armchair carbon nanotubes with radii in the range 3.42 to 10.85 Å. That corresponds to tubes between the (5,5) and (16,16) in the standard nomenclature. In both cases, the ground state is either a liquid (helium second layer and tubes whose radii is greater than ~ 7 Å) or an incommensurate solid (for thinner tubes). In the former case, upon a density increase, the system undergoes a first order phase transition to another incommensurate solid. A study of the influence of the C-He potential (isotropic or anisotropic) on the phase diagrams is also presented.

P4.14 Evidence of Novel Quasiparticles in a Strongly Interacting Two-Dimensional Electron System: Giant Thermopower and Metallic Behaviour

V. Narayan^a, S. Goswami^b, M. Pepper^c, J. Griffiths^a, H. Beere^a, F. Sfigakis^a, G. Jones^a, D. Ritchie^a, and A. Ghosh^b

^aCavendish Laboratory, University of Cambridge, UK

^bDepartment of Physics, Indian Institute of Science, Bangalore, India

^cDepartment of Electronic and Electrical Engineering, University College London, UK

We report thermopower (S) and electrical resistivity (ρ_{2DES}) measurements in low-density (10^{14} m^{-2}), mesoscopic two-dimensional electron systems (2DESs) in GaAs/AlGaAs heterostructures at sub-Kelvin temperatures ¹. Our results indicate the existence of novel itinerant quasiparticles in the 2DES that render it metal-like as is evidenced by a linearly growing S as a function of temperature. Interestingly this metallicity is not Drudé-like, showing several unusual characteristics: i) the magnitude of S exceeds the Mott prediction valid for non-interacting metallic 2DESs at similar carrier densities by over two orders of magnitude; ii) ρ_{2DES} in this regime is two orders of magnitude greater than the quantum of resistance h/e^2 ; and iii) ρ_{2DES} and S show an intriguing decoupling in their density-dependence, the latter showing striking oscillations that are completely absent in the resistivity. We argue that the above observations are manifestations of the inter-electron Coulomb potential combined with quantum fluctuations and draw parallels with 2D supersolid behaviour ^{2,3}.

1. Narayan, V. *et al.* (submitted) (2012)

2. Koushik, R., Baenninger, M., Narayan, V. *et al.*, Phys. Rev. B **83**, 085302 (2011)

3. Baenninger, M. *et al.*, Phys. Rev. Lett. **100**, 016805 (2008)

P4.15 One-Dimensional Superfluid ^4He Adsorbed in Nanochannels

Taku Matsushita, Yuki Nakanishi, Takumi Endoh, Mitsunori Hieda, and Nobuo Wada

Department of Physics, Nagoya University, Nagoya, Japan

Systematic torsional-oscillator studies for ^4He adsorbed in one-dimensional (1D) straight channels of nanoporous FSM have shown that superfluids are observed even in the 1D-phonon states where longitudinal long-wavelength phonons are dominant in the heat capacities¹. By fine tuning of the channel diameter, we have observed whole temperature dependences of the superfluid ^4He in nanochannels 2.4 nm in diameter. Growth of the superfluid density with decreasing temperature is quite gradual around a characteristic temperature where a broad dissipation peak is observed. These features are of 1D superfluid, essentially different from those of 2D or 3D superfluid. The temperature dependence of the superfluid density qualitatively agrees with that calculated for finite-length 1D superfluid where 1D topological excitations with 2π -phase winding play a major role to determine the density. And, previous results in the other channel diameters are also well explained in this context. On the other hand, existence of the accompanying dissipation clearly indicates that the observed is a dynamic response of the 1D superfluid rather than the static superfluid density. In addition to dependences of the superfluid on temperature and densities, we will show preliminary experimental results for the frequency dependence to examine dynamics of the 1D superfluid.

1. N. Wada, Y. Minato, T. Matsushita, M. Hieda, *J. Low Temp. Phys.* **162**, 549 (2011).

P4.16 Critical behaviour of the liquid gas transition of ^4He confined in a silica aerogel

G. Aubry, F. Bonnet, M. Melich, L. Guyon, and P. E. Wolf

Institut Néel CNRS-UJF , BP 166, F-38042 Grenoble Cédex 9, France

We have studied ^4He confined in a 95% porosity silica aerogel in the vicinity of the bulk liquid gas critical point. Both thermodynamic measurements and light scattering experiments were performed to probe the effect of a quenched disorder on a liquid gas transition, in the context of de Gennes and Brochard proposition to view this transition in porous gels as an experimental realization of the Random Field Ising Model (RFIM). Far enough below T_c , we find that the measurements are consistent with the non equilibrium behavior predicted for the RFIM at zero temperature. In this paper, we focus on the temperature region close enough to T_c , with the aim to search for the equilibrium behavior of RFIM. We find that the hysteresis between condensation and evaporation present at lower temperatures disappears at a temperature T_{ch} about 30 mK below the critical point. In contrast to the situation at lower temperatures, slow relaxations are observed for temperatures slightly below T_{ch} , indicating that some energy barriers, but not all, can be overcome. Above T_{ch} , no density step is observed along the (reversible) isotherms, showing that the critical behavior of the equilibrium phase transition in presence of disorder, if it exists, is shifted to smaller temperatures, where it cannot be observed due to the impossibility to reach equilibrium. At all temperatures above T_{ch} , light scattering exhibits a weak maximum close to the pressure where the isotherm slope is maximal. However, this behavior can be accounted for by a simple model incorporating the compression of the helium close to the silica strands, rather than by thermodynamic fluctuations. Overall, our results suggest that the liquid gas transition of a fluid confined in aerogels does not allow to access the equilibrium behavior of the RFIM model.

P4.17 Many-Body Effects in the Spatially Separated Electron and Hole Layers in the Coupled Quantum Wells

V.S. Babichenko^a and I.Ya. Polishchuk^{a,b}

^aRNC Kurchatov Institute, Kurchatov Sq.1, 123182, Moscow, Russia

^bMax Planck Institute for the Physics of Complex Systems, Nöthnitzer Str. 38, D-01187 Dresden, Germany

Optical studies of excitations in semiconductor CQW systems created at intensive irradiation revealed a number of interesting effects, in particular, the observation of a luminescence ring. Sometimes, the ring was found to break down into number a of periodically arranged islands. A possible explanation of these experiments assumes a that the system is a non-equilibrium one which experiences a self-organization processes. At the same time, it is possible to explain the experiments solely within the bounds of equilibrium thermodynamics. In the paper the approach is proposed which describes an alternative scenario for the formation of the condensed phase in the space-separated electron-hole plasma in the CQW. It is demonstrated that, from the viewpoint of thermodynamics, the liquid state is the preferable one, the equilibrium charge concentration n_{eq} (in-plane charge per unit square of the quantum well) obeys the condition $n_{eq}R_{ex}^2$, R_{ex} being the exciton radius. It is shown that the bound energy per one electron-hole pair is larger than the exciton bound energy. This means that, if the concentration n of the electron-hole pairs (induced by the external pumping) is smaller than n_{eq} , then the initially created homogeneous state becomes a transient one. The electron-hole plasma experiences the fragmentation into islands with the equilibrium density n_{eq} instead. Thus our scenario does not assume that the system possesses the exciton Bose-Einstein condensation.

P4.18 Superfluidity of ⁴He in a well-controlled nanopore array

T. Tanaka^a, S. Murakawa^a, K. Osawa^a, Y. Shibayama^a, A. Nakahara^b, K. Honda^b, and K. Shirahama^a

^aDepartment of Physics, Keio University, Yokohama, Japan

^bDepartment of Biological Science and Chemistry, Yamaguchi University, Yamaguchi, Japan

Recent experiments have revealed that superfluidity of liquid ⁴He in nanoporous materials (pore size $d \sim 0.3\text{nm}$) is strongly suppressed under pressure¹. Since the suppression occurs at pore size much larger than the superfluid coherence length $\xi \sim 0.3\text{nm}$, it opens possibility of developing novel superfluid weak links with currently available technique of nanopore fabrication. In particular, the superfluid Josephson junction working not only near the λ point may be realized. Aiming at developing the weak link, we study superfluidity of ⁴He in a regular array of nanopores made of porous alumina (PA) in which the pore size is controlled by Au film evaporated on and inside the nanopores. We employ vibrating wire technique, in which the Au - evaporated PA is glued to a semicircular NbTi wire and is vibrated in superfluid ⁴He at various pressures. Suppression of superfluid transition is successfully observed as an abrupt change in resonant frequency accompanying a dissipation peak. The dependence of superfluid transition on pore size (thickness of Au film) will be discussed.

¹K. Yamamoto *et al.*, Phys. Rev. Lett. **93**, 075302 (2004).; K. Yamamoto *et al.*, Phys. Rev. Lett. **100**, 195301 (2008).; J. Taniguchi *et al.*, Phys. Rev. B. **82**, 104509 (2010).

P4.19 On Effective Mass of Charged Clusters in Cryogenic Electrolytes

I. Chikina^a, L. Mezhov-Deglin^b, S. Nazin^b, and V. Shikin^b

^aIRAMIS, LIONS, UMR SIS2M 3299 CEA-CNRS, CEA-Saclay, F-91191 Gif-sur-Yvette Cedex, France

^bInstitute of Solid State Physics of Russian Academy of Sciences, 142432, Chernogolovka, Russia

Discussed are available possibilities for determining effective mass M_i of charged clusters in cryogenic electrolytes. The technique widely used in the studies of 2D charged systems [1] is based on the existence of eigenfrequency ω_i in the potential well formed by the image forces and the pressing electric field E_{\perp} ($\omega_i^2 \propto M_i^{-1}$). The resonance $(\omega - \omega_i) \rightarrow 0$ is clearly observed in liquid helium as long as $\omega_i/\omega_{\eta} \gg 1$. Here ω_{η} is the hydrodynamic damping due to viscous Stokes force. In the opposite limiting case $\omega_i/\omega_{\eta} \leq 1$ which is important for both cryogenic and especially normal electrolytes, the resonance $(\omega - \omega_i) \rightarrow 0$ becomes practically indiscernible.

The suggested technique allows to extract information on M_i in the low-frequency range $\omega \leq \omega_i \leq \omega_{\eta}$ and is based on a special differential procedure. It employs simultaneous measurements of both planar $\sigma_{\parallel}(\omega, \omega_{\eta})$ and vertical $\sigma_{\perp}(\omega, \omega_{\eta})$ low-frequency conductivities in the 2D ion system formed at the surface of a cryogenic electrolyte in the presence of vertical field E_{\perp} followed by calculation of their difference $\delta\sigma(\omega) = \sigma_{\parallel}(\omega, \omega_{\eta}) - \sigma_{\perp}(\omega, \omega_{\eta})$. This model allows detailed discussion of effective associated mass δM_i^{ass} of charged clusters within the hydrodynamic approach (finite viscosity η is required) where $\delta M_i^{ass}(\omega) \propto \omega^{-1/2}$ [2].

1. V.Shikin, Yu.Monarkha. Two-dimensional Charged Systems in Helium. Moscow, Nauka, 1989.
2. L.Landau, E.Lifshits. Hydrodynamics. Moscow, Nauka, 1986.

P4.20 Low-temperature thermodynamic properties of nanocrystals

A.I. Karasevskii^a and V.V. Lubashenko^b

^aInstitute for Metal Physics, 36 Vernadsky str., Kiev, 03142, Ukraine

^bInstitute for Metal Physics, 36 Vernadsky str., Kiev, 03142, Ukraine

Size reduction of nanocrystals results in a change of the temperature and heat of phase transformations, shifts of the Curie point and the Neel point in the case of magnetic materials, increase in the temperature of the amorphous to crystalline transition, diffusion acceleration and increase in conduction, increase in the temperature of the superconducting phase transition etc. We propose a statistical theory of the nanocrystalline state. It is shown that size reduction of a crystal is accompanied with quantization of its vibrational energy, making the pressure of the phonon gas of the crystal increase [1,2]. At high temperature, such excess pressure of the phonon gas is inversely proportional to the crystal size, and the corresponding force is outward-directed. Analytical expressions are obtained for the crystal size dependence of changes in the temperature and heat of a phase transformation and other thermodynamic properties. In the case of low temperatures, the long-wavelength vibration modes with wavelengths longer than nanocrystal size are not excited. The probability of excitation of high-energy short-wave vibration modes is also low. These circumstances determine size-dependent rearrangement of the vibrational spectrum of a nanocrystal and, therefore, strong size dependence of both thermodynamic properties and temperature of phase transformations in nanocrystals. We present results illustrating low-temperature behaviour of thermodynamic properties of nanocrystals.

1. A.I. Karasevskii, V.V. Lubashenko, Eur. Phys. J. B 66, 375 (2008)
2. A.I. Karasevskii, Solid State Com., 151, 360 (2011)

P4.21 Instability of Small Deuterium Clusters in Superfluid Helium near the λ Point

N.V. Krainyukova^a, L.P. Mezhov-Deglin^b, and V.B. Efimov^b

^aInstitute for Low Temperature Physics and Engineering NASU, Kharkiv, Ukraine

^bInstitute of Solid State Physics RAS, Chernogolovka, Russia

We present the results of quasi-elastic small-angle neutron scattering study of deuterium clusters immersed in superfluid ^4He . Diffraction intensities exhibit a very strong change in a character at temperatures above 1.95 K but below the λ point. They are compared with calculations based on the assumption that clusters with different sizes and structures as well as single molecules may contribute in a total diffraction pattern with their particular varied relative weights. We have found that small clusters with $N < 300$ molecules intensively decrease in size and a big abundance of free deuterium molecules form inside superfluid ^4He below the λ point that evidences in favor of instability of smallest deuterium clusters while larger clusters undergo no noticeable changes.

P4.22 Superfluid Onset and 2D phase transitions of Helium-4 on Lithium and Sodium

P. Taborek, E. Van Cleve, A.E. Velasco, and F. Huisman

Department of Physics and Astronomy, University of California, Irvine, CA, USA

Lithium and sodium are predicted to be intermediate strength substrates which are strong enough to be wetted by He-4 but weak enough that solid-like layers do not form, so they are candidates for observing sub-monolayer superfluidity in direct contact with a metallic surface. We have fabricated lithium and sodium films on quartz crystal microbalances (QCM) using in situ low temperature pulsed laser deposition; these alkali metal films were subsequently used as substrates for helium adsorption experiments. The frequency shift (due to the clamped normal fraction) and dissipation of the alkali-coated QCM were measured as a function of helium pressure and chemical potential and used to construct the phase diagram of helium films on these substrates. A novel pressure measurement technique based on an RGA mass spectrometer was used to obtain accurate measurements even below 10^{-8} Torr. Helium adsorption isotherms and quenches between 0.5K and 1.6K on both lithium and sodium indicated continuous, sub-monolayer helium film growth and superfluid onsets in sub-monolayer films. Features below 1K indicate a collision between a classical 2D liquid/vapor phase transition and the Kosterlitz-Thouless superfluid phase transition. We see no evidence for the pre-wetting step instability predicted for helium on sodium. Preliminary measurements using ellipsometry to independently measure the total (normal+superfluid) coverage are also described.

P4.23 Relaxation of hot electrons on helium in ripplon scattering regime

A. Badrutdinov^a, M. Watanabe^b, K. Kono^b, and D. Konstantinov^a

^aOkinawa Institute of Science and Technology, Japan

^bLow Temperature Physics Laboratory, RIKEN, Japan

Surface states of electrons on liquid helium have been proposed as a potential candidate for qubit¹, providing the advantages of scalability and extremely high purity of the system. In the proposed scheme the Bloch sphere of a qubit consists of superposition of first two Rydberg states of single electron floating on helium surface, while evolution of qubit is caused by microwave radiation resonantly exciting the transition between these states. Coherence time of electron-on-helium qubit is limited by interactions of electron with helium vapor atoms and ripples (surface capillary waves' quanta), which may cause relaxation of electron from excited state. By lowering temperature concentration of vapor atoms drastically reduces, however, ripples still remain a significant source of decoherence. Uptodate, the knowledge about electron relaxation rate due to ripples is mainly theoretical, and values derived by different approaches vary significantly. In this work we report experimental study of the problem which allows to determine the actual timescale of electron-to-ripplon energy relaxation.

1. Platzman, P. M. and Dykman, M. I. (1999). "Quantum computing with electrons floating on liquid helium". *Science*, vol. 284, p. 1967.

P4.24 Superfluid ⁴He in Nanopore Array: Toward the Josephson Effect at Arbitrary Temperatures

S. Murakawa^a, K. Osawa^a, T. Tanaka^a, K. Honda^b, Y. Shibayama^a, and K. Shirahama^a

^aDepartment of Physics, Keio University, Yokohama, Japan

^bDepartment of Biological Science and Chemistry, Yamaguchi University, Yamaguchi, Japan

It has been recently revealed that superfluidity of liquid ⁴He confined in nanoporous materials (pore size ~ 3 nm) is anomalously suppressed¹. The transition temperature approaches 0 K by pressurizing liquid, indicating a quantum phase transition between superfluid and nonsuperfluid states. We propose that this remarkable confinement effect is utilized to superfluid weak link, i.e. Josephson junction. In superfluid ⁴He, a Josephson junction has been developed using an array of holes of 100 nm in diameter². The working temperature of such a junction is limited to the vicinity of the λ point, at which the coherence length is comparable to the size and length of the holes.

We propose an idea to utilize the confinement-induced superfluid suppression to develop novel Josephson junction working at arbitrary temperatures. A porous alumina nanopore array is prepared as a possible weak link device, on which gold film is evaporated to control (decrease) the pore size down to 5 nm³. We are currently preparing a SQUID-based diaphragm resonator² to measure the characteristics of the porous-alumina weak link. Current status and prospects will be discussed.

1. K. Yamamoto *et al.*, *Phys. Rev. Lett.* **93**, 075302 (2004); *Phys. Rev. Lett.* **100**, 195301 (2008).

2. E. Hoskinson and R. E. Packard, *Phys. Rev. Lett.* **94**, 155303 (2005).

3. T. Tanaka *et al.*, this conference.

P4.25 Collective Modes in Bilayer Dipolar Gases and the Drag Effect

B. Tanatar

Department of Physics, Bilkent University, 06800, Ankara, Turkey

We consider the collective modes of a bilayer dipolar Fermi and Bose systems in which the particles interact via long range ($\sim 1/r^3$) interaction. Assuming that each layer has a background flow which varies little and that the dynamics of the superfluid near $T = 0$ is the same as that of a normal fluid, we obtain the dispersion relations for the collective modes in the presence of background flow. Decomposing the background flow into two parts, the center-of-mass flow and counterflow, we focus on the properties of the counterflow. We first find an estimate of the change in the zero-point energy ΔE^0 due to counterflow for a unit area of double layers. Combining this with the free energy F of the system and taking the partial derivatives with respect to background velocities in the layers, we determine the current densities which reveal the fact that current in one layer does not only depend on the velocity in the same layer but also on the velocity of the other layer. This is the drag effect and we calculate the drag coefficient separately for Fermi and Bose systems. As in the case of charged systems¹ (electrons and charged bosons interacting via a $1/r$ potential) we find that the drag coefficient reflects the statistics of the dipolar gases.

1. B. Tanatar and A. K. Das, Phys. Rev. B **54**, 13827 (1996).

P4.26 SQUID-NMR of Helium-3 on a new Exfoliated Graphite Substrate

F. Arnold^a, B. Yager^a, K. Kent^a, C. Howard^{a,b}, J. Nyeki^a, B.P. Cowan^a, and J. Saunders^a

^aRoyal Holloway, University of London, UK

^bUniversity College London, UK

Low dimensional helium systems, such as ³He absorbed on graphite, provide model systems to investigate a variety of strongly correlated phenomena.

We present recent results of nuclear magnetic resonance measurements of submonolayer ³He-films adsorbed on a new exfoliated graphite substrate. New graphite substrates have been produced by potassium intercalation, ammoniation and subsequent exfoliation at elevated temperatures. The exfoliated graphites were characterised using x-ray diffraction, krypton absorption isotherms, electrical transport and magnetisation measurements. Magnetoresistance has been measured as a possible probe of substrate quality.

Nuclear magnetic relaxation times of submonolayer ³He films on exfoliated graphite have been measured using the SQUID-NMR technique at 1.8 and 4.2 K. We were able to measure the intrinsic transverse relaxation time T_2 of $2 \cdot 10^{19}$ ³He spins by applying spin-echo pulse sequences. The transverse relaxation time T_2^* has been extracted from FID lineshapes providing a signature of first layer promotion. A comparison of these results with previous data of ³He on Grafoil¹ and ZYX¹ substrates will be given.

1. H. Godfrin Prog. Low. Temp. Phys. **14** 213-320 (1995)

P4.27 **Effects of ^3He Impurities on the Superfluid Response of the ^4He Monolayer on a C_{20} Molecule**

Hyeondeok Shin and Yongkyung Kwon

Division of Quantum Phases and Devices, School of Physics, Konkuk University, Seoul, Korea

Effects of ^3He impurities on the superfluid response of the ^4He monolayer on a C_{20} molecule are studied with the path-integral Monte Carlo (PIMC) method. According to our previous PIMC calculation,¹ the monolayer on C_{20} is completed with 32 ^4He atoms to be a commensurate solid with a structure registered to the molecular surface. In addition, we found that mobile vacancy states could be activated to induce nanoscale supersolidity in this monolayer near its completion. For a partially-filled helium monolayer in a fluid state, the replacement of ^4He atoms with the same number of ^3He atoms is found to suppress the superfluidity of the layer, which is understood by ^3He impurities disrupting the exchange couplings among ^4He atoms. With the substitution of ^3He atoms for ^4He atoms in a near-complete monolayer, we observe the same crystalline structure as that of the pristine ^4He layer. Interstitial and vacancy defects promoted by larger quantum fluctuations of lighter ^3He atoms are expected to enhance the superfluidity of ^4He adatoms in a solid state while the disruption of exchange coupling due to the presence of ^3He impurities could suppress the superfluid response. Relative significance of these two conflicting impurity effects is now under investigation.

1. Y. Kwon and H. Shin, Phys. Rev. B **82**, 172506 (2010).

P4.28 **Structural and Superfluid Properties of the ^4He Monolayer on a C_{28} Molecule**

Byeongjoon Kim and Yongkyung Kwon

Division of Quantum Phases and Devices, School of Physics, Konkuk University, Seoul, Korea

We have performed path-integral Monte Carlo calculations to study ^4He adsorption on a single C_{28} fullerene molecule. The ^4He monolayer is found to show a commensurate structure at $N = 16$ with each of the 16 adsorption sites on the molecular surface being occupied by one ^4He atom while, as more helium atoms are added, it is in a mixed state consisting of 4 localized atoms at the hexagonal faces and the other atoms delocalized over the pentagonal faces. Another structurally-ordered state is observed at $N = 32$, where the helium layer shows the same platonic crystal structure with an icosahedral symmetry as observed for 32 ^4He atoms on a C_{60} molecule.¹ It is found that more ^4He atoms can be squeezed into the first layer to disrupt this icosahedral structure when enough ^4He atoms are added in the second layer. Finally we observe the reentrant superfluid response of the monolayer with superfluidity being quenched completely at the structurally-ordered states of $N = 16$ and 32.

1. H. Shin and Y. Kwon, J. Chem. Phys. **136**, 064514 (2012).

P4.29 A New Exfoliated Graphite Substrate for Measurements of Adsorbed Gases

K. Kent^a, C. Howard^{a,b}, F. Arnold^a, B. Yager^a, J. Nyéki^a, and J. Saunders^a

^aRoyal Holloway, University of London, UK

^bUniversity College London, UK

A new exfoliated graphite substrate for the study of 2D adsorbed systems is under development, potentially offering superior properties to those presently available. Helium on graphite provides a model system to investigate a broad range of problems in two dimensional strongly correlated systems; improvements in substrate quality are desirable.

The starting material is a natural graphite, intercalated to form a potassium-ammonia graphite intercalation compound. The exfoliation process has been studied systematically and is carefully controlled. An extensive comparative study of the physical properties of our substrate with those of existing graphite substrates, Grafoil¹ and ZYX, has been used to optimise the production process. Chemical analysis of the final substrate shows magnetic impurity levels lower than for Grafoil GTA and no residue from the intercalation process.

We compare crystallite sizes, inferred from peak broadening of the $hk0$ x-ray diffraction line, with those of conventional exfoliated graphite. Stepwise multilayer adsorption isotherms of krypton at 77 K have shown layer by layer growth with a specific surface area of $\sim 1 \text{ m}^2/\text{g}$.

1. Product of Union Carbide Corporation (GrafTech International)

P4.30 NMR Identification of Possible One-Dimensional Behaviour of Helium-3 in Nanopores

B. Yager, A. Casey, J. Nyéki, B.P. Cowan, C.P. Lusher, and J. Saunders

Royal Holloway, University of London, UK

³He confined in mesoporous media is a candidate system for the observation of one-dimensional Fermi behaviour at low temperatures.

We have made thermodynamic and NMR relaxation time measurements of ³He adsorbed in the one-dimensional 23 Å pores of zeolite MCM-41 down to 1.5 K.

Two systems have been studied, the first a multilayer isotopically pure ³He film and the second where 0.01 monolayer of ³He was added to a preplating monolayer of ⁴He.

The broadband NMR spectrometer with SQUID detection allowed the frequency and temperature dependences of the relaxation times to be measured.

The $T_1 \propto \omega^{1/2}$ behaviour observed in the mixtures film has been attributed to effective 1D motion. For the isotopically pure ³He measurement below monolayer the relaxation times were consistent with two-dimensional film behaviour exhibiting quantum tunnelling and thermally activated motion. At higher coverages the relaxation times could be analysed as the sum of two exponentials which we have attributed to relaxation times in the first and second layers. The behaviour of the second layer is consistent with mixtures film measurement where all of the ³He is expected to be in the second layer.

P4.31 Slippage of ^4He Films and Precursor Phenomenon of Superfluidity

K. Noda^a, K. Okamura^a, J. Taniguchi^a, M. Suzuki^a, and M. Hieda^b

^aDepartment of Engineering Science, University of Electro-Communications, Tokyo 182-8585, Japan

^bDepartment of Physics, Nagoya University, Nagoya 464-8602, Japan

We report QCM measurements using a 32 kHz tuning fork for ^4He films adsorbed on an exfoliated single crystalline graphite substrate. The QCM measurements for a Grafoil substrate was performed previously,^{1,2} and it is of importance to confirm the difference in slippage depending on a substrate. We prepared a graphite substrate exfoliated from a single crystal, which remains highly crystalline. In the present measurements, it was found that the decoupling of the film due to the slippage and the superfluidity is larger than that of Grafoil. The competition between the slippage and the superfluidity in three-layer films was also observed, which was confirmed in the previous measurements for Grafoil. In addition, the slippage is suppressed gradually at the higher temperature than the superfluid onset, T_c , during cooling process. For the film with $T_c = 0.2$ K, we measured the relaxation time concerning the slippage. At high temperatures, it increases with lowering temperature in accordance with the Arrhenius law, while it decreases at low temperatures. These two results for the single crystalline graphite suggest that the suppression of the slippage is a precursor phenomenon of the superfluidity.

1. N. Hosomi, J. Taniguchi, M. Suzuki, and T. Minoguchi (2009) Phys. Rev. B **79**, 172503.
2. F. Nihei, K. Ideura, H. Kobayashi, J. Taniguchi and M. Suzuki (2011) J. Low Temp. Phys. **162**, 559.

P4.32 Ultrasound Attenuation of Confined ^4He near the Quantum Critical Point

Y. Iwata, Y. Negishi, N. Yamanaka, S. Murakawa, Y. Shibayama, and K. Shirahama

Department of Physics, Keio University, Yokohama, Japan

In a previous torsional oscillator study¹, we discovered a quantum phase transition in ^4He confined in nanoporous Gelsil glass. The superfluid - nonsuperfluid transition occurs when the pressure is swept around 3.4MPa (critical pressure P_c) near 0 K. Theories with a classical analogue of quantum phase transition² predict that the characteristic time scales that dominate the quantum fluctuations diverge at the quantum critical point (QCP), same as classical dynamic critical phenomena. If the time scales characterizing superfluidity diverge at quantum critical point, some quantities, such as superfluid density, will become strongly frequency dependent near P_c .

We have used ultrasound technique to study the frequency effect on superfluid properties. The sound velocity and attenuation are measured by CW technique at frequency $10 < f < 110$ MHz using high harmonics of LiNbO_3 transducers. We have found that the sound attenuation shows a sharp peak at the superfluid transition temperature T_c . T_c increases with increasing f , suggesting a nature of dynamic criticality near T_c . More interestingly, a broad peak of sound attenuation is observed at around 1 K, and the attenuation becomes linear in T at the low-temperature side, as the QCP approaches. This T -linear attenuation is attributed to a general characteristic of quantum critical phenomena, the inverse- T divergence of characteristic time τ above the QCP, $\tau \propto T^{-1}$. This is the first clear evidence of quantum critical behavior in confined ^4He systems.

- 1 K. Yamamoto et al., Phys. Rev. Lett. **93**, 075302 (2004); Phys. Rev. Lett. **100**, 195301 (2008).
2. S. L. Sondhi et al., Rev. Mod. Phys. **69**, 315 (1997).

P4.33 Liquid and solid ^4He clusters adsorbed on graphene

L. Vranješ Markić^a, I. Bešlić^a, P. Stipanović^a, and R.E. Zillich^b

^aFaculty of Science, University of Split, Split, Croatia

^bInstitut für Theoretische Physik, Johannes Kepler Universität, Linz, Austria

The results of the recent study of small $^4\text{He}_N$ clusters, adsorbed on one and both sides of a graphene sheet will be presented. We assess the effect of corrugation on the binding properties of helium clusters, as well as the influence of the graphene-mediated McLachlan dispersion energy. The McLachlan interaction weakens the attraction between helium atoms, which has a significant effect on the binding energy and the shape of adsorbed ^4He clusters. We discuss the stability of liquid versus solid clusters as a function of the interaction potential model.

All the calculations have been performed using quantum Monte Carlo methods. At zero temperature the ground-state properties of $^4\text{He}_N$ for $2 \leq N \leq 40$ are determined using variational and diffusion Monte Carlo calculations, and in addition path integral Monte Carlo simulations at finite temperature have been performed for some selected cluster sizes.

We find that clusters adsorbed on both sides of graphene are bound but according to the He-He pair distribution function across the graphene sheet pair correlations are very small.

P4.34 Quantum Monte Carlo simulations of spin-polarized hydrogen in 2D and on the surface of liquid helium

L. Vranješ Markić^a, J. Boronat^b, and J.M. Marín^b

^aFaculty of Science, University of Split, Split, Croatia

^bDepartament de Física i Enginyeria Nuclear, Universitat Politècnica de Catalunya, Barcelona, Spain

The ground-state properties of spin polarized hydrogen $\text{H}\downarrow$ in two dimensions (2D) and quasi-2D space are obtained by means of diffusion Monte Carlo calculations. Quasi-2D space corresponds to the realistic model of hydrogen adsorbed on liquid helium. Using the most accurate to date ab initio $\text{H}\downarrow$ - $\text{H}\downarrow$ interatomic potential we have studied hydrogen gas phase, from the very dilute regime until densities above its freezing point. The solid phase in 2D has also been studied up to high pressures and gas-solid transition determined using Maxwell double-tangent construction. The comparison is made to universal equation of state at low densities. Significant differences appear in ground-state properties of the gas in 2D and quasi 2D model.

P4.35 ^3He Effect on 2D Superfluid in ^3He - ^4He Mixture Films on Gold

H. Yamaguchi, H. Tanaka, T. Oda, M. Hieda, T. Matsushita, and N. Wada

Department of Physics, Nagoya University, Nagoya, Japan

There have been a number of experiments exploring the nature of 2D superfluidity and the configuration of ^3He - ^4He mixture films on various substrates. So far, at $T \sim 0$, a possible structure of the film is proposed to be a simple layer model, ^3He /superfluid ^4He /solid-like ^4He /substrate, by torsional oscillator studies on Mylar [1] and porous gold [2], and the superfluidity is strongly affected by the coverage of ^3He overlayer. In the thick ^3He overlayer of $n_3 \sim 13$ layers [2], a large modification in the temperature dependence of the superfluid density ρ_s are observed, yet the mechanism has not been revealed. We undertook a QCM (quartz crystal microbalance) experiment to study the effect of ^3He on the superfluidity of the mixture films on flat gold. Our measurements are done by keeping ^3He coverage constant ($n_3 = 0, 0.3, 0.7, 1.8, 5.4, \text{ and } 8.8$ layers) and then incrementally adding ^4He . Increasing the temperature to the superfluid KT transition temperature T_{KT} , ρ_s generally decreases due to a temperature dependence of the background superfluid density and a screening effect of vortex pairs. With the addition of ^3He , this reduction of ρ_s rapidly increases and then saturates near $n_3 \sim 1$ layer. We suggest two possibilities as the ^3He effect, i) an extra localization of ^4He induced by a dissociation of ^3He into the superfluid ^4He at finite temperature and ii) a reduction of the superfluid vortex core energy by ^3He .

1. D. McQueeney, G. Agnolet and J. D. Reppy, *Phys. Rev. Lett.* **52**, 1325 (1984).

2. G. Csáthy, D. Tulimieri, J. Yoon, and M. H. W. Chan, *Phys. Rev. Lett.* **80**, 4482 (1998).

P4.36 Double torsional oscillator measurements for ^4He confined in 1D nano-porous medium FSM16 with 2.8-nm channel

Junko Taniguchi, Kenta Demura, and Masaru Suzuki

Department of Engineering Science, University of Electro-Communications, Japan

We have measured the frequency dependence of superfluid response for ^4He confined in a one-dimension nano-porous medium, FSM16, with 2.8-nm channel. The measurements were performed for an identical sample at two frequencies of 2 k and 500 Hz, by means of double torsional oscillator. It was made clear that for the low frequency mode the rapid growth of superfluid response occurs at several tens mK lower temperatures than those for the high frequency mode. The difference between the two frequency modes is enhanced by the application of pressure. The observed frequency dependence may be a signature of dynamical superfluid in one dimension.^[1]

[1] T. Eggel, M. A. Cazalilla, and M. Oshikawa, *Phys. Rev. Lett.* 107, 275302 (2011).

P4.37 Atomic motion in low-coverage helium film adsorbed in FSM nanochannels

Taku Matsushita, Atsushi Kuze, Ryosuke Kawai, Mitsunori Hieda, and Nobuo Wada

Department of Physics, Nagoya University, Nagoya, Japan

^4He and ^3He films adsorbed in straight nanochannels of FSM silicate have shown similar heat capacities¹ until coverages increase up to the quantum-fluid layer region over the first-layer completion n_1 . We have studied adsorbed state of ^3He in this low-coverage region for 2.4 nm channels, by measurements of pulsed-NMR at 2.4 and 3.3 MHz. The spin-lattice and spin-spin relaxation times T_1, T_2 of ^3He observed at 1.2–7 K were well described by the two-dimensional version of Bloembergen-Purcell-Pound (BPP) model, as previously reported for similar nanochannels MCM-41². Since in the model, T_1 and T_2 are determined by the second moment of adsorption line and the correlation time τ of magnetic field fluctuation, derived τ can be a measure for diffusive motion of adatoms. At coverages $0.4-2n_1$, minima of T_1 at 3.3 MHz were observed between 6 and 3 K, indicating τ on the order of 10^{-7} sec at these temperatures. With decreasing temperature, changes in T_1 and T_2 become small below about 1.5 K, which implies crossover from thermally-activated motion to quantum tunneling with T -linear heat capacities³. In contrast to large variations below n_1 , T_1 and T_2 are almost independent of coverages above n_1 , which is likely to indicate that τ is determined by interlayer exchange of adatoms. At present, the measurement has been extended to lower temperatures to find crossover to the localized state suggested in the heat capacities.

1. R. Toda et al., *Phys. Rev. Lett.* **99**, 255301 (2007).
2. C.P. Lusher et al., *J. Low Temp. Phys.* **134**, 619 (2004). B. Yager et al., *J. Low Temp. Phys.* **158**, 213 (2010).
3. R. Toda, M. Hieda, T. Matsushita, and N. Wada, *J. Phys.: Conf. Ser.* **150**, 032112 (2009).

P4.38 Heat Capacity of Very Dilute ^3He - ^4He Films on Graphite

Masashi Morishita

Faculty of Pure and Applied Sciences, University of Tsukuba, Japan

According to many experimental observations and theoretical calculations, the second adsorbed layer of ^3He films on graphite surfaces are believed to solidify from fluid into the so-called “4/7 phase” with an increasing areal density at low temperatures. ^4He films have also been considered to solidify into the 4/7 phase. However, a recent theoretical calculation has predicted that there is no commensurate second-layer phase in ^4He films.¹ Measurements of pure ^4He films cannot be expected to clarify this contradiction. The heat-capacity measurement of dilute ^3He - ^4He mixture films is a potential method that can be used to clarify the nature of a ^4He film.

In my previous heat-capacity measurements of dilute ^3He - ^4He mixture films, where the areal density of ^3He was fixed at 0.2 nm^{-2} and the areal density of ^4He was gradually increased, the ^3He - ^4He mixture films exhibited phase separation, and this prevents precise discussion about the solidification.

Herein, I present the results of heat-capacity measurements of even more dilute ^3He - ^4He mixture films, in which the areal density of ^3He is fixed at 0.015 nm^{-2} . The results do not show significant changes between the areal densities of the second-layer and third-layer promotions. The observations strongly suggest that the second layer of the ^4He film does not solidify before the third-layer promotion.

1. P. Corboz et al., *Phys. Rev. B* **78**, 245414 (2008).

P4.39 Imbibition of liquid helium in silica aerogels

P. Spathis, H. Delga, C. Malheiro, and P.E. Wolf

Institut Néel, CNRS, and Université Joseph Fourier, BP 166, 38042 Grenoble, France

We report optical measurements of the imbibition of liquid helium in a sample of silica aerogel with 96% porosity. Both direct imaging and light scattering experiments were performed to determine the dynamics of the liquid-gas interface in both the normal and superfluid phase of liquid helium. In the normal phase, a classical Lucas Wasburn behaviour is observed for the rise of the imbibition front confirming previous studies¹. Moreover our results show that the scattering of light at the interface increases with time implying that the rugosity of the imbibition front increases. The behaviour in the superfluid phase is markedly different, as the fluid invades the sample from all the sides with a constant speed. Besides, measurements at 1.8 K show a homogeneous increase of the scattered intensity from all the sample prior to the fluid invasion.

1. Nomura, R. (2006). “Dynamics of capillary condensation in aerogels”. Phys. Rev. E **73** 032601.

P4.40 Superfluid ³He Confined in a Single 100 nm Slab

L.V. Levitin^a, A.J Casey^a, B. Cowan^a, J. Parpia^b, and J. Saunders^a

^aDepartment of Physics, Royal Holloway, University of London, Egham, Surrey, TW20 0EX, UK

^bDepartment of Physics, Cornell University, Ithaca NY 14853, USA

We present our NMR study of superfluid ³He confined in a 100 nm thick slab. The slab is defined by a nanofabricated silicon cavity. The superfluid order parameter of such thin films is presently unknown.

In order for ³He to be superfluid in the slab of thickness D close to the Cooper pair diameter ξ_0 , ($\xi_0 = 16 - 77$ nm depending on pressure), the walls of the slab are required to scatter ³He quasiparticle specularly. Although scattering is diffuse at solid surfaces, it can be tuned specular by decorating the surfaces with a thick superfluid ⁴He film. To maintain this film on the walls of the cavity the fill line is interrupted with a superfluid-tight cryogenic valve installed at the mixing chamber.

Previous work using a 700 nm slab showed the A phase to be the stable superfluid phase at low pressures. With increased confinement, it is predicted that we approach the quasi-two dimensional A-phase, a gapped $\hat{p}_x + i\hat{p}_y$ superfluid.

P4.41 Self Oscillation of Electrons on the Surface of Superfluid ^4He

M. Watanabe^a, A. Badrutdinov^b, D. Konstantinov^b, and K. Kono^a

^aRIKEN, Saitama, Japan

^bOIST, Okinawa, Japan

Electrons on the liquid He surface move spontaneously and collectively in a certain condition. The frequency of the self oscillation is within audio frequency.¹ This phenomena is observed only in the zero resistant state of electrons on liquid He.²

The electron mobility on the liquid He is affected by irradiation of microwave and applied magnetic field. Microwave excites the electrons into the higher excited state in hydrogen-like potential composed of image charge in the liquid He and electric field applied vertically. In the presence of magnetic field, the electrons go into zero resistant state. In this zero resistant state, electrons move collectively on the liquid He surface.

The frequency range of the collective motion on ^3He is from 100 to 500 Hz, and the frequency changes periodically in the range. On the other hand, the frequency range for ^4He is a little higher than that of ^3He . In addition, the change of the frequency is not periodic.

In the presentation, we will discuss about the origin of this self-organized oscillation and difference of the electron oscillation between on ^3He and ^4He .

1. Konstantinov, D., Watanabe, M. and Kono, K., unpublished. "Self-excited audio-frequency oscillations in 2DES with a nonequilibrium carrier distribution"
2. Konstantinov, D. and Kono, K., Phys. Rev. Lett. 105(2010), 226801.

P4.42 Growth and Characterization of Anisotropic Silica Aerogel

A. Zimmerman, M. Specht, D. Ginzburg, J. Pollanen, J.I.A. Li, C.A. Collett, W.J. Gannon, and W.P. Halperin

Northwestern University, Evanston, Illinois

High porosity silica aerogel has been successfully used as a medium for studying impurity effects in quantum fluids such as $^3\text{He}^1$ and $^4\text{He}^2$. In order to perform such experiments it is important to have a good understanding of the structure of the sample being used, especially large-scale properties such as homogeneity and anisotropy. In previous work it has been shown that both small angle X-ray scattering and optical cross-polarization studies can provide good measures of aerogel anisotropy. These techniques were used to demonstrate that global anisotropy can be introduced to an aerogel sample by either compression or growth induced shrinkage.³ Anisotropic aerogels made using these methods have been used to study the phase diagram of superfluid $^3\text{He}^4$. Here, we present our work on aerogel growth and characterization, as well as new characterization results showing a relationship between aerogel stiffness and the magnitude of anisotropy induced by strain. We gratefully acknowledge support from the National Science Foundation, DMR-1103625.

1. W.P. Halperin, J.A. Sauls. "Helium-three in aerogel." arXiv:cond-mat/0408593v1.
2. M. Chan, N. Mulders, J. Reppy. "Helium in aerogel." Phys. Today. (1996) 30.
3. J. Pollanen, et al. "Globally anisotropic high porosity silica aerogels." J. Non-Crystalline Solids 354, 4668 (2008).
4. J. Pollanen, et al. "Identification of superfluid phases of ^3He in uniformly isotropic 98.2% Aerogel." Phys. Rev. Lett. 107, 195301 (2011).

P4.43 **A New Compact Rotating Dilution Refrigerator**

M.J. Fear^a, P.M. Walmsley^a, D.A. Chorlton^a, M.C. Sellers^a, S.J. Gillot^a, A.J. Crowe^a, D.E. Zmeev^a, H. Agrawal^b, G. Batey^b, and A.I. Golov^a

^aThe School of Physics and Astronomy, Schuster Building, Brunswick Street, Manchester, M13 9PL.

^bOxford Instruments NanoScience, Tubney Woods, Abingdon, Oxfordshire, OX13 5QX.

Rotating a superfluid is the analogue of applying a magnetic field to a superconductor and has thus proved to be a vital tool for investigating quantized vortices in superfluid helium. These can take the form of a rectilinear array of vortex lines during steady rotation, but in addition turbulent vortex tangles (quantum turbulence) can be created following rapid changes in angular velocity. We are constructing a new rotating dilution refrigerator that will complement the existing rotating microkelvin cryostat already present in Manchester. The design of the new instrument is based upon two coaxial rotating carousels that are driven synchronously. The pumps, gas handling system and other noisy electrical equipment are mounted on the upper carousel. Housing all equipment necessary for the running of the refrigerator and equipment required for experiments in the rotating frame means that the only two simple connections to the laboratory frame are required for helium gas recovery and a single phase mains electrical supply. The lower carousel supports a bespoke axially-symmetric wet dilution refrigerator (cooling power 300 microwatts at 100 mK, base temperature 12 mK) built by Oxford Instruments. A Joule-Thompson stage is used instead of a 1K pot to simplify the gas handling system. When it is fully operational, this cryostat will be used for a series of experiments that aim to understand the dynamics of quantum turbulence in the zero-temperature limit. We present an overview of the design and an update of the work in progress.

P4.44 **Thermometry in normal liquid ³He using a Quartz Tuning fork viscometer**

D. Garg, D.I. Bradley, M. Človečko, A.M. Guénault, E. Guise, S.N. Fisher, R.P. Haley, G.R. Pickett, M. Poole, and V. Tsepelin

Department of Physics, Lancaster University, LA1 4YB, Lancaster, UK

We have developed the use of quartz tuning forks for thermometry in normal liquid ³He. We have used a standard 32 kHz tuning fork to measure the viscosity of liquid ³He over a wide temperature range, 6 mK < T < 1.8 K, at SVP. For thermometry above 40 mK we used a calibrated ruthenium oxide resistor. At lower temperatures we used vibrating wire thermometry. Our data compare well with previous viscosity measurements, and we give a simple empirical formula which fits the viscosity data over the full temperature range. We discuss how tuning forks can be used as convenient thermometers in this range of temperatures with just a single parameter needed for calibration.

P4.45 A Compact Rotating Cryostat for Superfluid ^4He Studies

K. Shirahama and M. Taniguchi

Department of Physics, Keio University, Yokohama 223-8522, Japan

Rotation experiments of superfluid ^4He played an important role on understanding physics of superfluidity[1]. Recent discoveries of novel superfluid phenomena such as the superfluid Josephson effect[2] and a quantum phase transition in nano-scale confined ^4He [3] generates new demand of rotating cryostat. Since the great success of the Helsinki ROTA cryostat[4], efforts of developing rotating cryostats have been concentrated on realizing very low temperatures ($T < 1$ mK) and high rotation speed ($\Omega > 6$ rad/sec) with rather huge dewar and rigid structures. For studies of superfluid ^4He , however, it is best suitable to use a more compact cryostat with easier construction and handling.

Here we report on our effort of developing a compact, inexpensive, and easily-operated rotating cryostat focused on superfluid ^4He studies. It consists of a dulalumin rotation table of 1.2 m in diameter, on which an aluminum/FRP dewar and all electronic equipments are rigidly mounted. The upper end of the dewar is connected to a hollow ball bearing, which is fixed to a steel frame. A 1-K insert is installed from the hole of the bearing, then connected to a rotary pump via a O-ring rotating seal. The whole table is rotated directly by an AC servo motor located underneath the dulalumin table, up to 1 rev/sec. The performance test and future plans of experiments will be discussed.

[1] R. J. Donnelly, Quantized Vortices in Helium II (1991). [2] Y. Sato and R. Packard, Rep. Prog. Phys. **75**, 016401 (2012). [3] K. Yamamoto et al., Phys. Rev. Lett. **93**, 075302 (2004); *ibid.* **100**, 195301 (2008). [4] R. Blaauwgeers, S. Boldarev, V. B. Eltsov, A. P. Finne and M. Krusius, J. Low Temp. Phys. **132**, 263 (2003).

P4.46 Absolute Positioning Application of Capacitive Sensor

S. Jang and E. Kim

Center for supersolid & quantum matter research and department of Physics, KAIST, Daejeon 305-701. Republic of Korea

Positioning on a smaller scale is one of the most important techniques in nanoscale science and technology. A number of applications of capacitive sensors have focused on achieving high resolution with covering relatively long range^{1 2}. The limitation of the designs is that those sensors only measure relative change in position. Apart from these designs of capacitive sensors, we present a new design of capacitive sensor which can measure absolute position of system. Absolute positioning is achieved by introducing a set of position dependent area-varying capacitors.

1. Kim, M. and Moon, W. (2006). "A new linear encoder-like capacitive displacement sensor", Measurement 39, 481

2. Lee, S.-C. and Peters, R. D. (2009). "Nanoposition sensors with superior linear response to position and unlimited travel ranges". Rev. Sci. Instrum. 80, 045109

P4.47 **SRD1000 and CMN1000 sensors for precision thermometry below 8 K**

W.A. Bosch^a and R. Jochemsen^b

^aHDL, P.O. Box 691, 2300 AR Leiden, The Netherlands

^bKamerlingh Onnes Laboratory, LION, Leiden University, P.O. Box 9504, 2300 RA Leiden, The Netherlands

The SRD1000 superconductive reference device supports precision thermometry along the PLTS-2000 and ITS-90 by offering up to 13 calibrated reference points between about 15 mK and 8 K. A CMN1000 magnetic susceptibility thermometer supports continuous thermometry alongside the SRD1000 in the range from < 10 mK to 2 K. We report on recent developments to improve the quality of the SRD1000 reference points, and of the sensitivity, reproducibility and response time of the CMN1000 thermometer.

4.9 Invited Oral Presentations: Tuesday August 21st

O17.1 Physics of two-dimensional helium films: Recent studies of monolayer ^3He and ^4He on graphite

Hiroshi Fukuyama

Department of Physics, The University of Tokyo, Tokyo, Japan

I will review recent progress in experimental study of two-dimensional (2D) ^3He and ^4He systems adsorbed on graphite particularly emphasizing two different series of heat-capacity (C) measurements recently carried out in our group which disclosed several unknown properties in these systems. The first series is a study for the 2nd layer of ^3He on a Grafoil substrate preplated with the 1st layer of ^4He down to $100\ \mu\text{K}$. One unexpected finding here is many-body condensation of ^3He in strictly 2D forming liquid puddles of a very low-density.¹ Another is an observation of a detailed density evolution of the nuclear magnetism from a low-density commensurate (C2) phase ($4/7$ phase) to an incommensurate phase including a two-phase coexistence between them. We determined various higher-order ring exchange parameters reliably, from which we concluded that the interlayer exchange between the 2nd and 3rd layers is less important.² The second series is studies of the 1st and 2nd layers of ^4He on ZYX, an exfoliated graphite substrate with a ten-times larger platelet size, at high temperatures above 1 K. The observed C anomalies clearly support the existence of the C2 solid phase in the vicinity of the $4/7$ density.³ This finding is important from the viewpoint of possible bulk supersolidity in 2D solid ^4He since previous torsional oscillator experiments observed superfluid responses at similar densities.

1. D. Sato *et al.*, J. Low Temp. Phys. **158**, 201 (2010).
2. D. Sato, *et al.*, J. Low Temp. Phys. **158**, 544 (2010).
3. S. Nakamura, K. Matsui, T. Matsui and H. Fukuyama, to be published.

O17.2 Superfluidity and BEC of ^4He confined in a one-dimensional channel

Junko Taniguchi and Masaru Suzuki

Department of Engineering Science, University of Electro-Communications, Japan

We have studied the heat capacity and superfluidity of liquid ^4He confined in a uniform and straight nanometer-size channel. For 2.8 nm-channel, the heat capacity has a bend at a certain temperature T_B . Below T_B , ^4He atoms enter a BEC-like low-entropy state. At the same temperature, a small amount of the superfluid appears. Additionally, the superfluid shows a rapid growth at T_o of 0.9 K, far below T_B under low pressure, accompanied by a large and broad dissipation. This rapid growth has a large frequency dependence; T_o shifts to the low temperature by 40 mK by lowering the measuring frequency from 2 k to 500 Hz. It is the first experimental evidence of dynamical superfluid response peculiar to one dimension.

- J. Taniguchi, Y. Aoki, and M. Suzuki, Phys. Rev. B **82**, 104509 (2010).
J. Taniguchi, R. Fujii, and M. Suzuki, Phys. Rev. B **84**, 134511 (2011).

O17.3 ^3He and ^4He on graphene–fluoride and graphane: prediction of novel fluid, superfluid and supersolid phases

M. Nava^a, D.E. Galli^a, M.W. Cole^b, and L. Reatto^a

^aDipartimento di Fisica, Università degli Studi di Milano, via Celoria 16, 20133 Milano, Italy

^bDepartment of Physics, Penn State University, University Park, PA 16802 USA

We present a study of submonolayer He adsorbed on two derivatives of graphene: graphene-fluoride (GF) and graphane (GH). A semiempirical interaction with the substrate is used in state of the art quantum simulations. We predict that both isotopes ^3He and ^4He form anisotropic fluid states at low coverage. The commensurate state analogous to the standard $\sqrt{3} \times \sqrt{3}$ R30° phase that preempts fluid states on graphite turns out to be unstable relative to a fluid state. The commensurate insulating ground state on GF and GH is disfavored by the much smaller inter-site distance (below 1.5 Å) compared to graphite (2.46 Å), implying a large energy penalty for localizing He atoms. The ^4He ground state on both substrates is a self-bound anisotropic superfluid with anisotropic roton excitations and with a superfluid density ρ_s reduced from 100% due to the corrugation of the adsorption potential. In the case of GF such corrugation is so large that $\rho_s = 57\%$ at $T = 0$ K and the superfluid is essentially restricted to move in a multiconnected space, along the bonds of a honeycomb lattice. We predict a superfluid transition temperature $T \simeq 0.25$ (1.1) K for ^4He on GF (GH). At higher coverages we find two kinds of solids, an incommensurate triangular one as well as a novel commensurate state at filling factor 2/7 with 4 atoms in the unit cell. We have evidence that this 2/7 state is supersolid. We conclude that these new platforms for adsorption studies offer the possibility of studying novel phases of quantum condensed matter like an anisotropic Fermi fluid, possibly superfluid, an anisotropic Bose superfluid and a commensurate supersolid.

O17.4 Phases, transitions, and novel phenomena in monolayers of ^4He and other gases on individual carbon nanotubes

D. Cobden, H.-C. Lee, B. Dzyubenko, R. Roy, E. Fredrickson, J.M. Coy, and O.E. Vilches

Department of Physics, University of Washington, Seattle WA 98195-1560, USA

We are studying the adsorption of inert gases, from He to Xe, on individual suspended single-walled carbon nanotubes. The suspended nanotube itself as a vibrating mass balance with few-atom-level sensitivity. Adsorption and phase behavior analogous to that on planar substrates occurs, but the binding energies are small, allowing access to lower two-dimensional chemical potentials, and the cylindrical nanotube surface can be exceedingly homogeneous. Evidence for commensurability and size effects will be discussed. Adsorption, even of He, also has a significant effect on the electrical conductance of the nanotube, making it possible to detect phase transitions, obtain critical exponents, and observe transient behavior at phase transitions in cylindrical monolayers, and potentially allowing measurements at lower temperatures where the vapor pressure is negligible. Similar experiments are also under way on graphene.

1. Wang, Z. P. Morse, J. Wei, O. E. Vilches and D. H. Cobden, Science 327, 552 (2010).

O18.1 He-3 Superfluid as a Model for the Cosmic Landscape in String Theory

S.-H. Henry Tye

Department of Physics, Cornell University, Ithaca NY, USA

Institute for Advanced Study, Hong Kong University of Science and Technology, Hong Kong

String theory is likely to be the ultimate theory of everything (at least from a reductionist's viewpoint), with its deep concepts and rich properties. To describe our universe, we need to consider its numerous solutions. In particular, its 6-dimensional internal space may be described by a set of moduli, or scalar fields. This is a part of the cosmic landscape in string theory, which may be crudely described by an effective potential of these fields. Its understanding may lead to the explanation why we are where we are today. However, the complexity implies that this is a real challenge. To help tackle this problem, we are lucky to have the He-3 superfluid system, which may be described by a set of order parameters (or scalar fields) as well. The resulting effective potential (or free energy) displays the phases and their transitions in He-3 superfluid, the richness of which mimics that in the cosmic landscape. Here, experiments can be performed to test and study its properties, both quantum and classical, thus providing an excellent model to learn about some of the intricacies in the landscape. As a concrete step towards this direction, we like to address the puzzlingly fast A to B phase transition in He-3 superfluid and to explain how its resolution may impact on our understanding of the landscape.

5 Author Index

Abdurakhimov L.V.	P1.30
Abernathy D.L.	P1.36
Aboukassima A.	P3.1
Adamenko I.N.	P1.29
Agrawal H.	P4.43
Ahlstrom S.L.	P1.24 P3.5
Ahokas J.	O6.3
Alakshin E.N.	O11.2
Allen A.J.	P2.28
Anagama Go	P3.34
Ancilotto F.	O3.3
Anderson Brian P.	O3.2
Andersson N.	O1.1
Andreev A.F.	O16.1
Antsygina T.N.	P3.9 P4.3
Aoki Y.	P1.39
Aoki Yusuke	P2.15
Apaja V.	P2.2
Apushkinskaya D.	P2.32
Apushkinsky E.	P2.32
Arahata E.	P2.14
Arnold F.	P4.26 P4.29
Arrayás M.	P1.52
Assmann C.	P1.3
Astrakharchik G.	P2.3
Astrov M.	P2.32
Aubry G.	P4.16
Autti S.	P1.26 O11.3
Azuah R.T.	P1.36
Babichenko V.S.	P4.17
Babuín S.	O5.2
Badrutdinov A.	P4.23 P4.41
Baggaley A.W.	O5.4 P2.29 P2.34 P2.37 P2.48 O10.3
Bagnato G.	O6.4
Bagnato V.S.	O6.4
Balatsky A.V.	O9.3
Balibar S.	O9.1 P3.15 P3.40 P3.41 P3.42
Barengi C.F.	P1.19 O5.4 P2.26 P2.28 P2.29 P2.31 P2.34 P2.37 O10.3
Barragán J.	P1.25
Barranco M.	P1.25 P1.40
Batey G.	P4.43
Bešlić I.	P1.9 P4.33
Beamish J.R.	O9.1 P3.15 P3.40 P3.41 P3.42
Beck C.	P1.11
Beedle Christopher C.	P4.10
Beere H.	P4.14
Bennett R.G.	O2.3 P1.47
Berloff N.G.	O11.1
Birchenko A.P.	P3.31 P3.39
Blanc C.	P1.1 O12.2
Boltnev R.E.	O1.3 P3.30
Bonnet F.	P4.16
Borgh M.O.	P2.18
Boronat J.	P1.9 P2.3 P2.9 P4.12 P4.13 P4.34
Bosch W.A.	P4.47
Bossy J.	P1.35 P3.24 P3.36 P3.46
Bourgeois O.	P1.1 O12.2
Bowden Z.A.	P1.2

Bradley D.I.	P1.24 P1.54 P2.40 P2.46 P2.47 P2.50 P2.51 P3.5 P4.44
Braslau A.	P3.24 P3.46
Brazhnikov M.Yu.	P3.25
Brugarino T.	P2.45
Bukhari S.	P3.41
Bunkov Yu.M.	O11.2 P1.1 P1.26 O11.3 O12.2
Bykhalo I.B.	P3.30
Candela D.	P3.28
Capuzzi P.	P2.11 P2.22
Carbonell-Coronado C.	P4.12
Casey A.J.	P1.3 P1.4 O2.3 O2.4 P4.30 P4.40
Casulleras J.	P1.9
Cazorla C.	P4.12
Chagovets V.	P1.21
Chaib H.	P3.1
Chan H.B.	P1.14 O12.3
Chan M.H.W.	O14.4
Charlton T.R.	O8.2
Chaudhury R.	P3.3
Chikina I.	P4.19
Chishko K.A.	P3.9 P4.3
Cho S.U.	O7.2
Choi H.	P3.47 O14.2
Choi H.C.	P1.13
Choi J.	P3.38
Choi Jaewon	P3.45
Choi W.	P3.38 P3.47 O14.2
Chorlton D.A.	P4.43
Cleland A.N.	O7.1
Človečko M.	P1.24 P2.40 P3.5 P4.44
Cobden D.	O17.4
Cockburn S.P.	P2.10
Cole M.W.	P4.11 O17.3
Collett C.A.	P1.7 O13.1 P4.42
Collin E.	P1.1 O12.2
Corcoles A.	O2.3
Cowan B.P.	O2.3 O2.4 P3.27 P4.26 P4.30 P4.40
Cox T.	O4.1 P2.49
Coy J.M.	O17.4
Craighead H.G.	O7.3
Crowe A.J.	P4.43
Davis J.C. Séamus	O14.1
de Soto F.	P4.12 P2.12
Defoort M.	P1.1 O12.2
Delga H.	P4.39
Demura Kenta	P4.36
Devreese J.T.	P2.5
Devreese J.P.A.	P3.43
Diallo S.O.	P1.36
Dmitriev V.V.	O13.2 P1.44 P1.53
Down R.B.E.	P1.2
Drabbles M.	P1.40
Drung D.	P1.3
Dubyna D.S.	P3.2
Duda D.	P2.36
Dumont Matthieu F.	P4.10
Durajski A.P.	P3.4
Dzyubenko B.	O17.4
Efimenko E.E.	P1.53
Efimov V.B.	O16.3 P4.7 P4.21

Eltsov V.B. P1.26 O5.3 O11.3
 Endoh Takumi P4.15
 Eyal A. P3.12
 Fear M.J. P1.54 P2.38 P2.50 P4.43
 Fefferman A.D. O9.1 P3.15 P3.40 P3.41 P3.42
 Fernández J.M. O1.2
 Ferrari G. P1.8
 Fisher S.N. P1.24 P1.46 P1.51 P1.54 P2.40 P2.46 P2.47 P2.50 P2.51 O12.4 P3.5 P4.44
 Fomin I.A. O13.3
 Fredrickson E. O17.4
 Fujimoto K. P2.13
 Fukui A. P1.32
 Fukuyama H. O17.1
 Fukuyama Hiroshi P1.17 P1.50
 Galantucci L. P2.44
 Galli D.E. P1.37 P1.48 P4.11 O17.3
 Gallucci D. P2.10
 Gannon W.J. P1.7 O13.1 P4.42
 Ganshin A. P2.51 O16.3
 Garcell E. P1.14 O12.3
 Garg D. P1.24 P3.5 P4.44
 Gasparini F.M. O2.1
 Gazizulin R.R. O11.2
 Ghosh A. P1.43 P4.14
 Gillot S.J. P4.43
 Ginzburg D. P4.42
 Glyde H.R. P1.35 P1.36 P3.36
 Godfrin H. P1.1 P1.56 O12.2
 Golov A.I. P1.46 P2.38 P2.39 P3.25 O12.4 P4.43
 Golubchik D. O4.3
 Gonzalez M. P1.14 O12.3
 Goodkind J. P3.10
 Gordillo M.C. P2.12 P4.12 P4.13
 Goswami S. P4.14
 Graf M.J. O9.3
 Griffiths J. P4.14
 Grisenti R.E. O1.2
 Gritsenko I. P1.21 P1.22
 Guénault A.M. P1.24 P1.54 P2.40 P2.46 P2.47 P2.50 P2.51 P3.5 P4.44
 Guise E. P1.24 P2.40 P3.5 P4.44
 Guo W. P1.46 P1.51 P2.33 O12.4
 Guyon L. P4.16
 Hänninen R. O5.3 O10.2 P2.35
 Hakonen P.J. O7.2 O7.3
 Haley R.P. P1.24 P1.54 P2.40 P2.46 P2.47 P2.50 P2.51 P3.5 P4.44
 Hallock R.B. P3.23 O9.4
 Halperin W.P. P1.7 P1.47 O13.1 P4.42
 Hanai R. P2.21
 Harada S. P3.20
 Hartiti B. P3.1 P4.6
 Hata T. P1.31 P1.32 P2.30 P2.43 O10.4
 Hawthorne Dean L. P1.20
 Hayashi S. P2.17
 Haziot A. O9.1 P3.15 P3.40 P3.41 P3.42
 Heikkinen P.J. P1.26 O5.3 O11.3
 Hein B. P3.10
 Hernández E.S. P2.11 P2.22
 Hernando A. P1.40
 Heron J-S. O12.2
 Hieda M. P2.6 P4.15 P4.31 P4.35 P4.37

Hietala N.	P2.35 O10.2
Higashitani S.	P1.13 P1.41
Hill Stephen	P4.10
Hirashima D.	P3.44
Hitomi J.	O13.4
Hobbiger R.	P1.16
Holler R.	P1.16 P2.3
Honda K.	P4.18 P4.24
Hosio J.J.	P1.26 O5.3 O11.3
Howard C.	P4.26 P4.29
Huan C.	P3.28
Huber T.E.	P4.8 P4.9
Hufnagl D.	P2.2 P2.9
Huisman F.	P4.22
Idbaha A.	P4.6
Ihas G.G.	P1.46 P1.51 P2.33 O12.1 O12.4
Ikeda Ryusuke	P1.55
Ikegami H.	P1.12 P1.27 O15.2 O15.3
Inotani D.	P2.21 P2.24
Ishiguro R.	P1.45 O8.1
Ishikawa O.	P1.31 P1.32 P1.45 O8.1 P2.30 P2.43 O10.4
Ishino S.	P2.16 P2.17
Isozaki R.	P3.11 P3.21
Ito R.	O13.4
Iwasa I.	P3.10 P3.14
Iwata Y.	P4.32
Jackson, M.	P2.51
Jang S.	P3.38 P3.45 P4.46
Jochemson R.	P4.47
Jones G.	P4.14
Joseph E.M.	P1.43
Jou D.	P2.45
Kalinin A.	O1.2
Kalinin I.	O9.2
Kamada N.	P1.39
Kanemoto M.	O13.4
Karasevskii A.I.	P4.20
Kasamatsu K.	O6.2 P2.8
Kashimura T.	P2.19 P2.21
Kashiwaya H.	P3.7
Kashiwaya S.	P3.7
Kato C.	P1.31 P1.32
Kato Yusuke	P3.26 P3.34
Katz E.	O9.2
Kawai Ryosuke	P4.37
Kawakami T.	P1.34
Kawashima N.	P3.33
Keeping J.	P1.2
Kent K.	P4.26 P4.29
Khalatnikov I.M.	P1.30
Khmelenko V.V.	O1.3 P3.30
Kim Byeongjoon	P4.28
Kim Duk-Young	P3.45
Kim E.	P3.38 P3.45 P3.47 O14.2 P4.46
Kim S.S.	P3.28
Kimura Y.	P1.31 P2.30
Kinane C.J.	O8.2
Kirichek O.	P1.2 P1.36 O8.2
Kitamura A.	P3.20
Klimin S.N.	P2.5 P3.43

Klochkov A.V.	O11.2
Knowles Elisabeth S.	P4.10
Köhl Michael	O3.1
Koike Y.	P3.44
Kojima H.	P1.39 P3.10
Kolmakov G.V.	P4.7
Kondaurova Luiza P.	P1.5
Kondo K.	P1.32
Kono K.	P1.12 P1.27 P3.32 P3.47 O14.2 O14.3 O15.2 O15.3 P4.23 P4.41
Konopko L.	P4.8 P4.9
Konstantinov D.	P4.23 P4.41
Koren G.	O4.3
Korotash I.V.	P3.2
Koza M.	O9.2
Krainyukova N.V.	P3.35 P4.21
Krakovny A.A.	P3.2
Krasnikhin D.A.	P1.44 P1.53 O13.2
Krotscheck E.	P1.15 P1.16 O9.2 P2.3 P2.7
Krushinskaya I.N.	P3.30
Krusius M.	P1.26 O5.3 O11.3
Kubo H.	P2.43 O10.4
Kubo K.	P4.5
Kubota M.	P1.39 P1.45 O8.1 P3.20
Kühnel M.	O1.2
Kunimatsu T.	P1.45 O8.1
Kunimi Masaya	P3.26 P3.34
Kusumura T.	P2.25
Kuze Atsushi	P4.37
Kuz'min V.V.	O11.2
Kwon Y.	P3.44 P4.27 P4.28
La Mantia M.	P1.23 P2.36
LaloëF.	P2.4
Langlet M.	P1.40
Langridge S.	O8.2
Laurie J.	P2.37
Lauter H.J.	P1.56 O9.2
Lauter V.V.	O9.2
Lawson C.R.	P1.54 P2.50
Lebedev V.	O16.2
Lee D.M.	O1.3 P1.20 P3.30
Lee H.-C.	O17.4
Lee Y.	P1.13 P1.14 O12.3
Leiderer P.	O15.1
Levchenko A.A.	P1.30 P3.22
Levitin L.V.	O2.4 P1.4 P4.40
Li J.I.A.	P1.7 O13.1 P4.42
Li Jian	O7.2
Lichtenegger T.	P1.15 P2.3
Linfitt L.V.	P1.2
Lisunov A.A.	P3.8 P3.9
Livne E.	P3.12
Loginov E.	P1.40
Lubashenko V.V.	P4.20
Lulla K.	P1.1 O12.2
Lusher C.P.	P1.3 P1.4 P4.30
L'vov V.S.	O5.3
Machida K.	P1.34 O8.3
Macia A.	P2.9
Maidanov V.A.	P3.8 P3.9
Malheiro C.	P4.39

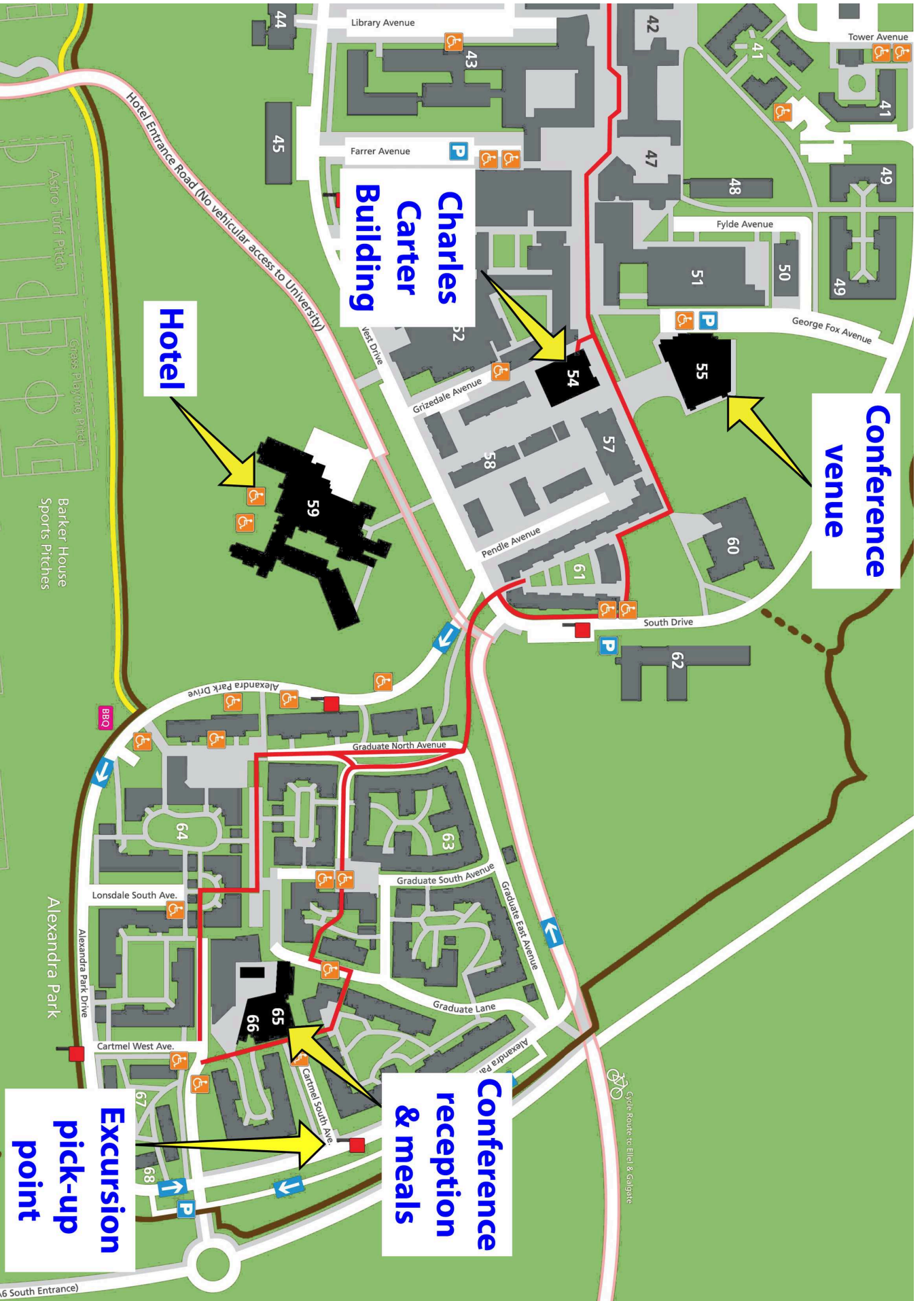
Malik G.P.	P2.1
Manninen M.S.	P3.13
Mao S.	O1.3
Marakov A.	P2.33
Marín J.M.	P4.34
Maris H.J.	P1.25 O8.4 P3.17
MarkićL. Vranješ	P1.9 P4.33 P4.34
Masuhara N.	P1.13
Masumoto R.	P3.11
Mateo D.	P1.25 P1.40 P2.7
Matsuda H.	P3.11 P3.21
Matsui K.	P1.17
Matsui T.	P1.17 P1.50
Matsumoto T.	P1.27
Matsuo Shigemasa	P1.41
Matsushita T.	P4.35 P4.15 P4.37
Matushita T.	P2.6
Mazzanti F.	P2.9
McClintock P.V.E.	P1.46 P1.51 O8.2 O12.4 O16.3
McKinsey D.N.	P1.46 P2.33 O12.4
Meisel Mark. W.	P1.13 P4.10
Melich M.	P4.16
Melnikovskiy L.A.	P1.33
Merdan M.	P3.48
Meschke M.	P1.56
Mezhov-Deglin L.P.	P3.22 P4.7 P4.19 P4.21
Mi X.	P3.16
Miah S.	P1.11
Mikhin N.P.	P3.31 P3.39
Mineda Y.	P2.41
Minoguchi T.	P1.48 P3.18
Mizushima Takeshi	O8.3
Momoi T.	P4.5
Monaco Roberto	O4.4
MongiovìM.S.	P2.45
Montero S.	O1.2
Moon B.H.	P1.13 P1.14
Morishita Masashi	P4.38
Moroni S.	P1.37
Moroshkin P.	O16.2
Motoyama G.	P1.39 P3.7
Motta A.	P1.37
Moutonet T.	O12.2
Mukharski Y.	P3.24 P3.46
Mukhin S.I.	P3.22
Mulders N.	P1.13 P3.37
Mullin W.J.	P2.4
Munday L.L.E.	P1.51
Murakawa S.	P4.18 P4.24 P4.32
Nafidi A.	P3.1 P4.6
Nagai K.	P1.13 P1.41
Nagato Yasushi	P1.41
Nago Y.	P2.43 O10.4
Nakahara A.	P4.18
Nakamura S.	P1.17
Nakanishi Yuki	P4.15
Nakano H.	P3.7
Nakatsuji A.	P2.42
Narayan V.	P4.14
Naruse K.	P1.50

Nava M.	P1.37 P1.48 P4.11 O17.3
Nayak Mukesh G.	P4.1
Nazin S.	P4.19
Negishi Y.	P4.32
Nema H.	P1.45 O8.1
Nemchenko E.K.	P1.6 P1.29
Nemirovskii Sergey K.	P1.5 P1.10 P1.28
Nesvizhevsky V.V.	P4.7
Nichols G.	P3.27
Nikolaenko V.A.	P4.2
Nikolaeva A.	P4.8 P4.9
Nikuni T.	P2.14
Nishijima A.	P2.43 O10.4
Nitta M.	O6.2 P2.8 P2.23
Noda K.	P4.31
Nomura R.	P3.11 P3.21 P3.29
Nussinov N.	O9.3
Nyéki J.	P4.26 P4.29 P4.30
Obara K.	P1.31 P1.32 P2.30 P2.43 O10.4
Ochi A.	P3.11 P3.21
Oda T.	P4.35
Ohashi Y.	P2.19 P2.20 P2.21 P2.24
Ohgoe T.	P3.33
Ohuchi H.	P3.29
Okamura K.	P4.31
Oksanen M.	O7.3
Okuda Y.	O2.2 P1.39 P3.11 P3.21 P3.29
Ollivier J.	P1.35 P3.36
Onorato M.	P2.26
Osawa K.	P4.18 P4.24
Ostaay J.	P3.22
Pach P.W.	P3.4
Pal A.	P1.43
Panholzer M.	P1.16
Panochko G.	P1.38
Papkour F.	P1.46 O12.4
Papoular D.J.	P1.8
Para Gh.	P4.9
Paraoanu G.S.	O7.2
Park Ju-Hyun	P4.10
Parpia J.M.	P1.47 O2.3 O2.4 P4.40 O7.3
Parshin A.Ya.	P3.13
Pelmenev A.A.	P3.30
Pepper M.	P4.14
Perron J.K.	O2.1
Pessoa Renato	P3.19
Pi M.	P1.25 P1.40
Pickett G.R.	P1.24 P1.54 P2.40 P2.46 P2.47 P2.50 P2.51 P3.5 P4.44
Pirkkalainen J.-M.	O7.2
Pistolesi F.	O12.2
Pitaevskii L.P.	P1.8
Polishchuk I.Ya.	P4.17
Pollanen J.	P1.7 P1.47 O13.1 P4.42
Poltavskaya M.I.	P4.3
Poltavsky I.I.	P4.3
Polturak E.	O4.3 P3.12
Poole M.	P1.24 P3.5 P4.44
Proment D.	P2.26
Proukakis N.P.	P2.10 P2.28 P2.31
Puchkov A.V.	O9.2

Rabi S.	P3.46
Reatto L.	P4.11 O17.3
Rees D.	O15.2
Remizov I.A.	P1.30
Reppy J.D.	P3.16
Risset Olivia N.	P4.10
Ritchie D.	P4.14
Rivers Ray J.	O4.4
Rogacki K.	P3.20
Rogova S.	P1.6
Rojas X.	O9.1 P3.15 P3.40 P3.41
Rotter M.	O5.2 P2.36
Rovenchak A.	P4.4
Roy R.	O17.4
Rubanskyi V.Yu.	P3.8 P3.9
Rubets S.P.	P3.8 P3.9
Rudavskii E.Ya.	P1.21 P3.8 P3.9 P3.31 P3.39
Rudenko E.M.	P3.2
Ruostekoski J.	P2.18
Rybalko A.S.	P3.8
Rysti J.	P1.49
Saini L.K.	P4.1
Salasnich L.	O3.3
Salman H.	P2.48
Salvat F.	P1.25
Sasaki Y.	P1.45 O8.1 O13.4
Sato D.	P1.50
Sato Masatoshi	O8.3
Sauls J.A.	P1.18 O13.1 O16.4
Saunders J.	O2.3 O2.4 P4.26 P4.29 P4.30 P4.40
Schanen R.	P1.24 P1.54 P2.50 P3.5
Schmoranzler D.	P1.23
Schober H.	P1.35 P3.36
Schurig Th.	P1.3
Sciacca M.	P2.44 P2.45
Seidel G.M.	O8.4
Sellers M.C.	P4.43
Senin A.A.	P1.44 P1.53 O13.2
Sergeev Y.A.	O5.4 O10.3 P2.29 P2.34
Sfigakis F.	P4.14
Sharma P.	O2.3
Sheludyakov S.	O6.3
Sherwin L.K.	P2.29
Sheshin G.	P1.21 P1.22
Shibahara A.	P1.3 P1.4
Shibayama Y.	P4.18 P4.24 P4.32
Shiddiq Muhandis	P4.10
Shikin V.	P4.19
Shimizu N.	P3.20
Shin Hyeondeok	P4.27
Shin J.	P3.38 P3.45
Shiozaki R.	O6.4
Shirahama K.	P3.32 P3.38 P3.45 O14.3 P4.18 P4.24 P4.32 P4.45
Shukurov A.	O5.4
Sigrist M.	P2.24
Sillanpää M.A.	O7.2 O7.3
Sindzingre P.	P4.5
Singh Chander K.	P3.1 P4.6
Skrbek L.	P1.23 O5.2 P2.36
Smith E.N.	P1.47

Silaev M.A.	O4.2
Smorodin A.V.	P4.2
Sokolov S.S.	P4.2
Song X.	O7.3
Sonin E.B.	O10.1 P3.6
Soucase B. Mari	P3.1 P4.6
Spathis P.	P4.39
Specht M.	P4.42
Stammeier M.	O5.2
Stamp P.C.E.	O4.1 P2.49
Stipanović P.	P4.33
Stringari S.	P1.8
Su J.J.	O9.3
Sugimoto N.	P3.7
Sullivan N.S.	P3.28
Sultan A.	P1.56
Sumiyama A.	P1.39 P3.7
Suominen K.-A.	O6.3
Suramlishvili N.	P2.34
Surovtsev E.V.	P1.42 O13.3
Suzuki Masaru	P4.31 P4.36 O17.2
Suzuki T.	P3.33
Syrkin E.S.	P3.8
Szcześniak R.	P3.4
Szybisz L.	P2.11 P2.22
Taborek P.	P4.22
Tagirov M.S.	O11.2
Takagi T.	P1.45 O8.1
Takahashi D.	P3.32 P3.47 O14.2 O14.3
Takahashi D.A.	P2.23
Takahashi T.	P3.29
Takeuchi H.	P1.13 P1.41 O6.2 P2.8 P2.16 P2.17 P2.25
Talham Daniel R.	P4.10
Tanaka H.	P4.35
Tanaka T.	P4.18 P4.24
Tanaka Y.	O13.4
Tanatar B.	P4.25
Taniguchi J.	P4.31 P4.36 O17.2
Taniguchi M.	P4.45
Tavares P.E.S.	O6.4
Taylor J.W.	P1.36
Tejeda G.	O1.2
Telles G.D.	O6.4
Tempere J.	P2.5 P3.43
Thompson K.J.	P1.51
Thompson L.	O4.1
Tinh B.D.	P2.27
Toda R.	P2.6 O13.4
Todoshchenko I.A.	P3.13
Toigo F.	O3.3
Tramonto F.	P1.48
Tsepelin V.	P1.24 P1.54 P2.40 P2.46 P2.47 P2.50 P2.51 P3.5 P4.44
Tsubota M.	O5.1 O6.2 P2.8 P2.13 P2.15 P2.16 P2.17 P2.25 P2.41 P2.42
Tsuchiya S.	P2.20 P2.23
Tsuiki T.	P3.32 O14.3
Tsutsumi Y.	P1.34
Tuoriniemi J.	P1.49
Tye S.-H. Henry	O18.1
Ueno K.	P3.11
Vadakkumbatt V.	P1.43

Vainio O. O6.3
 Vakarchuk I.O. P1.38
 Van Cleve E. P4.22
 Varga E. O5.2
 Varma V.S. P2.1
 Vasilev N.D. O8.2
 Vasiliev S. O6.3
 Vekhov Ye.O. P3.23 P3.31 P3.39
 Velasco A.E. P4.22
 Vilches O.E. O17.4
 Vinen W.F. P1.46 P1.51 P2.33 P2.41 O12.4
 Vitali E. P1.37
 Vitiello S.A. P3.19
 Volovik G.E. P1.26 O5.3 O11.3
 Wacks D.H. P1.19
 Wada N. P2.6 P4.15 P4.35 P4.37
 Walmsley P.M. P1.46 P2.38 P2.39 O12.4 P4.43
 Watanabe M. P4.23 P4.41
 Watanabe R. P2.19 P2.20 P2.21
 Wei W. O8.4
 Weir David J. O4.4
 Weis A. O16.2
 White A.C. P2.31
 Wilde Scott P1.20
 Williams P. P2.46 P2.47
 Wolf P.E. P4.16 P4.39
 Woods A. P1.24 P3.5
 Wouters M. P3.43
 Wu Hao P1.18
 Xia J.S. P3.28
 Xian Y. P3.48
 Xie Z. O8.4
 Yager B. P4.26 P4.29 P4.30
 Yagi M. P3.20
 Yamaguchi A. P1.39 P3.7
 Yamaguchi H. P4.35
 Yamanaka N. P4.32
 Yamashita K. P3.44
 Yang J.H. P1.51
 Yano H. P1.31 P1.32 P2.30 P2.42 P2.43 O10.4
 Yasuta Y. P3.20
 Yin L. P3.28
 Yoshii R. P2.23
 Yudin A.N. P1.44 P1.53 O13.2
 Zadorozhko A. P1.21 P1.22
 Zarembo E. P2.28
 Zavjalov V. P1.26 O11.3
 Zhelev N. P1.47
 Zheng P. P1.14 O12.3
 Zillich R.E. P2.2 P2.7 P2.9 P4.33
 Zimmerman A. O13.1 P4.42
 Zmeev D.E. P1.46 P3.25 O12.4 P4.43
 Zvezdov D. O6.3
 Zwierlein M.W. O6.1



**Charles
Carter
Building**

Hotel

**Conference
venue**

**Conference
reception
& meals**

**Excursion
pick-up
point**

6 South Entrance)